# Geology & geophysics of the Koonenberry Belt, far western New South Wales, and eastern Australian correlates:

## timing, development and prospectivity of a sector of the Late Neoproterozoic - Palaeozoic Gondwana margin

**Nicholas G. Direen** (Nicholas Gerard)

B.Sc (Hons) (UTas)

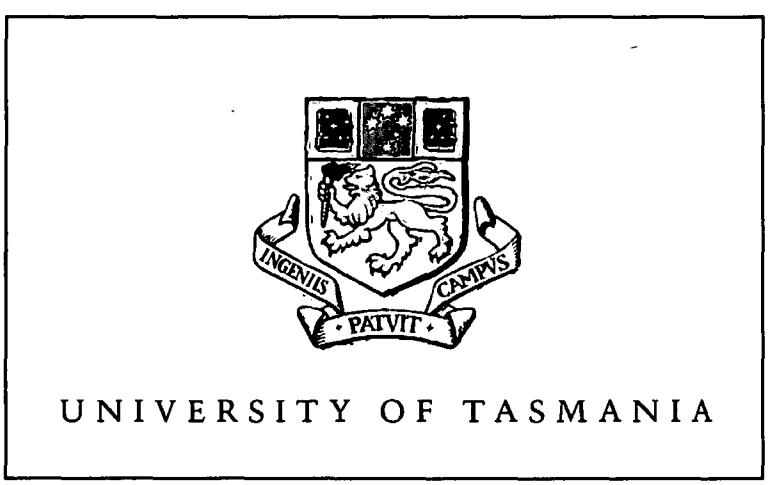


A thesis submitted in fulfilment of the requirements of the degree of Doctor of Philosophy at the University of Tasmania, Hobart, Australia

February 1999

## Statement

This thesis contains the results of research carried out from the School of Earth Sciences, The University of Tasmania, between 1996 and 1998. Part of the material presented in Chapter 3 has been published as:

**Direen N. G.** 1998. The Palaeozoic Koonenberry Fold and Thrust Belt, far western New South Wales: a case study in applied gravity and magnetic modelling. Exploration Geophysics **29**, 330-339.

This thesis contains no material which has been accepted or submitted for the award of any other higher degree or graduate diploma in any tertiary institution, and to the best of my knowledge and belief, contains no material previously published or written by another person, except where due reference is made in the text of the thesis.

This thesis may be made available for loan and limited copying in accordance with the *Copyright Act 1968.*

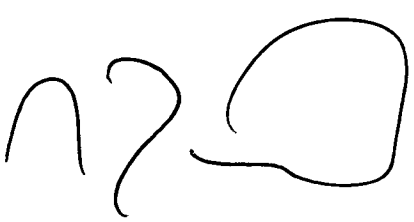

Nicholas Gerard Direen
University of Tasmania
February 1999

## Abstract

Consideration of the latest geophysical datasets and new mapping and stratigraphic data shows the Koonenberry Belt of far western NSW, to be an Early to Mid Palaeozoic fold-and-thrust belt.

This study presents the results of geologically-controlled qualitative interpretation and two-dimensional modelling of gravity and magnetic data which permit a new tectonic interpretation, relying upon the different petrophysical, structural and metamorphic attributes of three distinct tectonostratigraphic packages.

The oldest known sequence in the belt comprises shales, sands, dolomites and strongly magnetic transitional alkaline basalts, which are believed to exist in large volumes at depth, producing a major magnetic anomaly. These rocks are disconformably overlain by a regionally extensive ?Lower to ?Middle Cambrian turbidite sequence. The two packages represent Late Neoproterozoic continental rifting, dated at 587 Ma, and Early Cambrian volcanic passive margin formation. Dense, rifted blocks of Neoproterozoic sedimentary sequences are believed to underlie this remnant margin at depth, on the basis of high gravity signatures.

A second widespread rifting or crustal attenuation event is represented by marine shelf sequences interbedded with minor volumes of calc-alkaline volcanic rocks. This event has been dated around 525 Ma.

A series of highly deformed Cambrian to ?Early Ordovician quartz-rich turbidites and tholeiitic basaltic volcanics with E-MORB characteristics is believed to represent a marginal basin which formed in response to the 525 Ma rifting. These rocks are in faulted contact with older turbidites and broken shelf sequences along major regional faults, in some places marked by melanges. Further volumes of Cambrian to ?Early Ordovician rocks are implied at depth by both geophysical and structural considerations.

These relationships suggest that this package was thrust from the east over and onto a multiply rifted passive margin. The timing for this event is constrained by zircon dating of tuff horizons in the turbidites, and biostratigraphy of overlying syn- to post-collisional sedimentary rocks. These dates suggest that the deformation of the margin was a

diachronous event occurring from the late Middle Cambrian until at least the end of the Late Cambrian, and may have continued into the Early Ordovician.

In the Darling River Lineament-Scopes Range to the south of the main thrust belt, the Late Cambrian deformation is associated with two pulses of localised magmatism. The first is of medium- to high-K calc-alkaline character, and is believed to represent post-collisional volcanism dated between 508 and 486 Ma. A temporally later pulse of tholeiitic dykes is considered to mark an aborted rift phase.

Geological and geophysical considerations indicate that sequences up to and including the Ordovician were further deformed by folding and thrusting between the Middle Ordovician and the Late Silurian, before deposition of Late Silurian- Early Devonian red-beds.

The general style of faulting in the thrust-belt is constrained by analysis and modelling of geophysical data, which shows across-strike repetitions of various sequences, and listric fault geometries.

These features strongly suggest that the belt is both a polydeformed west-vergent fold-thrust belt that detaches in the mid-crust, and a zone of overlap between the Delamerian Orogen of South Australia, and the Lachlan Orogen of eastern Australia.

Comparison of the belt to sequences elsewhere, indicates tectonic equivalence between the early transitional alkaline volcanics, and alkaline volcanics in South Australia, picrite lavas in westernmost Victoria and on King Island, and tholeiitic volcanics in western Tasmania. These correlations support the hypothesis of widespread continental rifting and volcanic passive margin formation between 600 and 585 Ma.

Comparison of turbidite sequences in the belt and South Australia indicates fewer similarities than previously thought; equivalent passive margin sequences to those in western NSW may lie in westernmost Victoria.

Equivalents to the Cambrian shelf sequences exist within the Warburton Basin of northern South Australia, and indicate that the second episode of rifting dated at 525 Ma was widespread.

The late Middle Cambrian-Late Cambrian thrusting event and subsequent post-collisional volcanism in the belt is also believed to be represented in western Victoria and western Tasmania. In these locations, it is represented by allochthonous slices of intra-oceanic arc mafic-ultramafic complexes and overlying 'in situ' post-collisional volcanics. The structural and metamorphic character of these sequences, and their common timing, contrast strongly with the exposed sequences of the Adelaide Fold Belt and other portions of the Ross-Delamerian Orogen in Antarctica, and strongly suggest that the orogen is divided into internal and external zones. Analysis of differences in timing and character of deformation between the two zones suggests that the Delamerian Orogeny was a long lived, mantle-driven process with overprinting effects from short-lived plate-geometries. This model contrasts with earlier suggestions of a rigid arc-continent style collision.

Subsequent development of the Koonenberry and related fold-belts in an in-board position is related to long-lived accretion at the free plate margin to the east. Effects include major fold and thrust deformation in the Ordovician-Silurian, and widespread high crustal-level strike-slip deformation in the Devonian and Carboniferous. A second major mantle-driven thermal event in the Devonian found elsewhere in the Lachlan Orogen is absent within the Belt.

The tectonostratigraphic sequences and deformation style of the belt suggest significant prospectivity for a wide variety of base and precious metals, and diamonds. Correlations with equivalent sequences elsewhere support this conjecture. Petroleum prospectivity is also high, with known mature sources and reservoir facies; however, the structural complexity of the belt suggest all plays will have a high element of risk.

# Table of Contents

# List of Figures

**Chapter 5**

## Chapter 6



## Chapter 7

## Chapter 8



## Chapter 9



## Chapter 10

**Chapter 11**



**Chapter 12**

## List of Tables and Appendices

## List of common abbreviations and symbols used in this thesis

| | |
|---|---|
| ab | albite |
| act | actinolite |
| ap | apatite |
| AFB | Adelaide Fold Belt |
| AGSO | Australian Geological Survey Organisation |
| AMG | Australian Map Grid |
| bio | biotite |
| calx | calcite |
| carb | carbonate |
| chl | chlorite |
| clz | clinozoisite |
| cpx | clinopyroxene |
| Cr# | chrome number = atomic Cr/(atomic Cr + atomic Al) |
| crt | chrome spinel |
| D2000 | "Discovery 2000": a NSW government minerals exploration program |
| DRL | Darling River Lineament |
| epi | epidote |
| EPR | East Pacific Rise |
| FeO* | Total divalent iron |
| FTB | Fold-and-Thrust Belt |
| GPS | Global Positioning System |
| GSNSW | Geological Survey of New South Wales |
| GSV | Geological Survey of Victoria |
| gt | garnet |
| hbl | hornblende |
| hm | haematite |
| HFS | High Field Strength |
| HFSE | High Field Strength Elements (Ti, Y, Zr, Nb, etc.) |
| H.S. | Homestead (farmhouse) |
| il | ilmenite |
| KFB | Koonenberry Fold Belt |
| ksp | potassic feldspar |
| leuc | leucoxene |

| | |
|---|---|
| LFB | Lachlan Fold Belt |
| LILE | Large Ion Lithophile Elements (Rb, Ba, K, Th etc) |
| LOI | Loss On Ignition |
| Ma | Million years |
| MAR | Mid Atlantic Ridge |
| masl | metres above sea level |
| MAV | Mt Arrowsmith Volcanics |
| Mg# | Magnesium number = atomic Mg/(atomic Mg + atomic FeII) |
| MOR | Mid Ocean Ridge |
| MORB | Mid Ocean Ridge Basalt |
| MRV | Mt Read Volcanics |
| MSVC | Mt Stavely Volcanic Complex |
| mt | magnetite |
| mu | muscovite |
| MWV | Mt Wright Volcanics |
| NEFB | New England Fold Belt |
| NSW | New South Wales |
| NSWGS | New South Wales Geological Survey |
| NVL | North Victoria Land |
| ol | olivine |
| opx | orthopyroxene |
| PGE | Platinum Group Element (Pt, Pd, Ru, Os, Ir, etc.) |
| plag | plagioclase |
| pre | prehnite |
| pump | pumpellyite |
| py | pyrite |
| QFL | Quartz-Feldspar-Lithics |
| qz | quartz |
| RGB | red-green-blue image |
| rtp | reduced-to-the-pole |
| ru | rutile |
| SA | South Australia |
| SDRS | Seaward Dipping Reflector Sequences |
| ser | sericite |
| serp | serpentine |

| | |
|---|---|
| SHRIMP | Sensitive High Resolution Ion Micro-Probe |
| sil | silica |
| sp | sphene |
| SZ | subzone |
| TAM | Transantarctic Mountains |
| Tas | Tasmania |
| tm | tourmaline |
| TMI | Total Magnetic Intensity |
| Vic | Victoria |
| VIMP | Victorian Initiative for Minerals & Petroleum |
| zeo | zeolite |
| zrc | zircon |

| | |
|---|---|
| $\lambda$ | wavelength |
| $\lambda/2$ | half-wavelength |

## Acknowledgments

In a large-scale collaborative project such as this, there are many people and organisations to thank.

Primarily, I would like to acknowledge the help and advice of all my supervisors: Assoc. Prof. **Tony Crawford** (CODES) who imagined the whole project and got it off the ground; **Barney Stevens** (MRNSW), who flew with me as co-pilot and navigator during my sorties from Broken Hill; Dr. **Michael Roach** (CODES), who acted as a technical adviser with computers and equipment, and as my draughtsman; and my AGSO supervisors, Drs **Peter Gunn** (AGSO), and **Dick Haren** (now Managing director YAK 50 Gold Mining N.L), who provided resources and feedback from my chief sponsor organisation.

I would also like to thank Drs **George Gibson** (AGSO), and **Kingsley Mills** (MRNSW), who while not acting as supervisors, each provided timely advice, help and stimulating discussions worthy of one.

The project would not have been possible without the financial and logistical support of the chief sponsors, the **Australian Geological Survey Organisation**, and **Mineral Resources New South Wales**. I would especially like to thank **John Cramsie, Peter Lewis** and **Mick May**, from MRNSW for setting up the finances for work in NSW.

Students need an environment in which to study. This was more than adequately provided by my host institution, the **Centre for Ore Deposit Research, School of Earth Sciences** at the University of Tasmania. This place has been my alma mater for seven years now: a major part of my life. I would like to thank especially the long-suffering and ever-patient technical support staff, **Vagn Jensen** (electronics), **Phillip Robinson** (Analyst), **Darren Turner** and **Michael Harlow** (Computer Support), **Christine Higgins** (CODES manager), **June Pongratz** (publishing wiz), **Peter Cornish** (Lab manager), **Simon Stephens, Daniel Nicolle**, and **Maya Kamenetsky** (Lapidarists), **Kathi Stait** (Curator) and **Jeanette Harris** (ex-Geology Secretary). I am indebted to all of you, and without your hard work on my behalf, this project would have crash-landed long ago.

For stimulating ideas and discussion, I am also grateful to academic staff colleagues in Program 1: Drs. **Rob Scott, Sebastien Meffre, Carsten Munker** (University of Gottingen)

and **Dima Kamenetsky**, for technical and theoretical advice, assistance, and most of all for teaching me new things.

Others within the School who offered particular expertise, timely advice and reviews of my work are Drs **Clive Burrett** (School of Earth Sciences), **Ron Berry, Bruce Gemmell** and **Garry Davidson** (CODES).

As an aboriginal student, I have also enjoyed my association with **Riawunna**, the Centre for Aboriginal Studies at the University. I am indebted to Palawa elder **June Brown** for giving permission to use her artwork in the text.

While in the field on the mainland, I was assisted by many organisations, particularly the State Geological Surveys.:
**Mineral Resources NSW Broken Hill Office** provided a great deal of material assistance and technical support, as well as a friendly working environment over the last three years. Thanks especially to **Michael Hicks,** and **Kevin Capnerhurst** and **Gary Burton** (both now of Orange office) and secretaries **Gwen Carruthers** and **Caroline Molloy** (now moved on) for accepting an invader like me in your office.

Mineral Resources NSW Sydney Branch geophysics staff provided geophysical equipment along with technical advice on how to use it. **Dave Robson, Jamie McIntyre, Peter Ruskowski, Allan Willmore, Rob Hewson, Troy Macklin** and **Neil Watson** are thanked for this assistance. I would also like to thank **Dick Glen** of Regional Geology for challenging structural discussions and friendly ribbing when we were in New Zealand.

The **Geological Survey of Victoria** have provided a great collaborative team to work with. Perhaps more than anyone, they have driven my understanding forward with new mapping, and bold, adventurous interpretations. Their openness to sharing ideas is refreshing, and I stand in their collective debt. **Peter O'Shea** (Manager Geological Mapping), **Alan Willocks** (Manager Geophysics), and my friends **Simon Maher, David Moore, Ross Cayley & David Taylor** are thanked for their assistance, imagination and companionship.

Geophysics staff at AGSO are thanked for providing equipment and information relating to the gravity surveys undertaken in 1996; in particular **Alice Murray** and **Harry Reith** deserve mention. **Jane Mitchell** provided aeromagnetic data for Bass Strait.

While working on South Australian aspects of this project I enjoyed friendly assistance and advice from the Department of Primary Industries and Resources SA (**PIRSA**). **Wolf Preiss, Peta Abbott, Andrew Burtt, Colin Conor & Colin Gatehouse** of the regional geology section provided information and stimulating discussions; **Andrew Shearer & Domenic Calandro** of the geophysics section provided equipment and data; **David Gravestock** of the petroleum section provided much information on both the Murray and Warburton Basins; and **Brian Logan** and his staff at the Glenside Core Library let me get my grubby mitts on their core.

Dr. Peter (**Pierre**) **Kruse** of the Northern Territory Geological Survey is also thanked for his interest and information on the Cambrian Mt Wright and Antarctic faunas.

Various companies are thanked for providing finances and logistical support for the student field trip to Mt Wright in 1996, including **BHP Minerals Exploration** and **Aberfoyle Resources. Mark Dugmore (BHP), Steve Newbery (Pasminco)** and **Bob Richardson (Platsearch N. L.)** are thanked for giving me access to core and cuttings held by them for licences in the Koonenberry area. **Wolf Leyh** (Eaglehawk Consulting Pty Ltd.) also deserves thanks for his interest and enthusiasm, as well as donating of his time to help me stack and sort core at Broken Hill.

Various universities have also provided information, theses, maps, and advice. Dr. **John Foden** (University of Adelaide) and Assoc. Prof **Jim Jago** (University of South Australia), both graduates of this department, are also thanked for their help along the way.

Assistance and accommodation in the field was provided by various property owners and managers in the Koonenberry region: **Chris & Rachel Major** "Wonnaminta"; **Mark Andrews** "Wilandra"; **Bill & Biddy Gall** "Nuntherungie"; **Trevor & Shirley Medford** ex-"Nundora"; **George Siemer** "Koonawarra"; **Annie O'Connor** "Mt Arrowsmith"; and my friends **Bill, Helen & Jamie Anderson** of "Cymbric Vale".

Field work in 1996 at Mt Wright was undertaken by a willing band of slaves, known as the KEA 324 Exploration Geophysics class (**Duncan Latham, Greg Kunda & Ian Bellamy**). Their good humour and work ethic was admirable.

Access to the Mootwingee National Park was granted by the **NSW National Parks and Wildlife Service.** Traditional Owner-Senior Ranger **Matt Le Duc** and Senior Ranger **Rob McKinnon** are thanked for their speedy assistance in cutting through the red tape required to operate in a wilderness area studded with sacred and historic sites.

Finally, to those who have made the task mentally possible, I also give thanks. To my co-inhabitants of Room 202B, especially **Mark Duffett** for geophysical and GIS advice; to my fellow Ph.D students at CODES –for their good humour, and willingness to discuss ideas. In particular, **Peter Winefield, David (Rowdy) Rawlings, Steven Hunns** and **Ali Raos** deserve special mention.

My brothers and sisters in Disciples of Jesus Catholic Covenant Community in Hobart, Melbourne, Canberra and Adelaide branches, for welcoming us into their midst while we journeyed. Deserving of special mention are the **Moore, Horner, Hay, Kirk, Mullins, Nye, Wilson, Brennan** and **Jones** families, all of whom sheltered us for various amounts of time. Also to my extended family, particularly the **Garlepps**, who also put us up on various occasions.

To my companion **Nick MacFarlane**, and my "Barnabas", **Derek Tys**, for timely wisdom; and my very good friend **Shelley Greener**: for being there at the end, and providing understanding and encouragement.

And finally to my own family: to **Julian**, who helped with drafting diagrams; and to **Eilidh** (Bear), **Xavier** (Mr Snuffy); and my beloved, **Louise**: for believing in me, journeying with me, being my help-mate and comforter, and never looking back.

## Foreword and dedication: Geology, mapping and myth-making

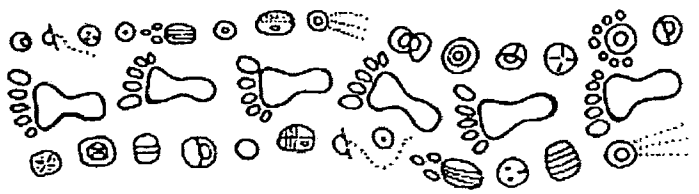

Artwork by June Brown, a Palawa elder: "Footprints", symbolising the relationship between the Palawa and the land. The symbols are also found in ancient Tasmanian petroglyphs or "rock writing".

The study which follows documents the nature and relationships of some ancient rocks in the interior of the Australian continent. It is a scientific study; it has involved travelling into the interior, making both descriptive and quantitative observations at various locations, and making records of "what" and "where", in terms of both space and time. This is the fundamental task of the mapping geologist: to accurately record facts about the rocks she has seen.

But this is not her only task, for in order to make a map, she must also relate the rocks of one place to another, taking into account their temporal and spatial relationships. At the very least, this is done by interpolation, filling the blanks on the map; but the science of geology does not end there, for the geologist seeks to answer a different, more important question than just "what" and "where"; that question is "why?". It is a question that is usually asked at different scales: from the atomic makeup of a single crystal, through to the dynamic behaviour of the largest portion of our planet, the mantle.

In my case, the process of filling in the blanks on the map was guided by the application of technology responding to the properties of rocks buried in the sub-surface, rocks that I could not see. These technologies allowed me to relate the rocks of far western New South Wales to others on the continental mainland, offshore islands, and finally across continents, to Antarctica. The relationships invoked precipitated more journeys and more observations, both my own, and those of my fellow geologists.

I then sought to explain why the rocks of the continental interior are like those in far away places. I sought more evidence, at different scales: unlocking the secrets hidden in individual crystals of spinel; relating the shapes of beds in sandstone; describing the chemistry of bodies of igneous rock in the crust; and imaging structures deep in the mantle.

And then I told a story; I created a **myth** around the observations I had made on my journeys, and I wove into it the stories of others who had gone before me. I tried to explain things that I have seen, things that I cannot see, and things that have happened long before I was born, before people walked the land.

What you are about to read is a myth about an ancient continent, the birth of an ocean and the raising of mountains from the sea; it is a story about great volcanoes and cataclysms in the earth; it is a tale of the genesis and obliteration of plants and animals. It is an epic myth, a myth of the large and the small over millennia. I choose to call my story a **myth** because it contains elements of fact, symbols, stories, and possibly, elements of fancy. Some if it may be proved wrong in the future, and some of it may be based on fundamental misunderstandings about the way our planet works. I hope that its eventual scientific obsolescence does not take away from its value as a story of exploration and explanation.

And if this is so, then I believe we must hold in equal regard the efforts of those who have gone before us, both those who have used our own methodology, and those who have not. For as I have gone about my journeys, and my story telling, I have realised that I am walking in the footprints of others. And as I look at the lands I have come to know, and have tried to explain them with my symbols and language, I see that these stories have been told before in other terms.

The aboriginal nations who owned these lands before western science came to be, were great geologists. They made journeys and observations, filling up songs and stories with the "what" and "where". They made maps, painted or etched in stone, symbolising the different features of the landscape and their relationships to each other, and their resources. And then they made myths: creating songs, stories and images around the observations they had made on their journeys, in order to try and explain things that they had seen, things that they could not see, and things that happened long before people walked the land. These stories were those of ancient lands, the source of the waters, and the raising of mountains; about great cataclysms in the earth; and of the genesis and obliteration of plants and animals. They too were epic myths of the large and small over millennia.

I believe though our methods, language and symbols were different, we have worked at the same tasks: exploration and explanation, a part of the human genius.

I dedicate this work to the descendants of those first explorers and storytellers: the Barkintji, Bandjigali, Wandjiwalgu, Kaurna, Wergaia peoples, and my own Palawa people, on whose lands I have explored. It is my hope that these ancient myths, of such beauty and value in understanding the landscape, and the cultures that cradled them, would be kept and alive and valued for what they really are.

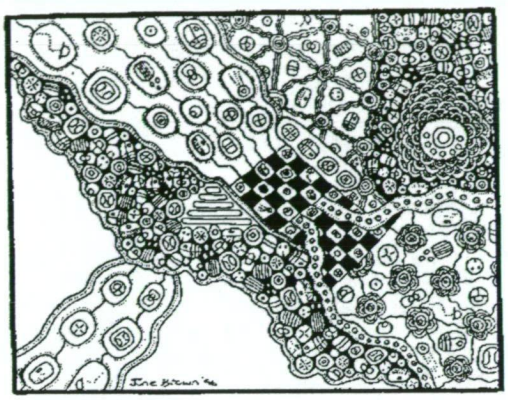

Artwork by June Brown, a Palawa elder: relationship of different parts of the land.

**Chapter 1: Introduction**

*1.1 Scope and Intent of Study*

*1.2 Study Areas*

*1.3 Comparative Study outline*

# Chapter 1 Introduction

## 1.1 Scope and Intent of Study

This thesis is principally intended to document a tectonic study of the Late Neoproterozoic and Palaeozoic rocks of far northwestern New South Wales, in eastern Australia.

The study was focussed on the structure of a poorly known and poorly mapped area known as the Koonenberry Belt-Bancannia Trough, and was to be guided by the acquisition of new, extensive public domain geophysical data over the area. What became clear as the study progressed, was that the Koonenberry Belt-Bancannia Trough contains geophysical structures of large magnitude, in the order of tens to hundreds of kilometres wavelength. When these features are viewed at a continental scale, which is their proper context, the Koonenberry Belt can be seen to be part of a much larger structural system (Figures 1.1.1 to 1.1.3).

This system extends from north of the Queensland border and through the initial study area following a general north-northwest trend. At the southern margin of the study area, it undergoes a 90 degree change in strike, following the course of the Darling River drainage complex in a southwesterly direction over the South Australian border. In the vicinity of Renmark, it undergoes a second right angle trend shift, to follow the Padthaway Ridge (Brown et al., 1988) southeast through the Wimmera region to terminate near Portland (Vic) on the Bass Strait coastline. For approximately 95% of its area, this system is obscured by the generally unconsolidated sediments of the Mesozoic Murray Basin and its Permian infrabasins.

This near-orthogonal system of continental-scale geophysical lineaments was first commented upon by Gunn (1996). Both Powell (1996) and Gunn (1996, 1997) thought that this feature represents the preserved eastern rifted-margin of the Proterozoic Rodinia Supercontinent. Gunn (1996) traced this margin into western Tasmania.

Any study of the Koonenberry-Bancannia region must therefore be placed in this context: that it forms one part of a continental-scale feature, and that processes that have operated on this region will include continental tectonic processes as well as local effects. The apparently coherent nature of the margin, at least from a geophysical perspective,

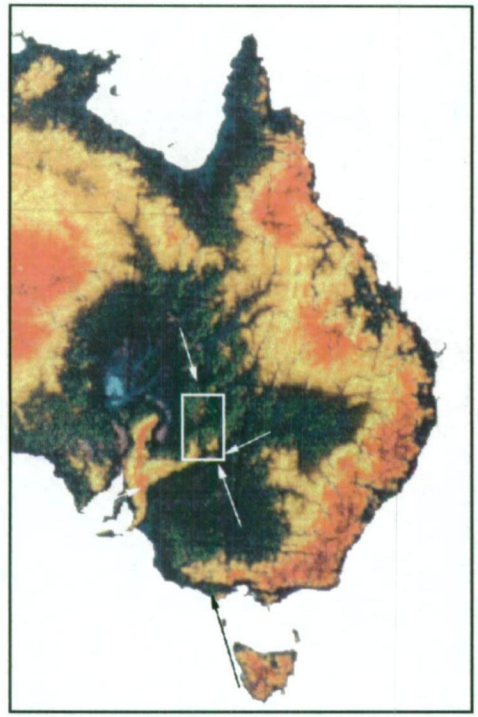

**Figure 1.1.1**
**Eastern Australia Digital Elevation Model**
Data from Auslig.
In all figures, arrows show approximate position of continental lineaments.
Box shows study area.

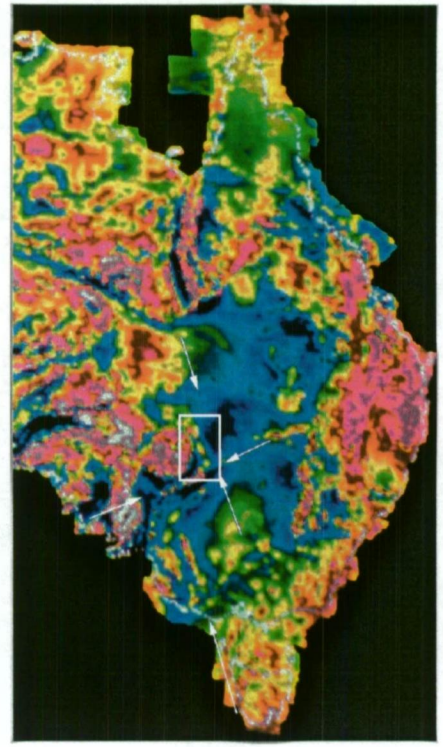

**Figure 1.1.2**

**Eastern Australia Total Magnetic Intensity**

modified from Tarlowski et al.,1996

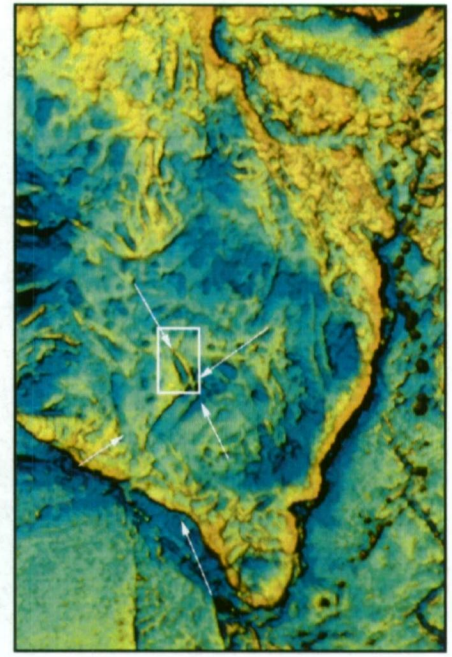

**Figure 1.1.3**

**Eastern Australia Bouguer Gravity**

modified from Morse et al., 1992

provides a unique opportunity to compare and contrast the structure and tectonic evolution of the Koonenberry-Bancannia area with other parts of this ancient margin. This will, in theory, allow the discrimination of the resulting effects of tectonic processes operating at different scales.

### 1.2 Study Areas and Methods

It is this method which has been adopted in the course of my study. Part 1 of this thesis deals with the Koonenberry Belt in some detail, outlining its stratigraphy and structure in four sub-regions: Nundora-Wonnaminta-Nuntherungie-Marrapina; Mt Wright-Cymbric Vale; Grasmere-Southern Koonenberry and the Darling River Lineament (Figure 1.2.1). These localities lie to the east and northeast of the city of Broken Hill. In these areas, the structure, sedimentology and geochemistry of some of the more extensive sedimentary and igneous units have been investigated in detail.

Because of poor outcrop conditions, and Mesozoic cover, potential field methods have been used to continue the study of structures beyond what can be usefully achieved by surface mapping. These methods, their acquisition, processing and results from modelling are outlined. The interpretation of these data has been constrained by acquisition of local petrophysical data.

Observations from geological and geophysical components of the study have been combined to produce an interpretive tectonic model for the Koonenberry-Bancannia region. This completes Part 1 of the study.

### 1.3 Comparative Study

Part 2 of the thesis presents the results of studying four other zones along the proposed Palaeozoic Gondwana margin in eastern Australia. These have been chosen for information on igneous and sedimentary units, usually from stratigraphic drilling provided by state Geological Surveys, or available in open file exploration licence reports. The characteristics of rock packages at these sites are then compared and contrasted with units of equivalent age in the Koonenberry-Bancannia region.

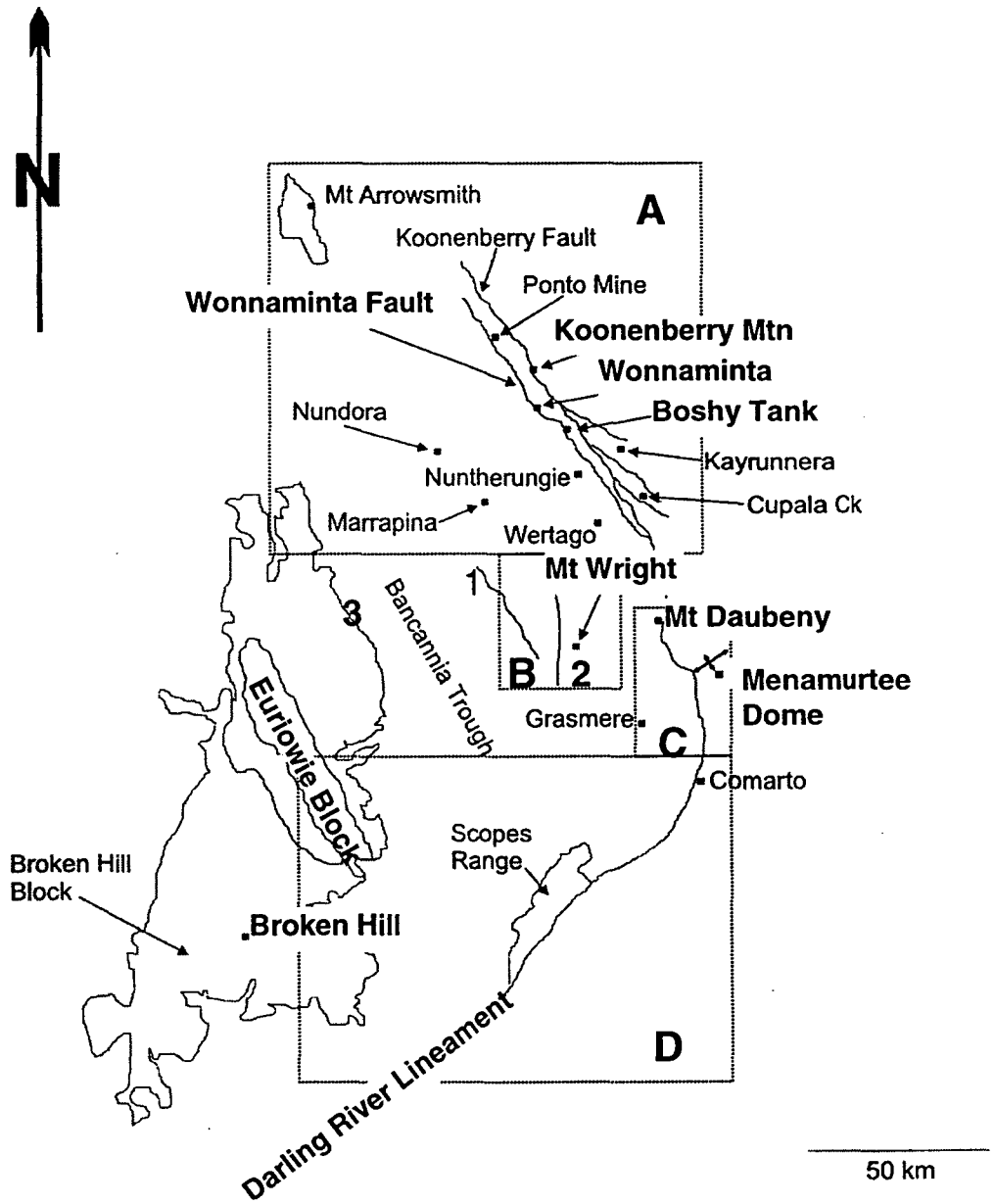


**Figure 1.2.1 Koonenberry Belt and Environs**
(modified after Mills, 1992)

Key: Boxes show study areas.
A = Nundora-Wonnaminta-Marrapina-Nuntherungie
B = Mt Wright-Cymbric Vale
C = Grasmere
D = Scopes Range-Darling River Lineament

1 = Lawrence Fault; 2 = Mt Wright Fault; 3 = Western Boundary Fault

These areas are (from north to south): Truro (eastern SA); Carrickalinga Head (central SA); Horsham-Dimboola (western Vic); King Island (Bass Strait, Tas) and the Smithton Trough (northwestern Tas) (Figure 1.3.1).

Information from the various regions has been analysed to determine the style, timing and extent of tectonic processes operating in common across the entire margin, and to separate these from more localised effects. This analysis is then used to build up a model for the Late Neoproterozoic and Early Palaeozoic evolution of the margin in southeastern Australia; the implications of this model for the distribution of resources are then briefly examined.

This study, therefore, is a work of synthesis, presenting new information about a little known area, and reviewing recent work in other similar areas. It includes results from stratigraphy, geochronology, geochemistry, economic geology, geophysics, structural geology and tectonics. The diverse nature of these topics, and the wide geographical area under consideration, demands an integrative approach, focussing on the links between datasets, rather than an in-depth treatment of any particular subject. It is hoped that this approach provides a better overall appreciation of orogenic tectonics in eastern Australia than a more rigorous treatment demanded by the purists of any one of these important sub-disciplines.

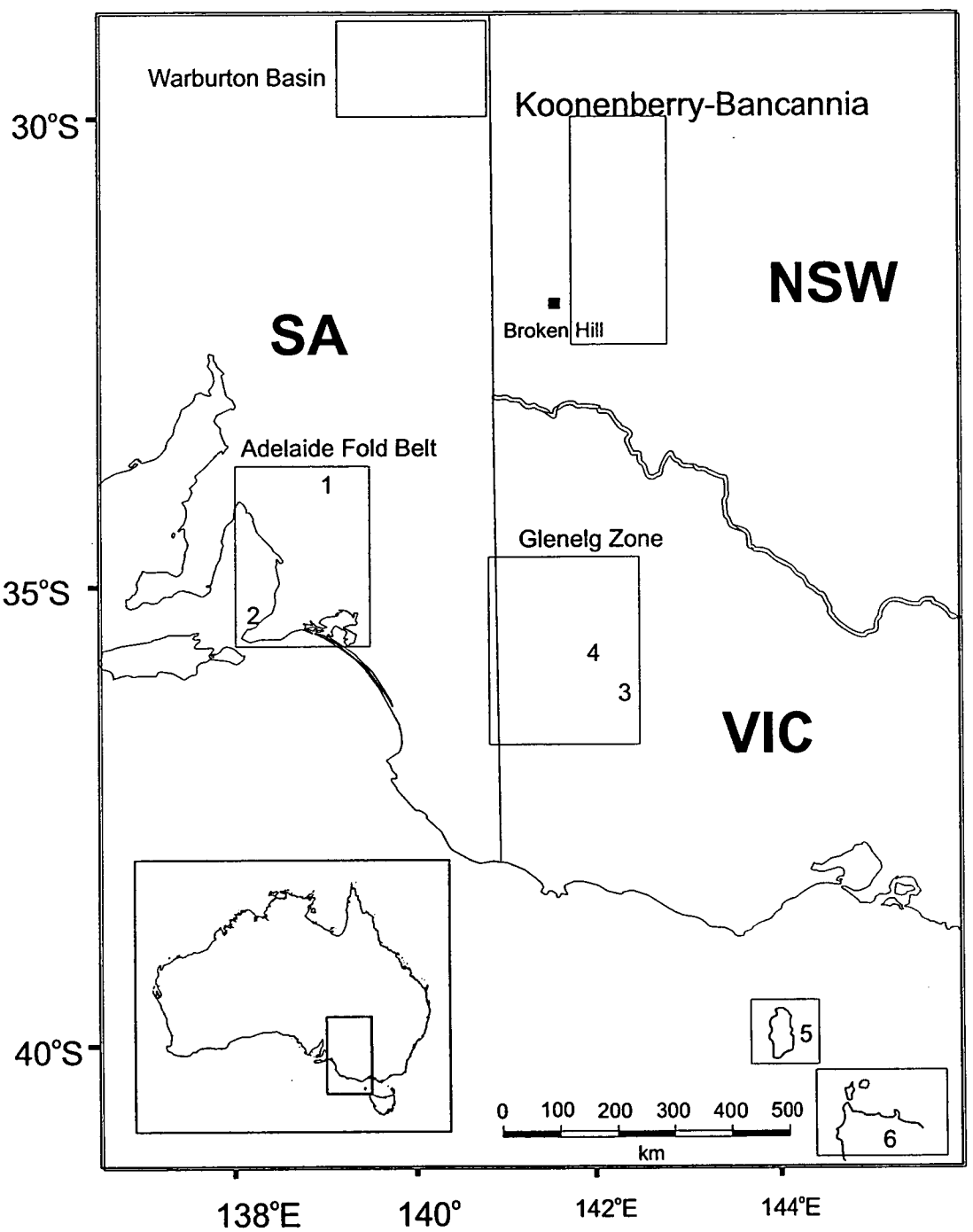


**Figure 1.3.1: Locality Map, southeastern Australia**

Key: 1=Truro; 2 =Carrickalinga Head; 3 = Horsham; 4 = Dimboola; 5 = King Island
6 = Smithton "Trough"

**Chapter 2: Overview**

# PART 1 KOONENBERRY FOLD BELT, NEW SOUTH WALES

## Chapter 2: Geology of the Koonenberry-Bancannia Region

### 2.1 Preamble

This chapter reviews the progress of regional geological mapping of the Koonenberry Belt. Mapping programs to the present have been of reconnaissance nature only, beginning in 1934 (Kenny, 1934) in the search for groundwater, and has proceeded in bursts since, e.g. 1967-1971 (maps at 1:250 000), 1979-1985 (various academic studies), 1989-1992 (regional mapping by the University of Sydney and University of NSW).

The year 1992 saw the publishing of a key summary paper by Mills, which for the first time, attempted to divide the Early Palaeozoic rocks of the region. Until that time, these sequences were grouped together as the "Wonominta beds" (cf. Scheibner, 1978). This brought about a profound change in the way the belt has been studied from that time.

As a result of this paradigm shift, much of the work prior to 1992 has been rendered less useful, strongly dividing the literature into "pre-" and "post-Mills", as will be seen in the following sections. This change in thinking has also necessitated remapping by the Geological Survey of NSW at 1:100 000 scale, which is still in progress. Further important contributions were made by Stevens et al. (1996) and Crawford et al. (1997), who challenged several of the correlations that had become axiomatic to work within the region.

Because of these factors, and relatively few papers published on the region since 1992, much reinterpretation of earlier studies has been required to understand their observations in the new scheme. This reinterpretation may account for apparent discrepancies between what can be found in the extant literature, and many of the interpretations I have chosen to incorporate into this study.

A further important development in the understanding of the region has been the acquisition of high-quality, closely-spaced regional aeromagnetic, radiometric and gravity data. In some cases, this permits resolution of units down to bed- or groups of

beds-scale (1-10m). This data has revolutionised the way mapping is carried out in this region, and forms the fundamental data source for this study.

## 2.2 A Note on Nomenclature

Following the example of Zhou (1993), it is necessary to define the sources of nomenclature for this study.

The Koonenberry region has a notoriously inconsistent scheme for nomenclature. This occurs because many of the geographic names are derived from the dialect of the local Barkintji aboriginal tribe. Because the tribal dialect is oral rather than written, it becomes possible to use different spellings for phonetic pronunciations. This nomenclatural ambiguity is compounded by historical precedents, which although incorrect, tend to remain entrenched in local lore. This has been further exacerbated by incorrect usage in geological literature. Several examples will serve to illustrate the nature of this problem.

The name "Koonenberry" has only recently been applied to the belt of rocks by the NSW Geological Survey in the 1995 release of new geophysical data. It is derived from Koonenberry Mountain, a striking topographic feature in the east of the belt. Nearby to the north lies East Kooningberry Tank.

Prior to this time the region was known as the "Wonominta belt". This name was derived from the historic pastoral property Wonnaminta. Zhou (1993) lists four spellings of this name in the geological literature, including "Wonaminta", "Wanaminta", "Wonnaminta" and "Wonominta". He concluded that, although geographically incorrect, historical precedent lay with "Wonominta" for geological purposes, while "Wonnaminta" should be used for the geographic locality around the homestead.

The Mt. Daubeny Formation (Neef et al., 1989) is named for the geographical feature Mt. Daubeny. Prior to the formal naming of this formation, it was known as the "Mt Daubney beds" (Edwards & Neef, 1979). These units incorporated an earlier informal stratigraphic unit known as the "Cootawundy beds" (Pogson & Scheibner, 1971), named for Cootawundy Creek which drains the Coturaundee Range on the property of Cootawundi. Warris (1969 *in* Packham) referred to this area as the "Cootawindy hills".

In naming new units, I have circumvented this sort of nomenclatural quagmire by using names found on the 1:100 000 topographic maps, and avoiding names where two or

more spellings exist. I have also made use of quotes "..." in describing pre-existing units that have been renamed or superseded, or that have spellings at variance with the currently accepted geographic names.

### 2.3 Regional Geology: outline of previous work

The first modern regional studies of the area were undertaken by geologists of the NSW Geological Survey in the preparation of 1: 250 000 and 1: 500 000 scale maps of the area (White Cliffs, Rose, 1966; Cobham Lake, Brunker, 1967; Broken Hill, Rose, 1968; Koonenberry, Brunker et al., 1971). These projects were assisted by the academic studies of Warris (1967) and Ward et al. (1969).

Mapping identified three main packages of rocks within the region: the low grade metasediments of the "Wonominta beds"; fossiliferous Cambrian and Ordovician sediments and volcanics; and Devonian red beds. These were overlain by the flat-lying and generally undisturbed sediments of the Murray Basin (Jurassic to Holocene).

The "Wonominta beds" (Rose, 1968) were described as a series of polydeformed metasediments, and correlated with either the Early Proterozoic Willyama Complex or the Late Proterozoic Adelaidean series.

The Copper Mine Range Beds are a sedimentary package of turbiditic aspect, occurring to the east of the Coturaundee Range (Pogson & Scheibner, 1971) were considered to be younger than the Willyama Complex, but pre-Late Cambrian, based on unconformable relationships with the "Wonominta beds", and Kandie Tank Limestone (see below).

The Gnalta Group, Acacia Downs beds, Wyarra shale, Wydjah Formation and Pincally Formation (Warris, 1967) are Cambrian fossiliferous limestone-bearing packages. The Gnalta Group, occurring in the Mt Wright area, contains "tuffs" and minor shale, was also shown to contain basaltic volcanics, interpreted as "spilites" and "keratophyres". The Wyarra shale, Wydjah Formation and Pincally Formation are equivalents of the Gnalta Group in the Mt Arrowsmith inlier further north, and contain essentially similar lithologies. The Acacia Downs beds, occurring on the property of that name, were a thin (c.100 m) series of quartzites and shales.

The Kandie Tank Limestone (Pogson & Scheibner, 1971) was defined to the east of the Koonenberry Fault, and assigned a late Cambrian age, based on fossils. A further,

trilobite-bearing limestone was recorded near the Koonenberry Fault at Kayrunnera airstrip, but left unnamed.

All of these Cambrian units occurred as small inliers and were suggested to be in-folded (Rose & Brunker, 1969), with demonstrated unconformity over the Adelaidean (Ward et al., 1969).

The Ordovician of the region was partially represented by the siliciclastic Mootwingee Group (Warris, 1967). The distribution of these rocks was found to be limited to the areas around the Bynguano Range. An equivalent section was defined by Warris (1967) for the Mt Arrowsmith inlier, comprising the Yandaminta Quartzite, Tabita and Pingbilly Formations. A slight angular unconformity was demonstrated by Warris (1967) between the Gnalta Group and the Mootwingee Group in the Bynguano Ranges.

Most of the less-deformed rocks of the region were initially referred to the Devonian, although containing few or no fossils. These included the Coco Range beds, Nundooka sandstone (Ward et al., 1969), Snake Cave sandstone and Ravendale Formation (Warris, 1967) which lay with marked unconformity over the Cambrian at the margin of the Bancannia Trough (Ward et al., 1969).

Petroleum drilling in the Bancannia Trough during the late 1960's intersected Mesozoic and Devonian packages, with one well bottoming in ?Cambrian andesites (Bancannia South No.1, Planet Oil P.L., 1969 *in* NSWGS, 1993).

Mineral prospecting in the Cymbric Vale area identified an ultrabasic unit termed the "Mt Wright Ultrabasic" (Johnson, 1972). This was thought to intrude the schists of the "Wonominta beds", but was not assigned a definite age.

In general, these lithotectonic sequences were correlated with time-equivalent units in the Flinders Ranges, South Australia, and were given interpretations accordingly. These emphasised the fixed nature of the Broken Hill cratonic block which was surrounded by a depositional basin ("geosyncline"). This basin was interpreted to have undergone occasional tectonic disturbance, producing folding and faulting (cf. Ward et al., 1969) in essentially a fixist, thick-skinned interpretation, involving only the upper crust.

A second phase of mapping was conducted in the late 1970's and early 1980's, resulting in the description of several new units.

Some alkaline volcanics at Mt Arrowsmith were described in detail by Edwards (1980) and were correlated with the volcanics of the Gnalta Group (e.g. Scheibner, 1978).

The fossiliferous, clastic Cupala Creek Formation, a Cambrian unit defined by Powell et al. (1981) was demonstrated to unconformably overlie the Copper Mine Range Beds.

The "Mt Daubney beds" and some andesites on "Wertago" were described by Edwards & Neef (1979), and assigned to the ?Late Silurian on the basis of some plant fossils. These superseded a description by Pogson & Scheibner (1971) of the "Cootawundy beds," which were assumed to be Devonian.

Three B.Sc (Hons) theses were compiled during this time. Davidson (1981) studied the geology of the Mt Wright-Cymbric Vale area. He defined several new units, including a serpentinite body on the Mt Wright Fault, and the ?Early Cambrian Wilandra beds inlier. Collins (1984) studied the sedimentology of the Copper Mine Range Beds, showing them to have an Early Cambrian age, on fossil content. Davies (1985) studied the "Wonominta beds" near the Ponto Mine area, describing 6 facies, including metavolcanics, and five deformation events.

Regional interpretations during this period began to make use of plate tectonic models, beginning with Scheibner (1972). In general, the "Wonominta beds" were still correlated with the Willyama Complex, and interpreted as representing the cratonic Precambrian crust. This craton was thought to have rifted to form a Bancannia marginal sea, which occupied a graben floored by volcanics. Outboard of this feature and to the east, lay a volcanic island arc and outer shelf environment, represented by the Cambro-Ordovician rocks. These were interpreted as having been deposited on a rifted basement fragment of the "Wonominta beds". Further to the east was the Palaeo-pacific ocean. This ocean was supposedly closed by the Late Silurian, with the onset of continental deposition marked by the Silurian and Devonian red beds. These events were considered to define a Wilson Cycle for the "Kanmantoo Fold Belt", which included correlated units of the Flinders Ranges.

Despite progress in the tectonic interpretation of the region, models remained essentially fixist and thick-skinned: that is, rocks were interpreted to have been deposited and deformed *in situ*, with vertical faults breaking up the sequence.

Third phase mapping was undertaken during the late 1980's and early 1990's. Again, several new units were discovered, with a key paper by Mills (1992) finally breaking up the "Wonominta beds" into three discrete units. This paper also caused the stratigraphy to be viewed in terms of four, rather than three, time packages: Proterozoic, pre-Delamerian, post-Delamerian-pre-Tabberabberan, and post-Tabberabberan.

The Ponto beds (Mills, 1992) were considered to be the oldest rocks of the region, consisting of polydeformed schists and tholeiitic volcanics. The Ponto beds were correlated with the upper part of the Willyama complex on the basis of at least four deformation fabrics, and on a dubious Sm-Nd age of 1.44 ± 0.24 Ga (Zhou & Mills, 1994). Amphibolite facies rocks of the Ponto beds were identified by Zhou (1993) to the east of the Mt Wright Fault, near Cymbric Vale homestead (H.S.).

The Kara beds were considered by Mills (1992) to be of Adelaidean to Early Cambrian age, with a possible correlation to the Torrowangee Group postulated on the basis of a now-discredited "tillite" near Nundora. The Kara beds were also tentatively correlated with the shale and limestone-rich Normanville Group of South Australia. Correlates of the alkaline volcanics described by Edwards were described interbedded within the Kara beds at Nundora and Packsaddle (Mills, 1992; Zhou, 1993).

The turbiditic Teltawongee beds, incorporating the Copper Mine Range Beds, were described by Mills (1992) as conformably overlying the Kara beds. The Teltawongee beds were assigned to the Early Cambrian on the basis of sponge fossils, and a possible correlation with the Kanmantoo Group postulated.

The Kayrunnera Group, overlying the Teltawongee beds with marked angular unconformity, was described by Webby et al. (1988), and given a late Cambrian age on the basis of its contained trilobite fauna. The boundary between these two units was interpreted as the signature of the Delamerian Orogeny (Mills, 1992).

The Mt. Daubeny Formation was also formally defined at this time, superseding the "Mt. Daubney beds" (after Neef et al., 1989; Neef & Bottrill, 1991). These rocks were re-assigned to the Early Devonian, rather than the previous Late Silurian age.

More recently, Stevens et al. (1996) overturned the correlation of the Ponto beds with the Willyama complex, based on a set of Late Cambrian and Early Ordovician radiometric zircon dates, and Crawford et al. (1997) divided the volcanic rocks at Mt Wright into two distinct packages with separate ages. These have Late Neoproterozoic and Early Cambrian ages, with the older package possibly correlated with the Truro Volcanics of South Australia.

The first paper to postulate allochthoneity of some or all of the units in the region was that of Leitch et al. (1987), which defined four tectonostratigraphic terranes with different tectonic histories. These terranes were defined using differences within the Cambrian rocks deposited on Proterozoic basement ("Wonominta beds") blocks, and were believed to have amalgamated during the Delamerian Orogeny. The "composite terrane" was then overlapped by Cambro-Ordovician post-orogenic flysch sequences. Relative movement between the terranes was thought to have been accomplished by large-scale strike-slip movements on the Koonenberry and Mt Wright Faults.

Mills (1992) expressly discounted major strike-slip movements along these faults, and by inference, rejected the allochthoneity of blocks. In doing so, he returned to the fixist position of a deformed, autochthonous continental shelf (Cambrian and Cambro-Ordovician deposits) developed over a rifted margin (Proterozoic deposits). The development of this shelf margin was punctuated by deformation attributed to the Delamerian Orogeny. Further deformation in the Middle Devonian triggered continental sedimentation. Mills (1992) again showed vertical faulting dominating the structure.

Crawford et al. (1997) interpreted two phases of rifting: a major, ocean basin-producing event in the Late Neoproterozoic, and a second, Early Cambrian event related to the development of the Kanmantoo Trough. The basins formed during these events were both deformed by the Delamerian Orogeny in the Middle to Late Cambrian.

The idea of allochthoneity of blocks, via thrusting, was revived by Crawford et al. (1997). This was required to explain contacts between more deformed, Late Cambrian-?Early Ordovician Ponto beds and less deformed ?Late Neoproterozoic Kara beds.

## 2.4 Summary

At present four main tectonostratigraphic packages are recognised in the Koonenberry-Bancannia region (Figure 2.4.1). The pre-Ordovician package (Direen, 1998) is a composite of Late Proterozoic to Late Cambrian sequences. It comprises the Mt Arrowsmith Volcanics, Kara beds, Teltawongee beds, Ponto beds, Wilandra beds, Acacia Downs beds and Macs Tank Ultramafic complex. All of these rocks were once thought to be Precambrian, and were termed the "Wonominta beds".

The Gnalta Group (Warris, 1967) is an Early to Middle Cambrian sequence of volcanic and sedimentary rocks, time-equivalent to the upper part of the "Wonominta Complex" (Mills, 1992). It is unique in containing diverse and numerous fossil faunas.

Both of these packages were believed to have been deformed by the Delamerian Orogeny (Mills, 1992).

Early and Middle Cambrian rocks are overlain with angular unconformity by "shelf" sequences of fossiliferous limestones and siliciclastics (Mootwingee Group and correlates, Kandie Tank Limestone, Kayrunnera Group), and also by the Early Devonian Mt Daubeny Formation.

This Late Cambrian to Early Devonian succession was deformed by the Tabberabberan Orogeny (Mills, 1992), and overlain, again with angular unconformity, by Late Devonian-Carboniferous red beds.

Tectonic interpretations of the area have evolved from an essentially autochthonous model of craton-mobile belts, to postulation of allochthonous elements. These later developments have been forced by new dating of several units within the pre-Ordovician package.

## 2.5 Review of Geophysics 1965-1994

The first geophysical methods to be used in the region were used in the search for petroleum during the mid-1960's. A combination of seismic reflection, seismic refraction, gravity and aeromagnetics were used to define potential structural traps. Use of these methods proved successful in delineation of regional structure, but inadequate for prediction of petroleum traps, as evidenced by a series of dry holes.

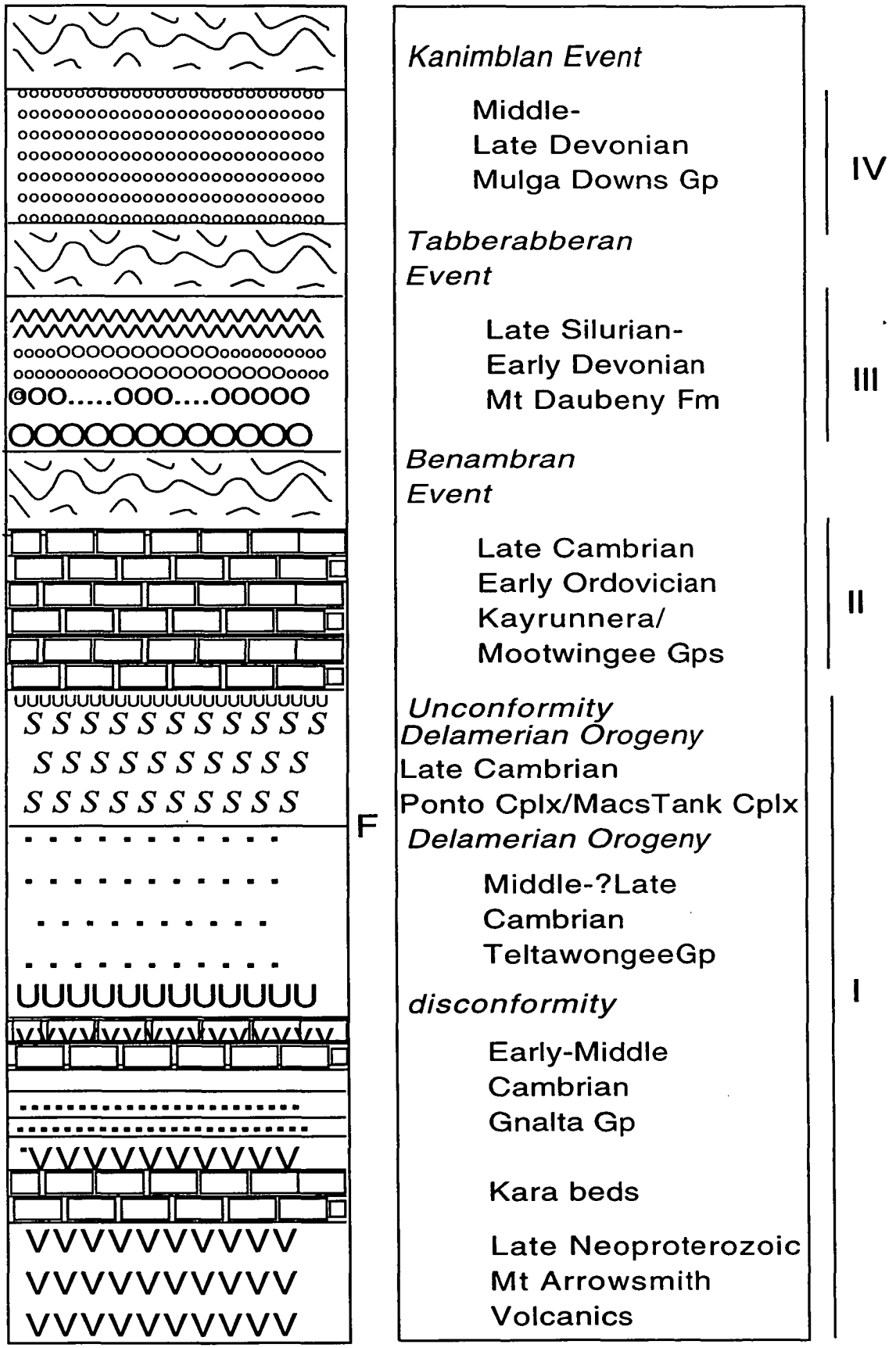


**Figure 2.4.1 Generalised Stratigraphy of the Koonenberry Belt and Bancannia Trough, and the four tectonostratigraphic packages**

Wilson (1967) qualitatively interpreted a 1965 aeromagnetic survey (Zarzavatjian, 1965 ref. Wilson, 1967) to define four distinct zones of differing magnetic character. These were separated by two north-northwest and east-northeast-trending sets of faults not revealed by photogeological interpretations. Zone 1, representing the Broken Hill block, was the western edge of the survey area and was characterised by high frequency north-northwest trending anomalies. Zone 2 was a zone of broad anomalies corresponding to the Bancannia plain, but also included the Mootwingee Range. This area had a depth to magnetic basement estimated at 3600 m maximum. Zone 3 contained high frequency anomalies that swung through c.90° from north-northwest to southwest. This was correlated with the "Precambrian" rocks between the Mt Wright and Koonenberry Faults. A magnetic high bounding this zone to the west was correlated with the volcanics at Mt Wright. Magnetic basement beneath "Gnalta sandstone" (= Ravendale Formation) was interpreted at ≤ 300 m in this zone. Zone 4 was characterised by a 200 nT anomaly in the vicinity of the Menamurtee Dome. Depth to basement in this zone was interpreted to deepen from 900 m to 3000 m from west to east.

Two reconnaissance gravity surveys were conducted (Stackler et al., 1965 ref. Wilson, 1967), the first in 1963 and the second in 1965. The 1963 survey was a profile along the Barrier Highway, and the second survey was an extension over the Bancannia plain. These surveys were able to delineate the boundaries of the Bancannia Trough, and the change in regional trends from north-northwest to southwest along the Scopes Range trend. The "Precambrian" of the Koonenberry belt was observed to form a regional gravity high, with steep gradients marking the Mt Wright Fault and its extension, the "Boorungie Fault."

Refraction seismic was used over the Bancannia Trough, after the abandonment of a reflection survey due to shot-hole difficulties (Wilson, 1967). This survey identified two main refractors. The first, with a velocity of c.4050 m/s occurred between depths of 150 and 880 m; this was correlated with the unconformity at the base of the Ravendale Formation. The second refractor, with a velocity of 4700 m/s occurred at depths of 650 m to 1800 m. This was thought to be related to an internal boundary in the "Mootwingee beds" (=Mootwingee Group). A further refraction survey undertaken at Menamurtee Dome identified a 6100 m/s refractor at a depth of 3050 m, thought to be either Precambrian basement or a Palaeozoic limestone (Wilson, 1967). Later drilling (Gnalta 1) encountered an orthoquartzite at 710m, which was assumed to be this refractor (NSW Oil & Gas N.L. ref. NSWGS Darling Basin Data Package, 1993).

A single-fold seismic reflection survey was shot over the Bancannia Trough in 1967, with subsequent drilling of Bancannia South No.1 well. Data from the well and the survey were jointly interpreted by Packham (1969). He identified four stratigraphic packages in the Trough, belonging to the Late Devonian and Ordovician. These were separated by four distinctive reflectors.

These boundaries were later extended by Evans (1977) to areas outside the Bancannia Trough. Evans' (1977) Horizon A marked the unconformity between ?Cambrian volcanics and the Devonian Snake Cave Sandstone encountered in Bancannia South No.1; horizon B (a disconformity) appeared to mark the base of the Middle Devonian; horizon C is the unconformity marking the boundary between the Middle Devonian and the Carboniferous, and horizon D marks the unconformity between the Palaeozoic and Mesozoic deposits.

The final episode of reconnaissance geophysics occurred in 1972. CRA, in their exploration in the Mt Wright area, discovered the "Mt Wright Ultrabasic" on the eastern side of the Mt Wright Fault. Johnson (1972) records the use of ground magnetometer traverses which were qualitatively interpreted to indicate that the body had a steep, easterly dip.

During the 1970's the Bureau of Mineral Resources (BMR) covered the region with a helicopter gravity survey on a 7.5 km grid (Tucker, 1983). In 1975 aeromagnetics were acquired with line spacings of between 1500 and 300 m, and clearance of 150 and 100 m respectively (Tucker, ibid.). These public domain datasets provided the material for interpretations by McIntyre & Wyatt (1978), Tucker (1983), Stevens (1986) and Encom (1994).

McIntyre & Wyatt (1978) provided a qualitative model for the structure of the Bancannia Trough. This invoked a large pile of magnetic andesite in the floor of a rift graben to produce the large wavelength and amplitude magnetic anomalies. They indicated that 2-dimensional forward models suggested that the anomaly was not due to either a vertical or horizontal slab. They also used profile matching methods to infer easterly dips of up to 30° for the "Mt. Wright Volcanics" (this study shows these anomalies of up to 300 nT to be caused by the Mt Arrowsmith volcanics, not the Mt.Wright Volcanics).

Tucker (1983) carried out a comprehensive potential field study of the Broken Hill block and its surrounds, backed up by petrophysical data. Although focussed on the

Proterozoic rocks, this study produced a quantitative 2-dimensional model for the Bancannia Trough indicating a maximum sedimentary thickness of 4 km.

Other important conclusions from Tucker's (1983) study include:

- Remanent components of magnetisation are not a major contributor to the magnetic field response. This was based on over 2100 measurements on drillcores.
- Response due to magnetic induction cuts out between 15 and 20 km, based on heat flow data from Cull (1982).
- The regional magnetic field is essentially flat.
- Weathering and oxidation of magnetite and pyrrhotite, the major phases contributing to the induced field, may be significant to depths of >100m. This observation was based on extensive drillhole susceptibility profiles.
- The best-estimate density of the Adelaidean successionis 2.75 t/m$^3$ to 2.80 t/m$^3$;
- A good estimate of the density of Devonian rocks is between 2.40 and 2.60 t/m$^3$
- Mesozoic cover sequences have densities typically 2.00 to 2.40 t/m$^3$.

Stevens (1986) used the regional gravity and aeromagnetic data to provide a qualitative interpretation of the structural blocks from the Queensland border to the Barrier Highway. Nine blocks were defined in the Koonenberry region, on the basis of gravity gradients or changes in strike of magnetic lineaments. Despite earlier quantitative modelling, Stevens (ibid.) suspected up to 8 km of Cambrian to Devonian sediments in the Bancannia Trough, overlain by up to 300 m of Mesozoic cover.

A further seismic survey was shot in 1986 near Alecs Tank, on the eastern flank of the Bancannia Trough. This was an 8-fold survey (NSWGS Open File Report SEIS 152, 1987), interpreted by Schroeder (1987). Data quality in this survey was poor, due to the presence of off-line structures and intense reverse faulting. Thrust faults were interpreted in the Cambro-Ordovician section, and were thought to extend into the Devonian.

McIntyre (1991) reiterated the findings of McIntyre & Wyatt (1978), inferring magnetic andesitic basement to the Bancannia Trough, invoking a high density volcanic basement to the Wonominta Block (terminology after Stevens,1986), and suggesting that the Koonenberry Fault was the margin to the "Kanmantoo Fold Belt" (after Scheibner, 1989). In addition, he noted that the Adelaidean sequences were essentially non-magnetic.

Encom (1994) produced four quantitative two-dimensional models for the region in the context of a regional petroleum prospectivity study. Unfortunately these models were flawed by the assumption of an average crustal density of 2.75 t/m$^3$ used to reduce the gravity data. This assumption increases the negative density contrast of the Devonian and younger rocks, causing their thicknesses to be grossly exaggerated; at the same time, it also decreases the density contrast of the Cambrian and Ordovician sequences, causing their modelled response to be negligible. No justification was given for this departure from accepted practice. An automated modelling process has also devalued these models, as the "best fit" computer solutions often have geologically meaningless geometries.

The general form of the Bancannia Trough given by these models is a graben or horst and two grabens. These are supposedly filled with between 5000 and 10000 m of (predominantly) Devonian sediments, although this figure is suspect for the reasons outlined above. The basement to the trough was thought to be Precambrian.

### 2.6 New Public Domain Data: Discovery 2000 Initiative.

In 1995 the NSW government began a program of acquisition of new geophysical data in collaboration with the Australian Geological Survey Organisation (AGSO). This was termed the Discovery 2000 Initiative. The first area to be targeted for data acquisition was the Koonenberry-Bancannia Region.

Over 4700 new gravity stations were acquired by Geoterrex on a 4x4 km grid (Figure 2.6.1). These were acquired using Lacoste & Romberg meters demounted from helicopter. Stations were reduced using a Bouguer density of 2.67 t/m$^3$ and the 1967 ellipsoid equation to produce a new Bouguer anomaly map of the region (Figure 2.6.2). Observed gravity for these stations was based on the Isogal 84 network (Wellman et al., 1985) stations at Broken Hill, and a set of 10 secondary bases throughout the area. Height control for this survey was provided by differential Global Positioning Systems methods, with sub-decimetre accuracy. None of the stations in this survey was terrain corrected. These assumptions and procedures give the survey an accuracy of ±0.01 mGal (Geoterrex Project Number 2-856, 1996).

Acquisition of aeromagnetic, radiometric and digital terrain data was undertaken by World Geoscience Corporation. Two separate specifications were made. Over the Bancannia Trough area, flight line spacings were to be 400 m, and flown as a 60 m

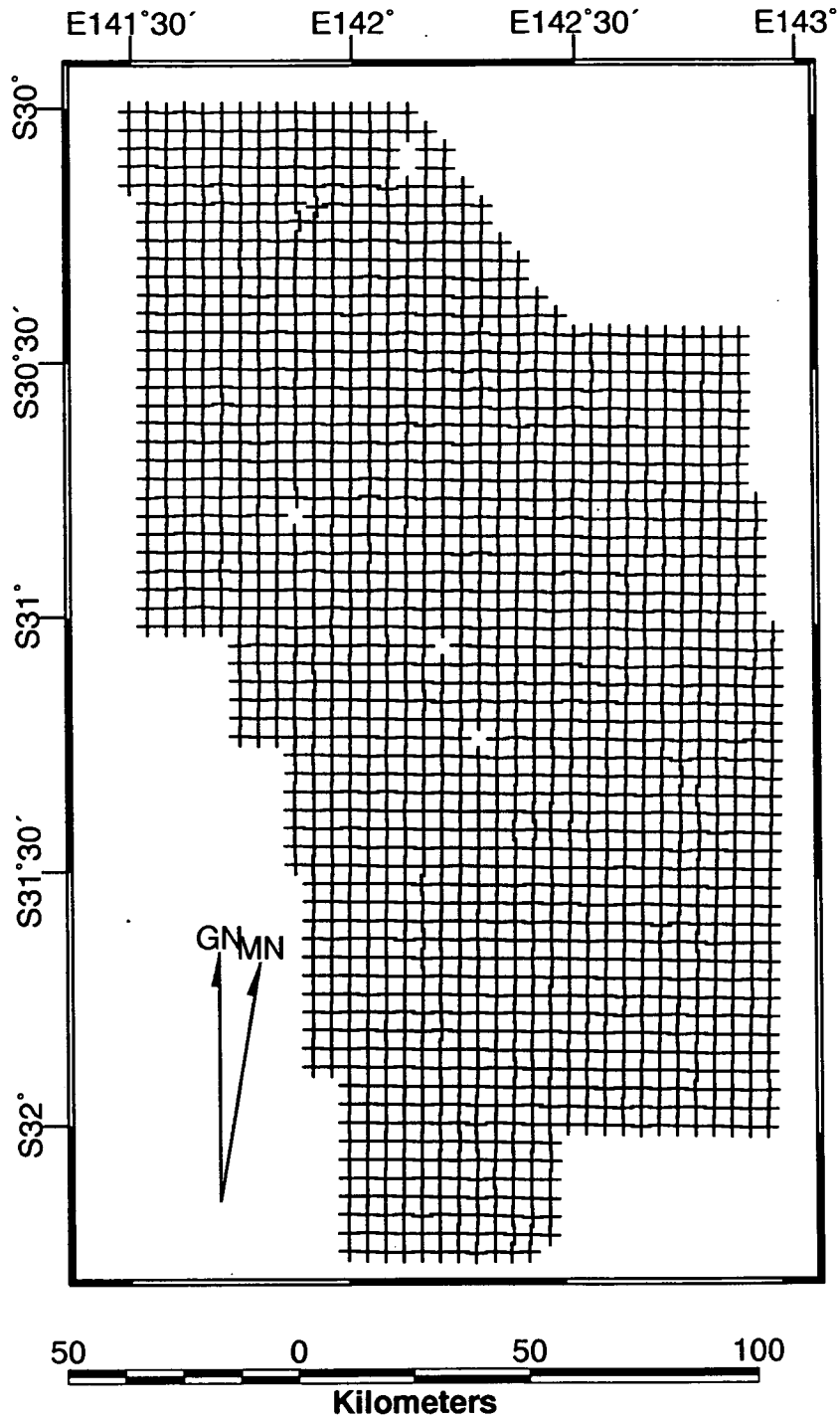


**Figure 2.6.1 D2000 gravity station distribution Bancannia Trough-Koonenberry**

(data courtesy MRNSW)

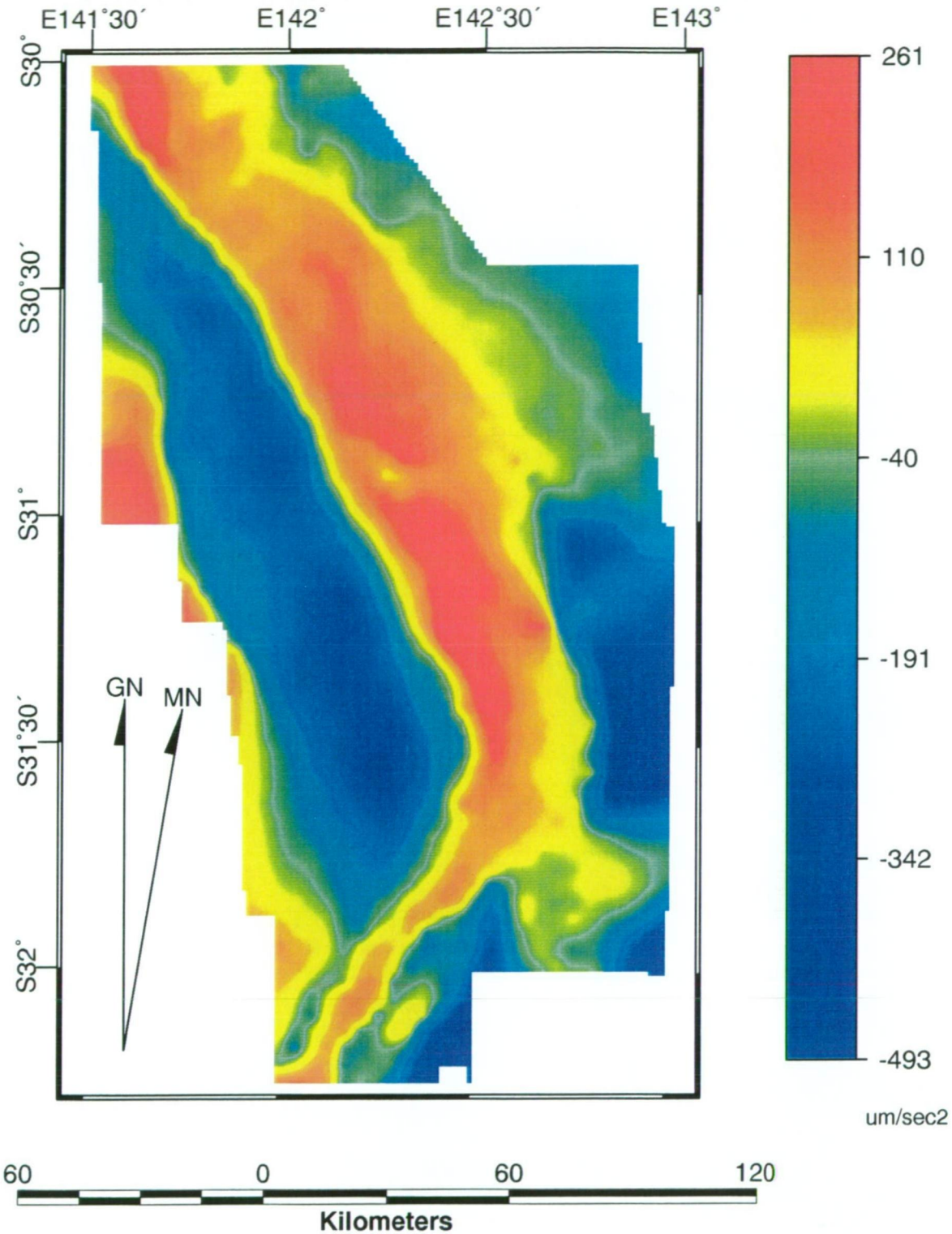


**Figure 2.6.2 D2000 Bouguer gravity data Bancannia Trough-Koonenberry**

(data courtesy MRNSW)

drape. Over the remainder of the area flight line spacings were to be 250 m, also flown as a 60 m drape. Both surveys used EW flight lines with NS tie lines spaced at 2500 m. The average sample interval along-line is given as 7 m (P. Ruszkowski, pers.comm., 1996).

The magnetometer used was a Scintrex "stinger" caesium vapour type, and the spectrometer used a 16 L NaI crystal, with 256 channel recording.

Aeromagnetic data were corrected for diurnal variation, microlevelling and parallax errors before removal of the IGRF and final gridding (Figure 2.6.3). Flight path data were recorded with real-time differential GPS to allow position-related corrections. The assumed level of the IGRF given as 56500nT (correct for the epoch 1995.5) was removed from the data. The claimed accuracy of the survey is 0.001 nT (P. Ruszkowski, pers.comm.1996).

Radiometric data were corrected for cosmic ray and environmental radionuclide responses (Cs137, Rn) before gridding. The data are presented as total counts, as well as channels at 0.41-2.81 MeV, 1.37-1.57 MeV and 2.41-2.81 MeV, corresponding to emissions of K, Th and U (P Ruszkowski, pers.comm.1996).

Digital terrain data were acquired through the use of radar altimeters and real-time differential GPS. They are position corrected (parallax and microlevelling) and are claimed to be accurate to 1 m (P. Ruszkowski, pers.comm.1996).

## 2.7 Interpretation of Discovery 2000 Data

A preliminary "solid geology" qualitative interpretation of the Koonenberry-Bancannia region was made in late 1995, and published as Hicks et al., (1996). This made use of the magnetic and radiometric datasets mentioned above. Subsequent ground checking of this interpretation has required revision of the interpretations, and a second edition interpretation is in progress.

New quantitative and qualitative interpretations of this data form the greater part of my investigations of the Koonenberry-Bancannia region, and are outlined in detail in subsequent chapters of this thesis.

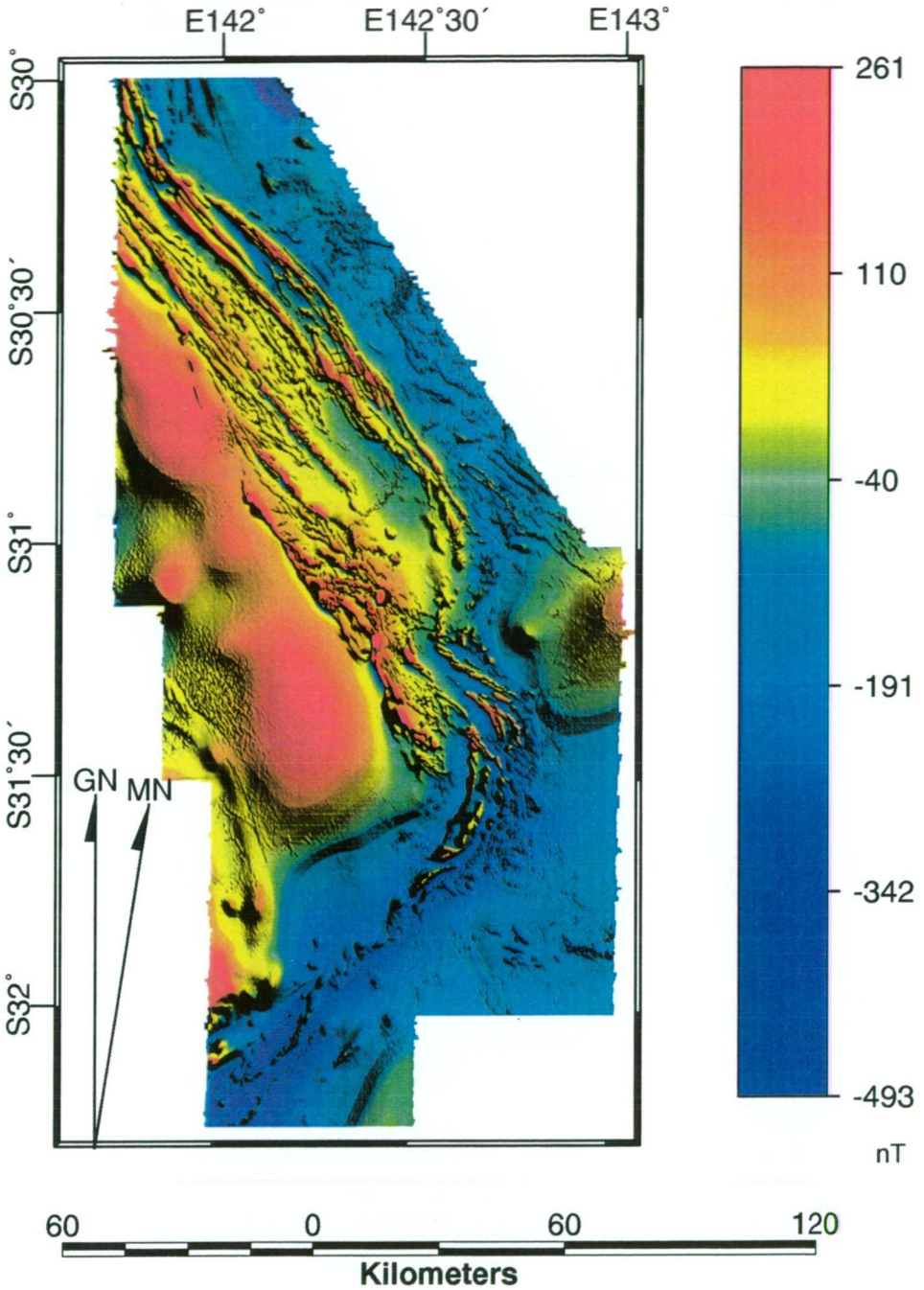


**Figure 2.6.3 D2000 Total Magnetic Intensity data, Bancannia Trough-Koonenberry**

(Sun shading at 45 degrees from NE. Corrected to IGRF 1990, epoch 1995; I = 57377.72 nT; Inclination -63.41 degrees; Declination 8.81 degrees. Data courtesy MRNSW)

**Chapter 3: Regional Stratigraphy and Petrophysics**

# Chapter 3: Regional Stratigraphy and Petrophysics

## 3.0 Introduction

This brief chapter serves to give a detailed overview of the stratigraphy of the Koonenberry Region as it was understood prior to the commencement of this study in January 1996. Findings of this study, and ongoing mapping by NSW Geological Survey geologists during the years 1996-1999 have forced revisions to this scheme, which will be outlined in later chapters.

The petrophysical properties of all the main lithologies within the Koonenberry region are also outlined here. The presentation of both sets of data together provides the framework for understanding the stratigraphic and geological studies outlined in following chapters.

## 3.1 Stratigraphy

### *3.1.1 Preamble*

The development of a stratigraphic scheme for the Koonenberry Belt has proceeded slowly due to the twin problems of large areal extent and extremely limited outcrop. Reconnaissance mapping by Rose & Brunker (1969) led to naming of only ten units at formation level, and two at group level. Much of the belt was assigned to the ubiquitous "Wonominta beds". However, the Nundora-Wonnaminta-Nuntherungie-Marrapina area retained its poorly divided stratigraphy until the work of Webby et al. (1988) and Mills (1992). Because of problems with correlation between widely separated outcrops, and the poor exposure of many contacts, many of the units discussed below are informal; that is they have not been formally accepted by the Australian Stratigraphic Nomenclature Board. Nevertheless, it is these informal units which are being applied to the latest generation of mapping being undertaken by the NSW Geological Survey. It is hoped that many of them will soon be defined with type sections, to avoid possible confusion. Formally defined units are indicated below using *italic* typeface.

### *3.1.2 Stratigraphic Nomenclature*

Late Neoproterozoic Mt Arrowsmith Volcanics (MAV)

This unit is used in the sense of Crawford et al. (1997), to describe a series of alkaline trachybasalt-trachyandesite lavas and dykes and alkali rhyolite lavas, their hypabyssal feeder systems, and their epiclastic derivatives. Volcanic facies described within the

MAV include lava flows, pillow lavas, breccias, hyaloclastites, epiclastics, a wehrlite-harzburgite plug, and a picrite cumulate body (Crawford et al., ibid.). The MAV are usually metamorphosed up to greenschist grade. This is an informal stratigraphic unit, despite a type section at Mt Arrowsmith described by Edwards (1978). It is also described at Conns Ck, within the study area (Edwards, 1978; Zhou, 1993; Crawford et al., 1997). In the type area, and at Conns Ck, the MAV remain undated.

In the Mt Wright area, the MAV includes isolated outcrops of trachybasalts on Mt Wright Creek (around 632500 mE, 6546800 mN), and along the Mt Wright Fault (around 633000 mE, 6542500 mN, and also around 635500 mE, 6537450 mN). All of these units are correlated on the basis of their trace element geochemistry and alkaline affinity (after Crawford et al., 1997). An alkaline rhyolite tuff from this sequence was dated by the above authors using the SHRIMP zircon U-Pb method at 587 ± 7 Ma.

Late Neoproterozoic-?Early Cambrian Kara beds

This unit is used in the sense of Mills (1992), describing a monotonous sequence of brown, black and white shales with occasional interbedded cross-bedded quartzite layers, outcropping between Teltawongee Tank (600832 mE, 6600250 mN) and Gums Creek on the Nundora -Wonnaminta Road (624000 mE, 6609000 mN). The base of this sequence is not observed, but the top is in disconformable contact with the Teltawongee beds (see below) at Teltawongee Tank. The apparent exposed thickness of this unit is c.16 km when the regional syncline in which it occurs is unfolded (Mills, ibid.). Such a thickness of black shale is unlikely, and this apparent thickness is probably indicative of cryptic thrust faulting (ibid.).

The Kara beds are interpreted as the host sedimentary sequence to the MAV (Mills, ibid.)

?Early Cambrian Teltawongee beds

This unit, also described by Mills (ibid.), is the predominant lithology in the Koonenberry Belt, if all the units referred to it are validly correlated. It is used to describe monotonous sandstone-shale interbeds of turbiditic aspect. These outcrop from the eastern margin of the Bancannia Trough in Nundora Creek (598100 mE, 6601000 mN) to Teltawongee Tank ("western sequence"); from Gums Creek to Wonnaminta airstrip (627300 mE, 6610600 mN)("central sequence"); and extend east of the Koonenberry Fault, to disappear under Mesozoic-Recent alluvium ("eastern sequence").

They are characterised by common occurrence of sedimentary structures such as ripple cross-beds, climbing ripples, graded bedding and flame structures, which allow their facings to be readily determined.

Sponge spicules were recovered from the central sequence, suggesting a maximum Early Cambrian age for the Teltawongee beds (Mills, 1992).

*?Early Cambrian Copper Mine Range Beds (CMRB)*

This unit was formally defined by Pogson & Scheibner (1971), and its type section lies to the east of the Coturaundee Range at The Hummock (651500 mE, 6586000 mN). It is unconformably overlain by the Kandie Tank Limestone (see above). It consists of interbedded laminated shale, siltstone, mudstone and poorly sorted lithic sandstones. The coarser units show graded bedding, load casting and flute casts. Soft sediment deformation structures are also common.

Collins (1984) found sponge spicules and radiolarian fossils that allow the sequence to be assigned to either the Early or Middle Cambrian. Mills (1992) incorporated the CMRB into the Teltawongee beds eastern sequence, although this link has no formal stratigraphic status.

?Early Cambrian Wilandra beds

This term was used by Davidson (1981) to describe a series of deformed, interbedded basalts, limestones, orthoquartzites and shales outcropping to the east of the Bald Hill Fault. These have been metamorphosed to greenschist facies (Davidson, ibid.). Basaltic clasts can be found within limestone lenses, showing intimate depositional-eruptive relationships.

The Wilandra beds are pre-Ordovician in age, being unconformably overlain by the Rowena Formation at Bald Hill (Davidson, ibid.), but have not been dated by fossils or zircon dating. Davidson (ibid.) tentatively correlated these rocks with the Coonigan Formation of the Gnalta Group on the basis of lithological similarity. He also suggested a possible correlation with the Copper Mine Range Beds. Mills (1992) grouped the Wilandra beds into the Kara beds, without recognition of the pre-existing informal name.

*Early-Middle Cambrian Gnalta Group*

The Gnalta Group was defined by Warris (1967), in the area bounded by the Bynguano Range, Mt Wright and Gnalta H.S. It consists of the Mt Wright Volcanics, overlain by the Cymbric Vale Formation, and the Coonigan Formation. Additions to the Cymbric Vale Formation were suggested by Davidson (1981), and modifications to the Mt Wright Volcanics were made by Crawford et al (1997).

The Mt Wright Volcanics (MWV) were described by Warris (op.cit.) as discontinuous, with severe faulting and folding disrupting the lithologies. The type section was in two parts, separated by a fault. However, Warris' (ibid.) original type sections were not provided with detailed maps or grid references, so they are not easily located in the field. The base of the MWV was not recorded by him; however, a transitional top to the Cymbric Vale Formation was defined. The southern, lower portion of the section was defined on an anticline, possibly at 633000 mE, 6542500 mN. The northern, upper section was defined in a creek, possibly at 632500 mE, 6547000 mN.

The lower section is described as 914 m of red to purple quartz + plagioclase-phyric volcanics, overlain by brown chert and mudstone.

The middle section (within the northern type section) is described as massive chert, altered basaltic volcanics, green shales and massive limestones. The limestones contain archaeocyathid faunae dated as Early Cambrian (Atdabanian) by Kruse (1982). The middle of the section is described as at least 762 m thick.

The upper section, separated by a fault from the middle section comprises at least 762 m of plagioclase + hornblende-phyric basaltic and andesitic lavas. The basaltic lavas were compositionally correlated with those in the middle section.

The Cymbric Vale Formation was defined as 1372 m of cherts, welded tuffs, silicicified siltstones, lithic to arkosic sandstones and organic limestones overlying the Mt Wright Volcanics (Warris, 1967). The type section is probably near 633000 mE, 6550000 mN. The base of the section is faulted, and the top is not exposed. A conformable contact with the MWV was proposed to the west of the type section. Arkoses and lithic sandstones within the formation were compositionally linked to basalts in the middle section of the MWV, suggesting a close spatio-temporal relationship. Siltstones in a correlated section west of the Lawrence Fault contain a Early Cambrian (Atdabanian-Toyonian) trilobite fauna (after Öpik, 1975).

The Coonigan Formation has a type section of only 113 m at 625000 mE,

6550000 mN (after Warris, 1967). It consists of discontinuous bodies of saprolite after micrites, shales and siltstones. The base is not defined, but the top is marked by a probable disconformity with a conglomerate at the base of the Early Ordovician Nootumbulla Sandstone; outcropping poorly at 627299 mE, 6548392 mN. It contains a Middle Cambrian (Templetonian) trilobite fauna (Öpik, op.cit.).

Davidson (1981) mapped several new Palaeozoic outcrops in the area of Baroorangee Creek (636087mE, 6537216 mN). One of these, adjacent to the Baroorangee Creek Serpentinite, consists of extremely immature feldspathic sandstones, rich in plagioclase and muscovite. These were compositionally correlated with the Cymbric Vale Formation.

Crawford et al (1997) investigated the geochemistry of volcanics previously assigned to the Mt Wright Volcanics and Cymbric Vale Formations, and defined two compositionally and temporally distinct units: an alkaline suite of basalts and rare alkaline rhyolites, which they dated at 586±7 Ma; and a calc-alkaline suite of evolved basalts and andesites with some rhyolitic volcaniclastics, previously dated at 525±8 Ma by Zhou & Whitford, (1994).

The older unit was correlated by Crawford et al (1997) with the Mt Arrowsmith Volcanics (described in Chapter 3), whereas the younger package envelopes the fossiliferous limestones described by Warris (1967), and dated by Kruse (1982). The two volcanic packages are separated by faults wherever they are found in the field.

Crawford et al (1997) noted that these observations were difficult to reconcile with the stratigraphy erected by Warris (1967), as the lower section of the defined Mt Wright Volcanics is the older alkaline suite, and the upper section is a composite of the alkaline and calc-alkaline packages. They reserved the name Mt Wright Volcanics for those units of the calc-alkaline suite of rocks spatially associated with the archaeocyathan limestones.

A corollary of these observations is that the contact between the Cymbric Vale Formation and the redefined Mt Wright Volcanics (*sensu* Crawford et al., 1997) is no longer defined. This is because the original contact described by Warris (1967) is with the Mt Arrowsmith Volcanics, and certainly a fault.

*Late Cambrian Cupala Creek Formation*

Formally defined by Powell et al. (1981), the Cupala Creek Formation type section is to the east of the Coturaundee Range at Cupala Creek (658900 mE, 6577200 mN). It is predominantly a sandstone succession with a basal conglomerate. The sandstone fines up to a siltstone which contains an abundant brachiopod-trilobite fauna of Late Cambrian (Idamean) age.

*Late Cambrian-Early Ordovician Kandie Tank Limestone*

This unit was formally defined by Pogson & Scheibner (1971), and its type section lies to the east of the Coturaundee Range at The Hummock (see above). It is a massive or thickly bedded biostromal limestone, consisting of biomicrites and crinoidal biosparite (Pogson & Scheibner, ibid.). It contains a conodont and inarticulate brachiopod fauna, and was correlated with the Nootumbulla Sandstone by Warris (1967). This gives it a Payntonian to Datsonian age (after Shergold, 1971).

Late Cambrian-Early Ordovician Ponto beds

The Ponto beds are the final unit proposed by Mills (1992), describing a polydeformed series of slates, schists and tholeiitic metabasalts outcropping in a 10 km wide strip immediately west of the Koonenberry Fault. The chemistry of the basalts was described by Zhou & Mills (1990), and Zhou (1993).

In the Cymbric Vale area, rocks referred to the Ponto Complex are polydeformed slates and mica schists, with rare interbedded metabasalts. Local lenses of calcite-quartz and haematite-quartz gneiss were also identified by Davidson (1981); these are volumetrically insignificant. The whole sequence reaches amphibolite grade to the east of the Mt Wright Fault (Zhou, 1993) and has been dynamically metamorphosed in the fault zone to form L-S tectonites (this study).

Although initially thought to be correlates of the Mesoproterozoic Upper Willyama Supergroup (Zhou, 1993; Mills, 1992; Zhou & Mills, 1990) on the basis of their higher metamorphic grades and Nd isotope signature, it is now known that these rocks are much younger.

SHRIMP zircon U-Pb radiometric ages have been obtained from a variety of samples from the Ponto Mine area, Bilpa and Grasmere. These gave an imprecise spread of ages from 484 ± 6 Ma and 488 ± 5 Ma at Ponto, and 516 ± 11 Ma and 497 ± 8 Ma at the other locations (BHP Exploration and Fanning & Stevens, unpubl. data). These dates span the Early Cambrian (Atdabanian) to Middle Ordovician (Chewtonian).

In view of their polydeformed, metamorphosed nature, I propose the use of the name Ponto Complex for these rocks. This name will be used throughout the remainder of this thesis.

*Late Cambrian-Early Ordovician Kayrunnera Group*

The Kayrunnera Group was initially defined by Webby et al (1988), with subsequent refinements by Wang Qizheng et al. (1989). It is divided into three formations, each with its own type section. All known outcrops of the Kayrunnera Group occur in fault splays of the Koonenberry Fault.

The basal Morden Formation, defined at Morden Creek (636150 mE, 6613281 mN) is a 1 to 6m thick medium-grained, cross-bedded quartzite, in the type section 2m thick.

This is succeeded by the Boshy Formation. Its type section is in JK Creek (641000 mE, 6608900 mN to 640900 mE, 6608900 mN), where it reaches a maximum thickness of 94.3 m. Elsewhere, its thickness is variable down to 15.7 m. It consists of interbedded fine sandstones, siltstones, with minor calcarenties and limestone lenses, and contains an abundant Late Cambrian (Mindyallan) trilobite fauna (Webby et al., 1988).

The uppermost formation of the Kayrunnera Group is the Watties Bore Formation, comprising a maximum of 2000 m of yellowish shales and siltstones. These are cut off abruptly by the Koonenberry Fault. The type section is southeast of Watties Bore (632100 mE, 6616700 mN to 630400 mE, 6614800 mN). The formation preserves an abundant trilobite-conodont fauna of Late Cambrian (Mindyallan) to Lowest Ordovician (Tremadoc-Datsonian) age.

Webby et al. (ibid.) and Wang Qizheng et al. (op.cit.) postulated that the Kayrunnera Group is a time-transgressive equivalent of the Cupala Creek Formation.

*Late Cambrian-Early Ordovician Mootwingee Group*

The Mootwingee Group is defined in the Bynguano Range and Mt Wright areas. Type sections were defined by Warris (1967), with subsequent amendment by Davidson (1981).

The basal formation is the Nootumbulla Sandstone that consists of a basal conglomerate overlain by a generally fining-upward sequence of gravels, arenites, biocalcarenites, siltstones, shales and limestone. The basal gravel conglomerate is

50 m thick in the type section, of a total thickness of 250 m (Warris, op.cit.; Davidson, op.cit). The Nootumbulla Sandstone contains an Late Cambrian (Payntonian) to Lowest Ordovician (Datsonian) trilobite fauna (Shergold, 1971). Mapping around 627299 mE, 6548392 mN shows the Nootumbulla Sandstone unconformably overlies the Coonigan Formation (Warris, 1967).

The upper formation is the Rowena Formation, which has a basal Bynguano Quartzite Member conformably overlying the Nootumbulla Sandstone at 627700 mE, 6544000 mN (Davidson, op.cit.). Davidson (1981) mapped the Rowena Formation unconformably overlying the Wilandra beds at Bald Hill (644500 mE, 6543300 mN).

The Bynguano Quartzite Member consists of pebbly quartzite layers, quartzite and siltstones, and is 320 m thick (Shergold, op.cit.). It contains an abundance of trace fossils, including *skolithos* and *rusophycus*, as well as an attendant trilobite population of Early Ordovician (Warendan) age (Shergold, ibid.)

The remainder of the Rowena Formation consists of arenites and siltstones, 1990 m thick (Davidson, 1981). These contain a mid-Arenig trilobite fauna. This section is faulted against Gnalta Group along the Lawrence Fault (Davidson, ibid.), and against the Snake Cave Sandstone of the Mulga Downs Group in the Bynguano Range (Warris, 1967).

*Late Cambrian-Early Ordovician Scopes Range beds*

This unit was first used by Rose (1968) used by Hicks & Mills (1997) to describe well-laminated white, maroon and red quartzose sandstones, quartzites and conglomerates. These crop out in the resistant Scopes Range, on the Bunda 7434 1:100 000 sheet. They are interpreted as shallow marine to estuarine facies, containing glauconite horizons, trace fossils (*rusophycus, skolithos*) and brachiopod and trilobite faunas. The top of the sequence contains well-developed cross-bed sets and quartz pebble conglomerates, and is considered to be a fluvial facies. According to Hicks & Mills (1997), the Scopes Range beds contain rare felsic volcanic rocks, but these are not described. The lower unit is estimated to be 1220 m thick, while the cross-bedded package is estimated as 500 m thick (Shergold et al., 1985). The upper package is correlated with the Bynguano Quartzite Member (Shergold et al., 1985).

Late Cambrian-Early Ordovician Bancannia intermediate volcanics

Although not a recognised package, this unit has been inserted into the stratigraphy because it has been accurately dated. It was drilled in the Bancannia South No. 1 well

(577900mE, 6559900mN; Planet Oil Co. P.L., 1968), and consists of welded crystal vitric rhyodacitic-dacitic and andesitic tuffs, and plagioclase-phyric dacite lavas which have a shoshonitic affinity (Barron, 1990). SHRIMP zircon dating of a sample of dacite gave an imprecise age of 497 ± 11 Ma, which is Middle Cambrian (Ordian) to Early Ordovician (Warendan).

*?Late Silurian-Early Devonian Mt Daubeny Formation*

First named by Neef et al. (1989), this sequence outcrops to the west of the Koonenberry Fault, as far west as Blue Well Tank (650500 mE, 6553800 mN). The thickness of the Mt Daubeny Formation is stated to be up to 6 km thick, although no coordinates are given for the top or base of the type section shown. Based on the probable location of a type cross-section (Neef et al., ibid., section K-L), the base is probably a ridge above Koonburra Creek (657700 mE, 6548100 mN) and the top cut by the Koonenberry Fault at 661300 mE, 6561600 mN

The Koonburra Creek Quartzite Member is defined above Koonburra Creek by Neef et al. (1989). It is a variably thick (75 to14m) grey cross-bedded orthoquartzite; its thickest extent is in the type section of the Mt Daubeny Formation, outlined above.

This is succeeded by red arenites and pebble conglomerates (c.400 m), coarse brown arenites and conglomerates (c.1000m), lithic arenites (c.2300m), fine-grained arenites and siltstones (c.1050m), orthoquartzite (c.650m) and lithic arenites and siltstones (c.600m). (Approximate thicknesses are based on Fig. 5, Neef et al., ibid.).

The fine-grained arenite interval contains plant fossils of Late Silurian (Ludlovian) to Early Devonian (Pragian) age.

Several andesite flows are interbedded within this sequence, together with their feeder dykes.

*Late Devonian-?Early Carboniferous Mulga Downs Group*

The Mulga Downs Group is defined far to the east of the Koonenberry Belt, in the Cobar region (Pickett, 1972), where it consists of the Meadows Tank Sandstone, Merrimerriwa Formation and Bulgoo Sandstone (Glen, 1979). These contain a Middle Devonian (Eifelian) fish fauna (Pickett, op.cit.) and Early Carboniferous (Tournaisian) microflora (Glen, op.cit.). The sediments also contain abundant pebble conglomerates, planar and trough cross-bedding, laminations and climbing ripples. The thickness of

the Mulga Downs Group is cited as 3500 m minimum (Evans, ibid.) and up to 4700 m (Roberts et al., 1972).

Wilson (1967) correlated units informally termed the "Ravendale beds" and "Gnalta sandstone" with the Mulga Downs Group on the basis of contained fishplate fossils and sedimentary structures. Rose and Brunker (1969) correlated the Snake Cave Sandstone (Warris, 1967) and Coco Range Beds (Ward et al., 1969) with the Mulga Downs Group, excluding the Nundooka Sandstone (Ward et al., ibid) and Ravendale Formation (Warris, 1967). Packham (1968), using evidence from seismic reflectors across the Bancannia Trough, rationalised the previous schemes, correlating the Coco Range Beds with the Snake Cave Sandstone, which were separated from the Nundooka Sandstone-Ravendale Formation by an unconformity. Evans (1977) again referred these groupings to the Mulga Downs Group.

The lower package of rocks consists of conglomeratic sandstones, red and white arenites with well-developed cross-bedding structures, together with red siltstone (Roberts et al., 1972). The upper package consists of soft-weathering white to red quartzite, with occasional red shale interbeds (Evans, op.cit.). These contain large-scale trough and planar cross-beds and pebble layers (Davidson, 1981).

The Snake Cave Sandstone, and its basal quartzite-pebble conglomerate, the Rock Holes Member (Warris, 1967), form most of the Mootwingee Range and Ramparts Hills; they also comprise the western drainage divide of the Bynguano Range.

The Snake Cave Sandstone-Coco Range Beds are dated as probable Late Devonian by a fishplate assemblage (Roberts et al., 1972). The Ravendale Formation-Nundooka Sandstone contains bivalves giving an Early Carboniferous age (after Mills, 1992), and Late Devonian (Famennian) to Early Carboniferous (Tournaisian) pollen assemblage in Blantyre No.1 (Roberts et al., 1972). Bembrick (1997) reviewed the pollen assemblages associated with this unit and concluded it was Late Devonian in age.

The maximum thickness of ?Early to Late Carboniferous Devonian sediments was encountered in Bancannia South No.1 well, reaching 1007.6 m, while the Middle to Late Devonian sequence measured 2035.5 m before intersection of unconformably underlying Cambrian dacites (Packham, 1969). At other locations in the Trough, the relative thicknesses of the Ravendale-Nundooka and Snake Cave-Coco Range are 368 m / 710 m (Bancannia North No.1; Packham, ibid.), and 850 m / 658 m (Jupiter 1; NSWGS, 1993).

The Ravendale Formation occurs in the Marrapina area, and the Turkaro Range forming low-lying, red hills. Its distribution in the Mt Wright area is strongly controlled by the Mt Wright Fault and its splays, forming the mesa of Mt Wright, and the range overlooking Cymbric Vale H.S. The formation is particularly distinctive, with a whitish to reddish weathering character, and forms strong cliff-lines, often with caves where more feldspathic zones have weathered preferentially.

### *3.1.3 Notes on the Early-Middle Cambrian sequences in the Cymbric Vale-Mt Wright Area*

Modifications to the established stratigraphy forced by new dating and geochemical investigations have necessitated reappraisal of the whole Early and Middle Cambrian stratigraphy in this area. Other considerations, such as the allochthoneity of several of the units, and the chaotic distribution of the Gnalta Group, have led to the hypothesis that the Gnalta Group may form a broken formation. This concept is examined in a further chapter 5.

## 3.2 Petrophysical studies

A comprehensive knowledge of density and susceptibility characteristics of rocks of the region is required before attempting detailed forward modelling. To this end a total of 45 density and 222 susceptibility measurements were made on 13 lithologies from the Nundora-Wonnaminta-Marrapina-Nuntherungie area, and a total of 66 density and 648 susceptibility measurements were made on 15 lithologies from the Mt Wright-Cymbric Vale area. All of these were conducted on outcrops or outcrop-derived samples. In the Grasmere area, 16 density determinations were made on samples from the Ponto Complex in addition to 410 susceptibility measurements. Of these, 5 density and 28 susceptibility measurements were made on drillcore; the remainder were conducted on outcrop or outcrop derived samples. In the Darling River Lineament, 26 density determinations were made, all on drillcore samples.

Magnetic susceptibility measurements were made in the field using a hand-held Exploranium KT-5 susceptibility meter. A minimum of 8 readings were made across each outcrop to provide a sample, and usually many outcrops of each rock-type were sampled to build up a picture of the natural variations in magnetic susceptibility. Results are summarised in Table 3.2 below, with the full datasets given in Appendix 2.

Density measurements were made at the University of Tasmania geophysics lab, using Archimedes' principle. All rocks were selected for minimal weathering characteristics in the field. A minimum of 500 g was then removed from outcrop for each sample. In the laboratory, these were immersed in water for a minimum period of 24 hours, to allow pore spaces to fill with water. After touch-drying, the saturated mass of the samples was measured using an electronic balance with a precision of 0.01 g. The immersed mass of the samples was then measured using the same balance with a cage assembly attached to an under-hook. Results are summarised in Table 1 below, with the full datasets given in Appendix 3.

**Table 3.2.1: Summary of Raw Petrophysical Property Data for Major Lithologies**

| Name | Locality | ρ (t/m$^3$) | nρ | type | kav (SI) | kmax | nk | Notes |
|---|---|---|---|---|---|---|---|---|
| Ponto phyllites | Wonnaminta | na | na | na | 0.0036 | 0.012 | 13 | Outcrop; "magnetic" |
| Teltawongee mudstones | Nundora | *2.74* | na | na | 0.00084 | 0.00084 | 7 | Outcrop |
| Kara mudstones | Wonnaminta | 2.29<br>*2.72* | 3 | AV | 0.00012 | 0.00024 | 21 | Outcrop |
| Kara mudstones | Wonnaminta | 2.45 | 2 | AV | na | na | na | Outcrop |
| Teltawongee sandstones | Nundora | 2.49<br>*2.66* | 7 | AV | 0.00024 | 0.0006 | 15 | Outcrop |
| Kara sandstones | Nundora | 2.51<br>*2.62* | 5 | AV | 0.00012 | 0.00024 | 17 | Outcrop |
| Mootwingee Group | Bulk value | 2.52 | na | WAV | 0.00008 | 0.0002 | na | |
| Ponto phyllites | Wonnaminta | 2.56<br>*2.71* | 5 | AV | 0.00024 | 0.0006 | 45 | Outcrop; "non-magnetic" |
| Ponto quartz-magnetite rocks | Wonnaminta | 2.62 | 4 | AV | 0.0072 | 0.0096 | 25 | Outcrop |
| Kayrunnera Group | Wonnaminta | 2.63 | 3 | AV | 0.00012 | 0.00012 | 15 | Outcrop; shales from Watties Bore Fm. K Wtd. 96:4 shale:ss |
| Copper Mine Range sandstones | Cotoraundee Range | 2.63<br>*2.66* | 3 | AV | na | na | na | Outcrop |
| Teltawongee Beds | Bulk value | 2.70 | na | WAV | 0.0006 | 0.00072 | na | |

| | | | | | | | | |
|---|---|---|---|---|---|---|---|---|
| Ponto Complex | Bulk value | 2.71 | na | WAV | 0.00036 | 0.036 | na | |
| Kara Beds | Bulk value | 2.71 | na | WAV | 0.00012 | 0.00024 | na | |
| Mt Arrowsmith Volcanics | Mt Arrowsmith | 2.75 | 3 | AV | 0.036 | 0.072 | 24 | Outcrop |
| Mulga Downs Group | Cymbric Vale | 2.30<br>*2.22* | 9 | AV | 0.00006 | 0.00018 | 20 | Outcrop |
| Mesozoic silcrete | Cymbric Vale | 2.51 | 4 | AV | 0.00006 | 0.00024 | 14 | Outcrop |
| Rowena Formation | Cymbric Vale | 2.52 | 3 | AV | 0.000084 | 0.000017 | 24 | Outcrop |
| Mootwingee Group | Bulk value | 2.52 | Na | WAV | 0.00007 | 0.0002 | na | |
| Cymbric Vale Formation | Cymbric Vale | 2.55 | 5 | AV | 0.0001 | 0.00024 | 75 | Outcrop; 2 localities |
| Ponto phyllites | Wonnaminta | 2.56<br>*2.71* | 5 | AV | 0.00024 | 0.0006 | 45 | Outcrop; "non-magnetic" |
| Wilandra sediments | Cymbric Vale | 2.63<br>*2.66* | 8 | WAV | 0.00036 | 0.00072 | 7 | Outcrop; Wtd. 84:15:1 shale:ss:LMS |
| Wilandra basalts | Cymbric Vale | 2.68<br>*2.75* | 3 | AV | 0.00036 | 0.0048 | 47 | Outcrop |
| Mt Arrowsmith Volcanics | Cymbric Vale | 2.72 | 4 | AV | 0.0096 | 0.048 | 70 | Outcrop |
| Ponto phyllites | Baroorangee Ck | 2.74 | 3 | AV | 0.0006 | 0.0012 | 19 | Outcrop |
| Mt Arrowsmith Volcanics | Mt Arrowsmith | 2.75 | 3 | AV | 0.036 | 0.072 | 24 | Outcrop |
| Mt Wright Volcanics | Cymbric Vale | 2.76 | 6 | AV | 0.024 | 0.084 | 217 | Outcrop |
| Mt Arrowsmith Volcanics | Nundora | 2.77 | 8 | WAV | 0.024 | 0.048 | 75 | Outcrop; Wtd. 90:10 basalt: UM. Excludes nundorite |
| Ponto phyllites | Cymbric Vale | 2.77 | 1 | AV | 0.0012 | 0.0024 | 4 | Outcrop |
| Ponto metabasalts | Cymbric Vale | 2.93 | 4 | AV | 0.0024 | 0.0048 | 7 | Outcrop |
| Ponto phyllites | Grasmere | 2.75 | 7 | AV | 0.085 | 0.0027 | 316 | Core |
| Ponto metabasalts | Grasmere | 2.93 | 7 | AV | 0.046 | 0.008 | 92 | Outcrop |
| Teltawongee sandstones* | Scopes Rg | 2.69 | 2 | AV | na | na | na | Core |
| Teltawongee sandstones* | Scopes Rg | 2.73 | 8 | AV | na | na | na | Core |

Key: ρ (t/m$^3$) = average density in t/m$^3$; type = averaging process used; AV = arithmetic mean; WAV = weighted according to ratio of lithologies in notes column; nρ = number of density determinations used in average; kav (SI) = average magnetic susceptibility

in SI units; kmax = maximum recorded susceptibility; nk = number of susceptibility determinations used in average.

Comments:

Evidently many of these density data will be affected to some degree by weathering. This is especially true for the sedimentary lithologies listed. In order to be useful for modelling, the data require checking and/or scaling. One method of checking the "quality" of a rock is to also measure the sonic velocity, which will be reduced if fractures or alteration are present. Sonic velocities for several of the lithologies are presented below.

**Table 3.2.2: Summary of Sonic Velocity Data for Selected (Meta-)Sedimentary Lithologies**

*P wave velocities only

| Name | Locality | Sonic Velocity (m/s) | Density ($t/m^3$) | Scaling? |
|---|---|---|---|---|
| Ravendale sandstone | Kara | 1310 | 2.31 | yes |
| Teltawongee sandstone | Nundora | 2232 | 2.42 | yes |
| Teltawongee sandstone | Nundora | 2817 | 2.49 | yes |
| Teltawongee sandstone | Nundora | 3333 | 2.36 | yes |
| Teltawongee sandstone | Nundora | 3509 | 2.47 | yes |
| Kara jointed siltstone | Kara | 3704 | 2.39 | yes |
| Teltawongee sandstone | Nundora | 3871 | 2.40 | yes |
| Kara coarse sandstone | Wonnaminta | 4531 | 2.47 | yes |
| Teltawongee sandstone | Nundora | 5581 | 2.62 | No |
| Teltawongee sandstone | Scopes Range | 5560 | 2.69 | no |
| Teltawongee sandstone | Nundora | 2232 | 2.42 | yes |
| Ravendale sandstone | Macs Tank | 4020 | 2.21 | no |
| Ravendale sandstone | Cymbric Vale | 4156 | 2.24 | no |
| Ponto phyllite | Baroorangee Creek | 4610 | 2.45 | yes |
| Rowena Fm sandstone | Bynguano Rg. | 5000 | 2.52 | no |
| Rowena Fm quartzite | Bynguano Rg. | 5000 | 2.42 | no |

In Australian conditions, unweathered sedimentary rocks metamorphosed up to greenschist grade are normally given "standardised" sonic velocities >4500 m/s (quartzites), and typically ≥5000 m/s (Greenhalgh & Whitely, 1977). The upper limit for velocity is between 5500 m/s and 6000 m/s, dependent on the minerals present. For unweathered quartzose sandstones, standard velocities are c.2400 m/s to 4500 m/s (ibid.).

Expected average "standard" densities of metasediments are 2.60 t/m$^3$ for quartzites, 2.65 t/m$^3$ for schists and metagreywackes, and 2.74 t/m$^3$ for phyllites. The upper and lower ranges for these lithologies is given as 2.5 to 2.8 t/m$^3$ (Berkman, 1995). For unweathered quartzose sandstones, standard densities average 2.35 t/m$^3$, ranging from 1.61 to 2.76 t/m$^3$ (ibid.).

These standard properties can be used to judge the accuracy of the petrophysical data derived from outcrop. These are divisible into two groups, metamorphosed and unmetamorphosed:
The unmetamorphosed group consists only of the Ravendale sandstone (3 samples). These have velocities and densities close to each other, and within standard ranges, Thus the average density for the Ravendale sandstone can be assumed to be c.2.22 t/m$^3$.

The metamorphosed group comprises the remaining lithologies. Of these, the Rowena quartzite and sandstone have velocities of 5000 m/s, so their densities can be accepted without modification at c. 2.42 t/m$^3$ and 2.52 t/m$^3$ respectively. This gives an average value for the whole Mootwingee Group dataset of 2.52 t/m$^3$.

Values for the (meta-)igneous rocks sampled vary between 2.68 t/m$^3$ and 2.93 t/m$^3$. These values compare with "standard values" of 2.70 t/m$^3$ to 3.30 t/m$^3$ (Berkman, 1995). The lower end of the range is the Wilandra basalts, which should probably be scaled up to c. 2.75 t/m$^3$, the average value for all greenschist facies metabasalts elsewhere in the belt. The 2.93 t/m$^3$ value is for amphibolite grade metabasalts near the Mt Wright Fault.

The Teltawongee sandstones from core, and one Nundora sample, preserve realistic velocities of c.5600 m/s. The average density for these three samples is 2.66 ± 0.03 t/m$^3$. This indicates that the remaining Teltawongee samples can be

disregarded. The average density of the Teltawongee beds must also be weighted for the c.50% which are pelites. These are very difficult to sample in the field, but if a density of 2.74 t/m$^3$ for these units is assumed, the bulk density becomes 2.70 ± 0.03 t/m$^3$.

By analogy, the value of the Teltawongee sandstones can be extended to the similar lithologies of the Copper Mine Range Beds, and the Wilandra Beds, that are similar in character and metamorphic grade. This would give these units bulk values of around 2.70 ± 0.03 t/m$^3$.

Two units from the Kara Beds have depressed velocities relative to the expected values, indicating a need for scaling. If a velocity of 4100 m/s is assumed for the (jointed) siltstone, and 4800 m/s for the coarse sandstone, the densities can be scaled pro rata, and become 2.72 t/m$^3$ and 2.62 t/m$^3$ respectively. As the Kara beds are predominantly finer grained (Mills, 1992), the average density can be assumed to be closer to 2.71 ± t/m$^3$, weighted 10:1 silt: sand.

Assuming a velocity of 5100 m/s for the Wonnaminta Ponto Complex phyllite, a pro rata scale can be applied to the density to give 2.71 ± t/m$^3$ as an average value for this sample. This is probably a more representative density than those listed for the Wonnaminta area, and more closely resembles data from the Cymbric Vale. Note that this is an intuitively reasonable bulk density for the Ponto Complex, as phyllites comprise the largest fraction of this group by volume.

## Chapter 4: Nundora-Wonnaminta-Nuntherungie-Marrapina area

# Chapter 4: Nundora-Wonnaminta-Nuntherungie-Marrapina area

## 4.1 Location of Study Area. Reasons for study.

This region is named for four of the larger pastoral properties situated within the study area, which falls within a box defined by the Australian Map Grid (AMG) coordinates 558880mE, 6593120mN - 652660mE, 6632100mN - 672890mE, 6581810mN - 578890mE, 6542530mN (Zone 54). This area falls over the Bancannia, Wonnaminta, Kayrunnera, Yancannia, Nuchea, Cobham Lake and Fowlers Gap 1: 100 000 map sheets.

This area was selected principally because of its well-developed north-northwest trending linear magnetic anomalies (Figure 4.1.1). These permit the assumption of off-line continuity in two-dimensional forward modelling of magnetic data.

Other advantages of this area include the availability of seismic reflection data near Alecs Tank, and a petroleum well, Bancannia South No. 1 (Figure 4.1.2). The area also includes the recent mapping undertaken by Mills (1992). All of these features give further control to forward modelling of gravity and magnetic data.

This chapter is divided into 6 main parts. The first part examines in detail the current state of knowledge of the stratigraphy and structure of the Nundora-Wonnaminta-Nuntherungie-Marrapina area, and poses several key unresolved questions. The second part (sections 4.6 to 4.8) is a stratigraphic and sedimentological study of the newly defined Teltawongee Group. The third part (section 4.9) is a geochemical investigation of two igneous suites, and their tectonic implications. The fourth part introduces a new tectonic model for the region based on geophysical interpretations, and the fifth part (section 4.10) presents geological and additional geophysical tests for this model. The final part (section 4.12) is a synthesis of new geophysical and geological data on the Ponto Complex.

## 4.2 Topography, hydrology, land use, access

The topography and road network are shown in Figure 4.1.2. The area is a relatively flat-lying plain dissected by an extensive dendritic drainage network. The principal points of relief in the area are the Coturaundee Range (420 masl), followed by Koonenberry Mountain (406 masl) and Mt.Lynn (Turkaro Range) (338 masl). To the west the Barrier-Coko Ranges rise to 420 masl above the Bancannia plain which has a minimum height of 120 masl. The flat-lying area of the Bancannia plain is an area of

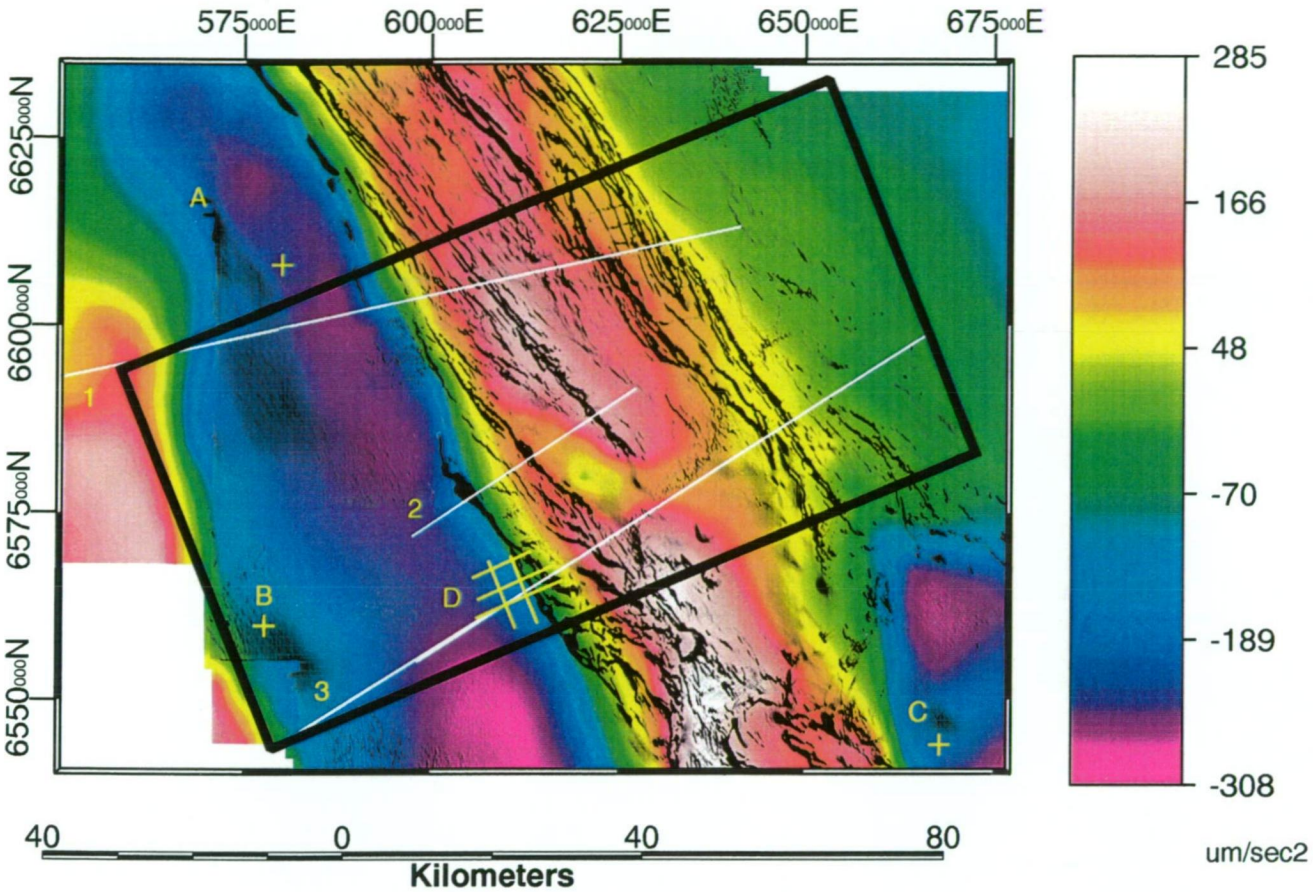


**Figure 4.1.1 Location of modelled traverses, Nundora-Wonnaminta-Marrapina-Nuntherungie area.**

Bouguer anomaly pseudocolour with TMI intensity layer shaded at 45 degrees from the NE. Grid is Australian Map Grid Zone 54.

Key: 1 = Nundora-Wonnaminta section; 2 = Turkaro Range section; 3 = Marrapina-Nuntherungie section; A = Bancannia North-1; B = Bancannia South-1; C = Gnalta-1; D = Alecs Tank seismic survey

**Figure 4.1.2 Digital Elevation Model and roads, Nundora-Wonnaminta-Marrapina-Nuntherungie area**

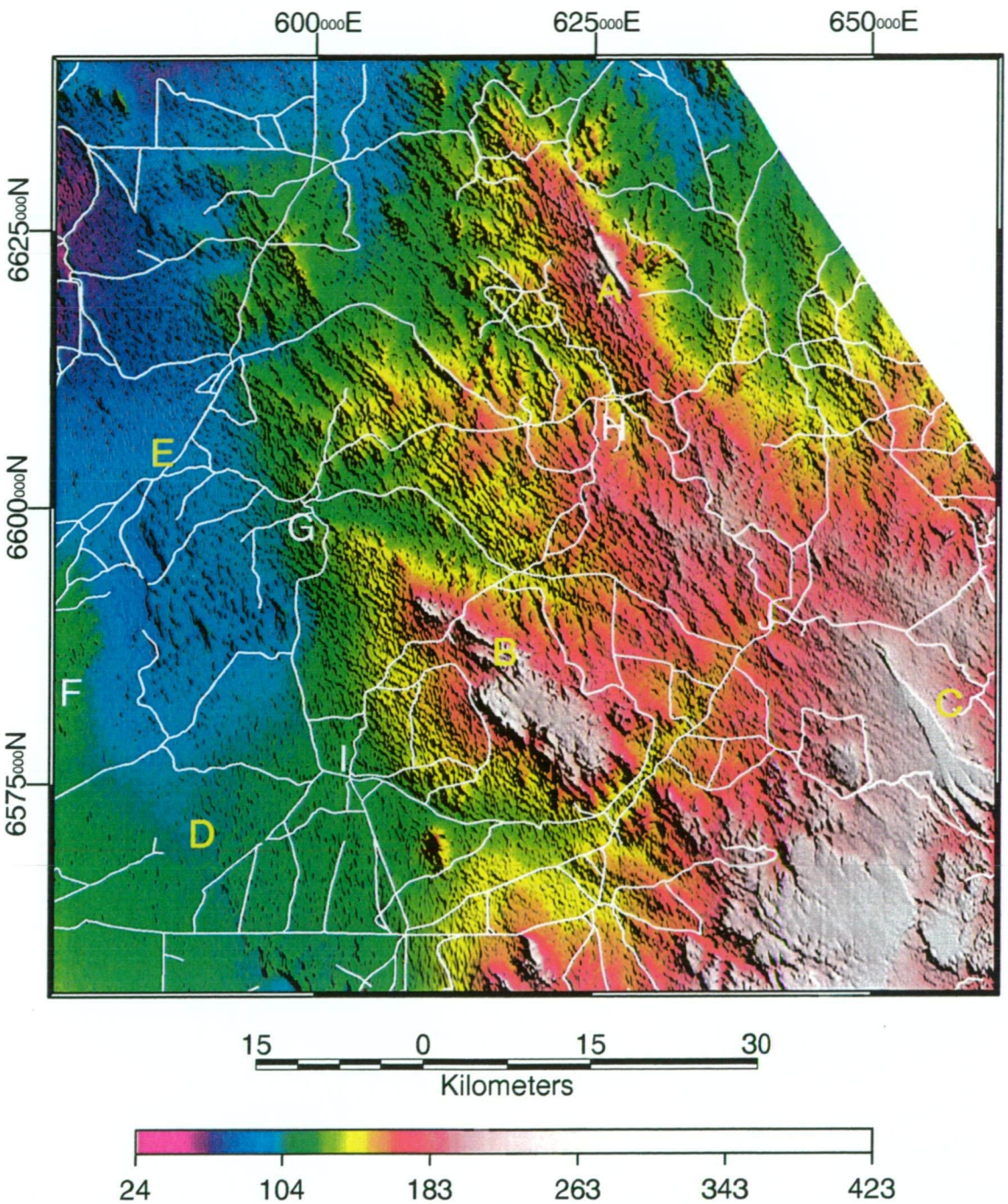


Digital Elevation Model pseudocolour and intensity layer shaded at 45 degrees from the northeast. Grid is Australian Map Grid Zone 54. Z Scale in masl.

Key: A = Koonenberry Mountain; B = Turkaro Range; C = Coturaundee Range; D = Bancannia Plain; E = Silver City Highway; F = Barrier-Coko Range; G = Nundora; H = Wonnaminta; I = Marrapina; J = Nuntherungie

internal drainage from the surrounding hinterlands, and is covered by an extensive ephemeral salt lake system.

Access to the area is afforded from the partially sealed Silver City Highway from Broken Hill to Tibooburra which runs through the west of the area, or from an unsealed road west from the opal mining settlement of White Cliffs. Two secondary roads connect the Silver City Highway with the road from White Cliffs; these are generally negotiable in conventional vehicles. A network of rough tracks maintained by the pastoral properties, gives four-wheel drive or motorcycle access to most parts of this area. However, all secondary roads and minor tracks in the area are unsealed, and are generally rendered impassable, even to 4 WD vehicles, by moderate to heavy rainfall (> 50 points or c.12mm).

### 4.3 Local Structure and Metamorphic Grade

Broad agreement exists that this portion of the belt is complex and polydeformed, but there is little agreement between authors about timing relationships of the various lithological groupings or their sequence of deformation.

The most recent structural synthesis of the belt was provided by Mills (1992).

The major regional fault in this area is the Koonenberry Fault, which is expressed as a gravity, aeromagnetic, topographic and aerial photo lineament. Mills (ibid.) described this feature as a Carboniferous west-side up dip-slip fault that deforms Late Devonian sandstones at Koonenberry Mountain.

The Western Boundary Fault (Nundooka Creek Fault of McIntyre & Wyatt, 1978; also Nundooka Fault of Stevens et al., 1996) is the western bounding fault to the Bancannia Trough (Neef et al., 1995); it is presently a north-northwest—trending normal fault that separates Early Neoproterozoic (Adelaidean) from Palaeozoic rocks (Stevens et al., 1996). It sinuously intersects the Nundooka Creek Fault (Neef et al., op.cit). The Nundooka Creek Fault appears to be post-Devonian (Ward et al., 1969), with evidence for Palaeogene and Quaternary movements (Neef et al., op.cit.).

The Lawrence Fault and its splays form the eastern margin of the Bancannia Trough (Crawford et al., 1997). These faults are reverse faults that appear to have been reactivated in the Carboniferous (Schroeder, 1987).

Mills (op.cit.) characterised the Ponto Complex, to the west of the Koonenberry Fault, as fault-bounded, with a near-vertical north-northwest—trending foliation. This foliation appears to be the axial planar surface to two overprinted sets of isoclinal folds, resulting from coaxial deformations. The early folding has been accompanied by biotite grade regional metamorphism.

Davies (1985) recorded five fabrics in the Ponto Complex from the Ponto Mine area, immediately west of the Koonenberry Fault. S1 in pelites was a slaty or disjunctive crenulation cleavage defined by chl-mu-Fe-oxides-qz-bio (sub-) parallel to S0. This was associated with "extremely rare" tight to isoclinal rootless F1 folds. Davies (1985) argued that a composite S0-S1 fabric has been rotated into parallelism with S2, and is now "strongly transposed".

Davies' (ibid.) S2 is the dominant fabric in the Ponto Mine area, purportedly refolding S1 and S0 in rarely preserved F2 folds. It is a spaced or crenulation cleavage also defined by chlorite-biotite-Fe oxides. Coaxial refolding of isoclinal F1 structures during F2 must produce spatially frequent and widespread reversals in younging direction. Despite this implication, Davies notes that reversals in younging are only minor, occurring in spatially limited F2 parasitic folds. His cross-section of the area also attests to this.

Davies' S3 is a kink banding or crenulation with sinistral sense; a rarer conjugate dextral kink banding was termed S3". S4 is a minor fabric with an inconclusive relationship to S3, also related to sinistral kink bands. S3 and S4 may be part of the same phase of deformation, hence Davies' nomenclature of these fabrics as S3/4.

Davies' (ibid.) S5 is the hinge surface to drag-related dextral kink bands that overprint S3/S4. This is limited to a zone immediately adjacent to the Koonenberry Fault, so is not a truly penetrative fabric.

S2 and S3/4 both occur in the Teltawongee beds in his area, suggesting a post-Lower Cambrian deformation. The F2 folds are present in carbonate rocks correlated with the Upper Cambrian-Lower Ordovician Kayrunnera Group (Davies subarea II), thus indicating a post-Early Ordovician age for this deformation. The "S2" cleavage does not occur in Upper Devonian rocks (Davies, subarea III), whereas "S3/S4" both occur in these rocks. This constrains the timing of "D2" to pre-Late Devonian. The post-"S2" cleavages may be Carboniferous or later.

The Kara beds described by Mills (op.cit.) are mainly situated in the core of a regional syncline with faulted-out limbs, thus preventing an estimation of the true thickness of this unit. Mills (ibid.) implied that the restored thickness of 16500 m, based on his regional cross section, might indicate unit repetition by obscured thrust faults. Very rare mesoscopic folds in the Kara beds are tight to isoclinal. The axial plane cleavage to these folds is sub-vertical, and has formed under chlorite-grade regional metamorphism. It is cut by a rare crenulation cleavage in exposures between Nundora and Conns Ck.

The Teltawongee beds disconformably overlie the Kara beds at Teltawongee Tank, as described elsewhere in this thesis. Mills (ibid.) described these rocks as similar in style to the underlying Kara beds: occupying a regional, limb-faulted syncline, tightly to isoclinally folded with a well-developed axial plane cleavage. The Teltawongee beds are also occasionally cut by a sinistral-kink crenulation cleavage (after Davies, op.cit.).

The Copper Mine Range Beds, considered part of the Teltawongee beds, are folded and faulted. Collins (1984) showed that the Copper Mine Range Beds have a statistically defined fold axis that plunges to 150°, and may form part of two asymmetric macroscopic synclines with overturned southwest limbs. Parasitic mesofolds on these structures plunge both northwest and southeast. Slaty cleavage in these rocks clusters about a vertical plane also trending to 150°.

The Teltawongee beds and Copper Mine Range beds are known to be intruded by a poorly known suite of diorites, dolerites and gabbros (Edwards, 1980; Zhou, 1993).

The Teltawongee beds and the igneous suite are unconformably overlain by the Late Cambrian to Lower Ordovician Kayrunnera Group at Morden Creek (Mills, op.cit.). The Kayrunnera Group is bounded by the Koonenberry Fault to the west, and forms a series of three thin, west-dipping wedges adjacent to it. These wedges contain open folding with a single, weak, spaced cleavage. The Kayrunnera Group has undergone chlorite-grade regional metamorphism (Wang Qizheng et al., 1989).

An equivalent of the Kayrunnera Group further to the south is the Late Cambrian Cupala Creek Formation (Powell et al., op.cit.), which occupies a fault-bounded open syncline to the west of the Koonenberry Fault at Cupala Creek. This syncline plunges gently to the south-southeast. It is unconformably overlain by the Late Devonian Mulga Downs Group that is not folded by the same events (Powell et al., ibid.).

Reconstructions of the pre-Late Devonian folding at Cupala Creek indicate a fold axis trace of 144° with overturned western limbs and axial plane surfaces that dipped steeply west.

The Early Devonian Mt. Daubeny Formation unconformably overlies the Ponto Complex to the west of the Koonenberry Fault on "Wertago" (after Neef et al., 1989; and K J Mills, unpubl. data). It contains interfering west-northwest and north-northeast—trending gentle folds (Figure 4.3.1) which form broad domes and basins. Brittle faults strike north-northeast (Figure 4.3.2), faulting out many north-northeast trending hinges. The formation contains no or very weak cleavage, being predominantly quartzites with low competency contrasts. Andesite flows interbedded in the formation contain the metamorphic assemblage chl-epi-ab-sp-mt ± carb-pre (Neef et al., op.cit.), indicating prehnite-pumpellyite facies metamorphism. Clearly, the deformation experienced by the Mt. Daubeny Formation was of different style and orientation to that found in older sequences.

The Late Devonian Mulga Downs Group, which unconformably overlies the Early Devonian, Ordovician and Late Cambrian sequences (Neef et al., ibid.; Powell et al., 1981; Davidson, 1981), is generally tilted rather than folded (Powell et al., op.cit.). Rarely developed buckle folds are open and asymmetric, with eastern limb dips shallower than western limbs. Axial planes plunge shallowly north-northwest—south-southeast. Bedding may be vertical to overturned where dragged into dip-slip faults (Powell et al., ibid.; Mills, op.cit.).

## 4.4 Summary

Structural studies of the Nundora-Wonnaminta area are fundamentally limited by lack of continuous exposures and a high degree of weathering. To date, there has been little or no agreement on the timing and sequence of deformation, a debate which was encouraged by a lack of age dating on the different lithologies, and hence an uncertain or incoherent stratigraphy for the area.

Now that absolute age parameters have been established for at least some of these rocks (Stevens & Fanning, unpublished data; Crawford et al. 1997), the following conclusions are possible.

The rocks that have traditionally been termed the "Wonominta beds" (Kara beds, Mt Arrowsmith Volcanics, Teltawongee beds-Copper Mine Range Beds and Ponto

# Figure 4.3.1 Folding within the Mt Daubeny Formation

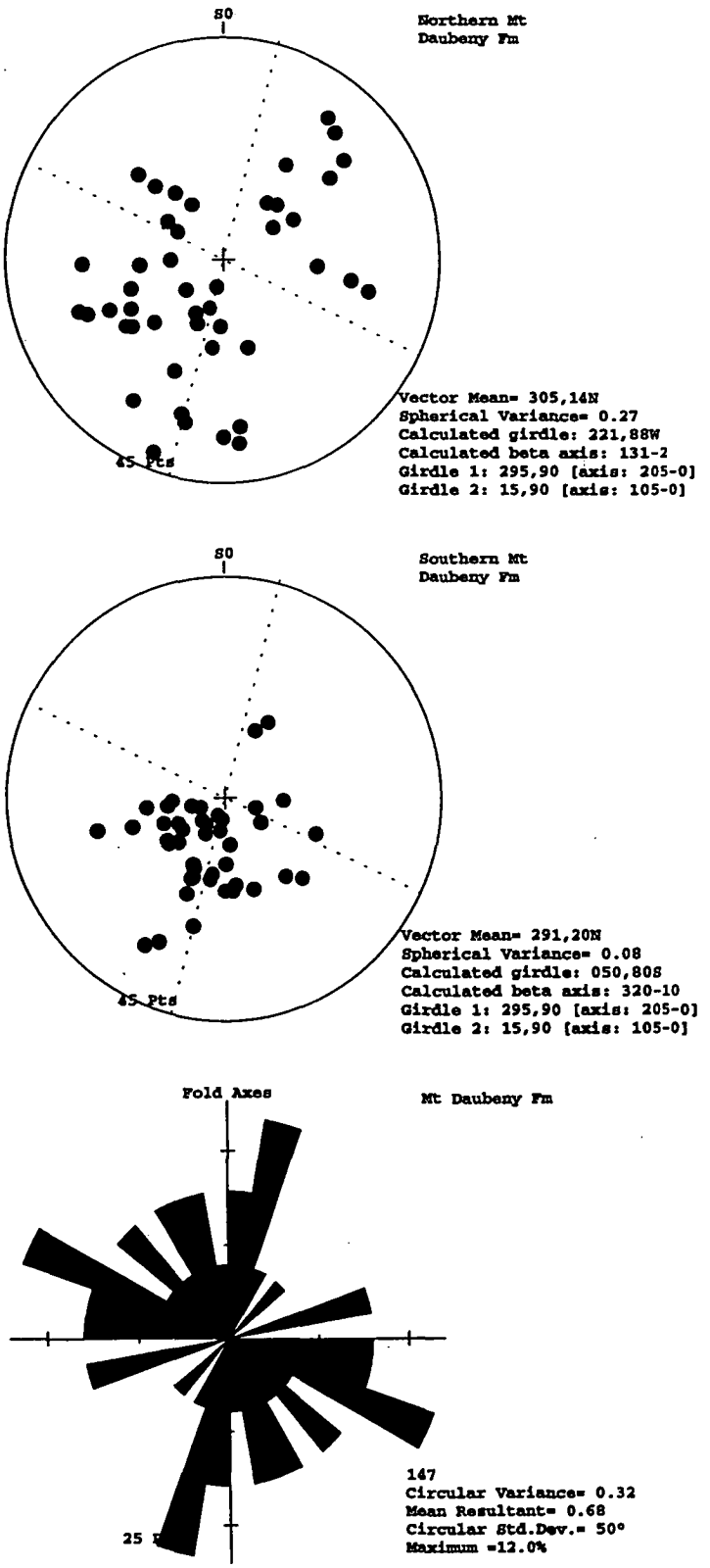


*divisions of Mt Daubeny Formation based on Neef et al., 1989.

## Figure 4.3.2 Fault orientations in the Mt Daubeny Formation

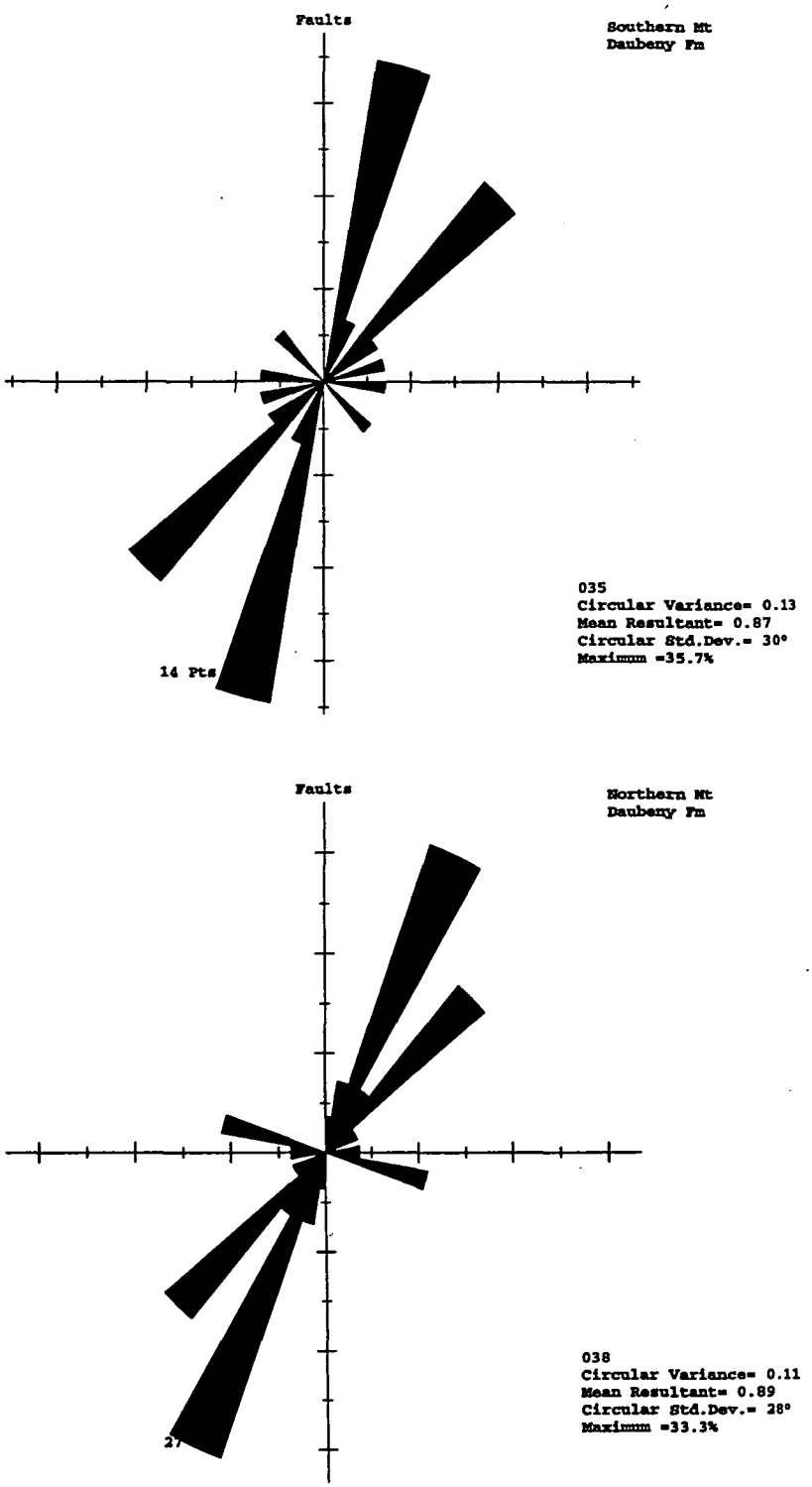


*divisions of Mt Daubeny Formation based on Neef et al., 1989.

Complex) are Late Neoproterozoic to Earliest Ordovician in age. The older rocks of this package (MAV to Teltawongee beds) have disconformable relationships and contain at least two cleavages; they are variably regionally metamorphosed, between chlorite and biotite grade for pelitic rocks, indicating a maximum lower greenschist facies metamorphic grade. The enigmatic Ponto Complex, which has been variably dated from Late Cambrian to Early Ordovician, contains three penetrative cleavages, and is also metamorphosed to biotite greenschist facies. The first cleavage formation in these metasediments seems to have formed during southwest directed compression.

This package is unconformably overlain by the Mootwingee Group and correlates, which are fossil dated as Late Cambrian (Mindyallan) to Early Ordovician (Arenig) (Wang Qizheng et al., op.cit.). These have undergone chlorite-grade regional metamorphism, similar to parts of the underlying sequence. They contain open folds with a weakly developed cleavage. These features may be due to a lack of competency contrast in a group that is dominantly quartzite (lower section) and monotonous shale (upper section).

The cleavage in the Mootwingee Group probably correlates with the second cleavage in the underlying rocks. It appears to have formed in conjunction with a second phase of isoclinal folding in the older rocks. The axes of the second folding in the lower package are generally coaxial to F1, resulting in strong transposition of S1 and S0.

The timing of the second deformation event is constrained to be earlier than the ?Late Silurian to Early Devonian (Gedinnian), (pre-deposition of the Mt Daubeny Formation; Neef et al., op.cit.) It is possible that this deformation may correlate with the Benambran event recognised in Victoria and eastern NSW (Gray & Foster, 1997b)

A third weak episode of deformation in the Mt Daubeny Formation is equated with the effects of the Middle Devonian Tabberabberan event in the Lachlan Orogen of NSW, Victoria and Tasmania (Gray & Foster, 1997b).

A fourth deformation has taken place sometime in the Carboniferous or later. This has in places buckled the Mulga Downs Group into open, low amplitude folds, but regionally has resulted in a more brittle style of deformation, reactivating earlier faults as dip-slip or strike-slip faults with crush zones. Mills (ibid.) correlated this deformation with the Kanimblan Orogeny recognised in central and eastern NSW.

### 4.5 Questions arising from previous studies

Several questions arise from the work of Mills (1992), and subsequent age dating of his sequences. The first concerns Mills' (1992) proposed correlation of the Kara beds-Teltawongee beds sequence with the Normanville Group-Kanmantoo Group of South Australia. Other than poorly-defined age equivalence, and a rough similarity in the style of stratigraphic contact, no convincing evidence has been suggested to support this hypothesis. A program of detailed stratigraphic logging and sedimentology is outlined below in an attempt to provide a comparable dataset with which to compare these two packages. The comparison is then outlined in chapter 9.

Related to the question above is Mills' (1992) inclusion of the Copper Mine Range Beds into the Teltawongee beds. Given a lack of type sections for both units, other evidence such as sedimentary provenance and sedimentary structures need to be investigated to support this correlation. Such a study is described below.

The timing of intrusion and tectonic significance of the mafic dyke suite that intrudes the Teltawongee and Copper Mine Range beds has not been dealt with in the past.

A new conundrum has been presented as a result of SHRIMP zircon U-Pb ages of volcaniclastic rocks within the Ponto Complex (described at 4.3 above). Why are these much-deformed schists and metavolcanics younger than the less-deformed rocks they are faulted against? Crawford et al. (1997) proposed that the Ponto Complex may be allochthonous. This concept is investigated via magnetic forward modelling of structures, and analysis of the stratigraphy and structure of these enigmatic rocks.

A further issue that has been contentious for over two decades, is the timing of development of the Bancannia Trough. Is this basin a Devonian rift, containing basement highs of Cambrian and Ordovician rocks (e.g. Webby, 1972), or a Cambrian rift floored by volcanics (e.g. Scheibner, 1972)? Intimately associated with the resolution to this problem is the true maximum thickness of the Devonian sediments: are they < 4000 m thick (e.g. Freeman, 1966) or up to 10 000m thick (e.g. Encom, 1994; B. Mullard, verb.comm. 25/2/97)? This question can only be solved by careful consideration of regional potential field data, together with stratigraphic, petrophysical and geochemical data from drillholes, as shown below.

The overarching question which links these inquiries, and which has not been satisfactorily addressed to date, is what tectonic setting (or settings) best accounts for

the observed mix of pre-Devonian facies and their present geometry? This question is clarified as the parts to the whole are answered.

## 4.6 Sedimentology of the proposed Teltawongee Group at Teltawongee Dam

### *4.6.0 Introduction*

The Teltawongee Group, is the most areally extensive unit in the Koonenberry Belt. At least three exposures were defined by Mills (1992), as described in Chapter 3. Earlier studies of the Teltawongee Group by Collins (1984), Davies (1985), Stevens (1991) and Mills (1992) showed that the rocks contain features that permit the Teltawongee Group to be divided into mappable formations; the objective of this study is to describe recent advances in mapping of the Teltawongee Group applying contemporary models of turbidite facies, and to describe the different formations that make up the Teltawongee Group using a combination of lithostratigraphic, sedimentological and geophysical criteria.

The western belt was thought to conformably overlie the undated Kara beds near Nundora Homestead (Mills, 1992), and an unknown thickness was shown under the Mesozoic cover of the Bancannia Trough. This package is characterised by the occurrence of coarse, sandy beds and red iron oxide cements (Mills, 1992). Cleavage is not well developed in this package, probably due to its sandy character. It is proposed that this unit be called the Nundora Formation.

Beds from the central belt around Wonnaminta H.S. shows classic turbidite couplets, and well developed sedimentary structures. The sandstones are unusually white mica-rich (phengite: Davies, 1985). Cleavage is well-expressed in mudstones as a fanning, slaty or phyllitic, continuous cleavage, whereas sandstones show a poorly developed, rough fracture cleavage. Kink bands are sometimes developed, but mesoscopic folds are extremely rare. This sequence is referred to below as the Mahomica Formation.

The eastern belt stretches from Koonenberry Mountain in the north to exposures near Grasmere (see Chapter 6), and incorporates the ?Early Cambrian Copper Mine Range Beds (CMRB) defined by Pogson & Scheibner (1971). The type section of these beds lies to the east of the Coturaundee Range at The Hummock (651500 mE, 6586000 mN). The eastern belt is bounded to the west by younger, unconformably overlying units, and appears to continue eastward for some kilometres (K. J. Mills, unpublished data). The area is cut by many suspected faults, and contains discontinuous outcrop and slump folding (Pogson & Scheibner, 1971; Collins, 1984).

Thus, the thickness of this section is unknown. Along strike, Davies (1985) mapped a minimum 300 m thickness of "Lower Palaeozoic metagreywacke" between the unconformably overlying Kayrunnera Group to the west, and younger silcrete cover to the east. The sediments in this belt are distinctively more muddy or shale dominated than in the other belts, and have a well-developed spaced or slaty cleavage. This unit is referred to below as the Copper Mine Range Formation.

In summary, it can be shown that the Teltawongee Group consists of at least three mappable units occurring in separate slices, with the minimum thickness of the total package being >3000 m.

*4.6.1 Methods and Parameters*

As indicated by Mills (1992), the softness of the Teltawongee Group sediments has led to poor weathering resistance. This in turn means that the outcrop distribution of these rocks is extremely discontinuous and poorly known. One of the approaches used by this study to overcome this limitation was the preparation of geophysical interpretations of "solid geology", guided by the different gravity, magnetic and radiometric responses of the fold belt. Because of the wide geographic distribution of the Teltawongee Group, I have chosen to focus this discussion on the Wonnaminta 7336 1: 100 000 map sheet, where all three map units are present, and most structural styles well-expressed. Detailed map interpretation and field work was also conducted on Cobham Lake 7337, Nuchea 7335, Kayrunnera 7436 and Grasmere 7435. The geophysical map boundaries of the Teltawongee Group have been the subject of detailed field traversing at c.1: 15 000 scale, recording stratigraphic and structural data where outcrop permitted.

In addition to mapping, a detailed stratigraphic and gamma ray log was constructed for the base of the sequence at Teltawongee Dam. Sedimentological observations were compiled for this section, and also for several traverses in the central and eastern belts; poor outcrop conditions did not permit the construction of detailed logs in these areas. For each traverse, a representative suite of sandstone samples was acquired to investigate similarities in grainsize, sorting and provenance between areas.

The term "bed" in this study is used to refer to a discrete layer of sediment, rather than a "sedimentation unit" as used by some authors (e.g. Powell et al., 1993). Graded beds have been distinguished from beds with gradational contacts using the methodology of

Bouma (1962). Sections have been thickness corrected using local dips, but have not been compensated for regional strain or volume loss during deformation.

Mills (1992) identified a section in Nundora Creek near Teltawongee dam as the basal contact of the Nundora Formation, conformably overlying the Kara beds. As part of the present study, a stratigraphic section was measured across the contact between cleaved, grey phyllites of the Kara beds, and the sandstone-mudstone package of the Teltawongee beds. The coordinates of the base of this section, are approximately 600830 mE 6600250 mN. The dip-corrected section extends for only 20 m, bearing 33° magnetic. Two subsidiary sections were measured; the first at 600980 mE 6600270 mN, for 11m bearing 35° magnetic, and the second at 600990 mE 6600270 mN for 13 m bearing 33° magnetic. A subsidiary traverse was also made through the discontinuous outcrops in Nundora Creek bearing west-southwest towards Nundora H.S.

The first section includes the boundary stratotype for the base of the Teltawongee Group. This is defined by the scoured base of a 0.5m thick medium- to fine-grained buff sandstone bed overlying grey, banded phyllite at the foot of the northern bank of the creek. The location of this stratotype occurs where a tributary joins Nundora Creek 40m south of Teltawongee Tank (see Figure 4.6.1).

Figure 4.6.2 shows the stratigraphic log for the principal section, and Figures 4.6.3 & 4.6.4 the subsidiary sections.

The base of the principal section was uncovered by flash-flooding in the creek during May 1997. Prior to this time, the boundary was thought to be conformable (cf. Mills, 1992), based on the exposure included in subsidiary section 1. Figures 4.6.5 shows that the contact in the principal section is erosional, with rip-up clasts of the underlying Kara beds found in the basal layer of the Teltawongee beds, and with a slight bedding discordance of c.5°. These features indicate that the boundary is disconformable.

Section 2 contains only one bed of the Teltawongee beds. This is a massive, grey coarse-grained arenite to granule sandstone. This bed is correlated with bed K in the third section, and bed F in the principal section. If this interpretation is correct, it means that the basal graded beds have been eroded or not deposited in section 2. Comparison of the thicknesses of this layer in each section (1.58m, 2.30m, 4.60m) suggest that the underlying substrate was channelled in some fashion, or had otherwise developed some local topography.

**Figure 4.6.1 Locality Map. Basal stratotype, Teltawongee Group (Nundora Formation)**

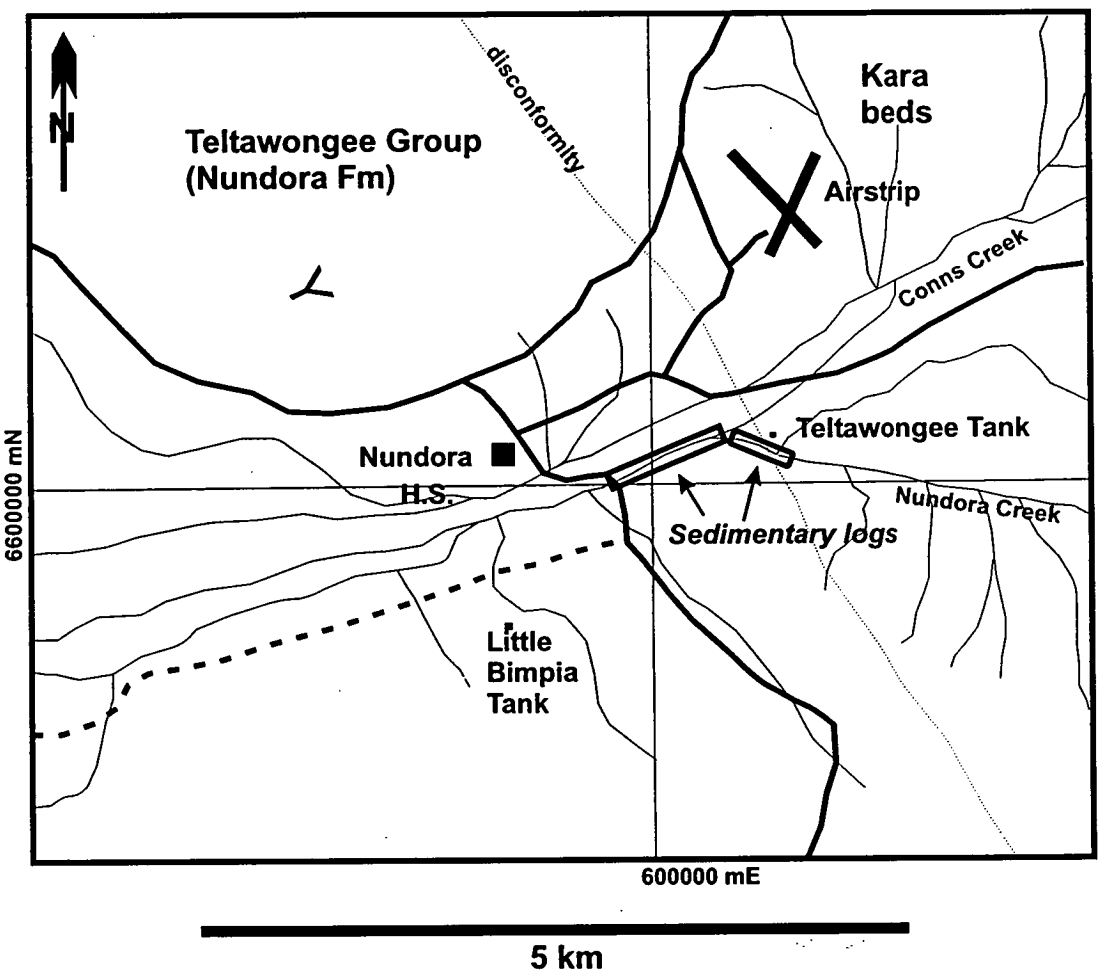

# Figure 4.6.2

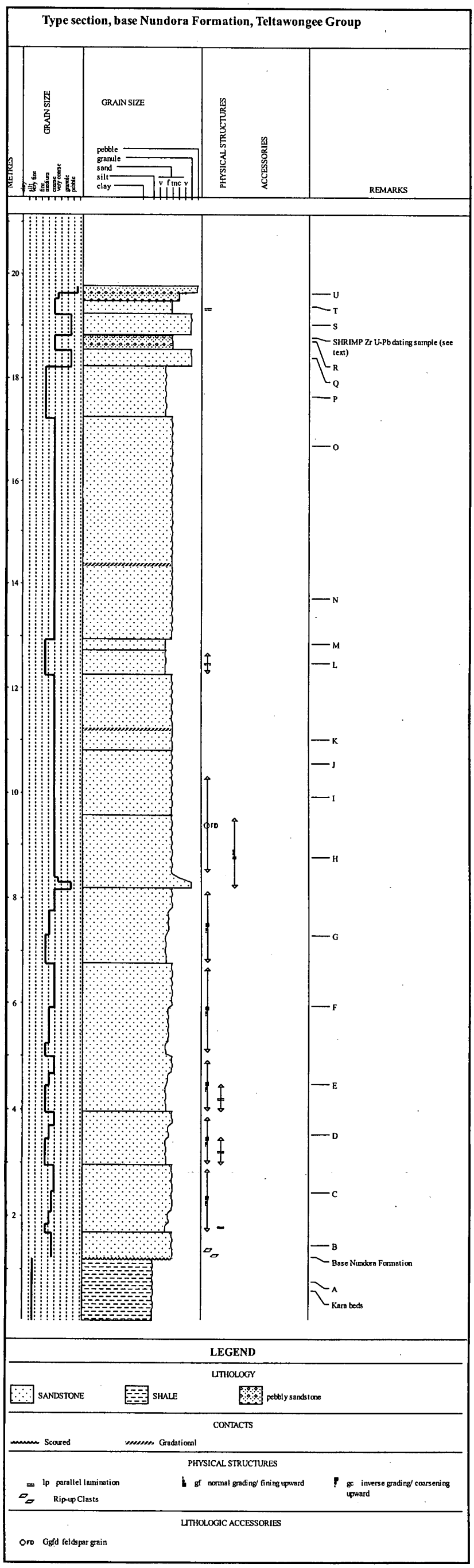
Type section, base Nundora Formation, Teltawongee Group
METRES
GRAIN SIZE
GRAIN SIZE
pebble
granule
sand
silt
clay
v f m c v
PHYSICAL STRUCTURES
ACCESSORIES
REMARKS
20
18
16
14
12
10
8
6
4
2
U
T
S
SHRIMP Zr U-Pb dating sample (see text)
R
Q
P
O
N
M
L
K
J
I
H
G
F
E
D
C
B
Base Nundora Formation
A
Kara beds
LEGEND
LITHOLOGY
SANDSTONE
SHALE
pebbly sandstone
CONTACTS
Scoured
Gradational
PHYSICAL STRUCTURES
lp parallel lamination
gf normal grading/ fining upward
gc inverse grading/ coarsening upward
Rip-up Clasts
LITHOLOGIC ACCESSORIES
Ggfd feldspar grain

# Figure 4.6.3

**A**

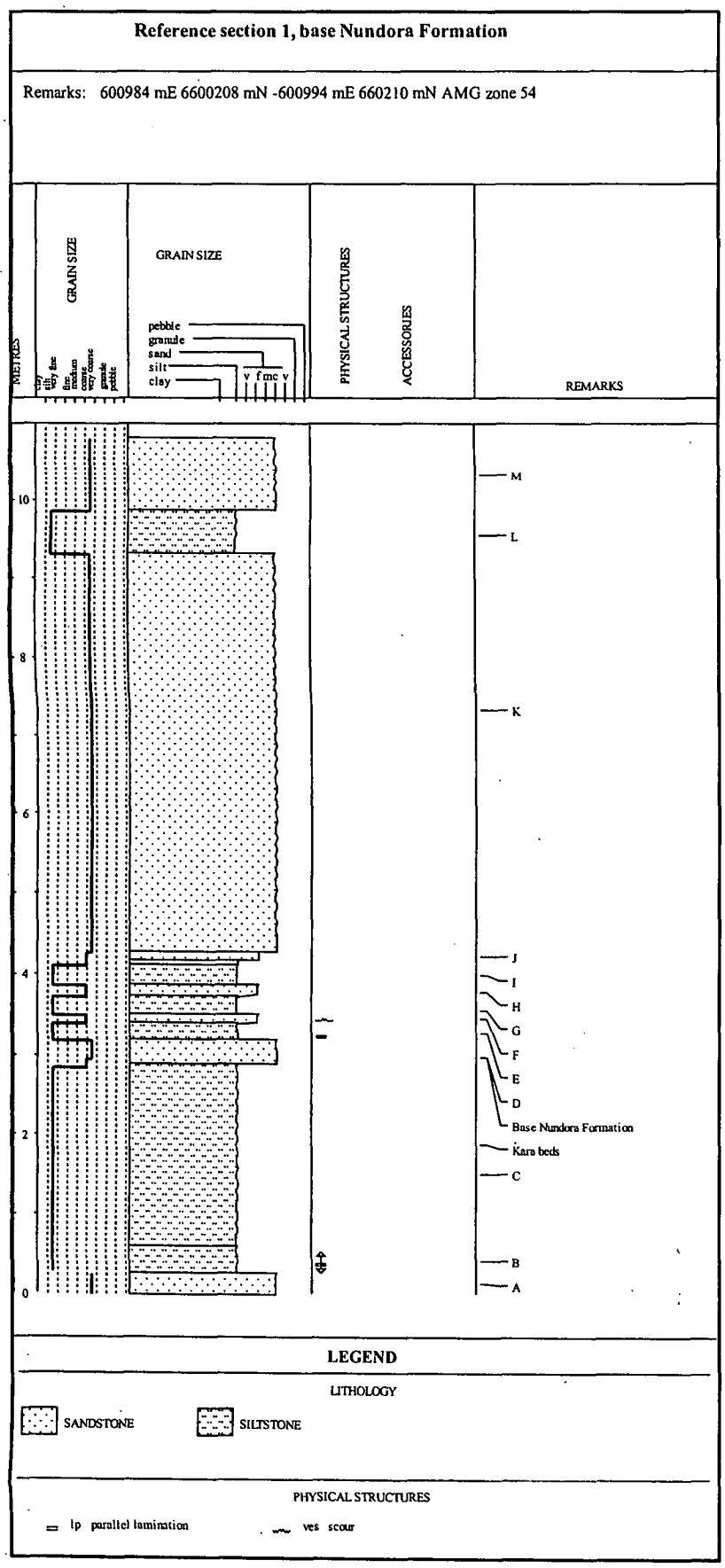


**B**

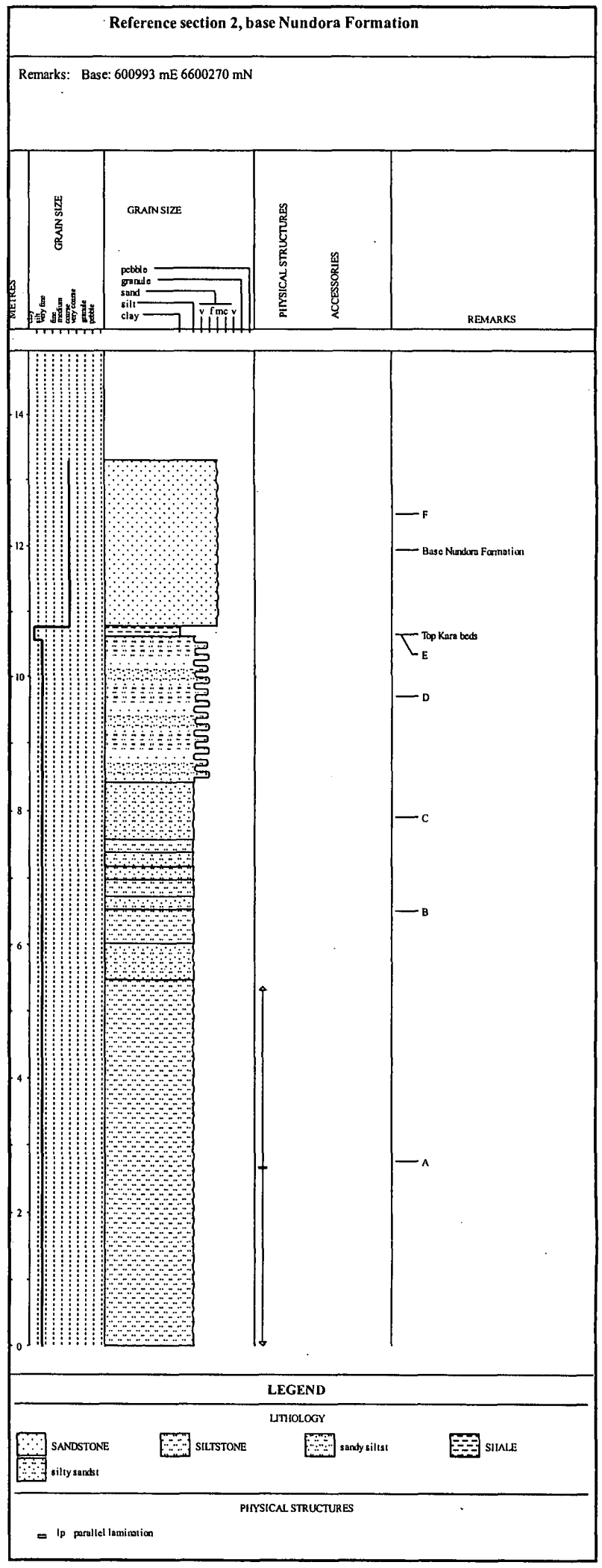

**Figure 4.6.4 Basal disconformity under the Nundora Fm**

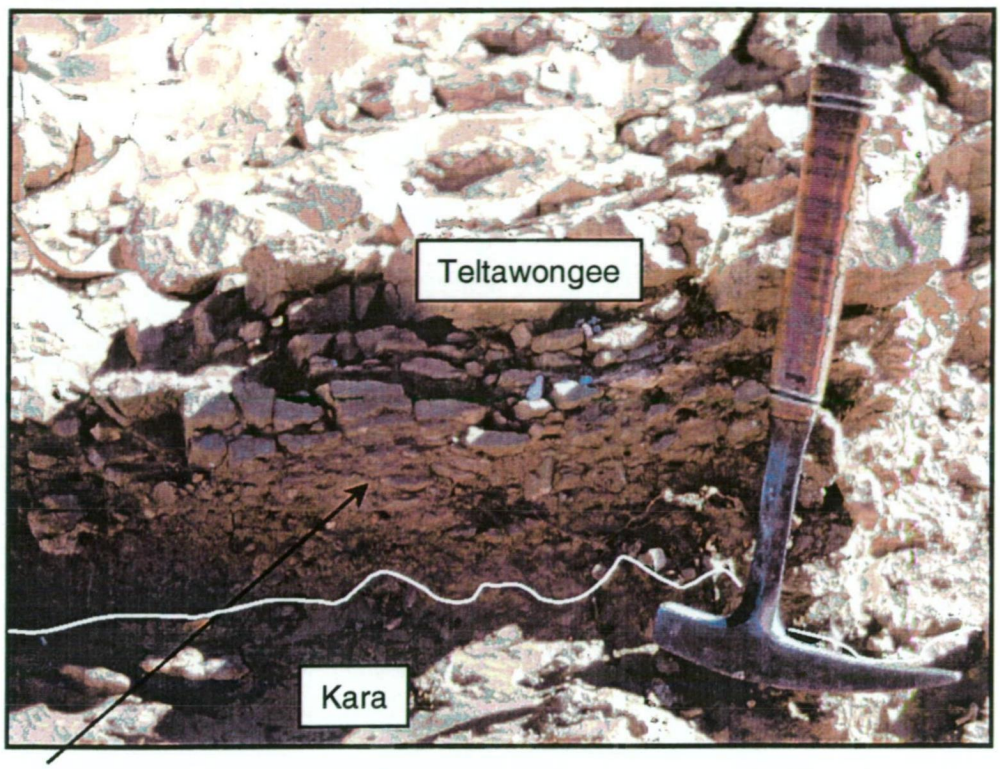


* Note angular rip-up clasts of underlying Kara beds in basal bed

**Figure 4.6.5 Gamma ray log of basal stratotype, Nundora Formation**

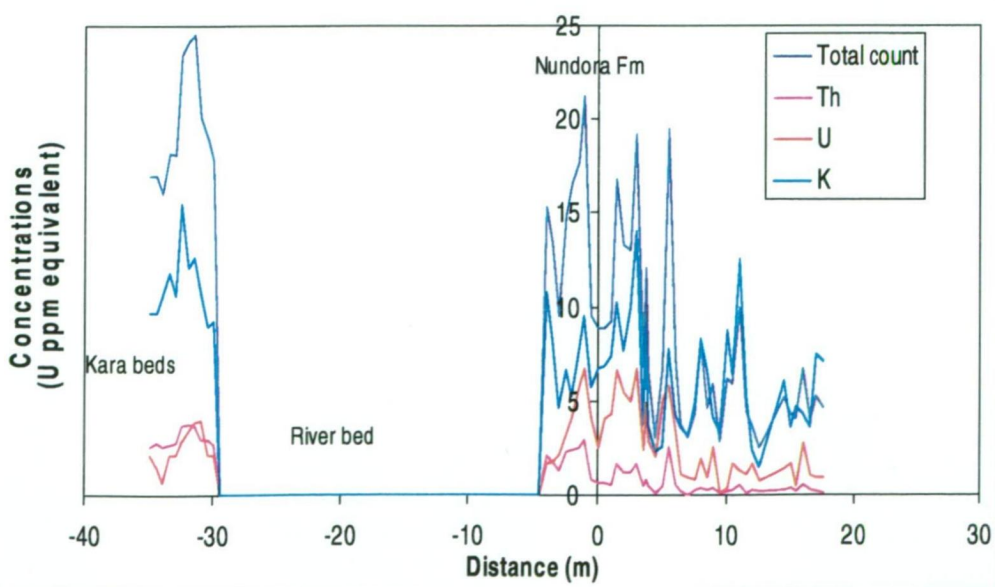

Section 3 contains both graded and massive beds, with the former occurring at the base.

A section was also walked out through the creek to the west of the type section. Recent alluvial sand drifts interrupt the continuity of the beds in this section, but they appear to be a monotonous series of sandstone-mudstone couplets with normal grading. Further to the northwest, near Nundora airstrip, sandstones and shales of this formation have a reddish colouration, probably due to iron oxide content.

*4.6.2 Gamma Ray Logging of the Basal Stratotype*

These data were acquired with a EG&G Geometrics 256 channel gamma ray spectrometer. This is a portable unit with a hand-held sensor with a crystal volume of 2.1L. The spectrometer is operable in two modes: full 256 channel acquisition capable of storing eight records, or window acquisition, capable of storing 60 records. The window mode was chosen with the following regions of interest used: channels 109-123 K, 192-214 Th, 131-149 U, 70-255 Total Count. Corrections for other naturally occurring radionuclides (e.g $Co^{60}$, $Rn^{222}$) have been made (see below)

Data were acquired at 50 cm intervals from 30 m beneath the datum for the proposed Nundora Formation to the limit of outcrop. As the average bed thickness is c.1m, this spacing avoids spatial aliasing of the gamma ray response. The reading interval for each measurement was 60 s, with the sensor held in contact with the outcrop.

The raw data were processed using a computer program supplied by EG&G. This applied corrections to the data for background counts and environmental nuclides other than the nuclides of interest. Data were then converted from counts to equivalent concentrations of U, expressed in parts per million equivalents (U ppm equiv.) using the matrix relationship outlined in the operations manual for the instrument.

The final dataset expressed as a function of distance above or below the datum is shown in Figure 4.6.6. Note that the gap in responses between -30 and -5 m is due to lack of outcrop. In any case, this interval is not within the proposed Nundora Formation, but the Kara beds.

It is clear from this diagram that the major response of the proposed Nundora Formation is in the potassium channels. The bimodal character is due to changes in

the concentration of this element in silty-shaly units (high concentrations) relative to sandy units (low concentrations).

### 4.6.3 Physical sedimentology of the proposed Nundora Formation

Type section: Nundora Creek at Teltawongee Dam

Thickness: 19.73 m logged. Reference sections: 11 m and 13 m. True thickness is much greater, in the order of hundreds of metres. However, poor outcrop conditions preclude logging the entire formation accurately.

Rock types: Using the classification of Folk et al. (1970), these rocks are very fine- to medium-grained sublitharenites (beds B to J) coarsening upward to medium- and coarse-grained subfeldsarenite and feldspathic litharenite. Occasional massive granule sandstones and interbedded mudstone-siltstone layers are also observed.

Geometry: coarser sand bodies have thick (up to 5 m) wedge and concave channel forms. Fine-grained sand and silt units have sheet geometry.

Contacts: basal contact with Kara beds is scoured with rip-up clasts. Most internal contacts are sharp, but channelling/scouring does exist (ref section 1, bed F), as do gradational boundaries. Massive sand beds have sharp bases in the reference sections (ref. Section 1 bed K; 2 bed F) but the equivalent bed in the type section has a gradational base. The upper part of the sequence is obscured by Recent alluvium.

Bedding: medium to very thickly bedded (0.25 to 5.5 m). The type section thins upwards. Silty bases to beds are thickly laminated (c.0.5 -1 cm).

Sedimentary structures: fine-grained heavy mineral laminations are common in the type section. Beds C to G are reverse graded. Bed H is normally graded. Channel structure was observed in reference section 1.

Petrographic texture: these units are all moderately to well-sorted arenites with sub-round to sub-angular grain shapes. Well-sorted units tend to have more round to sub-round grains. Grain size coarsens upward, and the feldspar content also increases up-section.

**Figure 4.6.6 Bedding features in the Nundora Formation**

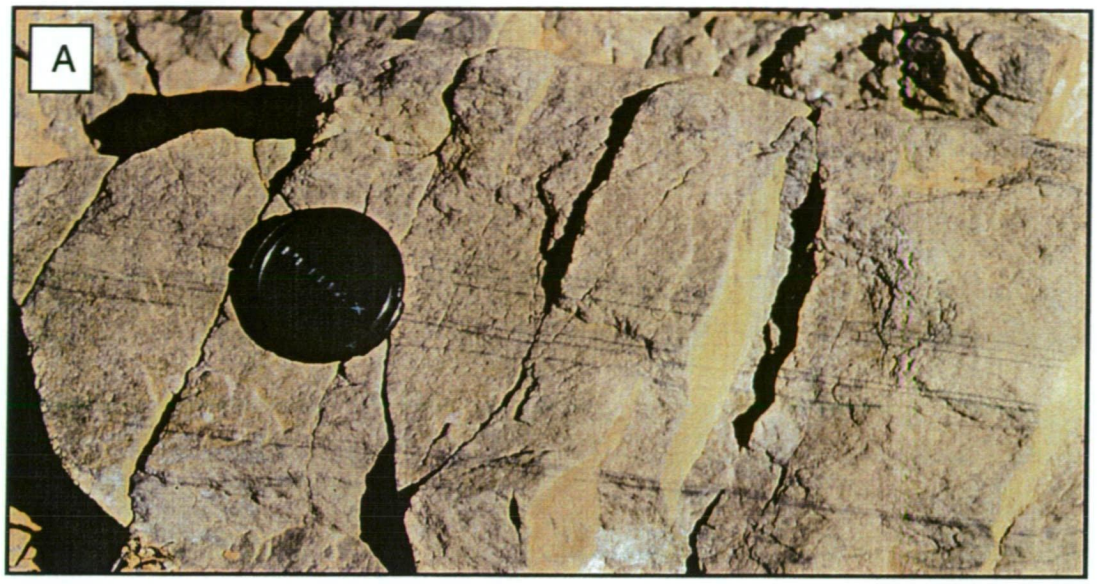


A = Heavy mineral (mainly ilmenite) laminations in medium-bedded sandstone

B = Medium-bedded medium-grained sandstone channels interbedded with thinly bedded fine-grained sandstone

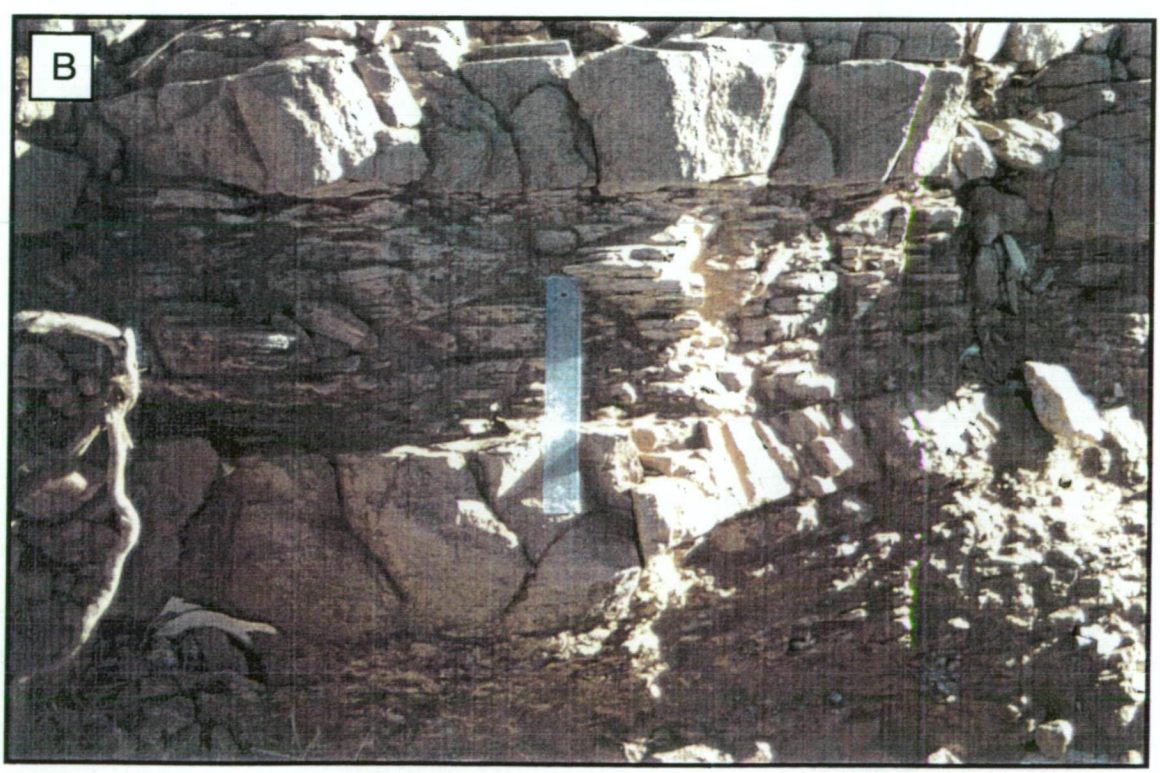

Heavy mineral assemblage: three samples giving high radiometric counts were selected for further investigation of heavy mineral populations. These samples, from beds B, D & F in section 3, were crushed in a jaw crusher and hydraulic press. The fine-grained sand fraction (63 to125 μm) was then removed by sieving in running water. Further concentration of the heavy minerals was achieved by flotation in heavy liquids (tetrabromoethane) and superpanning. The resulting separates were then rotated through a magnetic separator at different currents to separate more magnetic fractions (rutile, ilmenite, chromite, tourmaline) from less magnetic phases (monazite, zircon, garnet). These fractions were then mounted on a thin section, polished, and examined petrographically.

The heavy mineral assemblage of the Nundora Formation as determined by these methods is dominated by and ilmenite, with lesser, but significant, tourmaline, zircon and rutile. Garnets and chromites, common in eastern Australian sedimentary assemblages of comparable age (Berry et al., 1997; and S. Meffre, unpublished data) were not observed; however accessory microcline was common. Monazites, the assumed source of the Th anomalies related to these beds, were not observed.

Geophysical logging: calibration of the gamma log against the geological log shows the coarsening (increasing sand content) upward trend with the suppression of the K signal and total count channels. Zircons found in the heavy mineral laminae probably account for elevated U values in the base of the sequence. The differences between the underlying Kara siltstones and the graded sandstones of the types section are evident: the Kara siltstones have higher total counts (up to double that of the upper sand beds of the proposed Nundora Formation), with most of the contribution coming from elevated K counts. Conversely, U is generally lower, due to a lack of zircon-bearing sand.

Age: Samples of bed Q or R were taken by B. Stevens for detrital zircon SHRIMP U-Pb dating. Analysis of 25 grains returned a detrital population with a main peak at 1196 ± 21 Ma (Late Mesoproterozoic), and secondary peaks at 950 to 1000 Ma (Early Neoproterozoic), and out to 2680 Ma (Archaean). (Stevens & Fanning, unpublished data).

### *4.6.4 Facies Interpretation*

Mills (1992) briefly described the lower contact of the Nundora Formation as conformable with the underlying cleaved siltstones of the Kara beds, and described the

section as quartzofeldspathic lithic sandstone with graded bedding. He noted the presence of coarse-grained granule beds, and red iron oxide cements. These features were interpreted as indicating a proximal turbidite facies.

The new sedimentological data presented above allow a more detailed facies interpretation to be put forward, based on turbidite facies associations presented by Walker (1992) and Galloway & Hobday (1996).

The basic facies model for turbidites is the Bouma sequence, which is used by Walker (1992) to define the "classic turbidite" facies. It consists of a generally fining upward sequence of beds from A (massive coarse-grained, normally graded sands with scoured bases); B (parallel laminated sand); C (rippled and convolute rippled fine-grained sands); D (laminated mud and silt); and E (massive mud and hemipelagic mud). The classical turbidite facies is thought to represent levee and channel deposits in the fan system. It is clear that the sections observed do not represent any of the Bouma subdivisions, and are thus not "classical turbidites".

Several other facies associations were noted by Walker (1992), including massive sandstone facies; pebbly sandstone facies; conglomerate facies; and pebbly mudstone-slump facies. As descriptive/predictive models, most of these can be ruled out by the absence of pebbles and conglomerate material in the section. The massive sandstone facies however, provides a good descriptive model for the section at Teltawongee Dam.

This facies is defined as a gradation from thick-bedded classical turbidites, containing more evidence of erosion, channelling at the metre-plus scale, and the amalgamation of flows by scour elimination of hemipelagic mud. Bed thicknesses in this facies range from 0.5 m to many metres, with only the Bouma A division represented. Graded bedding is described as subtle or absent. All of these features are found in the type section of the proposed formation. A further feature not observed, but listed as common in this facies is the presence of dish-and-pipe structures resulting from fluid escape.

Walker (1992) argued that a thinning-upward sequence of massive sandstones passing into classical turbidites imply channel filling processes. This suggests that the environment of deposition of the proposed formation was a channel-levee complex. This interpretation is supported by idealised gamma log sections for this facies, which

show an upward thinning response similar to that observed (Galloway & Hobday, 1996).

*4.6.5 Provenance*

The main detrital age data peak at c.1200 Ma are anomalous in the context of eastern Australia. The most likely source of quartz, microcline, muscovite and accessory tourmaline, rutile, ilmenite and zircon, indicating a felsic igneous or quartzofeldspathic metamorphic source, is the Broken Hill block, some 130 km to the southwest. This derivation is supported by palaeocurrent observations made elsewhere in the old Teltawongee beds by Mills (1992), which show a southerly derivation. However, the stratigraphy of the Broken Hill Block has recently returned SHRIMP U-Pb zircon ages of between 1710 Ma and 1670 Ma (Donaghy et al., 1996), precluding these as the source. The Adelaidean sediments of the Torrowangee Series are also ruled out as a potential source terrain; these are correlated with the Adelaidean of South Australia which commences with the Willouran flood basalt province (Crawford & Hilyard, 1989), dated at c. 800 Ma (Fanning et al., 1986).

The closest source of 1200 to 1000 Ma zircons is therefore the Musgrave Block of central Australia (Ireland et al., 1995), a so-called "Grenvillean" source terrain (Ireland et al., 1998). However it is difficult to conceive a plausible mechanism whereby all of this material could be transported across a present-day distance of 1200 km, and yet still retain evidence of relative immaturity such as primary feldspars, angular grains, and abundant matrix. It is more likely that the heavy mineral grains such as zircon represent the product of at least two or more episodes of crustal recycling, and that the petrographic and sedimentological features are primary, related to a source to the south, possibly the Broken Hill Block. Such questions of source material also pertain to the Kanmantoo Group (cf. Ireland et al., 1998) with which the Teltawongee Group has been compared. These issues are addressed in Chapter 9.

## 4.7 Sedimentology of the proposed Copper Mine Range Formation (ex-Copper Mine Range Beds)

The sedimentology of the Copper Mine Range Beds (CMRB) was investigated in detail by Collins (1984), before the erection of the Teltawongee beds as a stratigraphic unit by Mills (1992). The CMRB were characterised as interbedded laminated shale, siltstone, mudstone and poorly-sorted lithic sandstones. The coarser units show graded bedding, load casting and flute casts. All of these features, also found within

the Teltawongee beds, led Mills (ibid.) to incorporate the CMRB into the Teltawongee beds.

Wang Qizheng et al. (1989) implicitly defined the upper boundary stratotype for the Teltawongee beds when they described the angular unconformity at the base of the overlying Mindyallan Morden Formation at Morden Ck. This boundary is the explicit lithostratigraphic (but not chronostratigraphic) correlate (Wang Qizheng et al., 1989) of the angular unconformity described between the Copper Mine Range Beds and the Idamean Cupala Creek Formation (Powell et al. 1981). Because of the lithostratigraphic correlation of these two boundaries and the lithostratigraphic incorporation of the CMRB into the Teltawongee beds by Mills (1992), any definition of the upper boundary stratotype is free to choose which location is the stratotype, and which the hypostratotype. Better outcrop conditions and the detailed sedimentological study conducted by Collins (1984) in the Coturaundee Range area argue that the upper stratotype for the proposed Teltawongee Group should be defined in this location.

In order to characterise the upper stratotype in similar terms to the lower stratotype, a reconnaissance of an area mapped by Collins (1984) was made in the headwaters of Cupala Ck. Eight samples of sandstone were collected between 657627 mE, 6581449 mN and 657583 mE, 6581523 mN. This is in the lower part of the section mapped by Collins (1984), with the sequence younging to the west. The basal contact of the originally defined CMRB is not exposed in the type area, but a fault contact was mapped at c.657500 mE 6817300 mN. Mills (unpubl. data) indicates that the units to the east of this fault, comprising black and brown shales, are probably a fault slice of Kara beds. Black shales, possibly belonging to the Kara beds were observed by the author at 657622 mE 6581669 mN in a tight asymmetric fold.

Unfortunately the exposures of the proposed Copper Mine Range Formation in this area are not continuous for more than a few metres, preventing the construction of a stratigraphic section and acquisition of gamma ray data.

### *4.7.1 Physical sedimentology of the proposed Copper Mine Range Formation*

Type area: Headwaters of Bunker Creek, west of "Morambie" airstrip, on the eastern pediment of the Coturaundee Range. A subsidiary area exists in the headwaters of Cupala Creek, between the Coturaundee Range and Spring Hill (= "The Hummock" of Collins, 1984).

Thickness: the thickness of the section in the type area is indeterminate, due to bounding by faults, possible internal faulting, discontinuous outcrop and slump folding (after Pogson & Scheibner, 1971; Collins, 1984). Hence no type section can be constructed. Along strike, Davies (1985) mapped 300 m of "Lower Palaeozoic metagreywacke" between the Kayrunnera Group to the west, and younger silcrete cover to the east.

Rock types: Collins (1984) mapped outcrops to the east of the Coturaundee Range as shale and siltstone, with an interval of "sandstone turbidites" in Bunker Creek. Sampling by the author showed these latter units to be medium-grained lithic arenites grading to mudstones, and fine-grained to very fine-grained lithic arenites. This accords with the description in Pogson & Scheibner (1971). Collins (1984) also recorded feldsarenites.

Along strike, east of Koonenberry Mountain, Davies recorded medium- to coarse-grained feldspathic litharenites. These were interbedded with thick metamudstones.

Geometry: Sheet geometries over strike lengths of 5 to 10 m were observed in Bunker Creek. In Cupala Creek, generally thin, lensoidal sand sheets were observed enclosed within large thicknesses of laminar shale.

Contacts: this area is in fault contact on both its eastern and western margins. Internal contacts are generally sharp and planar, although Collins (1984) noted the presence of some erosive scours with abundant rip-up clasts. Powell et al. (1982) described an angular unconformity between the proposed formation and the overlying Cupala Creek Formation.

Bedding: Bunker Creek contains both very thick (1-2 m) and medium bedded (10-30 cm) units. Laminations in graded bed tops are thin (1-2 mm). Very thick beds are massive. Cupala Creek contains generally thin sand beds within thickly (>4 mm) to thinly (< 1mm) laminated shales.

Sedimentary structures: the dominant sedimentary feature in Bunker Creek is reverse grading, which indicates tight, elliptical folding. Planar cross-bedding, and wavy and planar laminations are also common. Occasional load casts and small scale (< 0.2 m) chaotic slump folds were recognised in a few localities, whereas one distinctive bed at 657452 mE 6586624 mN contains perpendicular-to-bedding cylindrical features

interpreted as worm burrows. Collins' (1984) more extensive study also noted convolute laminations, climbing ripples and starved ripples. Pogson & Scheibner (1971) noted flute casts. The enclosing shaly facies is finely laminated.

The predominant feature of the enclosing laminated siltstone and shale units which was recorded by both Pogson & Scheibner (1971) and Collins (1984) was the presence of slump folding and other soft-sediment deformation (block sliding, bed disaggregation, chaotic bedding).

In the northern section, Davies (1985) noted reverse grading, and planar- and cross-laminations.

Petrographic texture: In the type section, these units are all moderately to well-sorted with distinctive angular, prismatic grain-shapes. In the northern equivalents, grain shapes are also angular, blocky, elongate or platy (Davies, 1985). These features indicate relatively immature sediment.

Age: Webby (1984) described trace fossils *Planolites* and *Chondrites* from the turbiditic sequence which were interpreted to indicate Early or Middle Cambrian age. Collins (1984) also found sponge spicules and unidentified radiolarian tests in both the turbiditic sequence and the enclosing shale; these are also indicative of an Early or Middle Cambrian age. Mills (1992) mentioned discovery of possible brachiopod fragments in the sequence; these have been described by Percival (1995) as a poorly preserved paterinide brachiopod fauna, giving a possible early Middle Cambrian biostratigraphic age.

### *4.7.2 Facies Interpretation*

Pogson & Scheibner (1971) interpreted this sequence as deep marine and "flysch like". "Flysch", describing impure marine calcareous sandstones and shales, interbedded with breccias, marls and conglomerates deposited in a syndeformational setting (Gary et al., 1972), is no longer recommended as a term to describe turbidites (Whitten & Brooks, 1972). Deposition was inferred to have taken place to the east of a fault scarp now represented by the Koonenberry Fault.

Collins (1984) interpreted the sequence as shelf storm surge deposits, with the laminated siltstones having been washed from the nearshore environment to the shelf during and immediately after storm events. This interpretation is inconsistent with the

current understanding of storm-dominated environments. Facies models proposed by Walker & Plint (1992) for storm-dominated shelves emphasise the presence of Hummocky Cross Stratification (HCS) and Swaley Cross Stratification (SCS) in these environments. HCS are isolated cross-stratified sand bodies, usually < 1 m in thickness, interbedded with shelf mudstones. They may contain shore-perpendicular sole markings (Walker & Plint, 1992). SCS is the product of amalgamated HCS, usually resulting in the elimination of mud interbeds. These units are by definition > 2 m in thickness, and contain distinctive elliptical swales as well as convex-up cross-beds. SCS is usually found stratigraphically above HCS, and below beach and shoreface deposits. Neither of these features is found within the proposed formation, suggesting that these units were not the products of storms in a shelf environment.

Walker & Plint (1992) specifically addressed the problem of parallel- and ripple cross-laminations (equivalent to Bouma divisions B & C) in shelf sand bodies. They concluded that true turbidites are unlikely to form in the shelf environment, as no modern examples are known, and no realistic shelf turbidity current-generating mechanism has been proposed. They further note that where these structures appear, they are associated with both HCS and SCS, and can be related to changes in wave velocity.

Mills (1992) thought the original Copper Mine Range beds were a lithological variant of the Teltawongee beds, but did not interpret their facies.

Again, the data compiled above allow a more detailed facies interpretation to be made.

Four facies associations appear to be present. The first is the "classical turbidite" facies (Walker, 1992), containing most of the primary divisions of the classical Bouma sequence. These include reverse graded sands (A), parallel laminated sand (B), rippled and convolute rippled fine-grained sands (C), and laminated mud and silt (D). Massive, hemipelagic muds are absent in Bunker Creek, but form the dominant lithology in Cupala Creek (see below).

Bouma sequences in Bunker Creek are generally < 30 cm thick, thus fitting the description of Walker's (1992) thin-bedded turbidites. In addition, these beds contains climbing ripples, abundant convoluted ripples, and rip-up clasts, which indicate that these facies lie within Walker's (1985) "CCC turbidites". Walker (1985, 1992) argued that CCC turbidites, with features suggesting rapid erosion followed by rapid deposition reflect levee or channel margin deposits.

Interfingered with these CCC turbidites are the very thickly bedded massive sandstone beds. These beds, which are a minor volumetric fraction of the entire formation, represent channels as described at 4.7.4. This facies is present both east and west of the Hummock Fault (Collins, 1984).

The third association comprises the slumped siltstone and shale facies. These are probably best described by Walker's (1992) "pebbly mudstone-slump facies", which contains three sub-groups: slumped shale and mudstone; slumped thin bedded turbidites; and angular slump blocks. Of these both the first and third group appear to be present. In the model presented by Walker (1992), slumped mudstone and shale represent slope failure away from channels, whereas angular slump blocks represent local channel-wall collapse.

The fourth facies comprises large thicknesses (10's of metres) of laminar shales interbedded with thin sand lenses; this association is found throughout the area between the Coturaundee Range, west of the Hummock Fault and east of the Cupala Creek Formation. The Cupala Creek exposures are typical of this facies, which probably represents hemipelagic sedimentation with occasional overchannel splays in interlobe areas.

The facies associations of the proposed Copper Mine Range Formation suggest that this sequence was deposited primarily on channel margins on an active slope. This slope was subject to periodic failure, inducing the collapse of established channels. The angular, prismatic grains preserved in the sand bodies indicate that the shelf sediment source was relatively close. It is unlikely that the current attitude of the slump folds is a reliable indicator of the palaeoslope direction, as the area has been subjected to tight folding and faulting. The interpretation of the proposed Copper Mine Range Formation as a more proximal facies than the proposed Nundora Formation precludes a simple palaeogeographic interpretation whereby more easterly variants within the Teltawongee Group represent deeper and deeper facies.

### *4.7.3 Provenance*

In thin section, the sand beds of the proposed Copper Mine Range Formation are quartz sandstones, rich in both detrital white mica and biotite, as well as microcline and plagioclase. Tourmaline and an acicular or platy opaque mineral, probably ilmenite, are also common (up to 10 modal %) with rare zircon and garnet as accessories. All of

**Figure 4.6.7 Bedding features in the Mahomica Formation**

A: Planar (a) and massive interbeds (b)

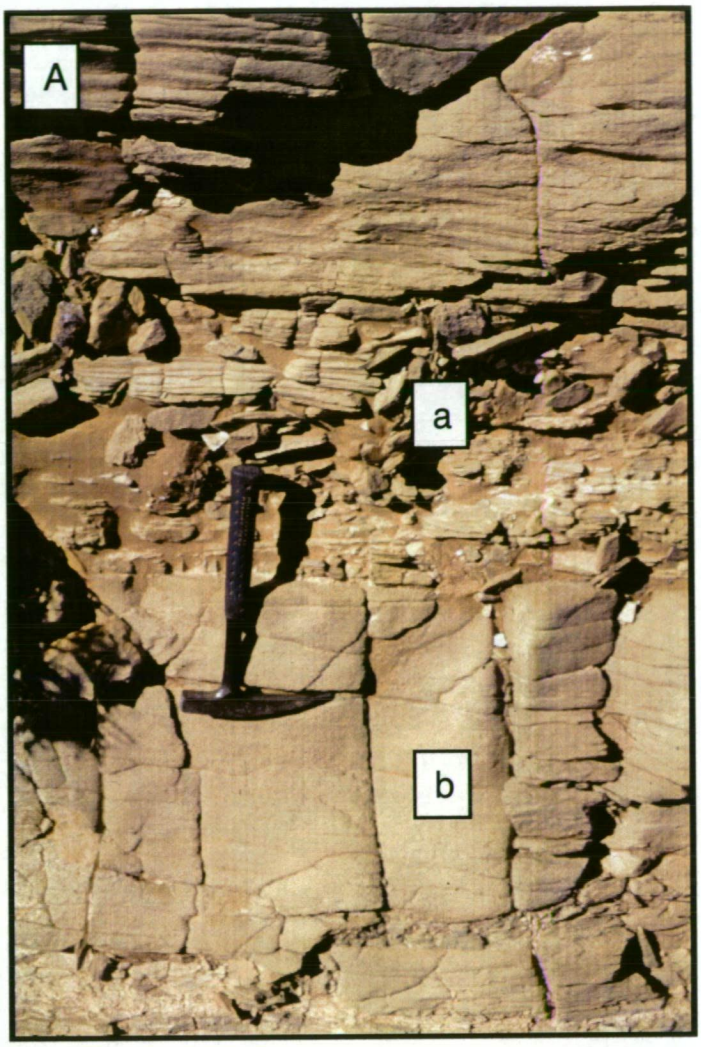


B: planar cross-bed sets

**Figure 4.6.8 Bedding features in Copper Mine Range Formation**

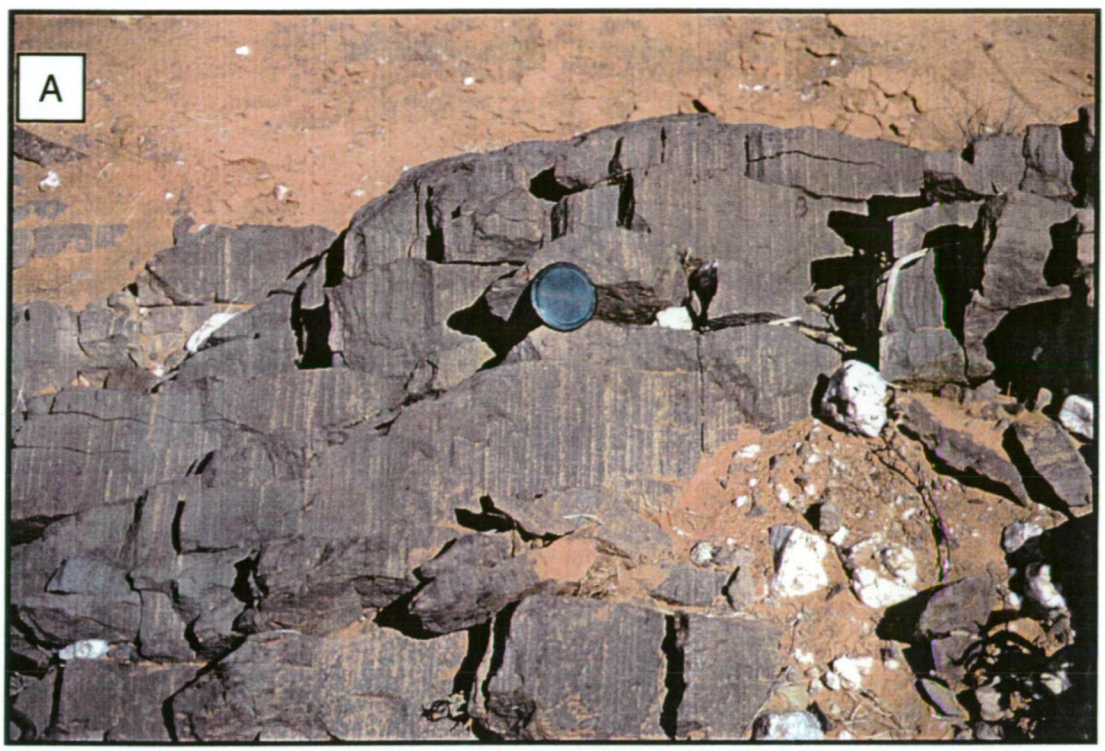


**A: Worm burrows (?*Skolithos linearis*)**

**B: Load casts**

these features indicate a likely metamorphic provenance for this sequence. Collins (1984) identified a northwesterly current pattern in cross-beds. As with the Nundora Formation, the most likely source for material from this direction is the Broken Hill-Euriowie cratonic block.

A key question arising from these interpretations is how the proximal facies of the proposed Copper Mine Range Formation is now outboard of the more distal Nundora Formation, when both were derived from a similar source.

*4.8.1 Sedimentology of the proposed Mahomica Formation*

Aside from the basal and upper stratotypes of the Teltawongee Group, there is a third exposure, running from Ponto Mine in the north, through "Wonnaminta" and "Nuntherungie" and disappearing beneath the unconformably overlying Mt. Daubeny Formation near Silverfield Tank on "Wertago". This has been referred to above as the "central Teltawongee sequence". The stratigraphic position of this body is investigated below.

The formation is named for Mahomica Tank, c.10 km east-northeast of Little Koonenberry Mountain, a location first described by Stevens (1991).

Type area: the type area is in Wonnaminta Creek, northwest of Wonnaminta H.S. A reference area exists to the north-northwest between Mahomica Tank and Ponto Mine.

Thickness: A maximum thickness of c.2100 m is preserved, apparently tightly folded around a regional syncline. This thickness accounts for folding, but does not take into consideration possible repetition or omission of beds by internal faulting.

Rock types: Davies (1985) recorded coarse- to medium-grained lithic arenites from the Ponto Mine area. These were interbedded with mudstones and occasional pebbly sand beds. Stevens (1991) correlated weathered phyllite and sandstones from Mahomica Tank with the Teltawongee beds. I have observed fine-grained lithic arenites and shale at Rocky Tank and in the headwaters of Ponto Creek. The lithic component is dominated by (up to 1mm) detrital white mica flakes, an observation also made by Stevens (1991). In the type section, lithic-feldspathic arenites and shale are common, with the lithic component again comprising significant coarse-grained white mica.

Geometry: Davies (1985) reported lensoid and pinch-out geometries of sand bodies within this sequence in the Ponto-Koonenberry area. Sheet geometries persisting for 10's of metres were found at Rocky Tank. In the type area, I observed sand wedges and mounds at sub-metre scales, along with sheet geometries (beds, laminations).

Contacts: This section is fault bounded by the Wonnaminta Fault to the east, and the Gums Tank Fault to the west.

Bedding: Davies noted massive sand accumulations of up to 50 m thickness. At Rocky Tank, thick sand and medium shale beds were interbedded averaging 0.65 m per couplet. However, one very thick (> 4 m) sand bed was recorded. Stevens (1991) described medium (0.1 m) and thickly (up to 0.4 m) bedded sands alternating with phyllite. In the type area, bedding was thick, averaging 0.4-0.5 m for both sand and shale. However, very thick departures from this were recorded with intervals of very thick turbidite couplets up to 2.4 m and occasional massive amalgamated sands from 2 to 30 m. Another interval contained 20 m of thinly laminated (1-2 mm) siltstone and shale, with occasional medium bedded (10-30 cm) sandstone interbeds.

Sedimentary structures: Davies (1985) observed Bouma divisions A (reverse graded sands), B (parallel laminated sand), D (laminated mud and silt) & E (massive hemipelagic mud), with only minor occurrences of the C division (rippled and convolute rippled fine-grained sands). In the Ponto Creek and Rocky Tank areas, normal grading is common, with no other structures observed. At Mahomica Tank, Stevens (1991) recorded high angle cross-beds, normal grading, ripples (division C) and rip-up clasts (division A). In the type section, normal grading is common throughout; at one location (624600 mE, 6614350 mN), possible liquefaction-injection structures (neptunian dykes) were observed. Cross-bedding was seen at 620856 mE, 6613097 mN, 400 m east of the Gums Tank Fault.

Petrographic texture: Samples of lithic arenite from the Ponto Mine area were moderately to poorly sorted with rounded to angular grains (Davies, 1985).

Age: No fossils have been recorded from any of the localities mentioned above. It is assumed that the Mahomica Formation. is either Lower or Middle Cambrian, based on its affinities to the rest of the Teltawongee Group.

*4.8.2 Facies Interpretation*

Davies (1985), using an early model by Walker (Walker, 1981) interpreted the sequence at Ponto Mine as stacked channel deposits in a mid- to lower fan turbidite lobe.

Occurrence of cross-bed sets, sand wedges and mounds, ripples and massive amalgamated sands supports interpretation of a channel facies association. The remainder of the formation fits Walker's (1992) description of thick bedded classical turbidites, representing individual flow and stacked levee deposits.

*4.8.3 Provenance*

At Ponto Mine, lithic arenites of this formation are rich in detrital micas (phengite 25%, muscovite+biotite 5%), and metamorphic quartz (35%) (Davies, 1985). The conspicuous presence of detrital mica throughout this formation is useful in discriminating it from the Nundora Formation. which is more feldspathic in character. The heavy mineral assemblage of this formation was not assessed.

*4.8.4 Summary: stratigraphy of the Teltawongee Group*

A summary stratigraphic column is presented in Figure 4.8.1. The ?Lower Cambrian Teltawongee Group comprises three distinct, mappable formations. The lowest unit, disconformably overlying inferred Late Neoproterozoic rocks is the Nundora Formation. It consists of well-sorted fine- and medium-grained quartzo-feldspathic sandstones, deposited in massive sand bodies, grading up to classical turbidites. This formation represents channel filling on a submarine fan, and implies considerable water depths and a cratonic sedimentary source. In uncertain stratigraphic position above the Nundora Formation lies the Mahomica Formation. This is made up of poorly sorted fine-grained lithic sandstones and interbedded shales, rich in detrital mica. These were deposited in channels and levees on a submarine fan lobe, again implying a basin floor environment. The structural top of the Teltawongee Group is represented by the Copper Mine Range Formation. It is composed of well-sorted immature lithic-feldspathic sandstones and voluminous shale. Sediment geometry and imposed soft-sediment deformation both suggest deposition on a continental slope, or bathymetric high close to a continental source.

# Figure 4.8.1

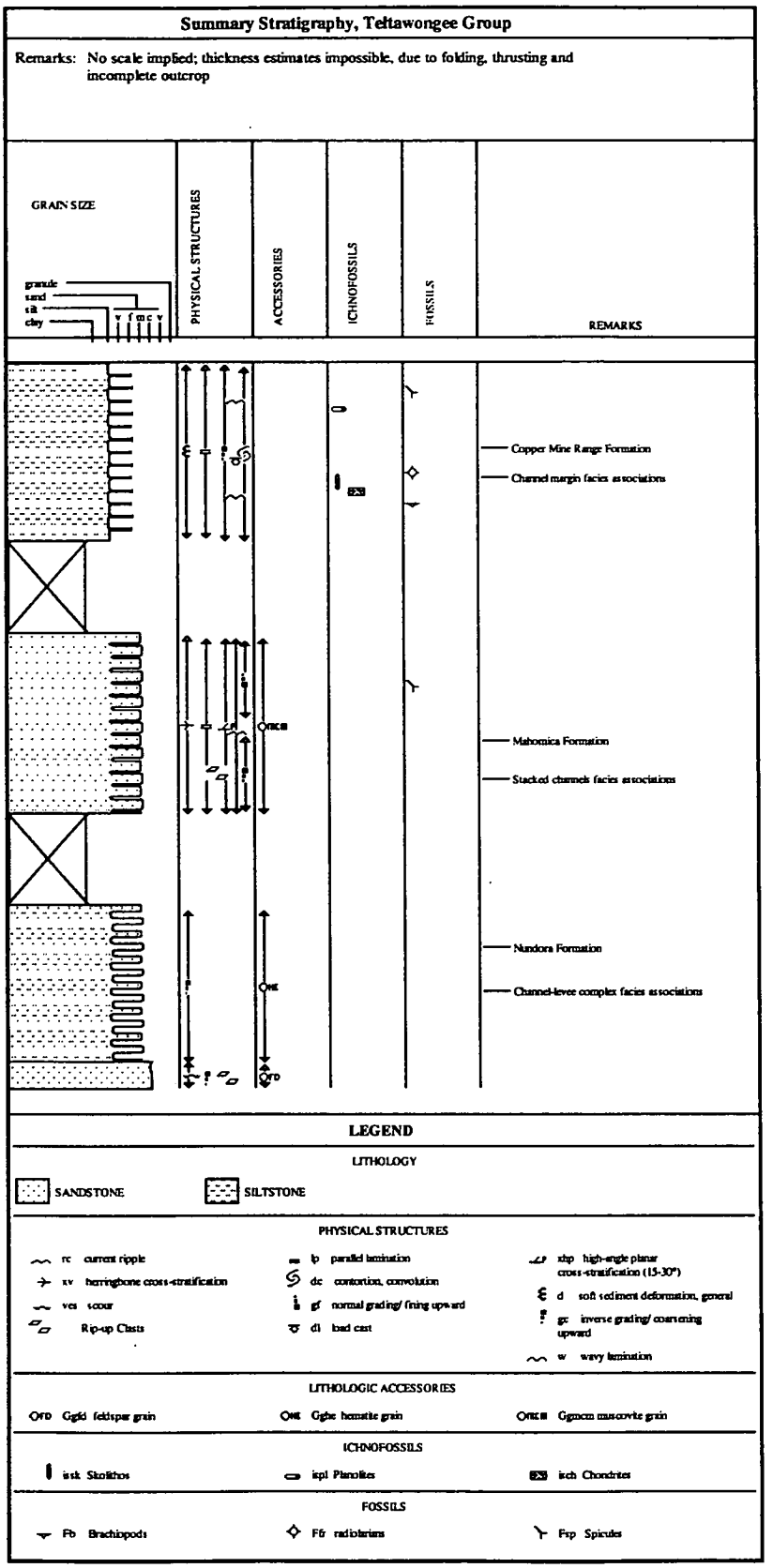
Summary Stratigraphy, Teltawongee Group
Remarks: No scale implied; thickness estimates impossible, due to folding, thrusting and incomplete outcrop
GRAIN SIZE
granule
sand
silt
clay
v f m c v
PHYSICAL STRUCTURES
ACCESSORIES
ICHNOFOSSILS
FOSSILS
REMARKS
Copper Mine Range Formation
Channel margin facies associations
Mahomica Formation
Stacked channels facies associations
Nundora Formation
Channel-levee complex facies associations
LEGEND
LITHOLOGY
SANDSTONE
SILTSTONE
PHYSICAL STRUCTURES
rc current ripple
xv herringbone cross-stratification
ves scour
Rip-up Clasts
lp parallel lamination
dc contortion, convolution
gf normal grading/ fining upward
dl load cast
xhp high-angle planar cross-stratification (15-30°)
d soft sediment deformation, general
gc inverse grading/ coarsening upward
w wavy lamination
LITHOLOGIC ACCESSORIES
Gfd feldspar grain
Ghe hematite grain
Gmcm muscovite grain
ICHNOFOSSILS
isk Skolithos
ispl Planolites
ich Chondrites
FOSSILS
Fb Brachiopods
Fr radiolarians
Fsp Spicules

## 4.9 Geochemical studies of some igneous rocks in the Northern Koonenberry

The geochemistry and petrology of many of the mafic rocks outcropping within the Koonenberry Belt was dealt with in detail by Zhou (1993) and Edwards (1980). The validity of most of the findings of Zhou (1993) still stands, rendering a further detailed petrological-geochemical study redundant. The work described in this section therefore has only limited aims: to briefly characterise the geochemistry of post-?Early-Middle Cambrian and pre-Late Cambrian-Early Ordovician mafic dykes and to compare these with similar age dykes of the Adelaide Fold Belt; and to examine the affinities of a poorly exposed, newly mapped series of pillow lavas and volcaniclastic sediments cropping out to the west of Mt Arrowsmith. In keeping with the broad aims and integrative nature of this study, only geochemical data pertinent to the determination of tectonic affinities will be presented in this and following chapters. Detailed petrological studies on many of these rock suites can be found elsewhere in the literature, and where possible, these sources are referenced.

### *4.9.1 Gneilwonga Intrusive Suite*

This suite is named for Gneilwonga Tank, near Wonnaminta H.S. where most of these rocks occur. They form sills, dykes and small plugs intruding the Mahomica Formation, and the Kara beds between Ponto Mine and Boshy Tank (Figure 4.9.1: = Wonnaminta 7336 Map, back pocket). Other exposures have been recorded intruding the Copper Mine Range Formation. around Bunker Creek and Nuntherungie Creek (this study; Mills & Hicks, unpublished mapping). These rocks were only briefly dealt with by Zhou (1993), who analysed just two samples, and thus warrant further study herein.

Contacts between sills and the intruded sediments (e.g. at 625406 mE, 6614821 mN) are sharp, and not characterised by peperitic textures, implying that the sediments were lithified and dewatered at the time of intrusion. A further key age relationship occurs on the Kayrunnera 7346 map sheet, where a gabbroic plug is unconformably overlain by Late Cambrian-Early Ordovician limestones equivalent to the Kayrunnera Group (K. J. Mills, pers.comm.). This constrains the age of intrusion to pre-Mindyallan.

Petrographically, samples from this suite are lower greenschist grade rocks, but retain doleritic textures, and in many cases, primary mineralogy, which appears to have been plag-cpx-mt, with one gabbro showing relict opx. Recognisable intersertal and ophitic textures indicate that these were dolerites. The alteration assemblage comprises epi-

chl-ab-act-qz-carb-mt, which is typical of greenschist metamorphism of original basaltic compositions.

Six samples were analysed for major and trace elements using standard whole rock XRF techniques (Norrish & Hutton, 1969). Sample selection and preparation was conducted according to the procedure outlined in Crawford et al. (1997), to avoid contamination of the geochemical signature through sampling alteration products. Major and trace element data for these rocks are shown in Table 4.9.1. Data are recalculated volatile free, with loss on ignition values reported separately. The mobility and immobility of the various major and trace elements in basaltic rocks under hydrothermal and greenschist facies metamorphism is now relatively well understood (e.g. Humphris & Thompson, 1978; Gelinas et al., 1982). These, and other studies, predict that in most circumstances Ti, Zr, Nb, Y, Al and Ni are immobile, and can be used with some confidence. Inferences from other elements must be treated with caution. CIPW norms have not been calculated, as mobilisation of some elements during metamorphism and weathering violates the underlying assumptions inherent in this procedure.

Major oxide data are plotted against MgO in Figure 4.9.2, as MgO is a better indicator of evolutionary stage in mafic rock suites with a limited range of $SiO_2$ contents. A selection of trace elements expected to have been immobile under the alteration conditions is plotted against FeO*/MgO as the index of fractionation.

Increasing $SiO_2$, FeO* and $P_2O_5$ with decreasing MgO are indicative of olivine, clinopyroxene and plagioclase fractionation from tholeiitic magma. The tholeiitic affinities of the suite are borne out by examination of plots against FeO*/MgO, which show increasing $TiO_2$, Zr and FeO* at more evolved compositions. V appears to have been mobilised during alteration, and shows non-magmatic scatter. The limited low range (1-2%) of $TiO_2$ with decreasing MgO, and the lack of ferrobasalts with FeO* > 16 and FeO*/MgO > 3 suggests that these were not particularly evolved rocks. A plot of Zr/Ti v Nb/Y (after Winchester & Floyd, 1977) confirms the sub-alkaline affinities of these rocks. In summary, these samples are tholeiitic dolerites and gabbros.

N-MORB normalised incompatible elements (Figure 4.9.3) show distinctive MORB-like flat patterns in Nb, La, Ce and the HFS elements (Nd, Zr, Ti, Y), but elevated LILE (Rb, Ba, Th, K and Pb). This signature is characteristic of both early backarc basin-type tholeiites in which the excess LILE are thought to come from the subducted slab (e.g.

**Table 4.9.1 Whole-rock analyses recalculated volatile-free for the Gneilwonga Intrusive Suite**

| Sample | 9614 | 762904 | 9615 | 9724 | 9809 | 9814 |
|---|---|---|---|---|---|---|
| Rock | Diorite | Gabbro | Gabbro | Dolerite | Diorite | Dolerite |
| SiO2 | 53.09 | 47.02 | 49.76 | 50.82 | 49.17 | 49.88 |
| TiO2 | 1.27 | 1.32 | 1.16 | 1.23 | 0.91 | 0.95 |
| Al2O3 | 14.54 | 17.62 | 14.91 | 15.43 | 15.69 | 15.43 |
| Fe2O3 | 11.47 | 10.77 | 11.51 | 11.90 | 10.79 | 10.60 |
| FeO* | 10.32 | 9.69 | 10.36 | 10.70 | 9.71 | 9.54 |
| MnO | 0.20 | 0.17 | 0.19 | 0.21 | 0.17 | 0.18 |
| MgO | 6.20 | 7.72 | 7.54 | 6.78 | 8.32 | 8.21 |
| CaO | 9.49 | 11.66 | 11.72 | 9.24 | 12.56 | 11.61 |
| Na2O | 2.52 | 2.83 | 2.69 | 3.75 | 1.94 | 2.27 |
| K2O | 1.08 | 0.74 | 0.41 | 0.53 | 0.40 | 0.77 |
| P2O5 | 0.15 | 0.16 | 0.10 | 0.11 | 0.06 | 0.11 |
| LOI | 5.24 | 3.06 | 2.26 | 2.10 | 1.99 | 2.15 |
| | | | | | | |
| Th | 3 | N/A | <1 | <1 | <1 | <1 |
| Nb | 5 | 3 | 4 | 3 | 2 | 2 |
| La | 13 | N/A | 6 | 5 | 2 | 3 |
| Ce | 28 | 28 | 10 | 14 | 8 | 13 |
| Nd | 16 | 84 | 8 | 8 | 6 | 10 |
| Zr | 115 | N/A | 59 | 73 | 39 | 57 |
| Ti | 7622 | 7905 | 6980 | 7361 | 5486 | 5697 |
| Y | 33 | N/A | 22 | 28 | 19 | 21 |
| Ni | 42 | N/A | 63 | 40 | 73 | 69 |
| Cr | 198 | 7 | 195 | 126 | 227 | 292 |
| Sc | 41 | 381 | 47 | 44 | 49 | 47 |
| V | 258 | 22 | 289 | 3 | 297 | 252 |
| Zn | 115 | N/A | 83 | 87 | 71 | 76 |
| Cu | 58 | N/A | 69 | 86 | 99 | 81 |
| | | | | | | |
| FeO*/MgO | 1.66 | 1.26 | 1.37 | 1.58 | 1.17 | 1.16 |
| Nb/Y | 0.15 | N/A | 0.16 | 0.10 | 0.10 | 0.09 |
| Zr/Ti | 0.02 | N/A | 0.01 | 0.01 | 0.01 | 0.01 |

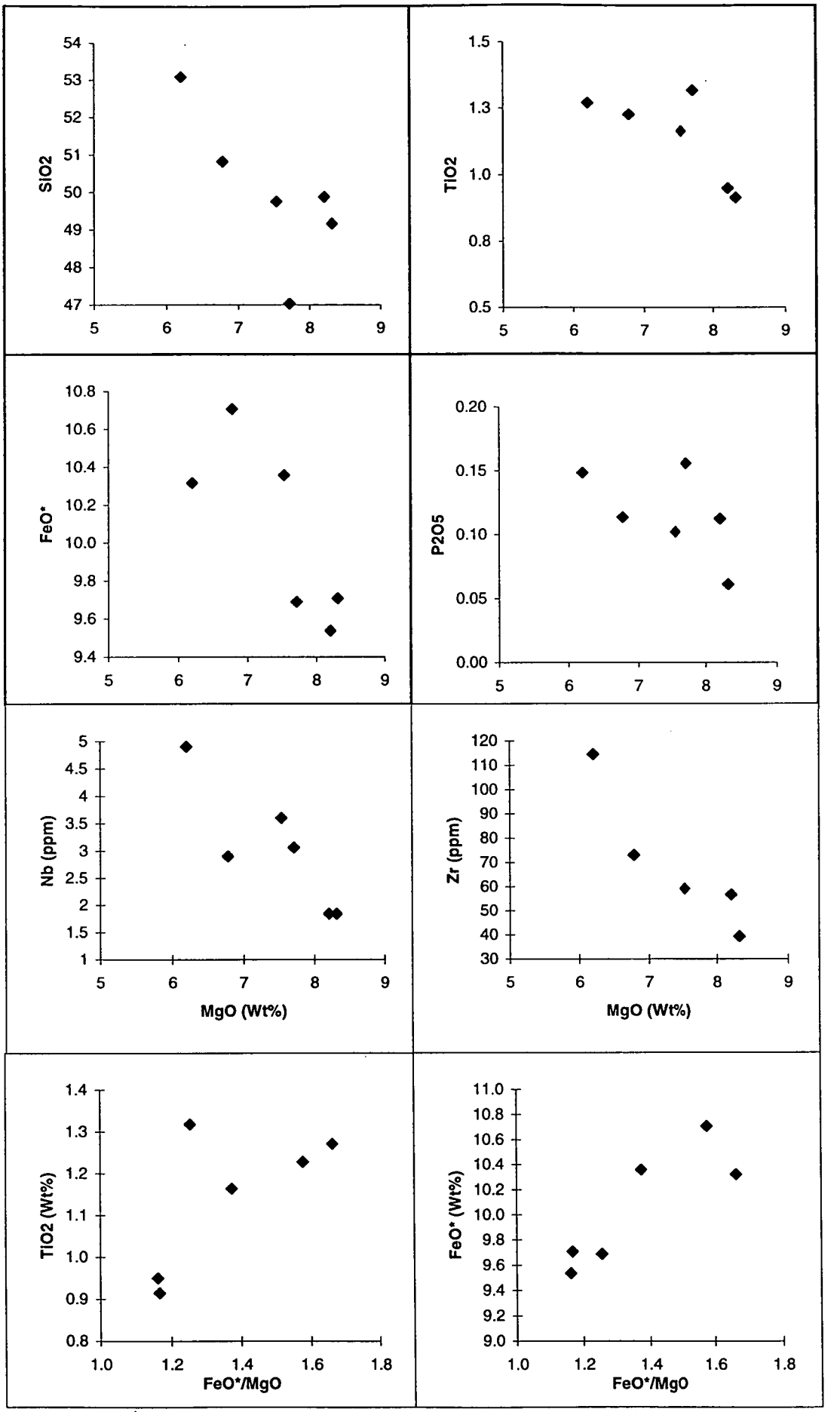


**Figure 4.9.2 Major element diagrams, Gneilwonga Intrusive Suite**

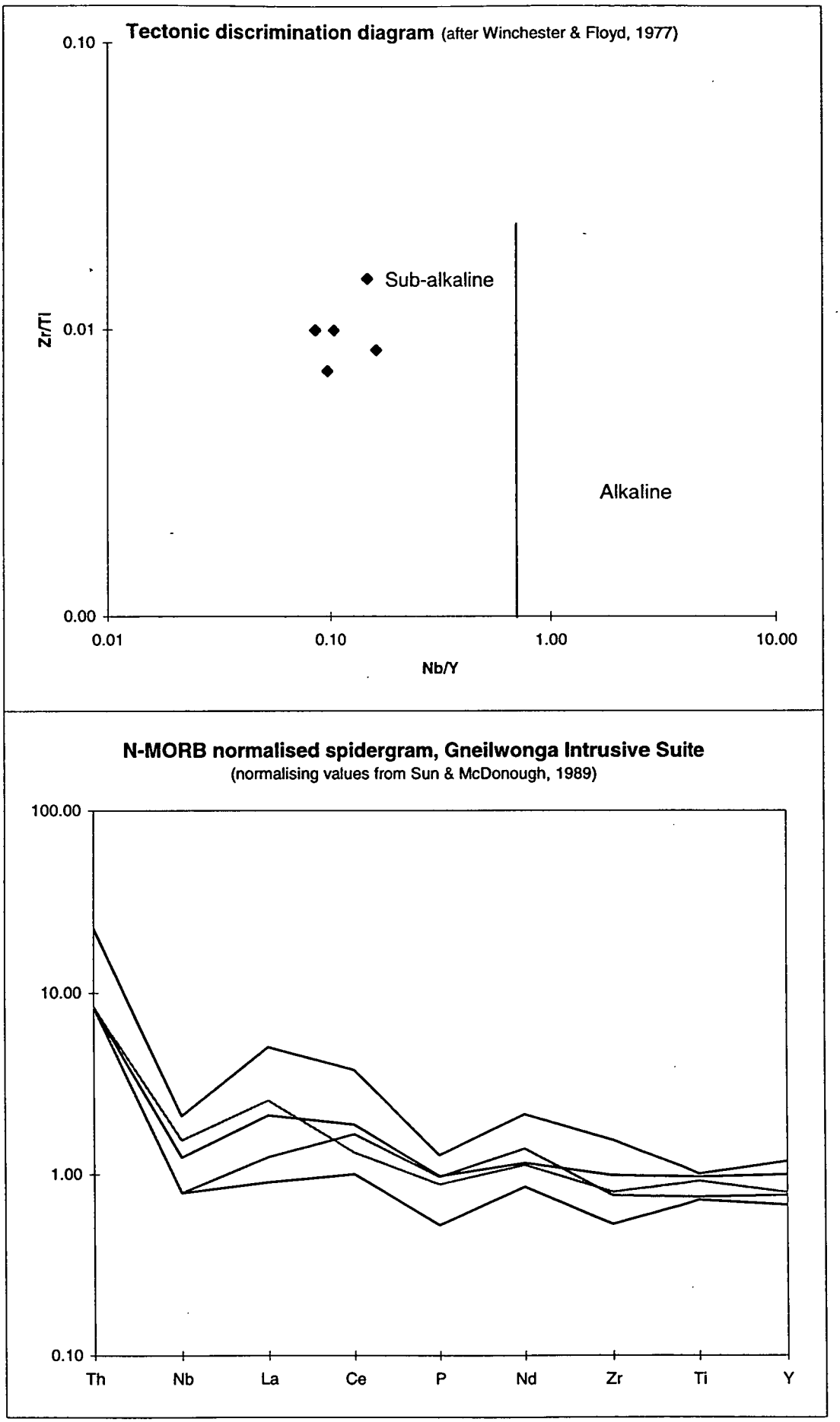


**Figure 4.9.3 Immobile element diagrams**

South Sandwich Is, Pearce et al., 1984) or rift tholeiitic basalts intruded into and through continental crust, the latter providing excess LILE (Thompson et al., 1983).

The Gneilwonga Intrusive Suite shares some characteristics with the contemporaneous Henty Dyke Swarm of western Tasmania; these latter rocks intrude the Middle Cambrian Central Volcanic Complex of the Dundas "Trough", but are not known to intrude Late Cambrian rocks of the Tyndall Group (Crawford et al., 1992). Similarities of the Henty Dyke Swarm to the Gneilwonga Intrusive Suite include tholeiitic compositions, relatively low $TiO_2$ (c.1.5% at 5% MgO) and Nb compared to normal MORB tholeiites (>2.5% at 5% MgO). Crawford et al (1992) suggested the Henty Dyke Swarm was related to aborted post-collisional rifting of a recently assembled crustal collage.

Liu & Fleming (1990a, b) described tholeiitic dykes, sills and plugs in the Adelaide Fold Belt which they considered to be syn- to post-tectonic to the Delamerian Orogeny. One sample of post-tectonic metadolerite was dated using an isotope dilution method on zircons (Chen & Liu, 1996), returning an age of 510 ± 2 Ma, which is latest Atdabanian (Early Cambrian) (after Shergold, 1995). These rocks intrude the partly turbiditic sedimentary rocks of the Early Cambrian Kanmantoo Group. Although major oxide and trace element data for the South Australian rocks remain unpublished, precluding direct comparison, Liu and Fleming (1990a) list some key features of these rocks. They include: typical Rb 3-6 ppm; $K_2O$ < 0.2 Wt%; Sr 110-120 ppm; Nb 2-5 ppm; La 3-4 ppm; Zr 70-80 ppm; $TiO_2$ c.1.3 Wt%; Y c.29 ppm. In addition they describe these rocks as possessing "flat REE patterns...and spidergrams" closest to E-MORB in extensional environments. (Liu & Fleming, 1990a). These features are similar to the Gneilwonga Intrusive Suite (cf. Table 4.9.1). The similar relative ages, and similarities between the host rocks (see for example Mills, 1992) indicate a potentially widespread event.

### *4.9.2 Pimbilla volcanics, west of Mt Arrowsmith*

Wopfner (1966) and subsequent workers (Warris, 1967; Edwards, 1980; Edwards & Neef, 1981) mapped two fault-bounded synclines containing Middle Cambrian and Lower Ordovician rocks, cropping out to the west of Mt Arrowsmith between McDonalds Tank and Tobacco Bush Creek (Figure 4.9.4). The eastern syncline contains the Lower Ordovician Yandaminta Quartzite, Tabita and Pingbilly Formations, which are the equivalents of the Nootumbulla Sandstone, Bynguano Quartzite and Rowena Formation of the Mootwingee Group in the Mt Wright area (see Chapter 5).

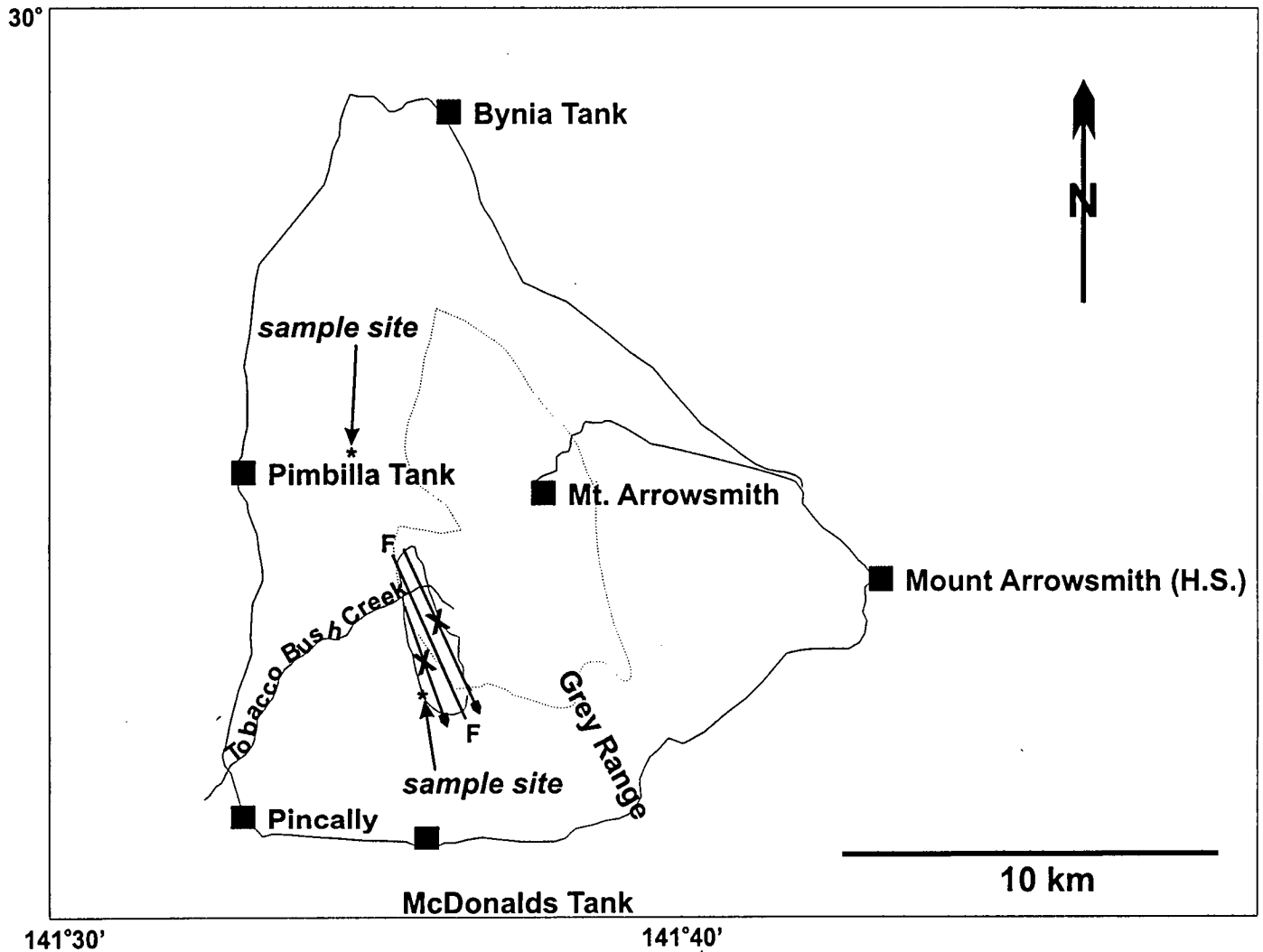


Figure 4.9.4 Locality Map. Mount Arrowsmith and environs.

The western syncline contains the basal Pincally Formation, correlated with the Coonigan Formation at Mt Wright, the Wydjah Formation and the Wyarrah Shale (Edwards & Neef, 1981). Edwards & Neef indicated that the Pincally Formation contained volcaniclastic material, although they described neither the affinity nor the source of these. Recent reconnaissance mapping along strike to the northwest near Pimbilla Tank reported lavas (B. Stevens, pers. comm., 1998) unlike those mapped around Mt Arrowsmith by Edwards (1980). These rocks and the volcaniclastic sandstones of the Pincally Formation form the subject of this investigation.

Three samples of black to grey, gritty lithic volcaniclastic medium-grained sandstone were acquired during traversing the Pincally Formation around 557345 mE 6661590 mN, within c.20 m of the base of section. This part of the formation contains distinctive Hummocky Cross Stratification (Figure 4.9.5) indicating water depths below fair weather wave base but above storm wave base (Walker & Plint, 1992). Some distance along strike at 555955 mE 6669200 mN, two samples of rubbly, glassy basaltic pillow lava were acquired from isolated outcrops in gutters on the main north trending ridge east of Pimbilla Tank (Figure 4.9.4).

The lithic sandstones of the Pincally Formation contain diverse volcaniclastic grains including clinopyroxene, sericitised plagioclase, K-feldspar, rhyolitic pumice, devitrified glass, and embayed quartz, as well as micaceous and cherty lithics and opaque minerals, often in heavy mineral laminae. These rocks are chemically and texturally immature, with angular to subrounded grains, but moderately to well sorted; they are cemented by void-filling carbonate; a felsic source is implied.

The two lava samples proved highly altered with haematite as the dominant alteration phase. Both contained a relict groundmass of altered plagioclase laths with a trachytic texture. Sample 9866 appeared to contain ghost clinopyroxene phenocryst shapes, altered to chl-hm. Sample 9867 contained both relict sericitised plagioclase glomerocrysts and clusters of relict olivine phenocrysts, altered to hm-talc-chl. Both samples contain amygdules rimmed by an opaque mineral and filled with carbonate.

Two samples (hereafter "Pimbilla Volcanics") were analysed for major and trace elements using standard whole rock XRF techniques. Major and trace element data for these rocks are shown in Table 4.9.2. Data are recalculated volatile free, with loss on ignition values reported separately. Note that the high ignition losses (14.54 and 13.25%) mean that these data must be treated with caution. These data have been supplemented with seven analyses from lavas collected to the north and east of the

**Figure 4.9.5 Hummocky Cross Stratification in Pincally Formation, Mount Arrowsmith**

Bed is medium-grained volcanoclastic sandstone

| | "Pimbilla volcanics" | | | | "West Arrowsmith volcanics" | | | | | | |
|---|---|---|---|---|---|---|---|---|---|---|---|
| Sample | Ep2/9864 | Ep3/9865 | Ev1/9866 | Ev2/9867 | AR50a | AR50 B | AR51 A | AR51 B | AR52 A | AR52 B | AR50 A |
| Rock | volcaniclastic | volcaniclastic | basalt | basalt | basalt | basalt | basalt | basalt | basalt | basalt | basalt |
| SiO2 | 64.51 | 51.02 | 49.40 | 48.07 | 43.08 | 45.10 | 47.59 | 47.78 | 44.24 | 46.88 | 43.00 |
| TiO2 | 0.73 | 2.28 | 1.96 | 1.95 | 1.88 | 2.12 | 3.13 | 3.30 | 1.85 | 3.23 | 1.86 |
| Al203 | 12.52 | 9.88 | 13.30 | 13.93 | 13.41 | 13.42 | 13.44 | 13.88 | 16.44 | 13.73 | 13.43 |
| Fe2O3 | 4.01 | 8.15 | 9.01 | 10.52 | 10.66 | 9.14 | 12.42 | 12.10 | 9.32 | 12.20 | 10.74 |
| FeO | 0.24 | 0.35 | 0.11 | 0.15 | 3.02 | 2.84 | 3.42 | 2.89 | 4.22 | 3.42 | 3.08 |
| MnO | 1.25 | 1.09 | 5.71 | 3.41 | 0.14 | 0.18 | 0.16 | 0.18 | 0.16 | 0.15 | 0.15 |
| MgO | 10.32 | 22.08 | 13.77 | 15.87 | 4.71 | 7.10 | 4.27 | 3.40 | 4.51 | 2.21 | 4.68 |
| CaO | 3.77 | 3.24 | 5.77 | 5.05 | 15.15 | 12.10 | 6.73 | 7.65 | 10.37 | 9.04 | 15.06 |
| Na2O | 2.26 | 1.45 | 0.69 | 0.79 | 3.50 | 5.06 | 5.04 | 5.65 | 2.69 | 5.59 | 3.50 |
| K20 | 0.41 | 0.45 | 0.27 | 0.25 | 1.81 | 0.43 | 0.59 | 0.41 | 2.22 | 0.37 | 1.79 |
| P2O5 | 100 | 100 | 100 | 100 | 0.22 | 0.26 | 0.49 | 0.54 | 0.23 | 0.46 | 0.22 |
| FeO* | 3.61 | 7.34 | 8.11 | 9.47 | 13.69 | 11.99 | 15.83 | 14.99 | 13.54 | 15.61 | 13.83 |
| LOI | 8.63 | 15.62 | 14.54 | 13.25 | 16.20 | 15.05 | 6.20 | 5.74 | 7.34 | 9.11 | 16.20 |
| Rb | 83 | 56 | 11 | 14 | 49 | 13 | 9 | 10 | 54 | 8 | 49 |
| Ba | 1336 | 367 | 273 | 166 | 270 | 172 | 256 | 192 | 555 | 216 | 293 |
| Th | 15 | 12 | <1.5 | <1.5 | 1.4 | 1.6 | 3.31 | 3.42 | 1.39 | 2.26 | 1.4 |
| Nb | 20 | 34 | 20 | 20 | 16 | 16 | 34 | 37 | 17 | 27 | 15 |
| Pb | 23 | 14 | <1.5 | <1.5 | 4 | 3 | 4 | 5 | 5 | 9 | 3 |
| Sr | 272 | 288 | 278 | 455 | 275 | 239 | 330 | 339 | 483 | 341 | 271 |
| P | 1792 | 1993 | 1189 | 1119 | 7953 | 1885 | 2579 | 1815 | 9777 | 1636 | 7896 |
| Zr | 240 | 424 | 140 | 138 | 117 | 137 | 255 | 272 | 119 | 200 | 123 |
| Ti | 4356 | 13652 | 11763 | 11712 | 11245 | 12709 | 18778 | 19778 | 11111 | 19377 | 11164 |
| Y | 47 | 38 | 18 | 17 | 21 | 20 | 35 | 39 | 19 | 29 | 18 |
| Zr/Ti | 0.06 | 0.03 | 0.01 | 0.01 | 0.01 | 0.01 | 0.01 | 0.01 | 0.01 | 0.01 | 0.01 |
| Nb/Y | 0.42 | 0.88 | 1.12 | 1.17 | 0.76 | 0.80 | 0.97 | 0.95 | 0.89 | 0.93 | 0.83 |

**Table 4.9.2 Whole-rock analyses recalulated volatile-free for the "Pimbilla volcanics" and "West Arrowsmith volcanics"**

| | "Pimbilla volcanics" | | "West Arrowsmith volcanics" | | | | | | | | |
|---|---|---|---|---|---|---|---|---|---|---|---|
| Sample | Ep2/9864 | Ep3/9865 | Ev1/9866 | Ev2/9867 | AR50a | AR50 B | AR51 A | AR51 B | AR52 A | AR52 B | AR50 A |
| Rock | volcaniclastic | volcaniclastic | basalt | basalt | basalt | basalt | basalt | basalt | basalt | basalt | basalt |
| Ni | 7 | 5 | 118 | 199 | 198 | 199 | 77 | 61 | 99 | 57 | 179 |
| Cr | 12 | 40 | 489 | 546 | 207 | 216 | 10 | 10 | 53 | 20 | 197 |
| V | 63 | 172 | 279 | 298 | 205 | 206 | 297 | 319 | 241 | 295 | 209 |
| Sc | 9 | 18 | 34 | 38 | | | | | | | |
| Cu | 34 | 23 | 48 | 53 | 140 | 66 | 75 | 60 | 112 | 85 | 136 |
| Zn | 37 | 39 | 61 | 69 | 65 | 84 | 109 | 108 | 73 | 80 | 61 |
| La | 48 | 47 | 14 | 14 | 14.9 | 16.7 | 33.2 | 34.9 | 15 | 21.8 | 15.1 |
| Ce | 111 | 96 | 32 | 31 | 33.2 | 36.4 | 72.7 | 74.8 | 33.8 | 48.9 | 32.9 |
| Nd | 55 | 46 | 19 | 16 | 17.5 | 20.2 | 37.1 | 38.2 | 18.7 | 27 | 18.1 |

**Table 4.9.2** (cont.)

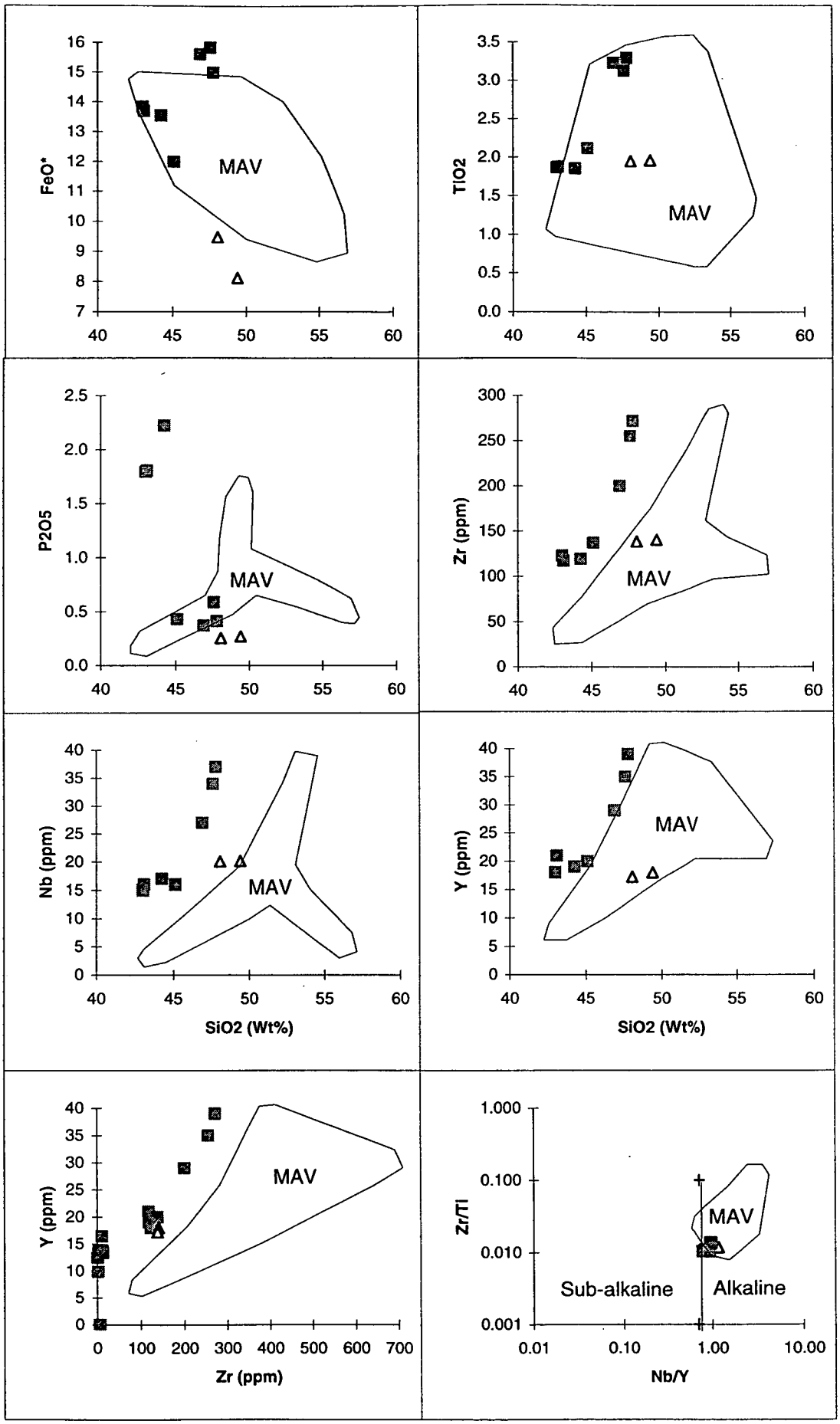


**Figure 4.9.6 Major element diagrams, "Pimbilla volcanics"**

squares = west Mt Arrowsmith; triangles = Pimbilla volcanics; field for MAV from Crawford et al., 1997.

sample area ("West Arrowsmith"; B. Stevens, unpublished data). These latter samples were analysed by Analabs Perth, using a proprietary combination of XRF and INAA. All data are presented as major and trace element Harker diagrams, with three immobile trace element diagrams based on Ti, Nb, Y and Zr (Figures 4.9.6a/b). Also presented for reference is a field for the Mt Arrowsmith Volcanics lavas ranging from picrite through to trachyte, published in Crawford et al. (1997) ("MAV").

Despite the scattering effect expected from hydration, the Pimbilla and West Arrowsmith lavas group is well within the MAV in the major element plots. In the more reliable immobile element Harker diagrams, the lavas define clear trends of increasing Zr, Nb, Y and Ti with increasing fractionation. The tectonic discrimination plot (Zr/Ti v Nb/Y, after Winchester & Floyd, 1977) shows both the Pimbilla and West Arrowsmith lavas to have alkaline affinities like the MAV. On the basis of this evidence, I confidently correlate the Pimbilla and West Arrowsmith lavas with the MAV.

Given the age difference between the MAV (586 ± 7 Ma; Crawford et al., 1997) and the Pincally Formation (Templetonian; Wopfner, 1966), and the lack of regionally significant tectonic events in this time span, it is unlikely that the MAV is the source of the fresh volcanic detritus in the Pincally Formation. It is more likely that correlates of the Mt Wright Volcanics and Cymbric Vale Formation supplied volcaniclastic material into these formations. These may still be present at depth, and under cover to the west, or may have been faulted out in the post-Ordovician tectonic event represented by the faulted synclines in this area. The felsic nature of the detritus supports this correlation.

## 4.10 Geophysical studies of structure in the Northern Koonenberry

A large proportion of the following section has been published as DIREEN N. G. 1998: The Palaeozoic Koonenberry Fold and Thrust Belt, far western New South Wales: a case study in applied gravity and magnetic modelling. Exploration Geophysics **29**, 330-339. A reprint is included for the reader's reference.

### *4.10.1 Methods*

Gravimetric and magnetic methods were chosen to continue the study of structures in this area for two reasons. The first was the availability of the Discovery 2000 data, allowing appraisal of locally developed models in a regional context, with the possibility

of profile modelling across the entire area. The second was the generally satisfactory past record of these methods of providing useful structural information in the region.

*4.10.2 Gravity survey: acquisition and processing*

Gravity data, described in Direen (1998) were acquired using a Lacoste & Romberg Model G gravimeter, serial no. 651, and were processed according to the following algorithm.

1. Removal of tidal drift from base repeats (based on AGSO charts for relevant days/times).
2. Removal of linear instrumental drift from all stations based on non-tidal residual loop error.
3. Correction for instrument scale Lacoste & Romberg G651 for all stations;
4. Calculation of observed gravity (G obs) by difference to base. The base station for the gravity survey was at Fowlers Gap airstrip. This is located at 31°05'04.8954"S 141°40'51.4912"E, with observed gravity of 97931.32 mGal. This station is a second order base to the Isogal 84 network station at Broken Hill airport. Details of this station are recorded in an appendix.
5. Calculation of theoretical gravity: latitudes for this calculation were converted from AMG northings for zone 54 using the FORTRAN program NSWUTM. AMG coordinates were recorded from 1:100 000 map sheets controlled by handheld Magellan GPS and surveying. The program uses the ellipsoid and theoretical gravity function of Coron (1972) ref. Wellman et al (1985).
6. Calculation of Free Air Anomaly and Bouguer Anomaly: an integrated calculation performed using the FORTRAN program NSW1967. The assumed Bouguer density is 2.67 $t/m^3$.
7. Addition of Terrain Correction: required for about 20% of stations. The maximum correction did not exceed 0.5 mGal. Terrain corrections were manually calculated using the method of Hammer (1939) to zone M, where curvature of the earth begins to be significant.
8. Data were checked by comparing their fit into the existing data acquired by Geoterrex (Figure 4.10.1). The fully reduced data are included in Appendix 1.

To allow two-dimensional modelling, fully reduced station values were projected onto the line joining the first and last stations of each traverse.

To permit modelling of the Bancannia Trough, further data were then added to each projected traverse on the south-western side. These data were extracted from gridded

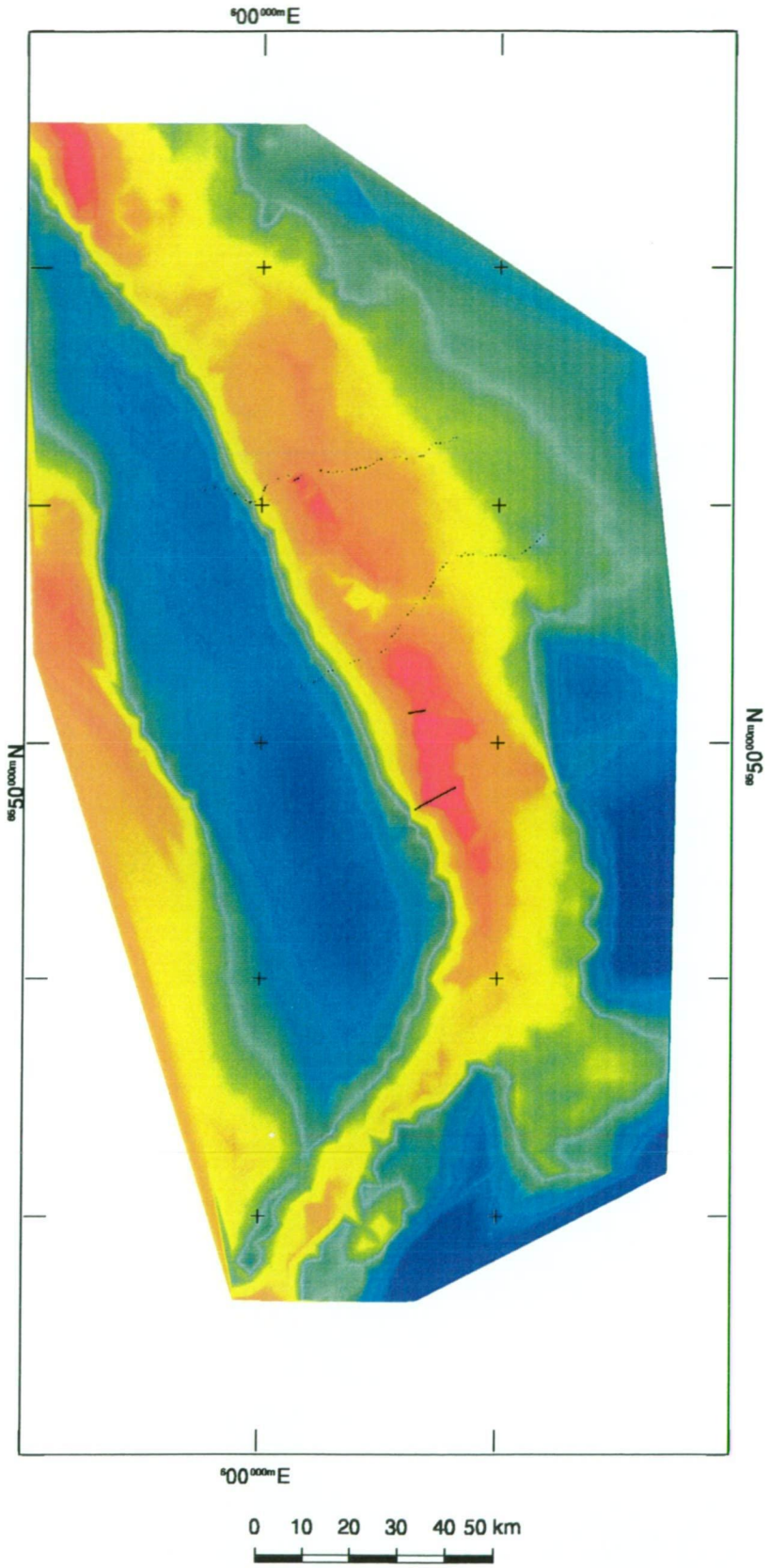


Figure 4.10.1 Bouguer Anomaly, Bancannia Trough-Koonenberry region, incorporating D2000 data and this study; Grid is AMG Zone 54

gravity acquired by Geoterrex P.L. The acquisition parameters of these data are described at 2.5.

Extraction of data from the grid was carried out using the View Traverse function of ER Mapper v.5.2. The start point of the additional data was the westernmost station of each gravity traverse, with the end point occurring 5 km west of the inflection point marking the western boundary of the Bancannia Trough. An additional traverse, from 597538 mE 6571820 mN to 627321 mE 6591568 mN, was also extracted, to allow construction of a model across the Turkaro Range area. All additional data were transformed from (x, y, value) to (x', value) using a modified version of the BASIC program ERMObs by Michael Roach.

### *4.10.3 Magnetic data*

The length of the gravity profiles acquired precluded acquisition of ground magnetic data for logistical reasons. Instead, three lines of data were extracted from the gridded aeromagnetic coverage acquired by World Geoscience Corporation P.L. The acquisition parameters of these data are also described in section 2.5.

Extraction of data from the grid was again carried out using the View Traverse function of ER Mapper v.5.2. The start- and end-points of traverses were defined by projections of the line joining the first and last stations of each of the three gravity traverses. The extracted data were transformed and subsampled by a factor of 2 in a similar fashion to that outlined above (4.10.2).

### *4.10.4 Modelling Parameters*

Two-dimensional forward models were constructed using Model2d v3.1a by Michael Roach. This uses the algorithms of Talwani (1965) and Talwani et al. (1959) to calculate the potential field responses of bodies of arbitrary shape in two dimensions. There is an assumption of body continuity in the third dimension inherent in this method.

Model variables include scale and sign of the physical properties of bodies, body geometry, and the field base-level. Typically, both the physical properties and the base level are controlled variables, thus allowing prediction of the subsurface geometry of the various units contributing to the field.

In the study area, none of the variables is completely controlled. It is therefore appropriate to list how these limitations have been approached, and the way in which they are expressed in the models.

First, petrophysical properties must be measured from outcrop samples rather than fresh drillcore, the implications of which have been examined in Chapter 3. Second, the level of accurate mapping of important units at surface is limited by essentially flat-lying Jurassic-Recent sediments. Third, there is no consistent, published method of removing the regional field (e.g. as a third order polynomial surface) from the gravity field in NSW.

In addressing the second limitation, known boundary locations e.g. from Mills (1992) and Mills (unpublished mapping) have been rigorously incorporated into the models at surface. Where this has not been possible, boundary placement has been guided by gradients or other linear features displayed in regional maps of the total magnetic intensity. In many cases, projections of these features correspond with outcropping locations of boundaries. Where neither of these methods is of use, a boundary or body may be inferred via projection from another traverse. Where several possibilities exist, separate solutions have been generated and compared using the RMS error of fit between the two calculated and two observed fields.

The lack of removal of the regional gravity field has required a static shift of the calculated field with respect to the observed field in all of the models. Leaman (1994) outlined possible reasons for these shifts, and stipulated that where they occur, they should be of the same sign and value. If this condition is not fulfilled, the model solutions must be invalid.

*4.10.6 Two-dimensional forward models*

Three model sections are presented for this area, incorporating modelled structure through the Nundora-Wonnaminta Rd, the Turkaro Range, and the Marrapina-Nuntherungie Rd. A variety of alternative models is presented, illustrating various geometric and petrophysical permutations. The field parameters used in these models are specifically:
G static shift (best fit) 11 mGal
M field base-level 57170 nT, inclined at –63.53°, with a declination of 9.3° E.

*4.10.7 Nundora-Wonnaminta Interpretation*

This model is dealt with in detail by Direen (1998), to which the reader is referred.

Adelaidean (Neoproterozoic) rocks are not known from in the Koonenberry Belt, but crop out in the Euriowie Inlier to the west of the Bancannia Trough. Here, they comprise dolomite, diamictite, conglomerate and mudstone, and are broken up by east-dipping ?Delamerian thrusts, including the major Corona Fault (NSWGS, 1998). Density data for the Adelaidean rocks of the Euriowie inlier are quoted by Tucker (1983) averaging between 2.75 and 2.80 $t/m^3$, but with a range from 2.61 $t/m^3$ (quartzite) to 3.00 (dolomites). Rare ironstones (NSWGS, 1998) reach densities of up to 3.25 $t/m^3$, although these are relatively unimportant volumetrically. The unmodelled slice of Adelaidean may contribute significantly to the DC shift of 11 mGal applied to the field. A model illustrating the potential contribution of slices of Adelaidean rocks at depth is shown in Figure 4.10.2. Bodies in this model have been given average densities of 2.70 $t/m^3$, indicating a major contribution from slates, greywackes and siltstones (after Tucker, 1983). Because of the depth of these sources, it is very difficult to constrain the geometries involved. In order to avoid over-complication in other models, this deep basement source is omitted from modelling and the equivalent DC shift applied. The implication of Adelaidean sequences in a duplex at depth, and involved in Cambrian thrusts in the Euriowie Inlier to the west, means that the Corona Fault may be the eastern boundary thrust of a Koonenberry Fold and Thrust Belt. By this definition, the fold and thrust belt must also include the Bancannia Trough.

Further implications, regarding the presence of crustal decolléments, and the nature of the Bancannia Trough, are also described in Direen (1998).

*4.10.8 Comments.*

It has been suggested (K J Mills, pers.comm. 1996) that the high-amplitude, 10 km wavelength anomaly corresponding to the central outcrop of the Teltawongee Beds may be related to east-west trending hornblende lamprophyre dykes. These were mapped in the area by Zhou (1993), and are spatially related to an east-west trending fault that intersects the road c.1km southeast of Wonnaminta H.S.

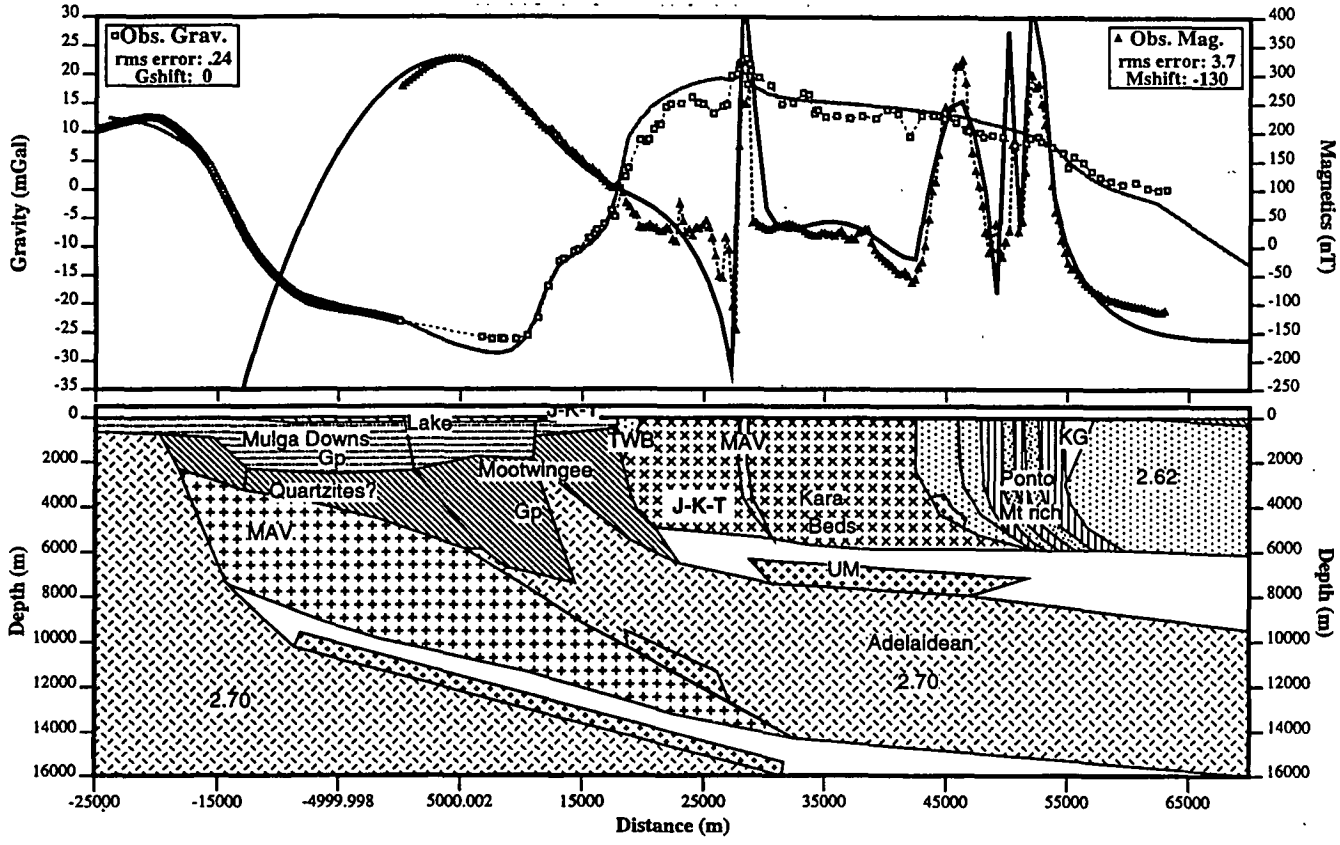


## Figure 4.10.2 2D gravity & magnetic model illustrating potential contribution from Adelaidean sources at depth (Nundora-Wonnaminta section)

V. E. = 5.9. Key: densities quoted in t/m$^3$. Lake = Quaternary Bancannia Lake; J-K-T = Murray Basin sequences; TWB = Teltawongee Group; MAV = Mt Arrowsmith Volcanics; Ponto Mt rich = magnetite rich Ponto Complex; KG = Kayrunnera Group; UM / + = serpentinised mafic-ultramafic complexes;Quartzites = possible Mootwingee group correlates.

With regard to this proposition, the following should be noted. The magnetics are extracted from gridded airborne coverage in which the lines were flown east-west at minimum spacings of 250 m. North-south tie lines were flown at 2500 m intervals (Mitchell et al., 1997). These acquisition characteristics will suppress anomalies directed east-west with dimensions of < 400 m width and lengths < 2.5 km. East-west units with dimensions greater than these will be aliased. Ground traverses over the east-west striking lamprophyre dykes by the author revealed that these dykes are commonly <1 m in width and <20 m in length. The units have magnetic susceptibility values ranging up to 0.024 SI.

It is therefore highly unlikely that an east-west striking dyke of these properties could produce a high-amplitude, continuous northwest-southeast striking anomaly with $1/2\lambda$ of c.8 km. These conditions demand a body striking at a high angle to the direction of acquisition, at depth, and with a high k value. This has been provided by the serpentinite modelled.

As the section has been projected north of the road, it is unlikely that a dyke in an east-west fault following the road would have been sampled at all: it is only poorly expressed in the aeromagnetic coverage.

The position of the section, although to the north of the road, is not to the north of Wonnaminta H.S. Given the scale of modelling, and the relative width of the strike- slip fault plane (as evidenced by a "blade" of quartzite fault gouge along the road at 630660 mE 6609706 mN), it is considered that the overall disposition of units would still be adequately sampled some tens to hundreds of metres north of the fault. I do not think that this assumption, although providing a small inaccuracy in the model, affects the overall style of solution. It is my opinion that repeat observations 2 to 3 km north of the road would show similar style and thickness of units as modelled in this section nearer the road.

In any case, it is impossible to construct a two-dimensional model to test these ideas without aliasing the response. This is because the near-parallelism of the dykes to the line of section violates the assumption of orthogonality of structure and section that underpins the method.

*4.10.9 Alternative Genetic Models.*

In order to discriminate between two competing, geologically feasible solutions, a parameter measuring the goodness of fit between the observed data and the modelled data is required. This parameter is called the objective function.

The objective function used for this purpose is the RMS error between observed and calculated responses, given by

$$\text{RMS error} = 1/[\Sigma(Zo\text{-}Zc)2/n]^2$$

where Zo are the observed values, Zc the calculated values and n the number of values.

Any model has particular variables (physical parameters which vary from place to place) including potential field strength and orientation, DC shifts applied to the calculated data, body positions and geometry, and body density and susceptibility.

In the comparison of two competing models, only some of these variables are free to change, because the two scenarios under consideration will be the same in many respects. For example, the surface geology and potential field parameters should be the same in any two models of the same area, as these are determined independently of any modelling. The remaining variables (those unconstrained by the real world) are termed degrees of freedom. Any of these can be fixed by making assumptions in the model, but must be balanced by changes in at least one other degree of freedom if the objective function is to remain constant. For example, for the objective function to remain constant, the density of a near surface body (one degree of freedom) may be increased. This can occur only if the density of a deeper body (another degree of freedom) is decreased proportionally, or the geometry of either body (two more degrees of freedom) changes. Thus a degree of freedom is defined as a variable set by a modelling assumption which requires a change in another variable in order to keep the objective function constant. Note that the more geological and petrophysical controls available, the fewer degrees of freedom exist in a model.

The purpose of comparing two alternative models is to see which combination of degrees of freedom produces a solution which best fits the observed data. When the objective function reaches a global minimum, the value of a free variable in the model is considered to be optimised for a specific combination of fixed degrees of freedom.

The curvature of the objective function in the vicinity of the global minimum indicates the sensitivity of the variable to further changes: if the slope approaching the minimum is steep, the variable is considered sensitive, meaning few values satisfy the optimum state. However if the slope is shallow or flat, the variable is insensitive, meaning that further changes in the variable will have no significant effects (after Roach, 1994). Note however that in any complex model solutions, there may be many free variables that are unable to be fixed.

This approach has been tested below, in general, keeping densities and susceptibilities as fixed degrees of freedom, and comparing RMS errors of different geometric solutions.

Using this approach, Direen (1998) showed the sensitivity of the preferred solution to the position of the primary décollement surface, defining a unique solution at c.8 km.

In order to further test the thrust concept, a model was developed for the local region between Nundora H.S. (c.598650 mE 6600690 mN) and near Wonnaminta H.S. (625440 mE 6609670 mN). This is shown in Figure 4.10.3. The model uses only the gravity data across the range 5 to 24 mGal, and assumes a constant 50 m depth of weathering . The higher frequency, multiple-observation gravity anomalies can be shown to fit a structural model that contains significant lateral density changes within the Kara beds. The full density range of the Kara beds in this scheme is from 2.61 $t/m^3$ to 2.78 $t/m^3$. This contrasts with outcrop measurements of 2.43 ± 0.11 $t/m^3$ , or velocity scaled approximations of 2.71 ± 0.06 $t/m^3$. These changes, outside the statistical error of the experimental density data, may represent subtle, continuous changes in metamorphic grade. Alternatively, repetitions of facies-related density variations could also explain this feature. Both alternatives are consistent with thrusting.

If higher density bodies represent increased metamorphic grades, and thus lower portions of the sequence, and a constant westerly direction of transport is assumed, this model demands a minimum of four thrust faults within the Kara beds, in order to place lower stratigraphic sections over higher (less dense) sections. This also assumes a subtle gradation of density from west to east between the faults.

An alternative model invoking only changes in thickness of alluvium to produce the gravity variations is shown in Figure 4.10.4. The density of the alluvium in this model is 2.00 $t/m^3$. This model was rejected because it requires thicknesses of alluvium and weathering in excess of 500 m. This was considered unreasonable, given that

## Figure 4.10.3 2D gravity model for the Kara beds, Nundora to Wonnaminta

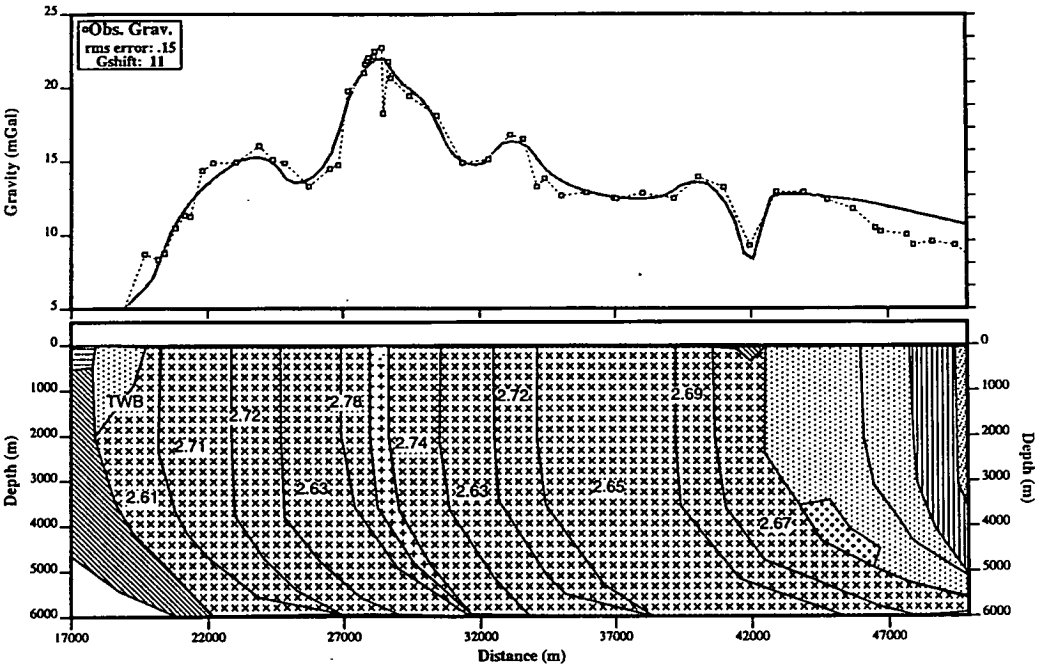


V. E. = 5.4. Key: Variable densities for the Kara beds quoted in t/m$^3$. + = Mt Arrowsmith Volcanics; x = Kara beds; dot stipple = Teltawongee Group; Vertical Stripe = Ponto Complex; Diagonal stripe = Mootwingee Group

## Figure 4.10.4 Alternative 2D gravity model for the Kara beds, Nundora to Wonnaminta

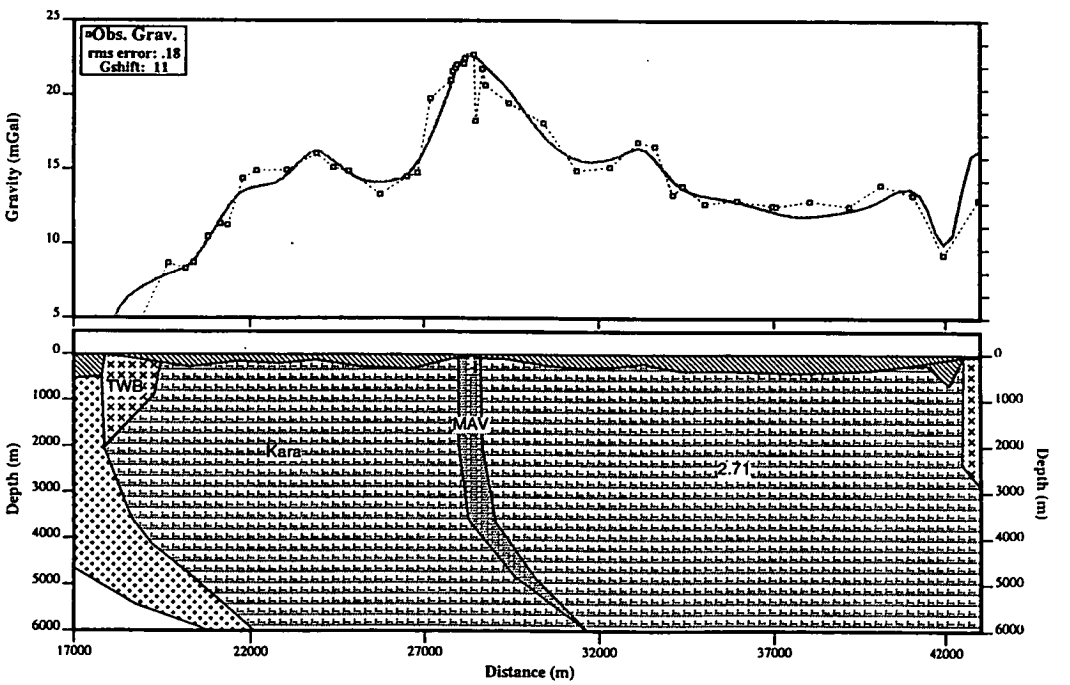


V. E. = 5.4. Key: Diagonal stripe = regolith; x/TWB = Teltawongee Group; MAV = Mt Arrowsmith Volcanics; + = Mootwingee Group. Kara density constant at 2.71 t/m$^3$.

relatively fresh Kara beds outcrop or shallowly subcrop (depths < 2 m) over most of the section.

If the validity of a thrust model is accepted for the reasons outlined above, several structural permutations still exist. Back-thrusting is potentially able to preserve the geometric constraints of vertical and horizontal surfaces, also maintaining the density distributions noted at the surface. Direen (1998) analysed several such solutions.

Several contrasting tectonic models can be proposed for the Bancannia Trough which do not invoke thrusting of the basement beneath the basin. These include published models (e.g. McIntyre & Wyatt, 1981) and theoretical models, including rift-graben and "steers-head" basin geometries. Models approximating these concepts have been constructed (Figures 4.10.5 –4.10.7), and are discussed below.

An in situ fossil rift with an inverted margin is shown in Figure 4.10.5. This model requires an 8 km thick pile of basalt, 40 km wide. These basalts have been attributed a susceptibility of 0.11 SI and a density of 2. 90 t/m$^3$ in order to fit the shape of the major anomalies. The form of the body required indicates this thickness must have been preserved without tectonic thickening.

Such an extreme in situ thickness of 100% basalt probably mitigates against this being a valid solution. Because the body required is symmetrical, it is obvious that full-scale continental break-up could not have occurred if this scenario is correct. This no break-up constraint allows comparisons to be drawn with other well-studied failed rifts such as the Oslo and US Midcontinent Rifts. Neumann et al. (1995) produced a gravity and magnetic model for the Vestfold Graben segment of the Oslo Rift, with a basaltic body of similar form and density (2.95 t/m$^3$). The thickness of this body was only 2 km between depths of 8 km and 10 km, and had a width extent of 20 km (aspect ratio 0.1). Allen et al. (1995) showed an 18 km thickness of Keweenawan basalts developed in the Lake Superior segment of the Midcontinent Rift. These were given a density of 2.90 t/m$^3$ and a susceptibility of 0.007 cgs, with both positive and negative remanence. The model for the Keweenawan rift basalts, constrained by seismic reflection data, showed the body to be saucer-shaped with a width of 160 km. The aspect ratio (0.1) of the Keweenaw rift is thus half the proposed alternative solution for the Bancannia Trough (0.2).

## Figure 4.10.5 2D gravity and magnetic model of inverted basin geometry, Nundora-Wonnaminta section

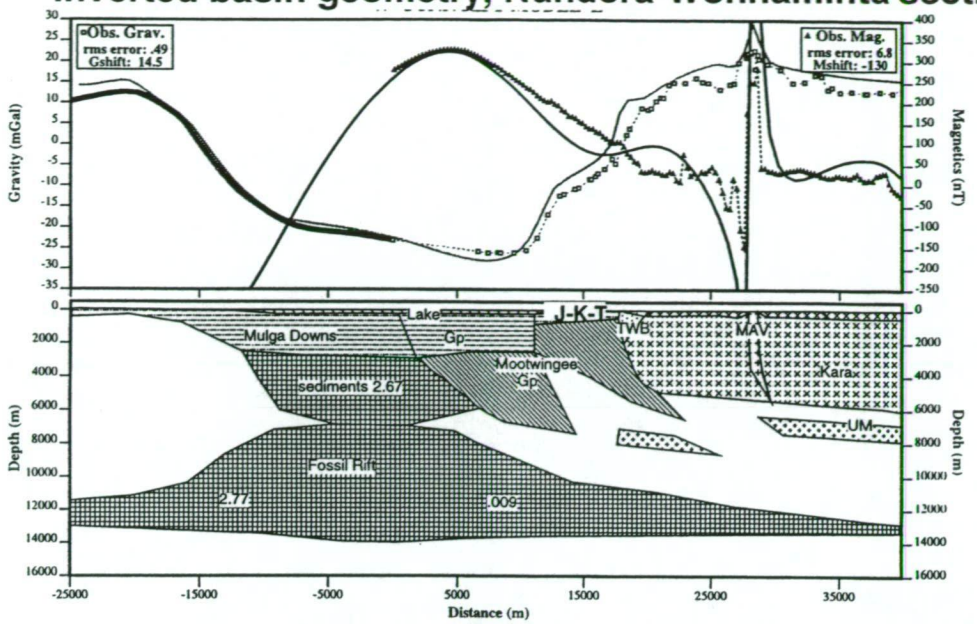


V. E. = 4.375. Key: J-K-T = Murray Basin sequences; MAV = Mt Arrowsmith Volcanics seds = possible Cambro-Ordovician section in Bancannia Trough; UM = serpentinised Mafic-Ultramafic slices; TWB = Teltawongee Group; Fossil Rift = basalt with properties shown in t/m$^3$ and cgs.

## Figure 4.10.6 2D gravity and magnetic model with "steer's head" basin geometry, Nundora-Wonnaminta section

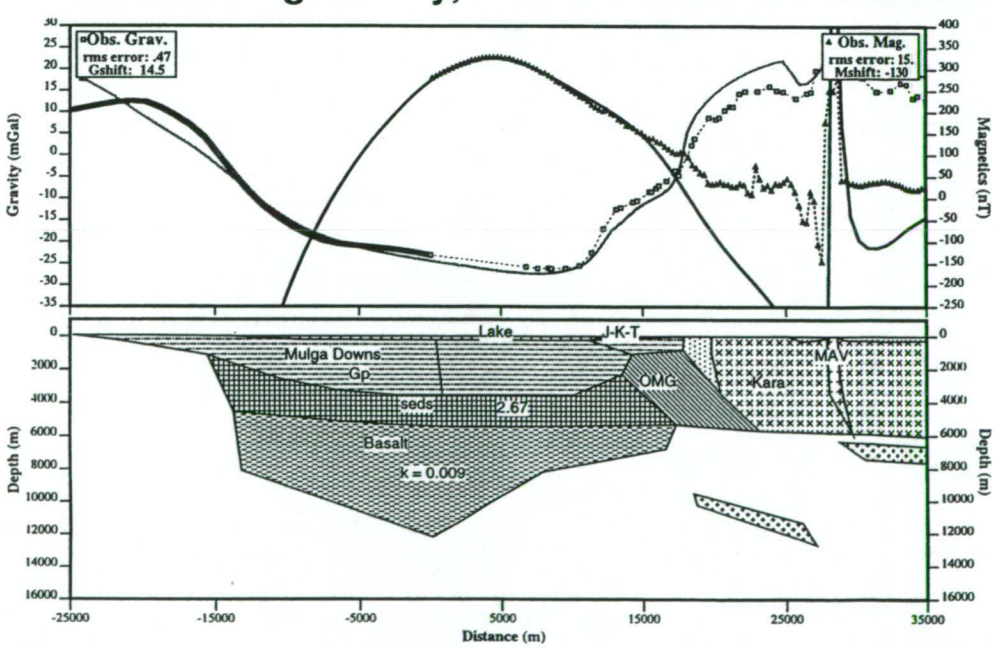


V. E. = 3.75. Key: Lake = Quaternary sequence; J-K-T = Murray Basin sequences; MAV = Mt Arrowsmith Volcanics; seds = possible Cambro-Ordovician section in Bancannia Trough; OMG = Ordovician Mootwingee Group; + = serpentinised Mafic-Ultramafic slices; ... = Teltawongee Group

Thus comparisons with other failed rift systems suggest that a failed rift is unlikely beneath the Bancannia Trough, on the grounds of aspect ratio of the proposed rift basalt complex.

Another genetic possibility for the Bancannia Trough geometry is the "steer's head" basin form, shown in Figure 4.10.6. This also requires an extreme thickness of basalt (7 km) at very high susceptibility to fit the magnetic profile.

Another possibility for the Bancannia Trough basement is the presence of downfaulted Proterozoic units of the Curnamona craton. The most magnetic of these, lying to the south of Broken Hill, are schists and gneisses of the Redan Block (B.Stevens, verb.comm., 1996). Some 72 magnetic susceptibility measurements were made on 8 samples of "magnetic" schist and gneiss of the Redan Block, provided by the NSWGS. These gave an average k of 0.0024 ± 0.0024 SI, with a maximum value of 0.011 SI. These values are significantly lower than those recorded for the Palaeozoic basalts in the Wonominta Complex. A model displaying Proterozoic basement beneath the Bancannia Trough is shown in Figure 4.10.7, with reasonable fit for the major magnetic anomaly. To produce this fit, the model invokes susceptibilities of 0.036 SI, more than three times the measured values.

A further model, based on a graben floored by dacitic volcanics (after McIntyre & Wyatt, 1981) was tested by Direen (1998), and also found to contain significant problems.

### *4.10.9 Synthesis for Nundora-Wonnaminta section*

This examination of alternative models shows that the most reasonable solution for the Nundora-Wonnaminta section is an imbricate fan with detachments at 8 km, and 14 km-16 km. The direction of thrusting is probably to the west, with the thrust stack involving the (non-crystalline) basement to the Bancannia Trough. However, the possibility of at least some hinterland-vergent thrusting cannot be ruled out by two-dimensional forward models. Other tests must still be applied to discriminate between these alternatives.

### *4.10.10 Turkaro Range Interpretation*

A non-genetic model for this section is shown in Figure 4.10.8. This model, like the initial model for the Nundora-Wonnaminta section, attempts to explain the magnetic

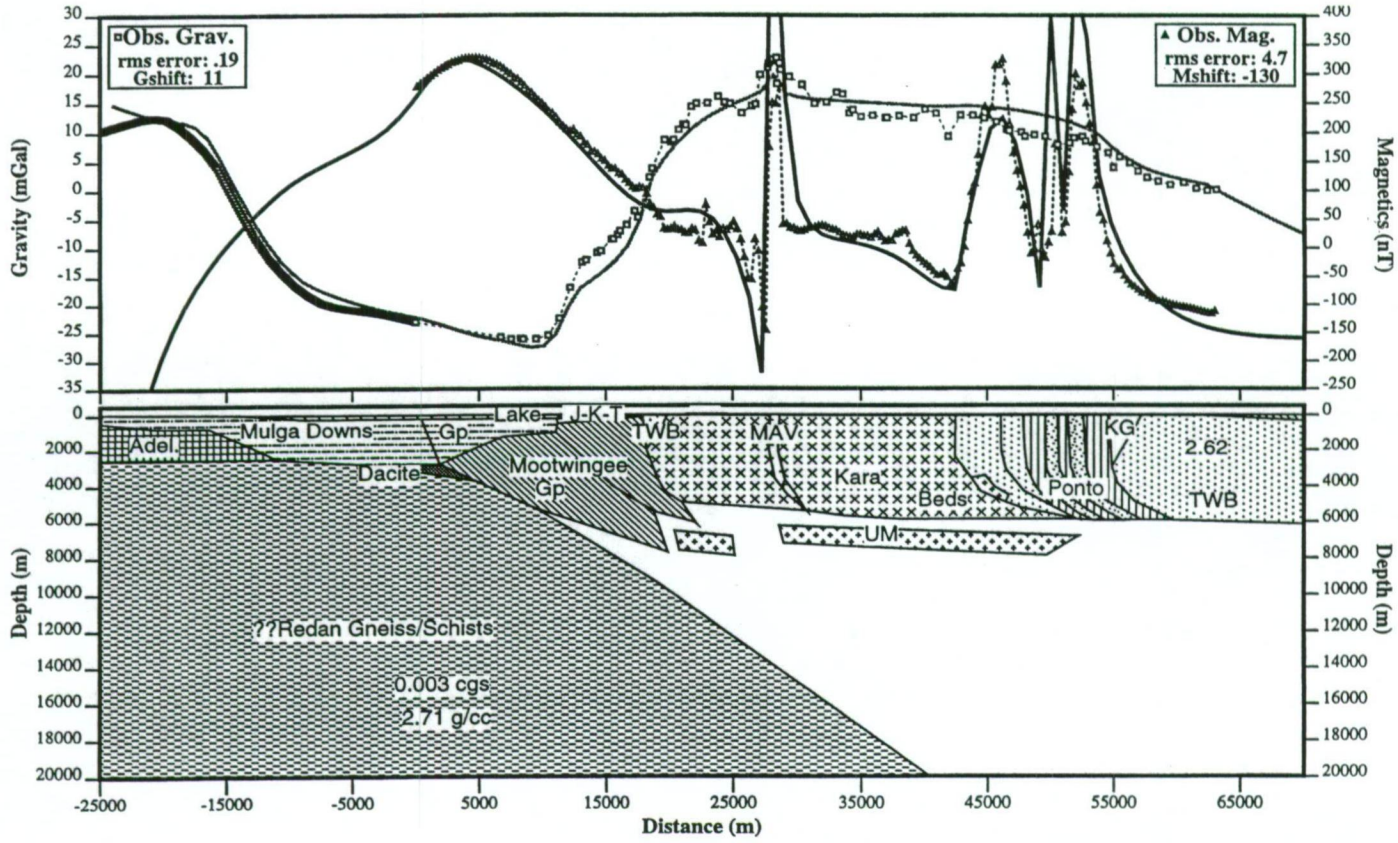


V. E. = 3.5. Key: Adel. = Adelaidean. KG = Kayrunnera Group; Dacite = dacitic volcanics intersected in Bancannia South-1; Ponto = Ponto Complex; for other abbreviations, see Figs 4.10.5/6.

**Figure 4.10.7 2D gravity and magnetic model, with Proterozoic Redan block beneath the Bancannia Trough**

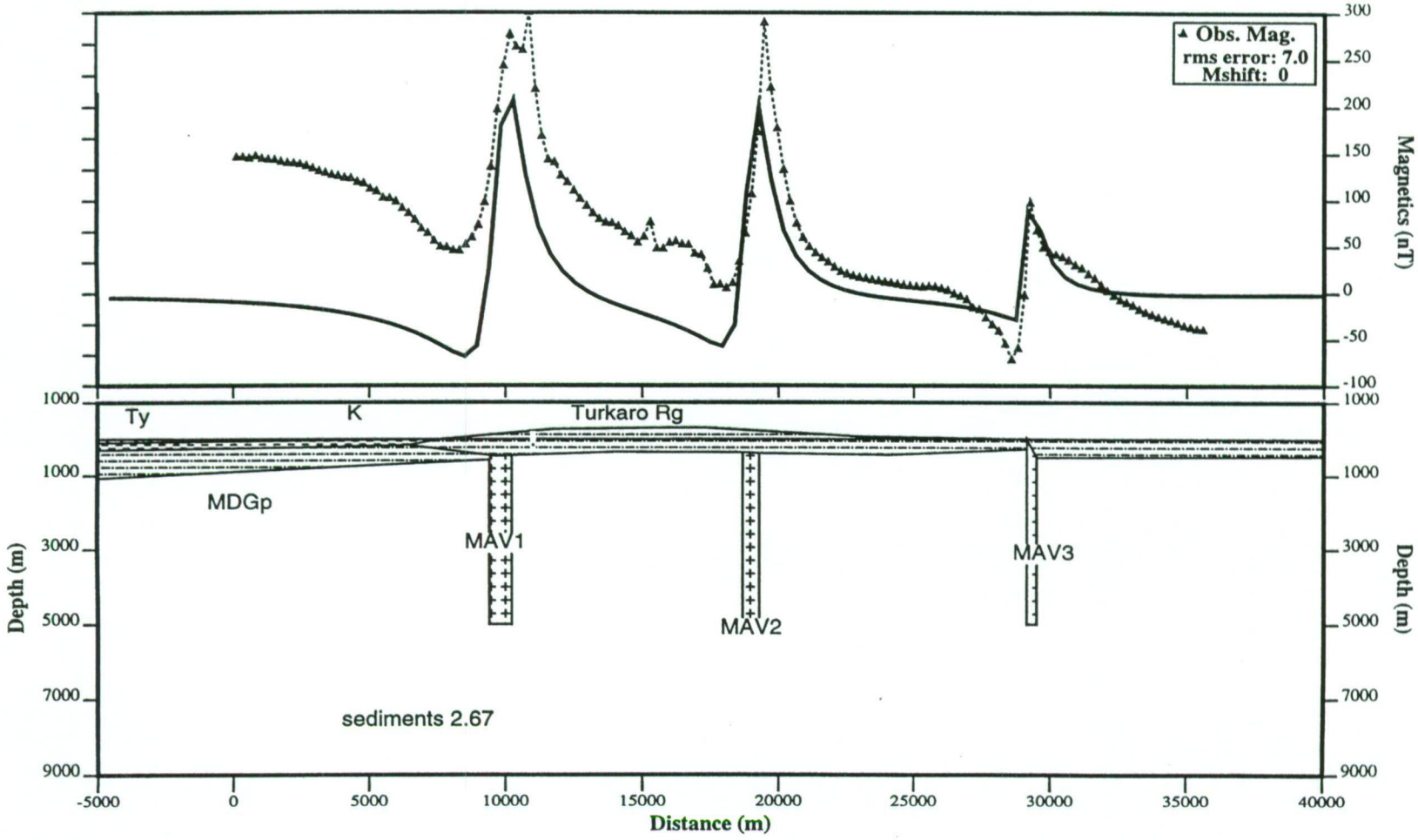


V. E. = 5. Key: Ty, K = Murray Basin sequences; MDGp = Mulga Downs Group; MAVx = slices? Of Mt Arrowsmith Volcanics

**Figure 4.10.8 2D magnetic model for Turkaro Range with simple vertical geometry**

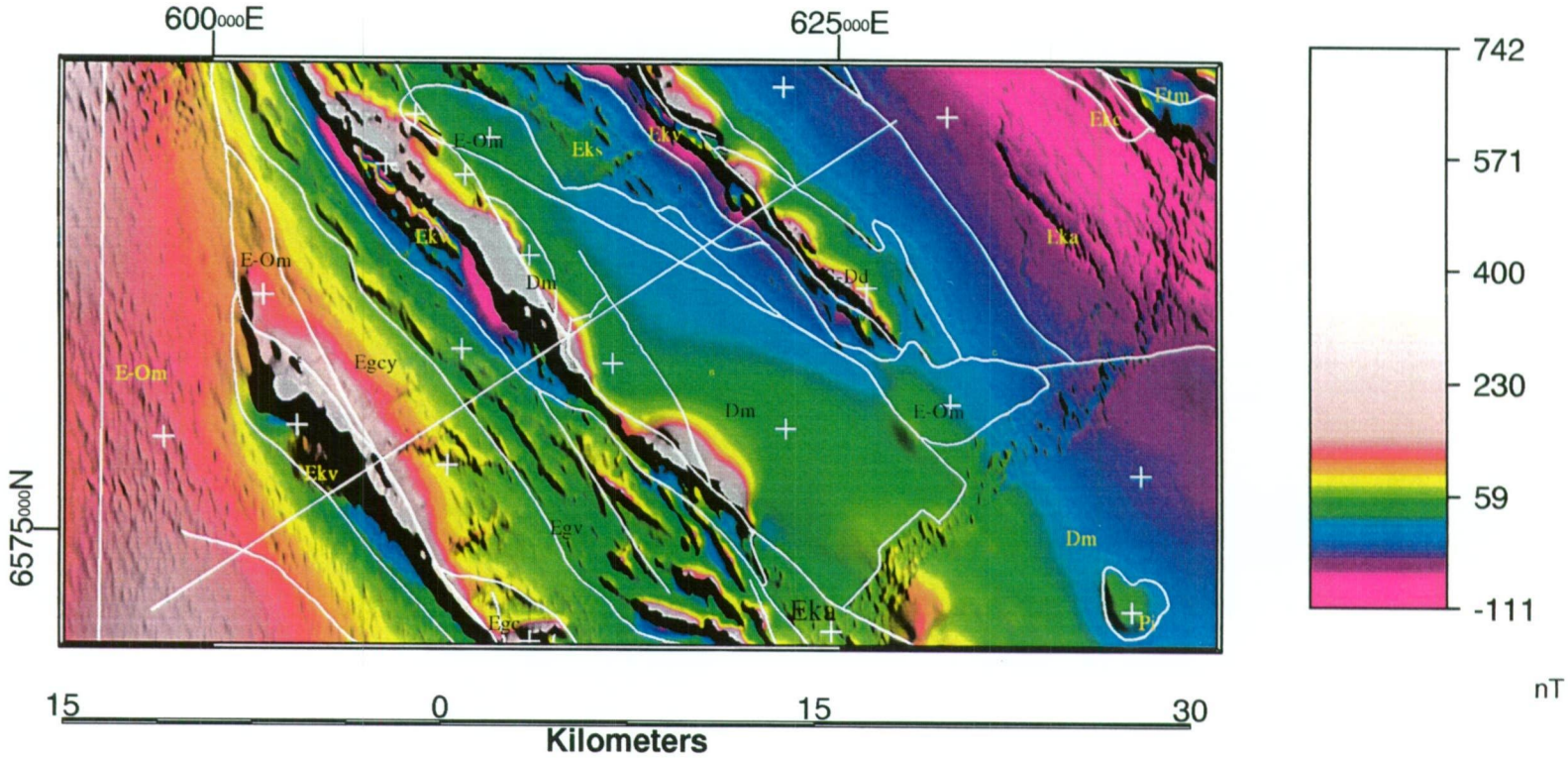


**Figure 4.10.9 TMI image and interpretation, Turkaro Range area.**

Line of modelled section shown.
For ciphers, see discussion in text, and key, Wonnaminta 7336 1:100 000 sheet, back pocket.

## Figure 4.10.10 Alternative 2D magnetic model, Turkaro Range

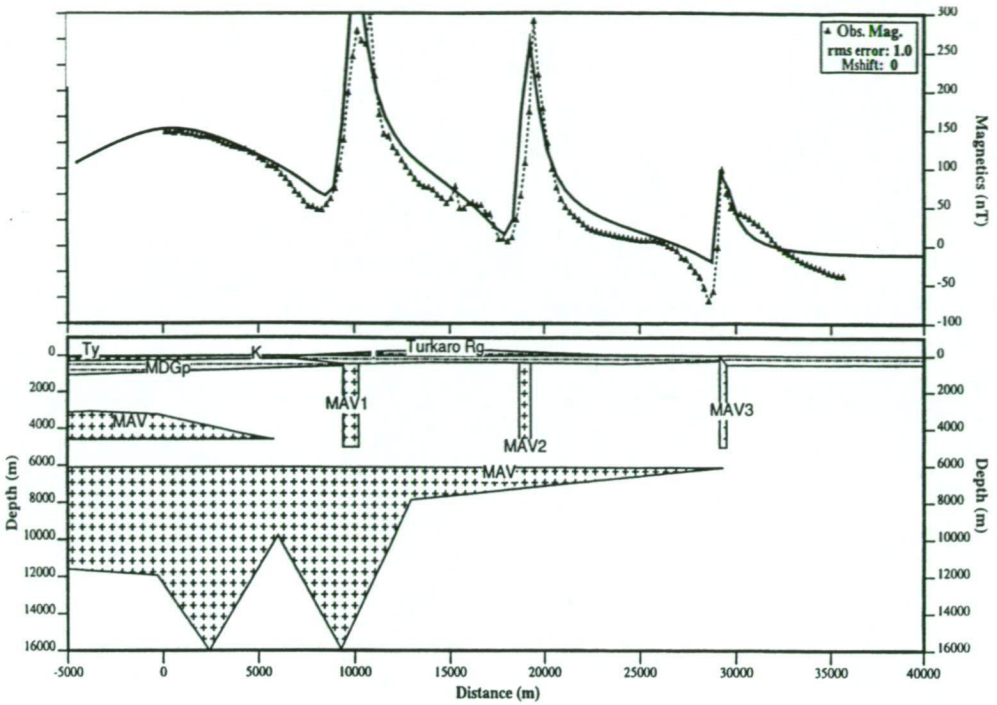


V. E. = 2.81. Key: as for Fig.4.10.8.

## Figure 4.10.11 Alternative 2D gravity & magnetic model, Turkaro Range

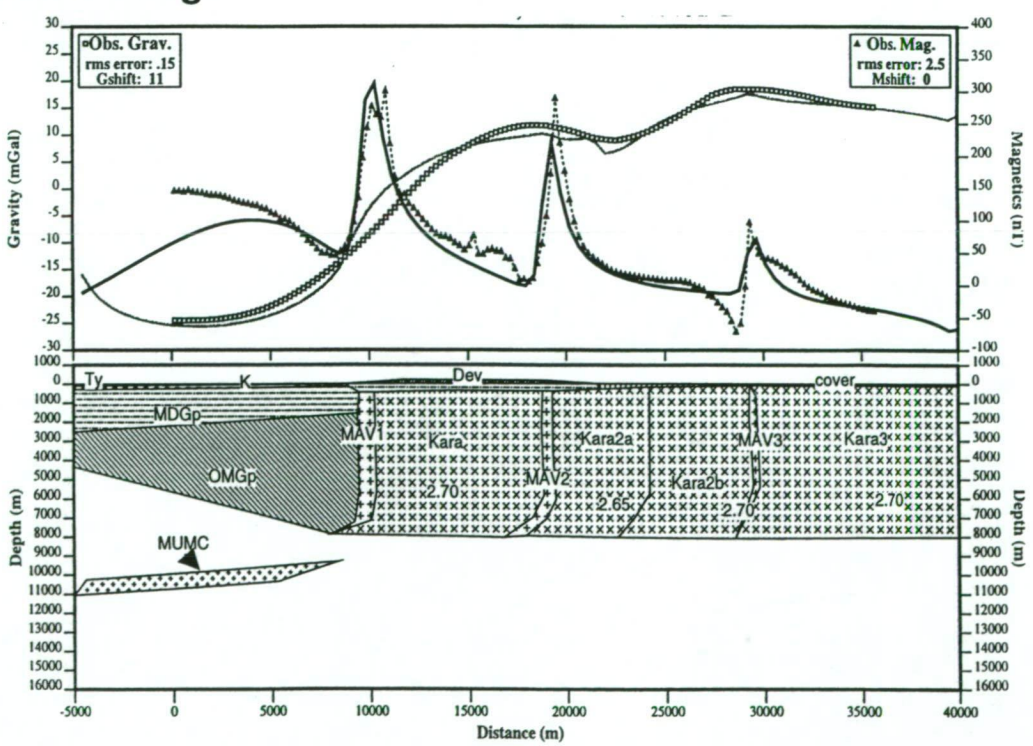


V. E. = 2.81. Key: Dev = Mulga Downs Group; OMGp = Ordovician Mootwingee Group MUMC = Mafic-Ultramafic complex; Kara x = thrust slices of Kara beds, densities shown in t/m3; remaining abbreviations as for Fig.4.10.8.

anomalies with the vertical geometry and the minimum number of bodies. The poor magnetic fit again illustrates the need for both vertical and sub-horizontal components in modelling the magnetic field, a fact that was first recognised by McIntyre &Wyatt (1981).

A fold-and-thrust solution for this section is described in Direen (1998), with four thrusts identified, involving packages up to the Ordovician Mootwingee Group.

*4.10.11 Comments; Alternative Models*

Figure 4.10.10 shows a model that attempts to provide the mid-crustal magnetic response with igneous bodies having the same properties as the Mt Arrowsmith Volcanics. As shown, a better fit can be obtained, but the geometry of the solution defies reasonable interpretation, with up to 10 km of irregular basaltic intrusions. This style of solution is typical of the approach applied by Encom (1994).

The final model (Figure 4.10.11) was constructed to determine whether the Turkaro Range section was sensitive to the dip ambiguity inherent in the Nundora-Wonnaminta section. Again, the model shows that although an easterly dip is the best RMS error solution for the Bancannia Trough basement, the solution may contain easterly- or westerly- dipping thrust planes in the Kara beds.

*4.10.12 Turkaro Range synthesis*

The accepted model, derived using the same properties and assumptions as the preferred solution for the Nundora-Marrapina section, shows the same style and ambiguities.

*4.10.13 Marrapina-Nuntherungie Interpretation*

An east-dipping imbricate fan model is analysed in Direen (1998).

*4.10.14 Alternative Model*

An alternative model involving westerly-dipping units is shown in Figure 4.10.12. This model possesses essentially the same geometry as the westerly-dipping model for the Nundora-Wonnaminta section. The RMS errors of this alternative pair of solutions are

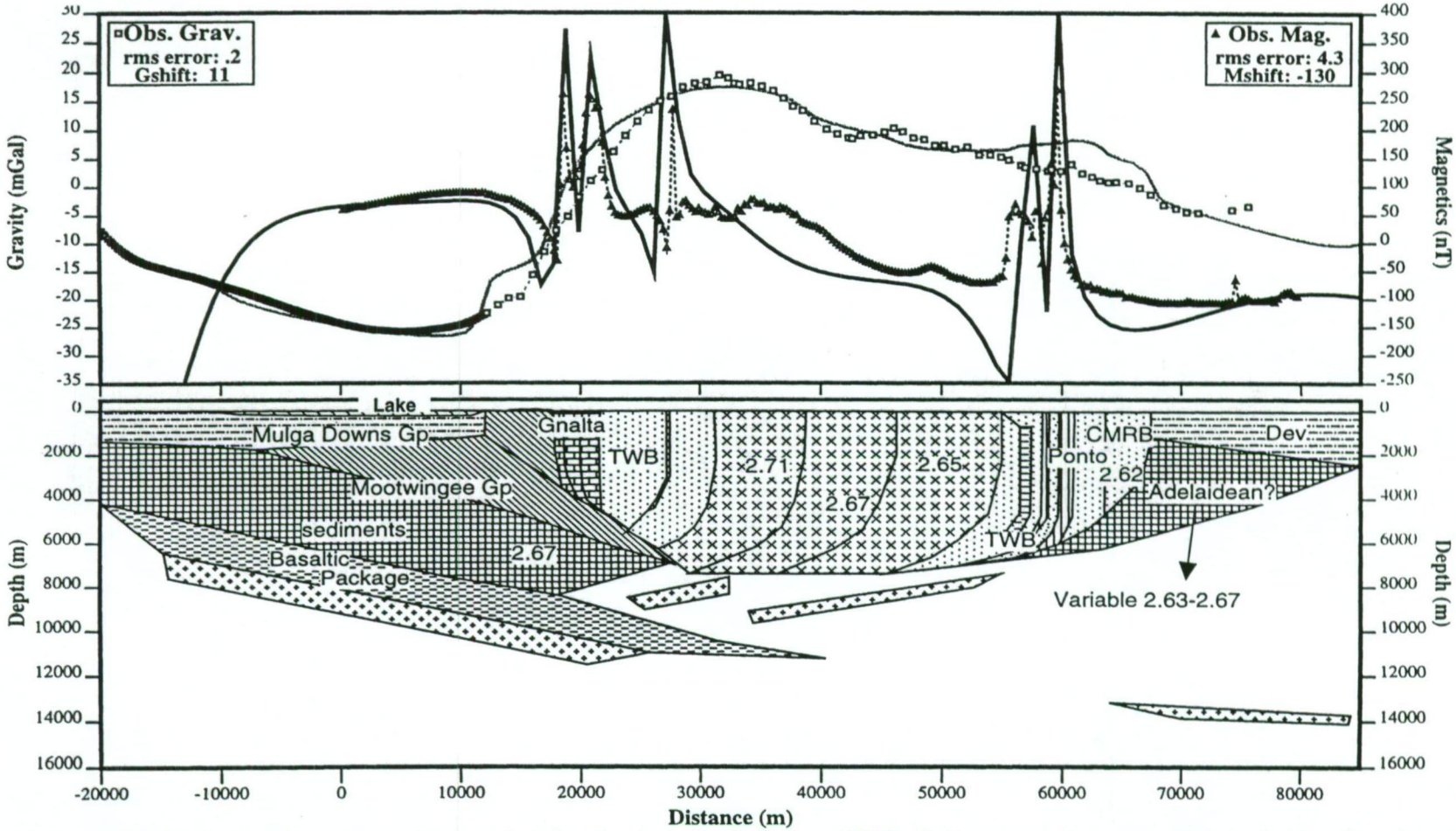


V. E. = 5.31. Key: Lake = Quarternary Bancannia Lake; Gnalta = Gnalta Group; TWB = Teltawongee Group; x = Kara beds, densities shown in t/m$^3$; Ponto = Ponto Complex; CMRB = Copper Mine Range Formation of the Teltawongee Group; Dev = Mulga Downs Group; Adelaidean? = possible Adelaidean metasediments or Ordovician section; sediments = possible Ordovician section; + = Mafic-ultramafic slices

**Figure 4.10.12 2D gravity and magnetic model of east-vergent thrust geometry, Marrapina-Nuntherungie section**

equivalent, signifying good model correspondence. However, it is significant that the RMS errors of the east- and west-dipping versions of the Marrapina-Nuntherungie section favours the east-dipping model due to an error reduction of about 40%. The comparative error decrease for alternative east- and west-dipping versions of the northern line is about 25% (gravity) and 10% (magnetics).These comparisons may help constrain the direction of thrusting.

*4.10.15 Marrapina-Nuntherungie synthesis*

This section can be constructed using equivalent geometry and assumptions to the sections to the north. This produces a good fit for an easterly-dipping imbricate thrust stack detaching in the upper crust at about 8 km, and again in the mid-crust at c.14 km. All units from the Neoproterozoic to the Ordovician are involved in thrusting, which had terminated by at least the Late Devonian. Significant improvement of model fit (up to 40%) can be made by accepting an easterly-dipping thrust stack over an alternative west-dipping model.

*4.10.16 Mt Arrowsmith Area*

In order to confirm the validity of the interpretation of large piles of Mt Arrowsmith Volcanics and serpentinites under the Bancannia Trough, the following investigation was undertaken. The type area for the MAV is at Mt Arrowsmith, approximately 60 km to the northwest of the Nundora-Wonnaminta section. The MAV at Mt Arrowsmith occur as steeply (70-80°) east-dipping fault slices up to 4.5 km total thickness. The volcanics preserved include magnetic basalts and trachybasalts, and non- or weakly magnetic volcanogenic sediments (Edwards, 1980; magnetic data, this study). These are in fault contact to the east with slices of non-magnetic Kara beds equivalents (Mills, 1992). To the west lies a faulted syncline of Ordovician sedimentary rocks equivalent to the Mootwingee Group; fault juxtaposed against this further west lies a second syncline containing Middle Cambrian sedimentary and volcaniclastic rocks equivalent to the Gnalta Group (Wopfner, 1966). The Mt Wright Volcanics are not observed at surface, although they may be present at depth (see section 4.9.2)

Older vintage aeromagnetic data were obtained from AGSO to check: a) if the MAV give rise to a significant magnetic anomaly; and b) whether the properties of the MAV at Mt Arrowsmith could generate the anomaly under the Bancannia Trough if a sufficient volume were present. Unfortunately the data obtained was a grid extracted from the magnetic map of Australia (Tarlowski et al., 1996), and no information was

available regarding the flying height, line direction, filtering or grid cell size (D. Souter, pers. comm. 1998). These problems mean that the solutions presented in the following models are not as certain as others presented above, and must be treated with a degree of caution. Gravity data are unavailable at appropriate spacings in this area to improve the interpretation.

A line of section was extracted from the magnetic grid between 548000 mE 6675500 mN and 562500 mE 6681000 mN, in the vicinity of Bynia Tank along strike of the Mt Arrowsmith massif (Figure 4.10.13) Although a line through the region of outcrop would have been preferable, an along strike projection was used to avoid non-two dimensional effects due to convergence of two anomalies in that region. The extraction was performed using the procedure outlined above. The simplest possible model for the area is shown in Figure 4.10.14. The parameters for this model are given in Table 4.10.1.

**Table 4.10.1 Mt Arrowsmith Model Parameters**

| **Parameter** | **Value** |
|---|---|
| Total Field intensity | 57300 nT |
| Inclination | -63.53° |
| Declination | 9.3° E of N |
| Line azimuth | 50° |
| Equivalent Height | 400 m |

The model shows three separate bodies of MAV with similar magnetic susceptibilities ($3000 \times 10^{-5}$ to $4000 \times 10^{-5}$ SI). The body to the west is a simplification of several off-line bodies giving rise to linear anomalies visible in map view, as opposed to the magnetic tail in the section. The main thicknesses of MAV in the centre of the model dip east at 11° and 76°. Between these two bodies, in inferred fault contact with the MAV and each other, are two non-magnetic wedges. These represent the along-strike projection of the two fault-bounded synclines of Gnalta and Mootwingee Group equivalents outcropping near Tobacco Bush Creek. The total thickness represented by the two main slices is approximately 2700 m, which is a minimum thickness not accounting for the simplified geology to the west.

A second model using the same data with identical parameters was constructed over the Bancannia Trough using the properties of the main mafic wedge and ultramafic slices in the fold-and-thrust solutions of section 4.9.7. The approximate apparent thickness of this body is 3600 m.

## Figure 4.10.13 2D magnetic model, Mt Arrowsmith

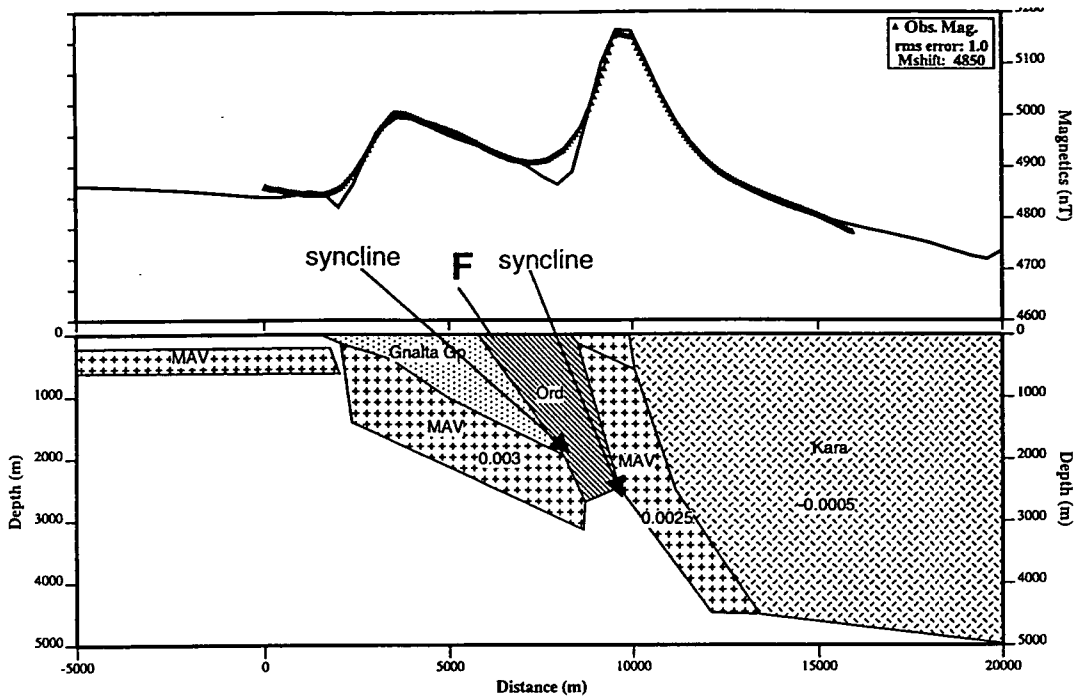


V. E. = 5. Key: MAV = Mt Arrowsmith Volcanics; Ord = Ordovician Mootwingee Group correlates; Kara = Kara beds. Magnetic susceptibilities quoted in cgs.

## Figure 4.10.14 Magnetic model for the Nundora-Wonnaminta section using properties derived from the model above

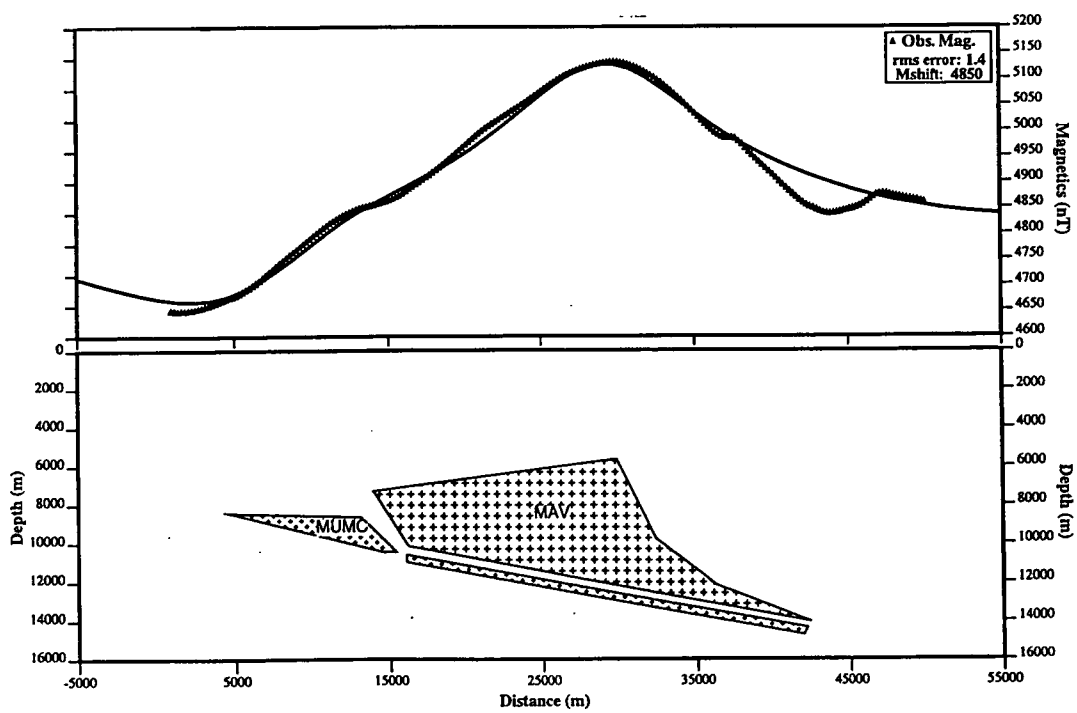


V. E. = 3.75. Key: MAV = Mt Arrowsmith Volcanics; MUMC = serpentineised Mafic-Ultramafic Complexes

**Figure 4.10.14a Magnetic Forward Model Traverse Locations, Mt Arrowsmith and Bancannia Trough**

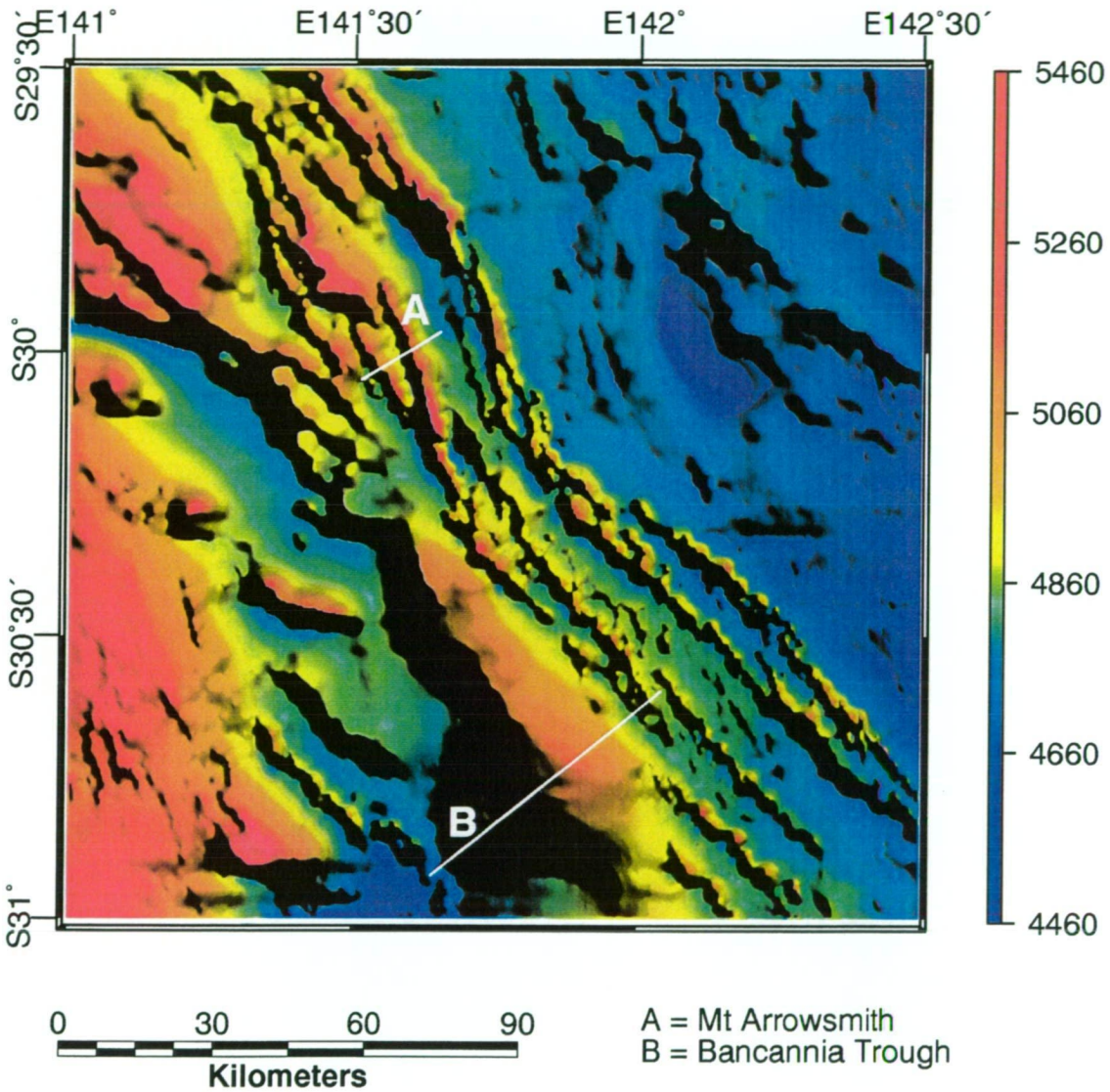


TMI pseudocolour and intensity layer shaded at 45 degrees from the northeast. Z scale in nT. Unknown base level and processing. Data courtesy AGSO.

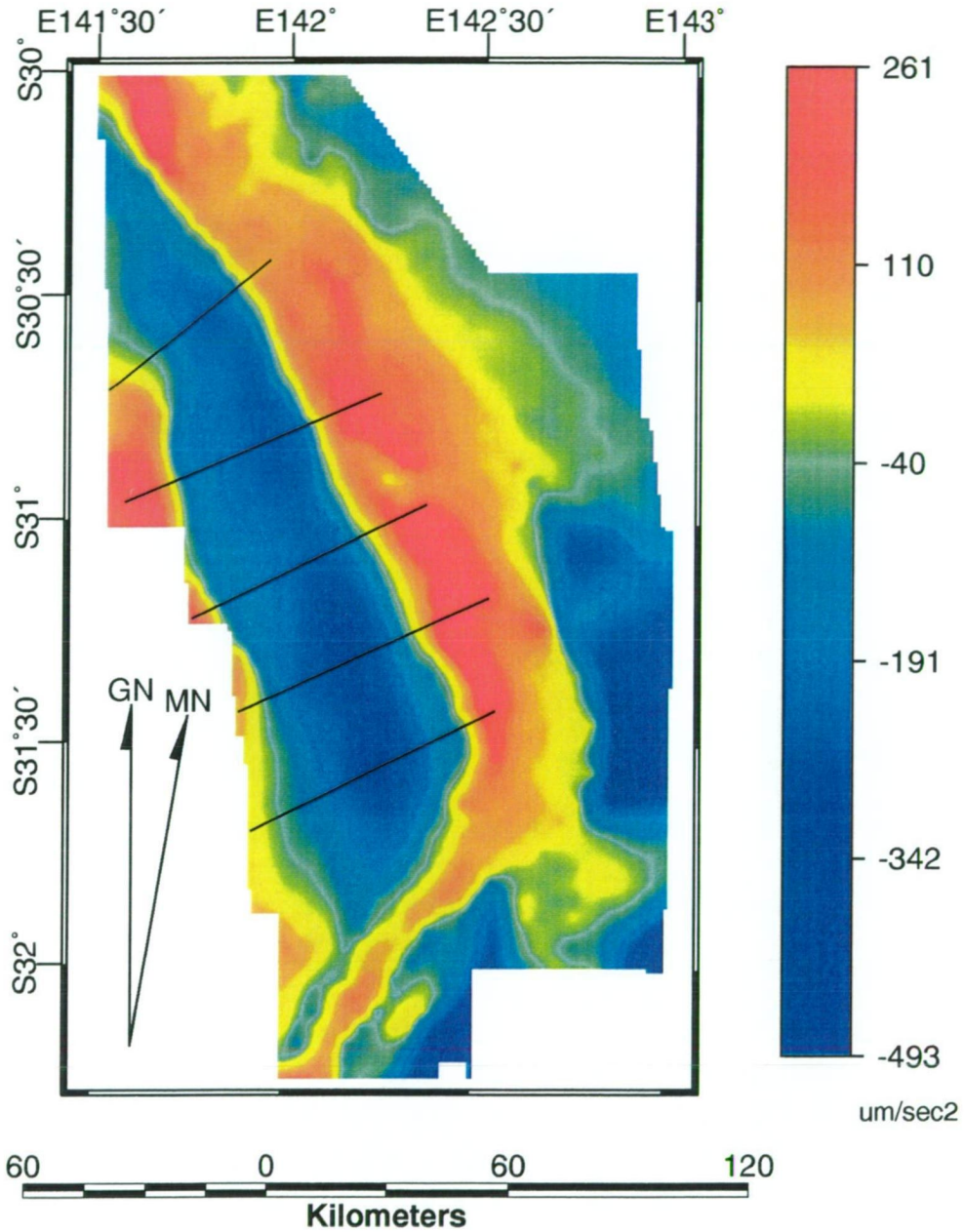


**Figure 4.10.15 Gravity model sections for testing Devonian section thickness, Bancannia Trough**

Bouguer Anomaly pseudocolour image

*"Caloola Ck" = Adelaidean sediments of the Caloola Creek Syncline, west of the Bancannia Trough; Wonominta = Koonenberry pre-Ordovician.

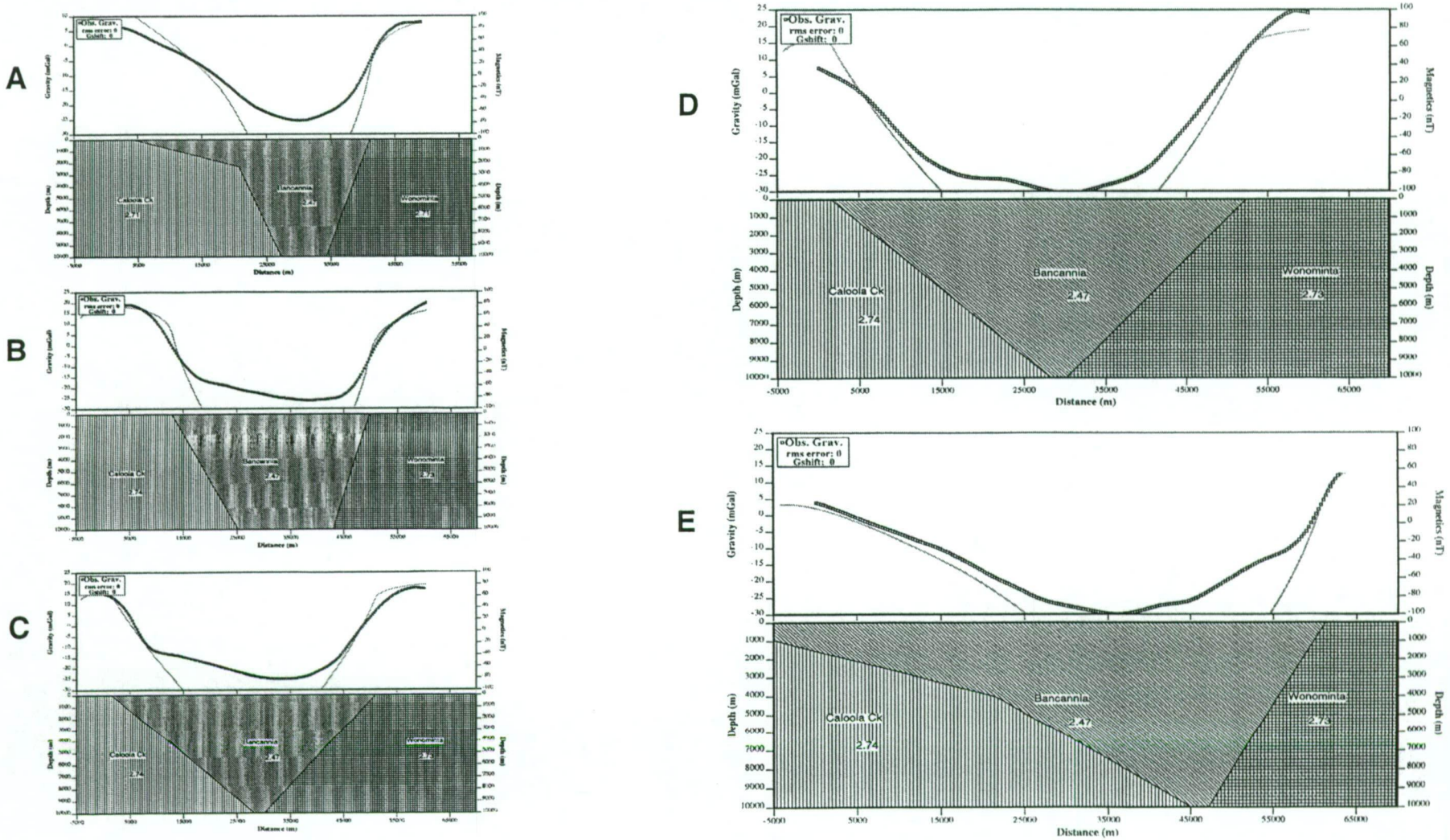


**Figure 4.10.16 Test of Encom (1994) model for Devonian section thickness, Bancannia Trough**

These models simply demonstrate the following:

1. the Mount Arrowsmith Volcanics occur as a series of fault bounded slices in the type area;
2. magnetic susceptibility of this suite is consistent across the belt;
3. the properties and minimum thickness of MAV in the type area are close to that required to generate the major anomaly present under the Bancannia Trough, 60 km along strike.

*4.10.17 Bancannia Trough*

Encom (1994), postulated that the Bancannia Trough may contain up to 10 km of Devonian sedimentary sequences, a finding supported by Alder (1996). However, as noted in Chapter 2 (section 2.5), this interpretation was based upon an assumed Bouguer density of 2.75 t/m$^3$, giving a density contrast for the Devonian of -0.1 t/m$^3$, based on density logs elsewhere in the Darling Basin (Encom, 1994). The assumed Bouguer density also gives a negative contrast for the Late Neoproterozoic-Late Cambrian sequences.

In order to apply a realistic test to Encom's estimate of the Devonian section in the Bancannia Trough, a series of gravity forward-models was constructed using the averaged measured densities for both sections: 2.47 t/m$^3$ for the Devonian, and 2.71-2.73 t/m$^3$ for the Late Neoproterozoic-Late Cambrian. An inferred density of 2.71-2.74 t/m$^3$ for the Adelaidean ("Caloola Ck") was based on Tucker's (1983) measured averages. Five models were constructed along the lines of section shown in Figure 4.10.15. The models were constructed using very simple block geometries, in imitation of the approach used by Encom (1994), which assumed that the Bancannia Trough was a simple horst and graben structure. In the construction, some consideration was paid to fitting the gradients over the basin shoulders by varying the density and geometry of the "rifted" blocks; no attempt was made to accurately fit the trough geometry; instead the maximum Devonian sediment thickness implied by Encom (1994) was modelled (Figures 4.10.16a-e). What this series of models shows is that, when the locally derived petrophysical property estimates of both the Devonian and older sequences is taken into account , 10 000 m of Devonian section is a gross over-estimate. For this reason, the c.4000 m section modelled in previous sections and in Direen (1998), is considered a better estimate of the Mulga Downs Group thickness.

*4.10.18 Structural synthesis for Nundora-Wonnaminta- Marrapina- Nuntherungie area*

The use of two-dimensional potential field forward models has offered new insights into the structure and possible tectonic development in an area of limited outcrop.

Surface mapping, drillhole and seismic data, and a database of petrophysical properties all help to constrain models for this area. In addition, the comparison of several competing theoretical solutions against each other allows selection of a model with best overall fit with regard to a standardised parameter (the RMS error) in each model.

These models indicate that it is likely that the Koonenberry-Bancannia region is a fold-and-thrust belt of Silurian or Middle Devonian age. This places it in the Lachlan Orogen described by Glen (1992) and Gray & Foster (1997b). The direction of thrusting is most probably to the west, although this requires confirmation by other means. Comparison of models also indicates that it is likely that the basement to the Bancannia Trough is also allochthonous, and contains a major magnetic unit. It is possible that this is a pile of rift basalts related to the Mt Arrowsmith Volcanics. Other possibilities exist, but are less likely. A further corollary of these models is that the Bancannia Trough has only existed since the Late Devonian.

## 4.11 Geological testing of thrusting in the Northern Koonenberry region

*4.11.1 Structural and metamorphic characteristics of eroded duplexes and imbricate fans: case examples.*

If the Koonenberry Belt is a fold and thrust belt, it should contain structural features that support the interpretation made on geophysical grounds. Geophysical interpretation suggests that the belt is an emergent foreland-vergent leading imbricate fan with possible back-thrusting (terminology after Boyer & Elliott, 1982) or alternatively, an eroded duplex (see Boyer & Elliott, 1982).

The lack of significant, structurally-competent carbonate packages within the Koonenberry Belt invites comparison with other leading imbricate system fold-thrust belts in eastern Australia; in particular, both the Adelaide Fold Belt (AFB) and the Lachlan Fold Belt (LFB) have similar structural styles.

These eastern Australian fold-thrust belts are distinctive for their monotonous turbidite packages, which lack structurally-competent sequences. These features lead to steeply ramping thrust faults instead of the "stair-step" ramps of the "classic" fold-thrust belts, e.g. Scottish Dalradian (Boyer & Elliott, 1982), Rockies, Appalachians, Swiss Alps, Italian Alps (Gray & Willman, 1991b).

Even in the absence of a complete lithostratigraphy (e.g. Ballarat slate belt, Gray & Willman, 1991a,b; Kanmantoo Group, Jenkins, 1990) workers have been able to define thrust-related deformation on the basis of two key relationships:
that of cleavage development and chevron folds to fault planes (e.g. LFB, western Vic: Cox et al, 1991, Gray & Willman, 1991a, Gray & Willman, 1991b; AFB, SA and Vic , Gibson & Nihill, 1992; Flottmann et al., 1994;
and that of metamorphic grade indicators to fault planes (e.g. LFB, western Vic; Cox et al, 1991, Gray & Willman, 1991a,b).

These features are reviewed briefly below.

Boyer (1986), using North American examples, showed that folding within thrust sheets was almost universally of kink-band style, at all scales. He showed that thrust related folds have chevron, cuspate, flattened chevron or box geometries, with large limb-length to hinge-width ratios.

The western LFB (Gray & Willman, 1991a,b; Glen, 1992) is a zone of faulted and folded Cambrian greenstones, Late Cambrian cherts and Ordovician quartz-rich turbidites. The c.3 km thick turbidite sequence has no developed lithostratigraphy, as it contains frequent lateral and vertical facies changes.

The belt comprises numerous ramping imbricate thrust sheets that are bounded by a series of meridional, sub-parallel west-dipping listric faults. Faults have lengths between 25 and 100 km and surface dips of > 60°. However, seismic data confirm that they detach at two horizontal decollements at 4 to 6 km, and 7 to 10 km (Gray et al, 1991). The major faults separate sequences with differing ages, and often, structural vergence. In outcrop, the hangingwalls of these faults are often highly strained but may have a relatively unstrained footwall. Fault traces are often only a few millimetres wide, but may be marked by cataclasite or clay gouge (Gray & Willman, 1991b).

The structurally higher parts of the thrust sheets contain regular trains of upright to steeply east- or west-dipping, close to tight chevron folds, with average interlimb

angles (ILA) of between 35 and 50° (Gray & Willman, 1991a; Cox et al, 1991). Regional fold wavelengths are of the order of 10 to 15 km, with amplitudes of 1 to 2 km. These folds often have doubly plunging axial surfaces, producing characteristic "canoe" shapes on map projections (Gray & Willman, 1991a,b).

Deformation in these higher zones is coaxial, and has produced little or no flattening of XZ strain indicators (Gray & Willman, 1991b).

Cleavage development in the upper parts of the sheets consists of spaced or solution axial planar cleavages in psammites, and a crenulation solution cleavage in pelites and semi-pelites. These cleavages are developed parallel to the axial planes of folds, although fanning through stress deviation is observed in psammites (Cox et al., 1991). The early crenulated cleavage found in pelites/semi-pelites is developed in response to flow during preferential take up of layer-parallel slip (Cox et al., ibid.). These incompetent layers may also develop parasitic folds, and be chaotic in major hinges for the same reason.

The structurally lower parts of the thrust sheets are only emergent in the hanging walls of thrusts, and are typically up to 3 km wide (Gray & Willman, 1991b). They correspond to a ramping of the regional enveloping surface at the thrust (Cox et al., 1991). These zones show features related to non-coaxial high strains. Approaching any thrust, Gray & Willman (1991b) noted that there was a 2.5 km wide (max) zone where chevron folds became inclined toward the fault. This corresponds to rotational tightening of the folds such that ILA's become 20 to 30°. This is well beyond the theoretical lock-up angle of c.60° predicted for chevron folds. This tightening is accompanied by flattening of XZ strain indicators (up to 5:1) and a decrease in the spacing of cleavages. The angle between bedding and cleavage also falls to < 20°, due to fold rotation.

In the 500 m hangingwall zone, axial planes rotate into parallelism with the fault planes, folds are flattened with XZ strain up to 30:1 and ILA's drop below 20°. This is accompanied by development of an intense fault-parallel phyllitic cleavage and a down-dip mineral stretching lineation. Cleavage may be overprinted by crenulations related to transpression, or later wrench reactivation of faults (Gray & Willman, 1991a).

A key timing relationship is indicated by the fact that the faults cut regional folds, indicating that folding occurred prior to thrusting (Cox et al., 1991; Gray & Willman, 1991b).

The entire sequence of faults and thrust sheets is also cut at a high angle by late vertical wrench faults. These have maximum displacements of tens of metres (Gray & Willman, 1991a)

The characteristic feature of chevron folds being progressively flattened and rotated in the hangingwalls of emergent imbricate thrust systems was also demonstrated in the Glenelg River Complex of southwestern Victoria (Gibson & Nihill, 1992), and the southern Mt Lofty Ranges of South Australia (Flöttmann et al., 1994). These are both part of the west-vergent Adelaide Fold Belt.

Cox et al. (1991) found that the enveloping surfaces of the structurally higher zones of the Lachlan Fold Belt are regionally flat or very shallowly dipping (Cox et al, 1991), and the gross metamorphic grade is in the chlorite zone for pelites. This feature contrasts with the metamorphic grade attained in the immediate hangingwall of thrusts, which can reach amphibolite grade. Mylonites and cataclasites are also frequently developed in this position (Wilson et al., 1992). The metamorphic grade increase has also been noted in a sudden appearance of the biotite and garnet isograds as faults are approached (R.Cayley, pers.comm. 1997), corresponding to a ramping of the enveloping surface (Cox et al., 1991).

This feature is not present in the Adelaide Fold Belt, where the peak thermal conditions were attained after the thrusting event, resulting in isograds unrelated to the thrust-system geometry (Jenkins, 1990).

The following sections (4.11.2 to 4.11.5) outline attempts to confirm these thrust-related structures in the Koonenberry Belt.

*4.11.2 Determination of dips of fault planes*

Due to the inherent ambiguities apparent in larger scale magnetic models (see 4.10 above), further testing of the dips of inferred faults was required to facilitate structural analysis. This was carried out by modelling ten asymmetric magnetic anomalies adjacent to inferred faults at locations along strike from the previously modelled sections.

Traverses perpendicular to the strike of these anomalies were extracted from gridded TMI data using the ERMapper 5.2 View Traverse function and exported to Model2d

using the revised ERMObs program. Care was taken in selecting anomaly profiles with single wavelength profiles that departed from and returned to an identifiable base-level (classic single body anomalies).

The rationale for selecting these anomalies was to allow the construction of very simply-dipping dyke-like models of the magnetic sources. These simple models have few variables and more degrees of freedom compared to multiple-body models of complex anomalies. More degrees of freedom facilitates testing of single parameters such as the dip of the body or fault plane, as small changes in the spatial variables do not impact upon other parts of the model, changing the response in a complex fashion. The problem of complex models containing fewer degrees of freedom has not yet been overcome for this type of approach (Roach, 1994).

The modelling procedure applied to test the dips of the10 selected anomalies used the following initial constraints:

- the rock sequence responsible for the anomaly was determined from geological mapping, and a fixed magnetic susceptibility ascribed on the basis of collated petrophysical data (Chapter 3.2);
- a four-sided polygon (usually a parallelogram) with depth >> width and a maximum cut-off depth of 4 km was digitised to represent the source;
- a DC shift was applied to the magnetic field to account for "regional" effects on these short profiles;
- changes in depth to top, and side dip were made until a rough fit of calculated and observed profiles was achieved.

At this stage, the number of variables for each model was seven (susceptibility, depth to top, depth to base, dip of top, dip of base, dip of sides), excluding magnetic field parameters (intensity, inclination, declination, sensor height, sensor orientation) which are considered fixed. Three of these variables are considered degrees of freedom under the initial constraints (depth to top, dip of top, dip of parallel sides). The first two of these parameters were then kept fixed, whereas the dip of the parallel sides was subjected to systematic perturbation.

The perturbation was effected by applying a series of dip increments to the initial state. In order to assess the effect of the perturbation, the objective function chosen was the RMS error.

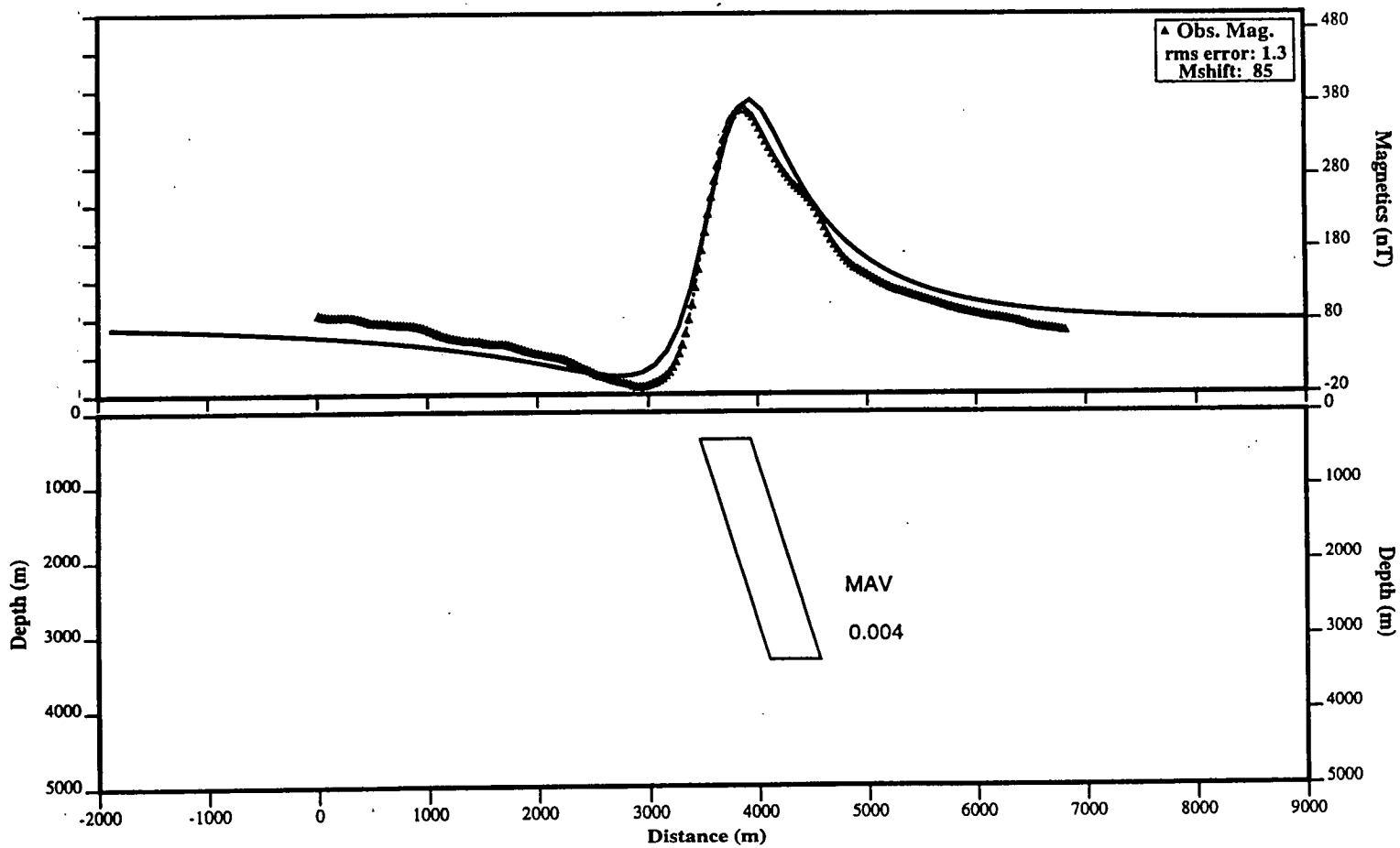


If the DC shift, shape, depth extent, depth to top, and susceptibility are kept constant, the model has only one degree of freedom which is the dip

**Figure 4.11.1 Simple 2D magnetic initial model for dip-sensitivity modelling**

Five degree dip increments were applied to the initial model between values of 90° and 60°, and 10° increments thereafter. This series of values was used because mapping indicates that faults and cleavages in this area are generally steeply dipping at the surface (Mills, 1992). For each successive increment, the value of the objective function was recorded. Both the intuitive dip direction (indicated by the "tail" of the magnetic anomaly) and the opposite dip direction were tested in this manner. With one exception (see below) the counter-intuitive direction always shows a strong increase in the objective function as small dip increments were applied. This supports the idea that direction of anomaly skew corresponds with direction of dip of a dyke-like body.

The results of this testing are summarised in Direen (1998).

*4.11.3 Summary*

The investigation and modelling of individual asymmetric magnetic anomalies is a useful tool in structural investigations hampered by poor outcrop conditions. Under a carefully defined set of simplifying assumptions, the investigation of ten anomalies yields useful and generally unambiguous dip information for 6 faults, only 3 of which had been mapped previously.

*4.11.4 Fold and cleavage development in the Nundora-Wonnaminta area*

Cleavage data from the Conns Creek area are shown in Figure 4.11.2, illustrating the footwall and hangingwall of a possible thrust system identified geophysically. This thrust separates the highly magnetic Mt. Arrowsmith Volcanics in the hangingwall from sediments of the Kara beds in the footwall. Near the contact, highly strained basalts have a foliation dip of 61° to 67° (T). This contrasts with average cleavage dips of 70° to 66° (T) for shales immediately west of the fault, and steep cleavage dips (79° to 58° T) in basalts and limestones 900 m further to the northeast. Cleavage 1.7 km to the northeast of the fault dips at c.80°. These observations lend weight to the interpretation that the Conns Ck Fault is a steeply east-dipping high angle or reverse fault, which has brought up slices of Mt Arrowsmith Volcanics from depth.

Cleavage data from two locations on the Wonnaminta Fault are shown in Figure 4.11.3. The Wonnaminta Fault separates the Mahomica Formation to the west from the Ponto Complex to the east. From geophysical interpretations, the Ponto Complex forms the hangingwall of this fault. Cleavage data show rotation to shallower easterly dips in the Ponto Complex, whereas dips in the Mahomica Formation dip steeply to both east and west, confirming the geophysical interpretation.

## Figure 4.11.2 Equal area nets, rock fabrics, Conns Creek thrust

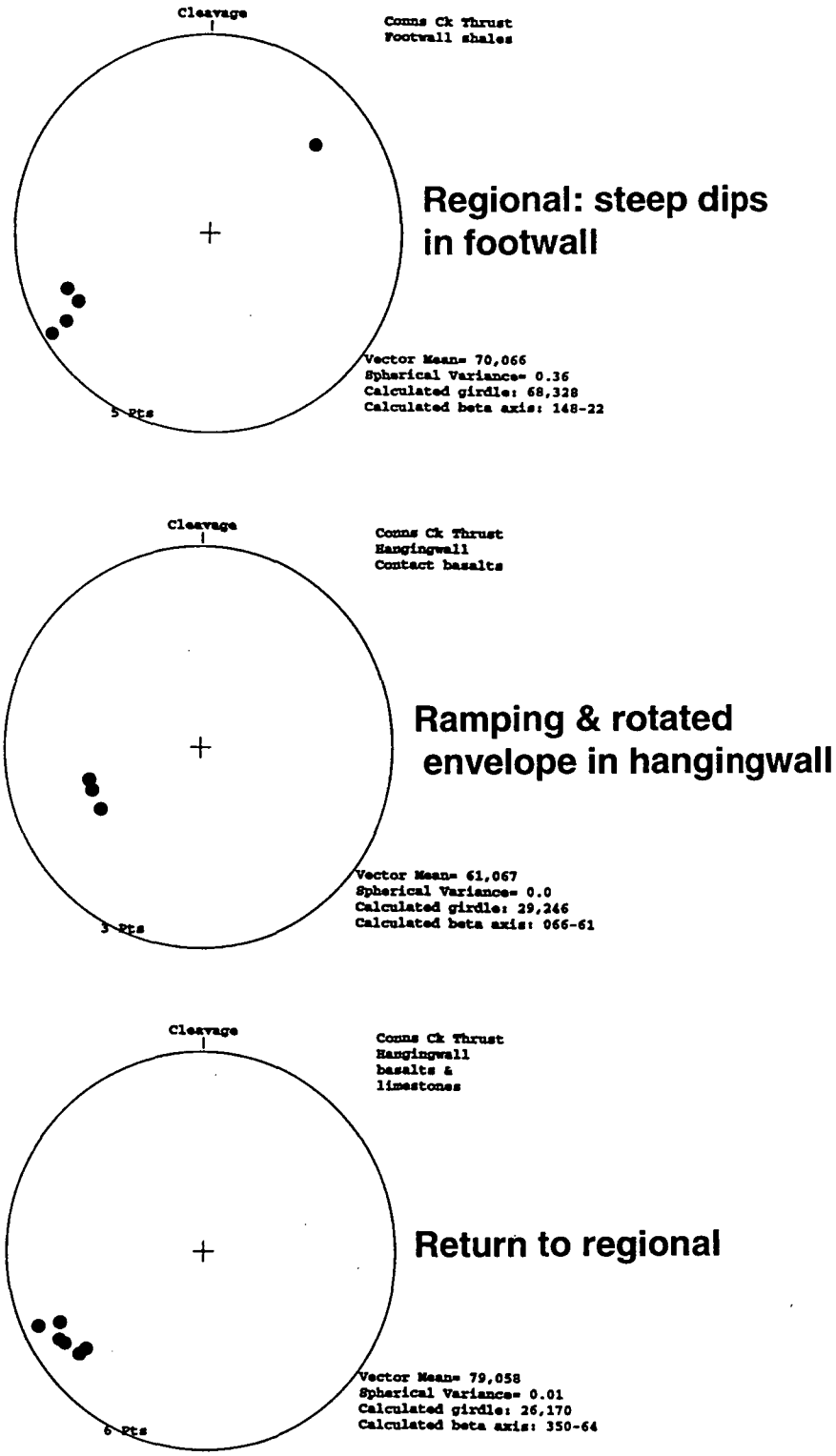


**Rotation of hangingwall cleavages with respect to footwall implies a listric fault geometry.**

## Figure 4.11.3 Equal area nets, rock fabrics from Wonnaminta Fault

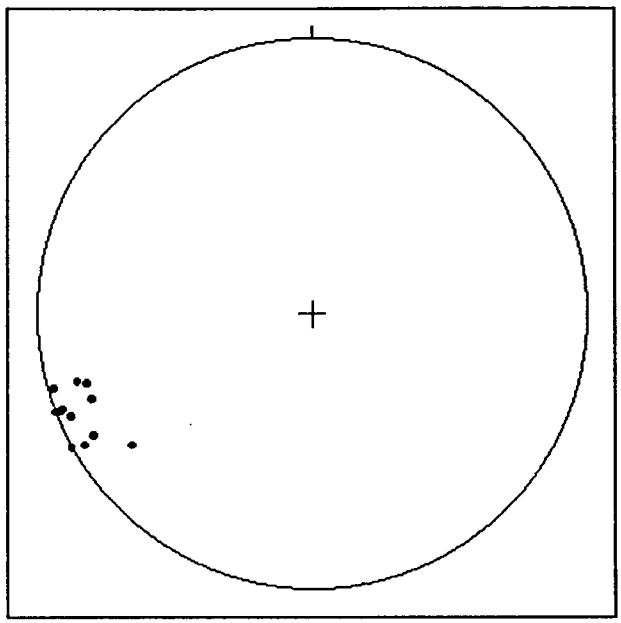

S1 cleavage in Teltawongee Group,
footwall of the Wonnaminta Fault

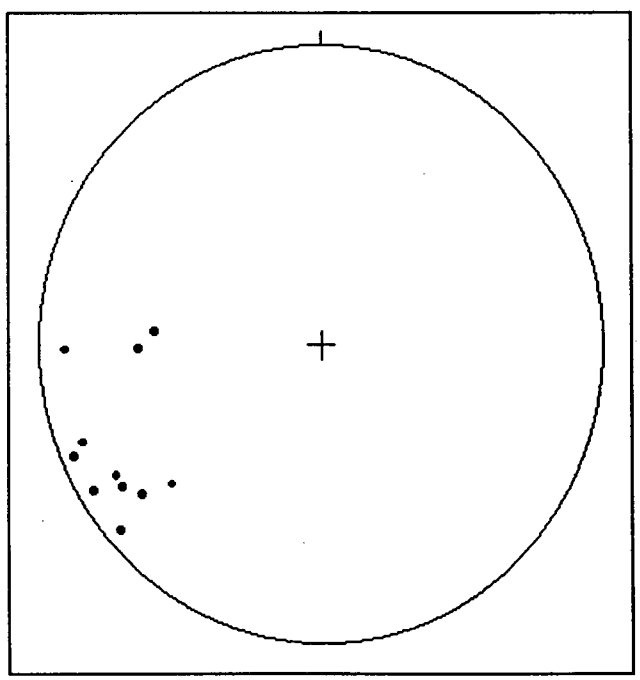

S1 cleavage in Ponto Complex,
hangingwall of the Wonnaminta Fault

Rotation of the fabrics in the eastern side of the fault with respect to the western side, implies a listric-to-the east fault geometry. Emplacement of younger (Late Cambrian) rocks over older (?Early Cambrian) rocks, implies a high-angle reverse fault.

The Gums Tank Fault is the boundary between the Kara beds to the west and the Mahomica Formation to the east. Cleavage data from traverses across this fault are shown in Figure 4.11.4. These data show rotation of cleavages to shallow easterly dips in the Mahomica Formation in contrast to bedding, which remains steeply dipping both east and west; cleavage in the Kara beds remains approximately constant, dipping 82° to 67°(T). These observations indicate a west-dipping high angle reverse fault.

In extensive field traverses throughout the Nundora-Wonnaminta- Marrapina-Nuntherungie area, only one mesoscale fold closure was observed. Measurements of bedding dip and facing can be used to infer sheared out or otherwise invisible synclinal closures in many areas e.g. Figure 4.11.5; this confirms the observations of Mills (1992). A possible explanation for this is given below at.

*4.11.5 Fold and cleavage development in the Cupala Creek area*

Collins (1984) reported structural observations from the proposed Copper Mine Range Formation in the Cupala Creek-Copper Mine Range area. Poles to bedding defined a pair of rounded macroscopic synclines separated by a fault. These synclines have statistical plunge of 18° to 150°, although mesoscopic fold hinges were noted plunging both southeast and northwest, implying a doubly plunging macroscopic fold or scissor faulting. Other observations by Collins (ibid.) suggested that the macroscopic folds were inclined to the southwest, with the southwest limb being slightly overturned.

These observations are supported by my fieldwork which noted parasitic and mesoscopic folds within both the Copper Mine Range Formation and the overlying Cupala Creek Formation. Folds in the Copper Mine Range Formation were tight (Interlimb Angles = ILA 5°, 28° & 45°) similar, asymmetric folds, with rounded, elliptical and chevron fold profiles. Fold shape appears strongly lithology dependent, with rounded folds observed in sandy lithologies and more angular fold shapes in shales. The asymmetry was to the southeast, with overturned southwest limbs; the plunge was c.10° between 140° and 175°). Measurements by K.J Mills on a newly discovered worm burrow bed indicate that the worm burrow traces are no longer perpendicular to bedding; this and the tight ILA imply fold flattening.

Observations of cleavage by the author in sandstones of the Copper Mine Range Formation show that this folding has been accompanied by cleavage formation sub-

## Figure 4.11.4 Equal area nets, rock fabrics, Gums Tank Fault

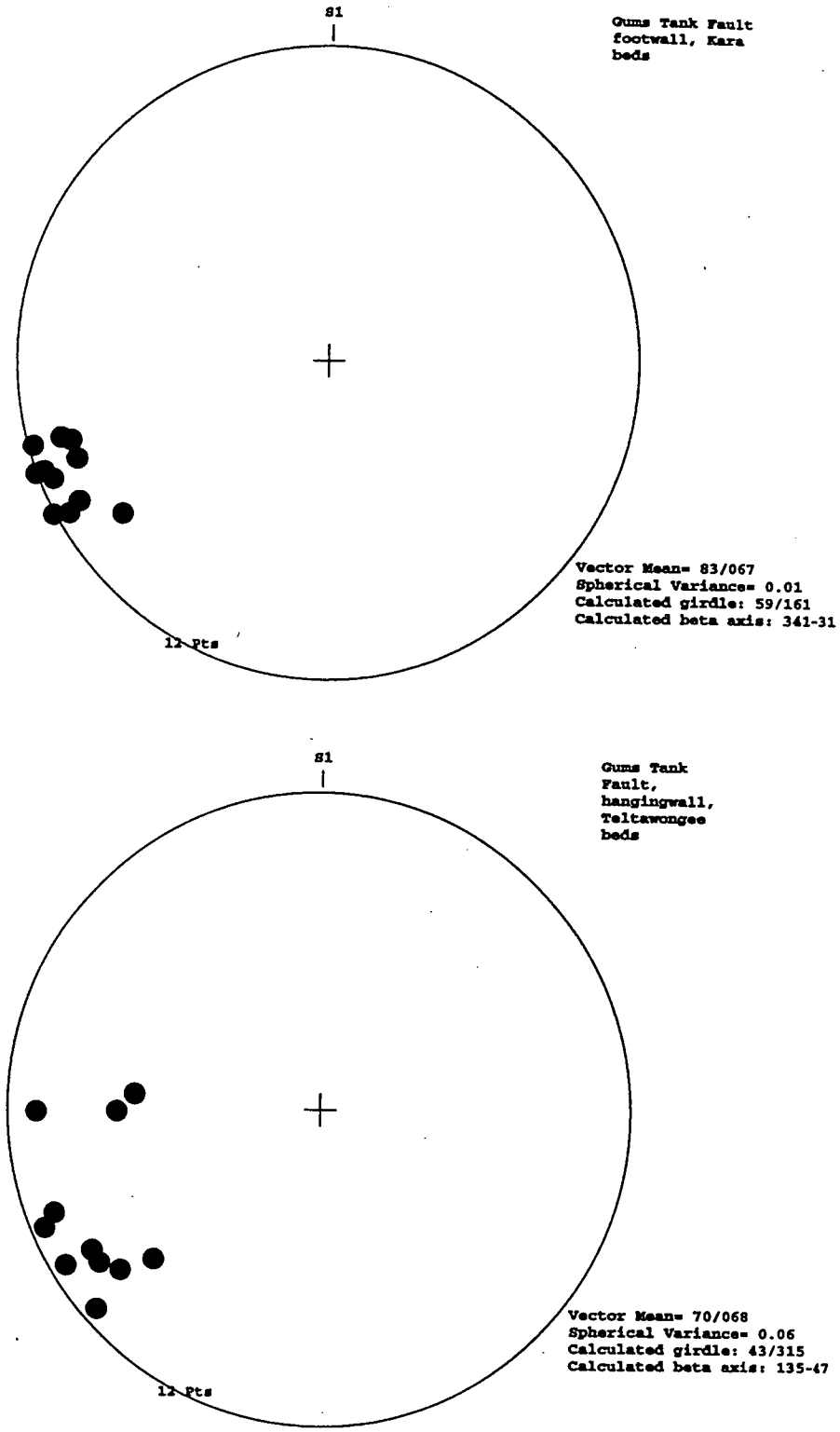


Rotation of the fabrics in the eastern side of the fault with respect to the western side, implies a listric-to-the-east fault geometry. Emplacement of younger (Early Cambrian) rocks over older (Late Neoproterozoic) rocks, implies a high-angle reverse fault.

**Figure 4.11.5 Schematic drawing of a possible inclined, isoclinal mesoscopic synclinal closure, in Mahomica Formation, Wonnaminta Creek**

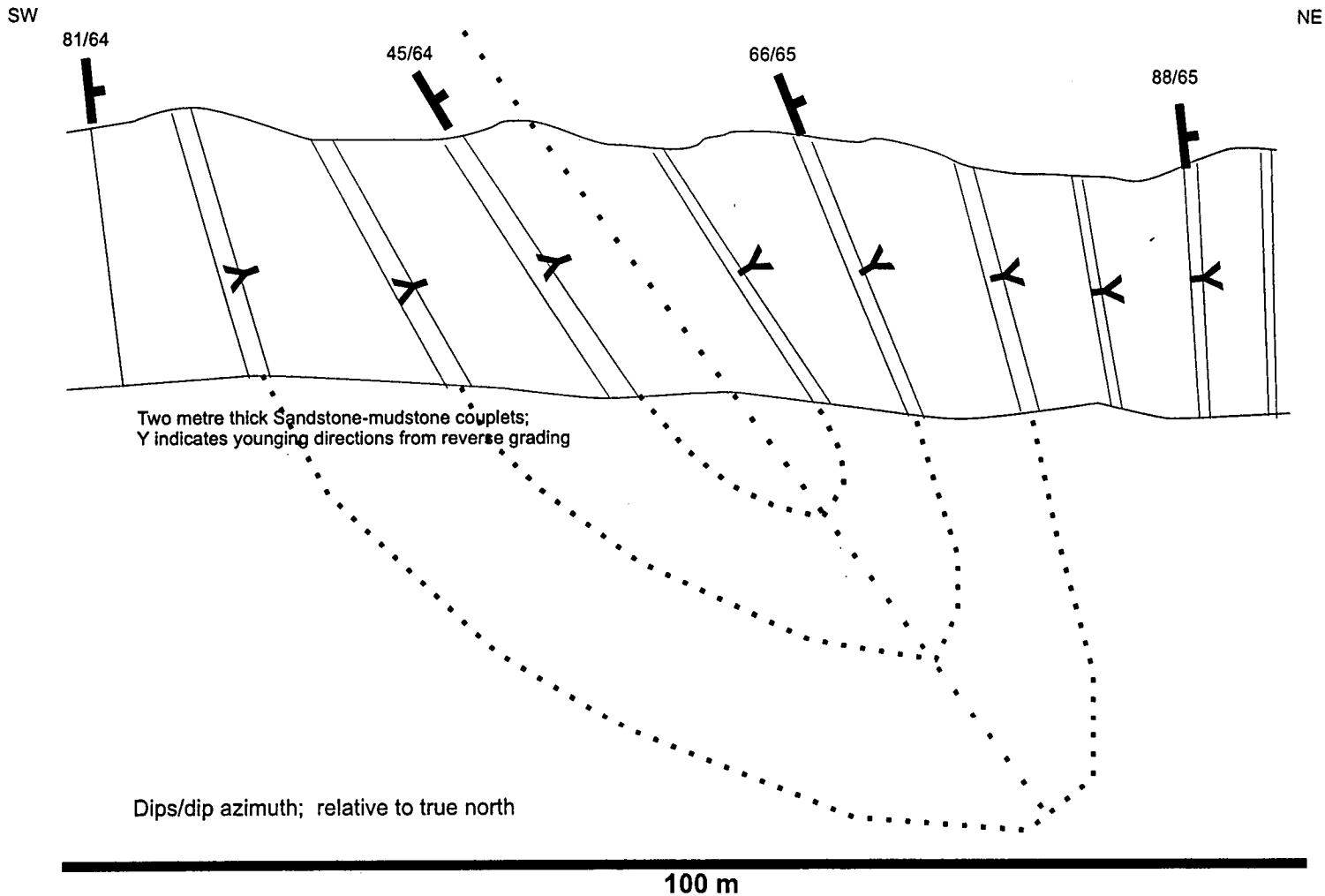

parallel to bedding on fold limbs; this is a weak spaced, disjunctive cleavage defined by biotite and Fe-oxides.

A mesoscopic fold hinge in phyllite in a possible fault slice of Kara beds at 657622 mE 6581669 mN is a tight parallel fold with an elliptical fold profile; this was apparently asymmetric toward the east. The plunge could not be recorded but the plunge azimuth was approximately north-south.

Mesoscopic folding also occurs in slates and pebbly sandstones of the Cupala Creek Formation. In Cupala Creek, these folds are open (ILA 140°), shallowly (10° to 13°, Powell et al., 1982) southeast plunging folds with a very weakly expressed spaced axial planar fracture cleavage.

In general, the presence of macroscopic asymmetric folds is consistent with an initial pre-Late Cambrian southwest-directed compression. When folds reached the maximum lock-up angle, deformation continued first by flattening and then possibly by thrusts breaching anticlinal cores. This mechanism explains the lack of macroscopic anticlines observed, as well as the other structural geometries in the area. The late open folds are interpreted to have formed in post-Ordovician and pre-Devonian time, as the overlying Mulga Downs Group does not contain folds of this type (Powell et al., 1981). Post-Devonian faulting accounts for tilting within the Mulga Downs group and some rotation of earlier fold axes (Powell et al., ibid.; Collins, 1984)

### *4.11.6 Metamorphic grades in the Nundora-Wonnaminta area*

A pilot study, consisting of a single traverse made over the east-dipping Wonnaminta Fault (described above) was conducted to determine whether significant metamorphic grade changes occur across the defined and inferred faults. Samples were acquired at 100 m intervals on either side of the fault for petrographic analysis. This provided three samples of the Teltawongee beds (thin sections 9724, 9725, 9726) including a metadolerite sill (9724), and six samples of Ponto Complex (9727 to 9732) which were examined for metamorphic mineral assemblages.

The metadolerite contains a metamorphic assemblage of hornblende and biotite replacing the clinopyroxene. Plagioclase is albitised. These features indicate this rock has been metamorphosed under upper greenschist facies conditions.

A

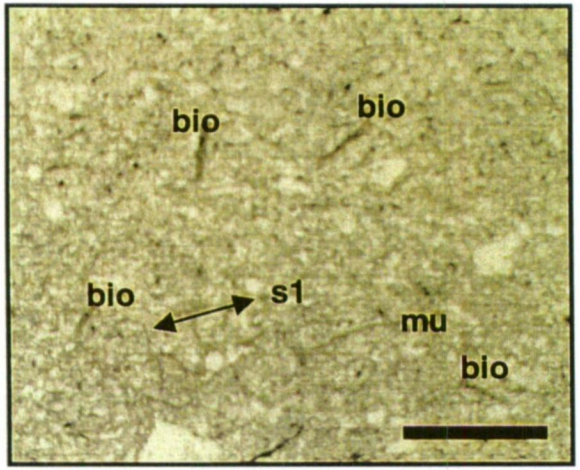


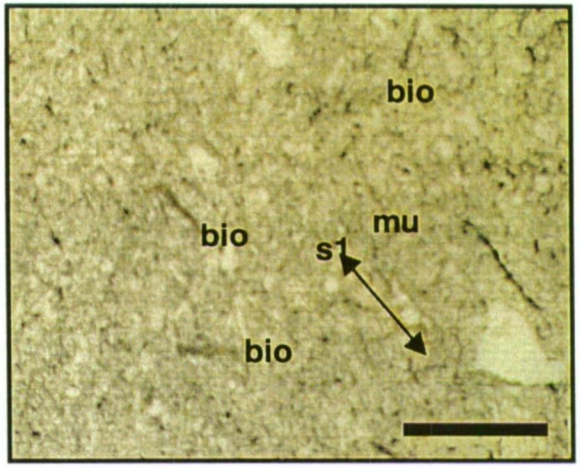


This sample was taken from west of the fault in the footwall block

Scalebar is 500 microns

Photomicrographs of sample 9725, Teltawongee Group sandstone. Taken in plane polarised light, 90° rotations. Large decussate metamorphic pleochroic biotites (bio) overgrow S1 cleavage defined by wispy white micas (mu).

B

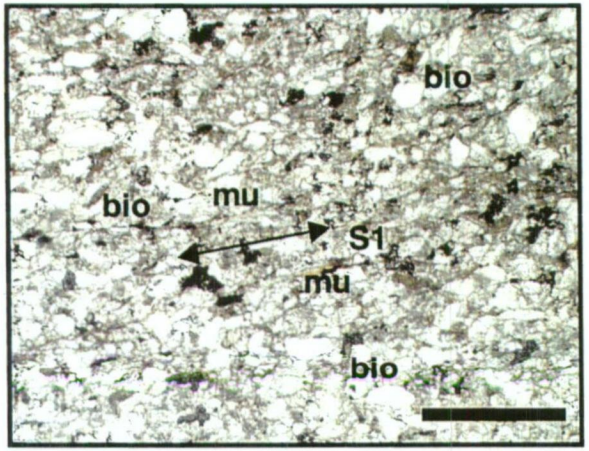


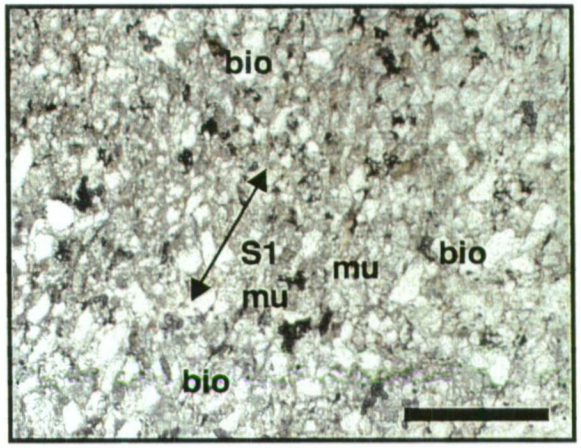


This sample was taken from east of the fault in the hangingwall block

The occurrence of decussate biotite in both blocks suggests peak metamorphic grade (greenschist facies) was achieved after reverse faulting

Photomicrographs of sample 9732, Ponto Complex sandstone. Taken in plane polarised light with rotated stage. Decussate metamorphic pleochroic biotites (bio) overgrow S1 cleavage defined by white micas (mu) and anhedral preferred orientation of quartz.

**Figure 4.11.6 Metamorphic mineral growth in sandstones adjacent to the Wonnaminta Fault**

The fine meta-litharenite (9725) and meta-lithic siltstone (9726) sampled to the east of the fault both contain a weakly-developed spaced disjunctive cleavage principally defined by non-detrital white mica. This is intergrown with biotite, indicating that these rocks also fall within the upper greenschist facies.

The pelites and psammite (9728) sampled from the Ponto Complex retain original sedimentary textures including unrecrystallised grain shapes, matrix and possible grading. These features all indicate relatively low strain. All samples contain a well-developed spaced cleavage defined by muscovite, or minor (sub-) parallel pressure solution domains with remobilised silica. The cleavage is overgrown in all samples by decussate biotite (Figure 4.11.6). This indicates that these rocks are also within the greenschist facies, but that they attained their peak metamorphic grade after cleavage formation.

Thus both the footwall (west side) and hangingwall (east side) of the Wonnaminta Fault have the same metamorphic grade, although this was achieved in the hangingwall after cleavage formation (post-?S2).

As it can be assumed that this tectono-thermal event must post-date all thrusts of the same generation as the Wonnaminta Fault, this line of inquiry was abandoned.

*4.12 Geophysical mapping and stratigraphy of the Ponto Complex*

The following discussions are based on extensive interpretation of geophysical data over the Koonenberry region. Interpretive "solid geology" maps have been produced at a scale of 1:100 000 for the map sheets Cobham Lake (7337) and Wonnaminta (7336) (these maps are located in a back pocket). Linework and attributes were constructed in ArcInfo using various processed images of the available aeromagnetic data, airborne gamma ray spectrometry and ground gravity data. These were compiled at scales between 1: 10 000 and 1: 100 000. Also incorporated into the map interpretation are structural, lithological and petrophysical data acquired during field traverses from 1996 to 1998 by the author, and some unpublished information courtesy of B. Stevens and K. Mills.

The suite of images used to produce the final interpretation included total magnetic intensity (TMI) reduced to the pole (RTP) pseudocolour with first vertical derivative (1VD) intensity layer sunshaded from the northeast; 1VD TMI RTP greyscale; potassium channel pseudocolour with 2VD TMI RTP intensity layer; total count

pseudocolour with intensity layer sunshaded from the northeast; gravity pseudocolour; gravity pseudocolour with TMI RTP intensity layer sunshaded from the northeast; Red-Green-Blue three colour composite for Potassium-Uranium-Thorium; and Digital Elevation Model pseudocolour with intensity layer sunshaded from the northeast. These images were produced at various scales and are too numerous to reproduce herein.

Ciphers in the following discussion refer to units on the two interpretation sheets. The discussion utilises the terminology of Moore (1996) to identify coherent geophysically distinctive packages. The following hierarchy is observed:

Domain ≈ Group/lithodeme

Sub-domain ≈ Formation/suite

Anomaly ≈ Member

This arrangement allows for ready extrapolation of stratigraphic units beneath cover rocks as equivalent geophysical units.

### *4.12.1 Stratigraphy, Volcanic Facies and Structure of the Ponto Complex, Ponto Mine Area*

A detailed study was carried out in this area by Davies (1985), prior to the establishment of the Ponto beds as an informal stratigraphic unit by Mills (1992). Davies' work identified phyllite, sandstone, metabasaltic pillow lavas, meta-andesitic flows, andesitic tuffs, cherty tuffs, tuffaceous phyllites, and quartz-magnetite rock, all of which are also found near Boshy Tank (Wonnaminta 7336).

Zhou (1993) completed reconnaissance mapping near the Ponto mine, and found metabasalts and two suites of metadolerites in eight distinct units. Geochemical analysis of seventeen samples indicated that all of these rocks were subalkaline with tholeiitic characteristics. Four samples were analysed by Zhou (1993) for REE; these showed MORB affinities, but with significant Nb depletion. One of the dolerites, probably belonging to the Gneilwonga Volcanics (section 4.9.1), displayed a significantly more depleted pattern to volcanics from the Ponto Complex.

**Palgamurtie Domain (Epp)**

Interpretation of the aeromagnetic data combined with detailed field traversing and mapping at 1: 25000 reveals the existence of 10 magnetic subdomains in the Ponto Complex on the Cobham Lake 7236 sheet. These form the Palgamurtie Domain (Eppa).

The entire Palgamurtie Domain can be traced for over 50 km strike length onto Wonnaminta 7336. Bedding and cleavage data are approximately parallel, with steep southwesterly and northeasterly dips, suggesting northwest-plunging isoclinal folds (Figure 4.12.1). The characteristics of the several subdomains comprising the Palgamurtie Domain are listed below:

**Table 4.12.1 Magnetic characteristics, Palgamurtie Domain**

| Subdomain | Symbol | Lithotypes | Mag.Susc. (SI) | Amplitude (nT) |
|---|---|---|---|---|
| Rocky Tank | Epro | Sandstones, phyllite | $20 \times 10^{-5}$ | -80 |
| Truganini | Eptr | Magnetic phyllite | $550 \times 10^{-5}$ | 200 |
| Bluff | Epbl | Phyllite~sandstone | $20 \times 10^{-5}$ | -100 |
| Ponto mine | Eppm | Magnetic phyllite | $1400 \times 10^{-5}$ | 300 |
| Stevens | Epst | Phyllite~sandstone | $20 \times 10^{-5}$ | -175 |
| Funeral Creek | Epfc | Volcanics | $400 \times 10^{-5}$ | 300 |
| Belah | Epbe | Sandstone, tuff | $50 \times 10^{-5}$ | |
| Nulla Nulla | Epnn | Magnetic phyllite, tuff | $300 \times 10^{-5}$ | 300 |
| Two Mile | Eptm | Phyllite>>sandstone | $20 \times 10^{-5}$ | -80 |
| Koonenberry | Epko | Phyllite, tuff, quartz-magnetite rock | $325 \times 10^{-5}$ | 30 |
| Little Wallaby | Eplw | Phyllite, tuff | $20 \times 10^{-5}$ | -100 |

Cleavage data from beds near the Wonnaminta Fault contact indicate that the Rocky Tank Subdomain has been subjected to west-directed transport, placing it over the Mahomica Formation. The footwall has steep, almost vertical, dips striking north-northwest.

The Ponto Mine Subdomain contains rocks listed by Davies (1985) as banded iron formation (BIF), hosting sulphides which have historically produced high-grade (18.5%) copper ore (Carne, 1908 ref. Davies, 1985). The absence of volcanic rocks in the ore

horizon (cf. Davies, 1985; Zhou, 1993) is similar to the pattern observed at Grasmere (see Chapter 6); in particular there is a possible correlation between the Ponto Mine and Grasmere Prospect Subdomains.

The Funeral Creek Subdomain contains outcropping volcanics, including metabasalt and coarse-grained volcanogenic sandstones interbedded with phyllite. Davies (1985) described a thick volcanic pile corresponding to the Funeral Creek Subdomain; this contained tuffs, BIF, cherts, basic pillow lavas, and andesitic tuffs. Evidence from pillow lavas suggests general eastward younging.

The Belah, Nulla Nulla, Two Mile, and Koonenberry Subdomains continue for 50 km south-southeast along the Koonenberry Fault hanging wall. These are described at 4.12.2 below.

Stevens & Fanning (unpublished data 1996) carried out sampling within the Little Wallaby and Koonenberry Subdomains. A cherty tuff sampled at 619740 mE 6632581 mN in the Little Wallaby domain has been SHRIMP U-Pb dated on the basis of volcanogenic zircon crystals, giving an age of 484 ± 10 Ma. This falls in the Arenig (Lower Ordovician).

*4.12.2 Stratigraphy, Volcanic Facies and Structure of the Ponto Complex, Boshy Tank Area*

Preliminary reconnaissance mapping was attempted by Zhou (1993), with the intention of tracing mafic dykes along strike. He found some (unexplained) evidence for "complicated stratigraphic repetition", which he thought prevented correlation between across-strike traverses.

The main contribution by Zhou was the recognition of 4 mafic dykes, striking between 120° and 145°(T). The longest of these is continuous for c.5 km along strike.

Twelve samples of volcanic rocks analysed by Zhou (1993) are petrographically metadolerite and metabasalt with the upper greenschist assemblage act-hbl-ab-ep-qz-chl-carb-mt-sp. Geochemical analysis of 9 samples (Zhou, 1993) using the immobile elements Nb, Y, Zr, and Ti suggests that the igneous rocks were subalkaline, tholeiitic basalts (Zhou & Mills, 1990); analysis of REE from two metadolerites indicated a MORB-like signature (Zhou, 1993).

Mills (1992) recognised that the Ponto Complex forms distinct, mappable packages of feldspathic lithic sandstones ("greywackes"); phyllite and mica schist; lavas, tuffs, sills, dykes and plugs; and banded quartz-magnetite rocks. He further recognised that these packages are variably magnetic, giving rise to the striped character of the magnetic field over the whole sequence.

**Palgamurtie Domain**

The solid geology map shows four distinctive magnetic subdomains.

The youngest part of the sequence is the Koonenberry Subdomain (Epko). This has the highest magnetic signature of the four packages identified in the Boshy Tank area, producing a 300 nT linear anomaly (Note: quoted peak values are relative to the regional datum, 57300 nT). Magnetic susceptibilities average 1880 x $10^{-5}$ SI (n = 17). Individual lithological components of this package include basalt, dolerite, tuff, volcanogenic lithic sandstone and quartz-magnetite rock, all interbedded with phyllite. The Koonenberry Subdomain contains all four of Zhou's (1993) mapped dykes. The true thickness is of the order of 400 m.

Thin sections from the Koonenberry Subdomain from representative samples near 637800 mE 6603300mN are of brecciated plagioclase-phyric evolved metabasalt lava, and a well-bedded, cleaved feldspathic volcaniclastic sandstone. These samples were taken from a thirty metre interval which also included cherty tuff bands. The volcaniclastic sandstone has an extremely well-developed cleavage defined by secondary biotite, indicating middle-upper greenschist facies metamorphism. This is consistent with the observation of metamorphic actinolite-hornblende in metabasaltic rocks by Zhou (1993). No evidence of a prior cleavage was found in these samples.

Thin sections from the Koonenberry Subdomain acquired near 634300 mE 6610400 mN, c. 8 km north-northwest along strike from the other samples, are of poorly sorted feldspathic arenite and quartz-magnetite rock. The sandstone contains a rough, spaced cleavage defined by white mica, iron oxides and possible clay minerals. These features indicate a lower metamorphic grade than those samples to the southeast.

The Koonenberry Subdomain's eastern margin is in faulted contact with the Teltawongee Group at the Koonenberry Fault. Zhou (1993) mapped a wide (10's of metres) crush zone at the fault, probably due to later (Carboniferous?) reactivation.

Magnetic modelling (Direen,1998) suggests that the Koonenberry Subdomain dips to the west at 70°, indicating that the Koonenberry Fault is a high angle reverse fault. This interpretation is consistent with higher metamorphic grades in the Ponto Complex approaching the fault from the west, and the consistent lower grade of the Teltawongee Group to the east, which implies a ramping of the structural envelope from west to east across the fault

The Two Mile Subdomain (Eptm) is a series of magnetic phyllites with a pronounced crenulation cleavage lying to the west of the Koonenberry Subdomain. In the aeromagnetic coverage, the Two Mile Subdomain is a magnetic linear high of 100 nT amplitude, which can be attributed to its measured average magnetic susceptibility of 250 x $10^{-5}$ SI.

A key feature of the Two Mile Subdomain is the repeated rotation of the primary slaty cleavage from angles of c. 80° to c. 20° (see Figure 4.12.2) over across-strike distances of between 2 and 15 m. This rotation occurs over a cumulative distance of at least 250 m. A well-developed, west-plunging down-dip lineation has formed at the loci of shallowest dips; these positions also correspond to maxima in magnetic susceptibility (see Figure 4.12.3). These relationships are best explained by mesoscale imbrication of the phyllite to form a series of horses.

The NullaNulla Subdomain (Epnn) lies to the west of the Two Mile Subdomain. It has a moderate aeromagnetic response of commensurate with an average magnetic susceptibility of 125 x $10^{-5}$ SI. This produces a broad peak of c. 75 nT amplitude. The NullaNulla Subdomain comprises c. 350 m of phyllites with rare psammitic interbeds.

The dominant slaty cleavage in the NullaNulla Subdomain is everywhere steeply dipping between 70° and 80°. This is crenulated by rare kink bands trending 80°-85° (T), equivalent to the lineation in the Two Mile Subdomain.

The Belah Subdomain (Epbe) is the westernmost unit identified in two traverses. It has low to moderate aeromagnetic response, with magnetic susceptibilities averaging 40 x $10^{-5}$ SI, giving a relative magnetic trough of –25 nT. The Belah Subdomain consists predominantly of phyllite, with medium-bedded, medium-grained feldspathic-lithic sandstone interbeds, and occasional medium-bedded cherty tuff bands. The Belah Subdomain's true thickness is c. 480 m.

## Figure 4.12.1 Equal area nets for fabrics within the Ponto Complex Two Mile Subdomain, Boshy Tank

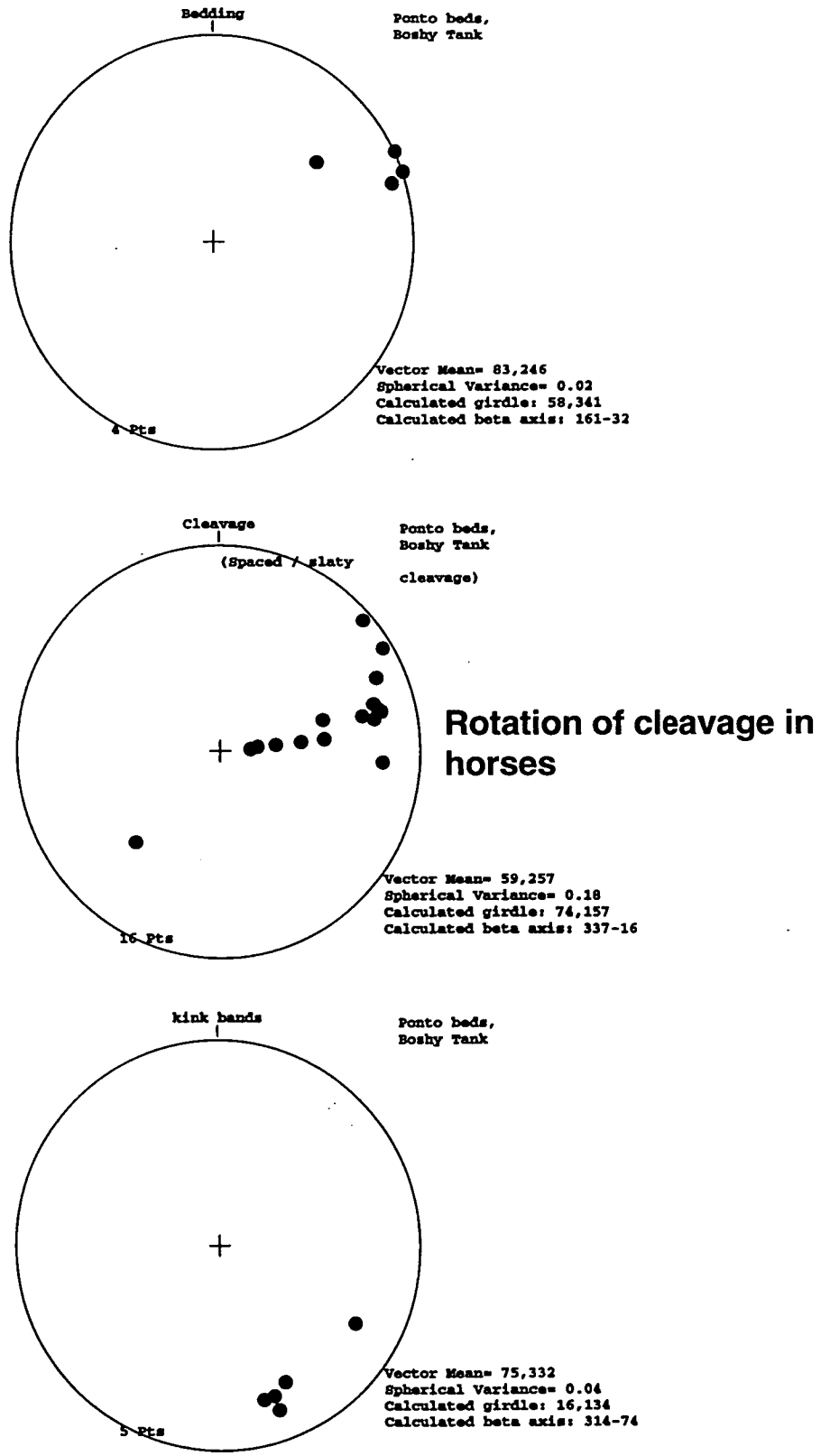

**Figure 4.12.2 Explanation of pattern of cleavage dips, Boshy Tank**

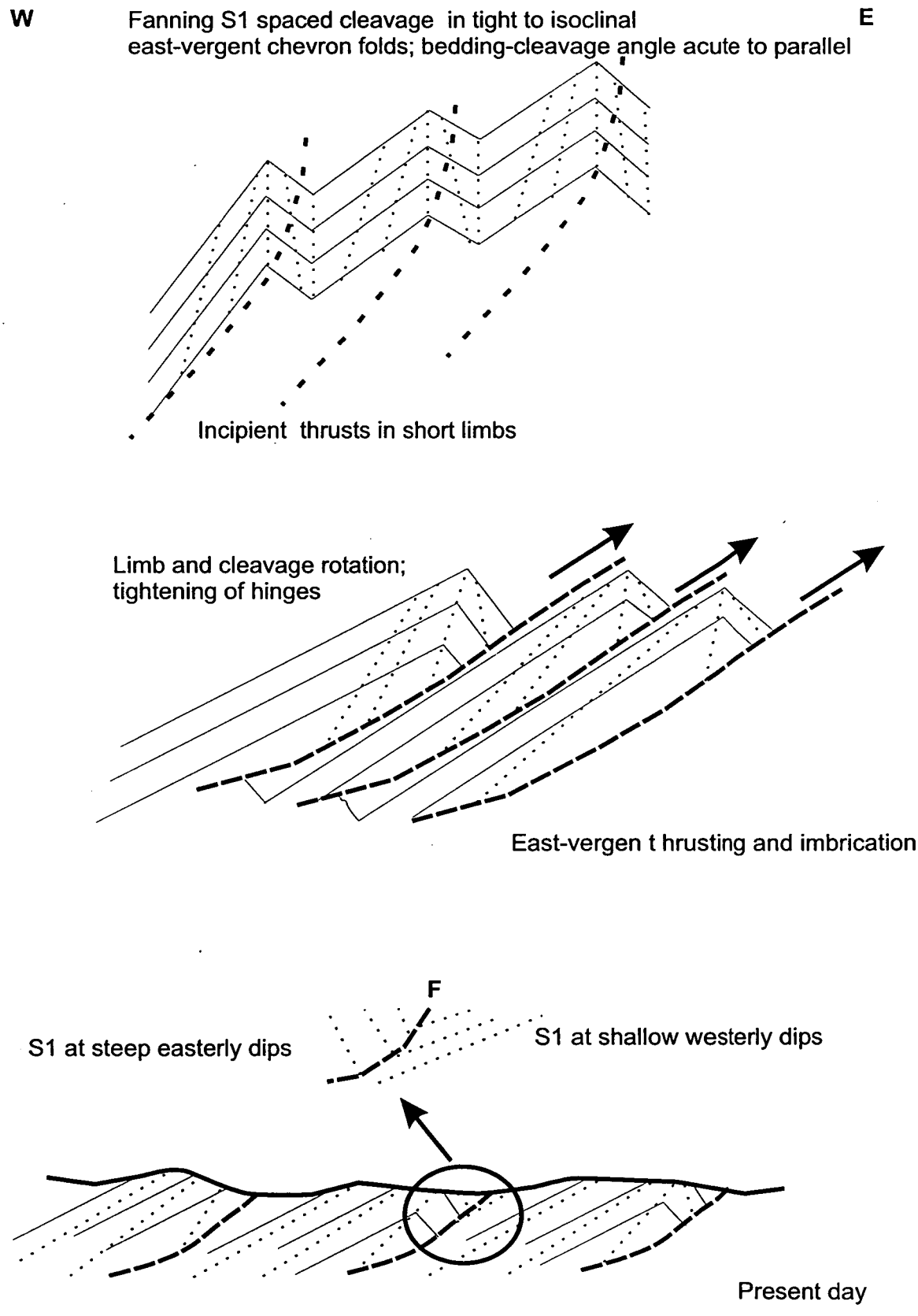

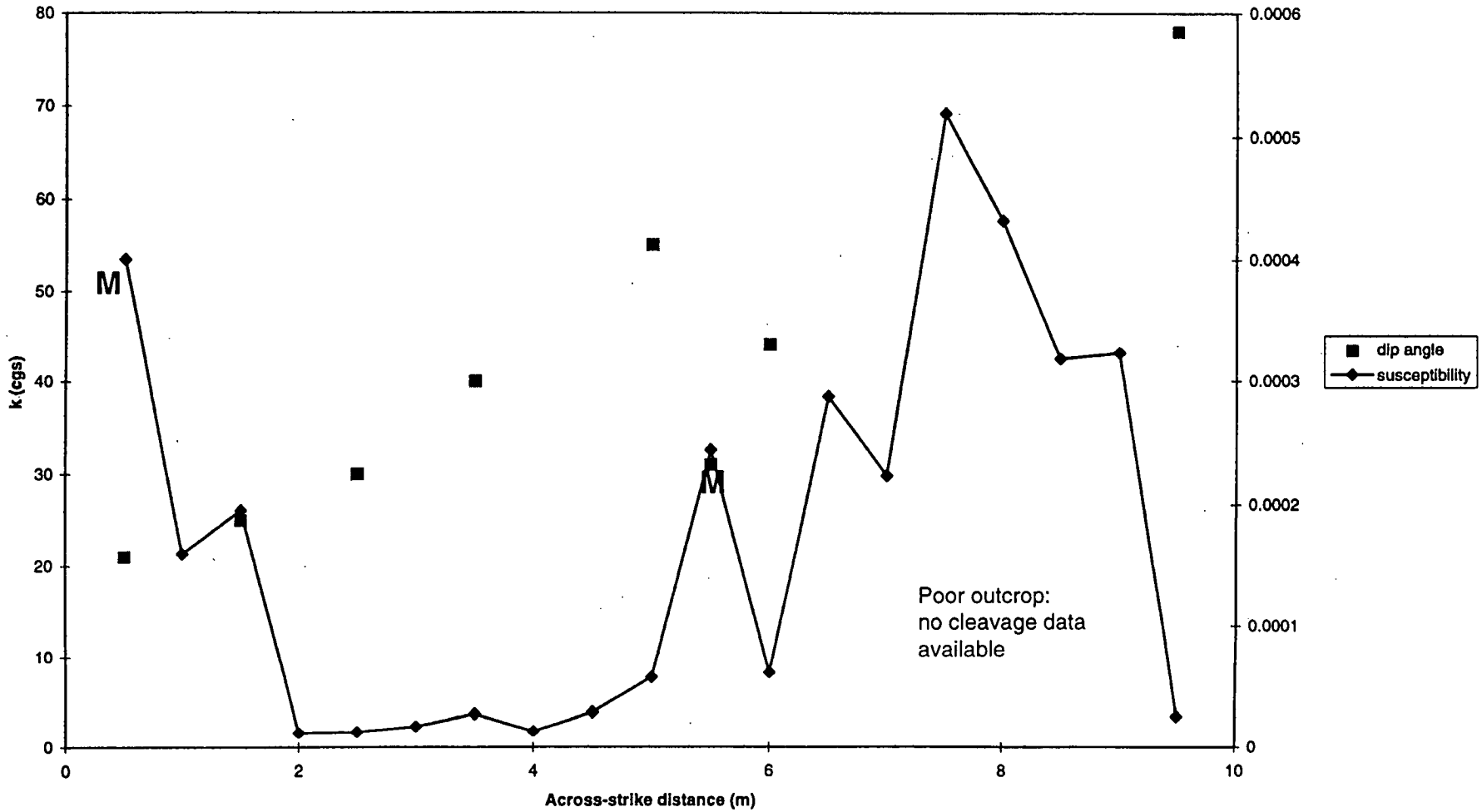


*Several maxima in magnetic susceptibility (M) appear correlated with cleavage dip minima

**Figure 4.12.3 Relationship between cleavage and magnetic susceptibility, Two Mile Subdomain**

Cleavage development in the Belah Subdomain increases to the east, with the spacing of the dominant slaty cleavage decreasing to < 1 mm within 2 m of the Wonnaminta Fault contact with the Teltawongee Group. Cleavage dip rotates from 72° near the fault contact, through 76°, 79°, to 87° at 100 m intervals from the fault. These relationships suggest that the Wonnaminta Fault is an east-dipping, high-angle reverse fault.

*4.12.3 Synthesis: the Ponto Complex in Area 1*

The Ponto Complex lies between two antithetic high-angle reverse faults, the east-dipping Wonnaminta Fault to the west, and the west-dipping Koonenberry Fault to the east. On both faults, the Ponto Complex forms the hangingwall block. Although the Ponto Complex is not everywhere appreciably higher in metamorphic grade than the Teltawongee Group rocks which they overthrust, they are considerably more deformed (see for example Davies, 1985). This deformation consists of refolded isoclinal folds with very high limb-length to hinge- width ratios (best seen in map view); imbricate stacking and repetition along minor thrusts; and intense phyllitic cleavage to transposition fabric formation, and dissolution crenulation cleavage. These features all imply that the Ponto Complex has been considerably shortened and flattened with attendant volume loss.

The timing of this deformation event is equivocal, considering only evidence from this area. Although SHRIMP zircon dates indicate eruptive ages for tuffs in the Arenig, the 10 Ma error on this date could take the age back into the Iverian (Late Cambrian). A Delamerian angular unconformity exposed at Morden Creek (Mills, 1992), which is pre-Mindyallan on the basis of fossil evidence, may also be related to this event.

The complete structural setting and kinematic history of the Ponto Complex remains ambiguous, with several permutations being possible. These include:

- the Koonenberry Fault being linked to the master detachment, and cutting off earlier formed east-dipping thrusts . In this case the Koonenberry Fault would be the major Fault in the Koonenberry Fold Belt. This would also imply that the Nundora and Mahomica Formations are not related in any way to the Copper Mine Range Formation;
- the west-dipping Koonenberry Fault as a relatively late-formed, minor backthrust (Figure 4.12.4). In this case, relatively flat-lying Ponto Complex rocks could be expected at depth underneath the Copper Mine Range Formation to the east. The depth to these could either be as little as 4 km or as much as 8 km. A flat-lying

**Figure 4.12.4 Sequential development of the Koonenberry Fault as a Cambrian backthrust**

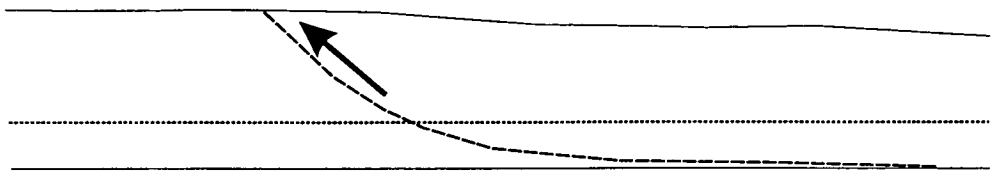

Thrust emplacement of the Ponto Complex over the Teltawongee Group

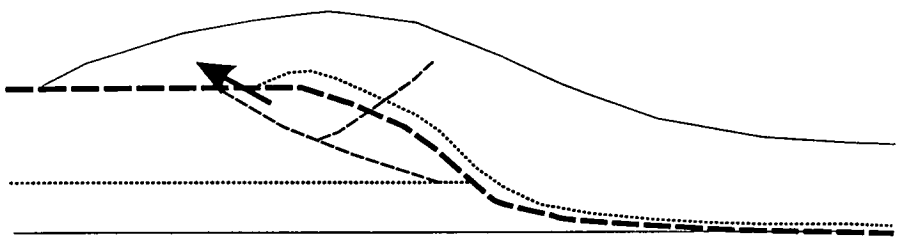

West-vergent imbrication of the thrust stack

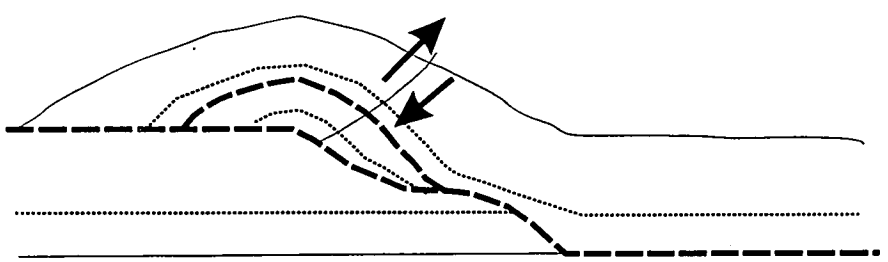

Incipient east-vergent back-thrusting

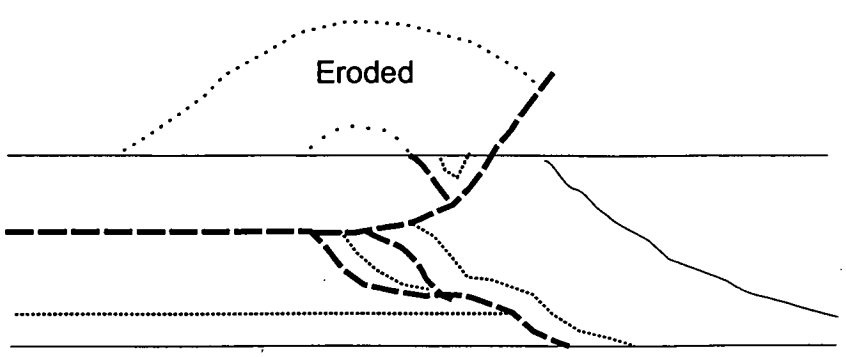


Reverse- and thrust-fault bound package of Ponto Complex at surface; more Ponto Complex implied at depth

magnetic package such as the Ponto Complex could explain the some of the bland magnetic character under the Murray Basin.

### 4.13 Summary

This chapter has sought to address the following questions:

*What are the stratigraphic and sedimentological characteristics of the Teltawongee Group, formerly the Teltawongee beds?*

*Should the Copper Mine Range Beds be incorporated into the Teltawongee Group?*

*What is the significance of the Gneilwonga Intrusive Suite (previously unnamed sills and plugs within the Teltawongee beds)?*

*Why is the highly strained Ponto Complex (formerly the Ponto beds) younger than the less-deformed rocks they are faulted against?*

*What is the age of the initiation of the Bancannia Trough, and how deep is it?*

A combination of geological, geophysical and geochemical techniques have been applied to these problems, and the following solutions suggested. The Teltawongee Group consists of three distinct formations, including the Copper Mine Range Formation, representing different facies within a continental slope-submarine fan system . These formations may be allochthonous with respect to each other.

The Gneilwonga Intrusive Suite represents a post-collisional extensional volcanic suite, similar, and contemporaneous, to the Henty Dyke Swarm of western Tasmania. These rocks are believed to relate to a rifting event after an arc-continent collision during the Late Cambrian.

The Ponto Complex represents a double hanging-wall block to two opposed thrusts. The initial emplacement of the Ponto Complex was from east to west over the continental margin wedge of the Teltawongee Group, probably during the Late Cambrian collision alluded to above. Subsequent structural rearrangement and back-thrusting caused deeper structural levels to be transported up the west-dipping Koonenberry Fault.

The Bancannia Trough is intimately involved in the thrust interpretation of the Koonenberry Belt. Its seismic basement formed during the ?Silurian thrusting event, with subsequent intra-cratonic sedimentation taking place in eroded relaxation basins during the Devonian. The structural depression has been the locus of further intra-cratonic depocentres in the Mesozoic and Cainozoic, with relatively unconsolidated sediments giving rise to a major negative gravity anomaly.

In conclusion, the generation of solutions to outstanding geological problems suggests that the Nundora-Wonnaminta-Marrapina-Nuntherungie area contains elements of a Late Neoproterozoic-Middle Cambrian continental passive margin, and an allochthonous Late Cambrian volcanosedimentary sequence. These were amalgamated in the Late Cambrian-Early Ordovician Delamerian orogeny. Subsequent reorganisation of these elements occurred in a Silurian deformation, probably equivalent to the Benambran event in the Lachlan Fold Belt. This area therefore represents the zone of overlap between the most outboard part of the Delamerian Orogen, and the most internal zone of the Lachlan Orogen; this in itself is sufficient to account for the relative structural complexity of the area.

**Chapter 5: Mt Wright-Cymbric Vale Area**

# Chapter 5: Mt Wright-Cymbric Vale Area

## 5.1 Location of the Mt Wright - Cymbric Vale area. Reasons for study.

This area is named for the major topographic feature and the pastoral property within this area. The area of study falls within a box defined by the Australian Map Grid (AMG) coordinates 620830 mE, 6558900 mN - 647310 mE, 6632100 mN - 647310 mE, 6533300 mN - 620830mE, 6533300 mN (Zone 54) (Figure 5.1.1). This area falls on the Wonnaminta 7336 and Nuchea 7335 1: 100 000 map sheets.

This area was selected for detailed study of the tectonics of the Mt Wright Fault, which controls two high amplitude magnetic anomalies, at Macs Tank and Baroorangee Creek (Figure 5.1.2). Detailed magnetic surveys, controlled by mapping (e.g. Davidson, 1981; Johnson, 1972) were designed to test the dip of fault. Previous reconnaissance had also indicated the presence of two ultramafic bodies on the fault; these types of bodies have major tectonic significance in other parts of the Lachlan and Delamerian Orogens (e.g. Berry & Crawford, 1988; Crawford & Berry, 1992), and thus warrant further detailed investigation.

## 5.2 Topography, Hydrology, Access

The topography and road network is shown in Figure 5.1.3. The southeastern part of the area contains rugged topography of the Bynguano and Mootwingee Ranges, and the Ramparts Hills which rise steeply to 380 masl. These contrast with the essentially flat, dissected plain that makes up the remainder of the area.

The western portion of the area lies within the Mootwingee National Park, which requires permits for geological access. The eastern half of the area lies on the sheep-farming properties "Cymbric Vale" and "Wilandra".

Access to the area is by two routes. The first uses the unsealed secondary road connecting the Silver City Highway and the White Cliffs road, and then proceeds via several rough tracks passing through the abandoned Gnalta H. S., arriving at "Cymbric Vale" from the north. The second is from the Barrier Highway via "Waterbag", "Boorungie" and "Wilandra", approaching "Cymbric Vale" from the east. Both routes are generally negotiable in conventional vehicles, although weather caveats apply. A four wheel drive-only route through the Mootwingee Ranges is not recommended, and may soon be closed by the National Parks and Wildlife Service. A network of rough

## Figure 5.1.1 Locality Map. Mt Wright-Cymbric Vale Area

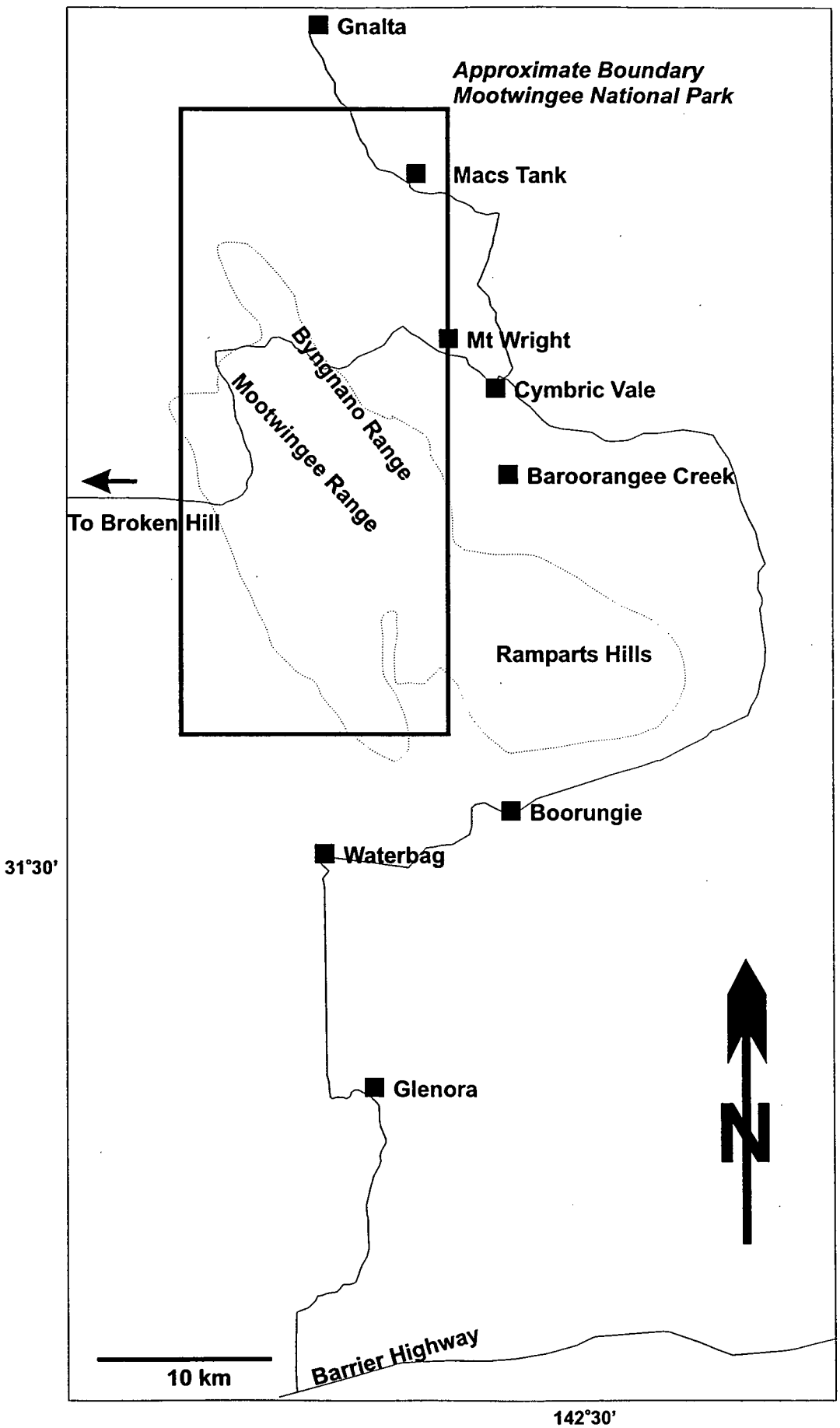

**Figure 5.1.2 TMI image of the Mt Wright Fault with interpreted geology**

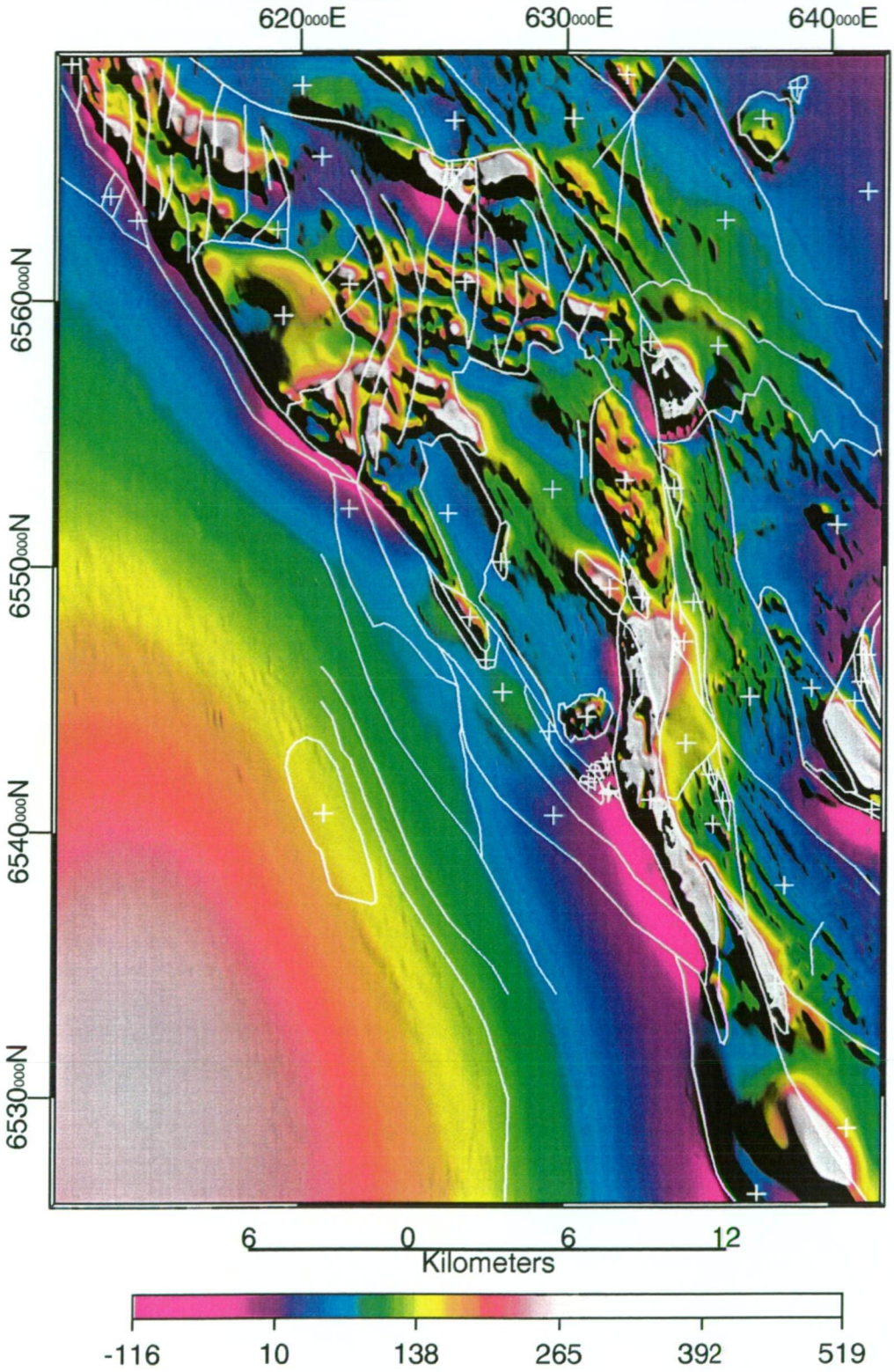


TMI pseudocolour with equalised stretch and TMI intensity layer shaded at 45 degrees form the northeast. Z zcale is in nT. Geology map based on image is included in rear pocket. Grid is AMG zone 54.

**Figure 5.1.3 Digital Elevation Model and roads, Mt Wright-Cymbric Vale area**

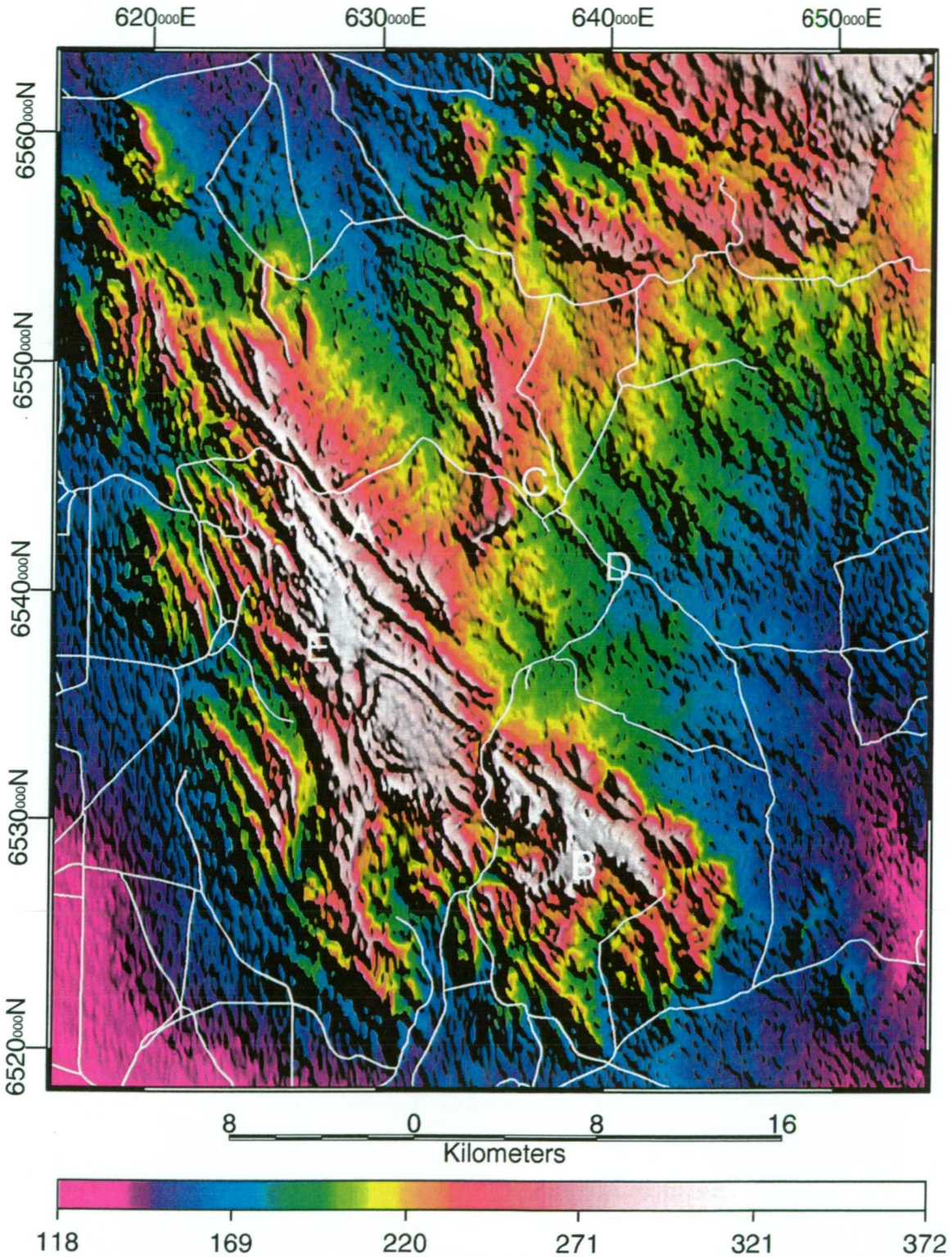


Digital Elevation Model pseudocolour and intensity layer shaded at 45 degrees from the northeast. Grid is AMG zone 54. Z scale is in masl. Key: A = Byngnano Range; B = Ramparts Hills; C = Mt Wright; D = Cymbric Vale; E =Mootwingee Range.

tracks on "Cymbric Vale" gives four wheel drive or motorcycle access to the eastern part of this area, weather permitting. Vehicular access in the eastern portion of the Mootwingee National Park is strongly discouraged, with a permit required for formed track use, and no off-road driving is permitted.

### 5.3 Local Structural & Metamorphic Geology

The most complete structural study of this area is that of Davidson (1981). This work was partially reinterpreted by Mills (1992) to incorporate further divisions of the defunct "Wonominta beds" (vis. Ponto Complex, Kara beds, Teltawongee Group).

Three major faults have been identified in the area. These are, from west to east, the Lawrence Fault, the Mt Wright Fault and the Bald Hill Fault (Davidson, op.cit.).

The Lawrence Fault is a composite fault, with dip-slip and strike-slip components (ibid.). Normal movement has downthrown the western block, and post-Ordovician transcurrent movement has caused drag folds in the Mootwingee Group in both hanging- and foot-wall.

The Mt Wright Fault marks the boundary between lower greenschist Mt Wright Volcanics (MWV) to the west, and upper greenschist to lower amphibolite facies Ponto Complex to the east (Crawford et al., 1997; Zhou, 1993). The schistosity of the Ponto Complex dips to the east, suggesting a west-directed thrust component (Crawford et al., op.cit.). At Baroorangee Creek, the fault is marked by a serpentinite melange (Davidson, 1981). Further north, the fault forms the boundary between the Cambrian MWV to the west, and the Late Devonian Mulga Downs Group to the east, and has been reactivated as a normal fault (Crawford et al., op.cit.).

The Bald Hill Fault forms the boundary between the Ponto Complex to the west and the Wilandra beds (see below) to the east (after Davidson, 1981; and Mills,1992). Davidson (op.cit.) indicated a late west-side up movement for this fault, with a more complicated (but undecipherable) early history.

The Ponto Complex reaches lower amphibolite facies adjacent to the Mt Wright Fault (Zhou, 1993). The metamorphic assemblage in metabasalts here is epi-act-hbl-qz-serp-clz. (Zhou, ibid.). Zhou also noted that the amphiboles of mafic rocks in this area are more Na-rich than in correlated areas, showing that pressures and temperatures of

regional metamorphism were higher in the Ponto Complex in the Cymbric Vale region than to the north around Wonnaminta.

Structurally, the Ponto Complex has been shown to contain four penetrative fabrics, together with localised late kinking (Davidson, 1981). S1 is a schistosity, defined by micas or amphiboles, generally parallel to S0, suggesting F1 was isoclinal. No F1 folds were observed by Davidson (ibid.). S2 is a rare crenulation cleavage or, more commonly, a spaced cleavage that is the axial planar surface of tight to isoclinal F2 folds. This cleavage is the main fabric observed in the area.

S3 is a crenulation of S2, developed in the hinges of open F3 folds. F3 folds plunge up to 20° to the southwest, while S4 is a slaty cleavage in the axial planes of open F4 folds that plunge 35° to the northeast. Nowhere does F4 fold S3, instead folding S2 to S0 (after Davidson, 1981). The similar style and c.180° difference in plunge azimuth between F3 and F4 may indicate a doubly-plunging fold relationship

The Wilandra beds, east of the Bald Hill Fault contain metabasalts with the metamorphic assemblage ab-chl-epi-act, indicating metamorphism under greenschist conditions (see discussion below).

The Wilandra beds are severely disrupted by faulting and outcrop poorly. Davidson (ibid) identified two phases of folding. F1 are tight folds plunging 10° to 330°, and paralleling the direction of the Bald Hill Fault. Stereographic data suggest these are asymmetric with the southwest limb dips steep to overturned (c.90°), and the northeast limbs shallowly dipping (c.50°). However, these folds have developed a vertical cleavage.

F2 are open or kink folds developed near the Bald Hill fault. These plunge 65° to 70°. They are probably related to late fault movements causing drag folding, as this orientation is not observed elsewhere in the area.

Crawford et al. (1997) described the MAV as containing a prehnite-pumpellyite metamorphic assemblage (ab-ser-carb-qz ± chl, epi, pre). This assemblage was also recorded by Warris (1967).

The Mt Wright Volcanics (MWV), that are intimately associated with archaeocyathan-bearing limestone lenses which have been dated as Early Cambrian (Kruse, 1982) are a calc-alkaline series of andesite lavas and dolerites that intrude the alkaline suite

(Crawford et al., ibid). These also contain a prehnite-pumpellyite metamorphic assemblage (ab-chl-epi-qz-ser-carb) (Crawford et al., ibid.).

The Middle Cambrian Coonigan Formation lies with slight unconformable relationship over the Cymbric Vale Formation in an anticline at the foot of the Bynguano Range (Warris, 1967). Outcrop is restricted to a series of narrow, fault-bound slivers on the east limb. The anticline plunges southeast, and is itself cut by the northwest-trending Lawrence Fault.

The entire Gnalta Group is described as being disrupted by severe faulting and folding, with individual beds being discontinuous (Warris, 1967; Kruse, 1982; Crawford et al., 1997). Because of the discontinuity of outcrop, only two fold closures have been described. The first is the one mentioned above, near the Lawrence Fault, and the second is a syncline-anticline-syncline structure c. 1km west of the Mt Wright Fault at 633000 mE, 6542500 mN. This latter structure was used by Warris (1967) to define the base of his "Mt Wright Volcanics". Davidson (1981) recorded no cleavage data for parts of the Gnalta Group exposed near Cymbric Vale. The lack of any axial plane cleavage to folds within the Cymbric Vale Formation has been confirmed by my mapping near the type section, and in a correlated exposure at the foot of the Bynguano Range.

The Mootwingee Group unconformably overlies the Coonigan Formation (Warris, 1967) at the foot of the Bynguano Range, and the Wilandra beds (Davidson, 1981) on Bald Hill. It is in fault contact with the Gnalta Group along the Lawrence Fault (Davidson, ibid.). The Mootwingee Group, consisting of interbedded calcareous clastics and limestones (Nootumbulla Sandstone) and pure quartzites (Rowena Formation), contains no indicators of relative metamorphic grade.

The Nootumbulla Sandstone is folded in a southeast-plunging anticline with the Coonigan Formation, near the Bynguano Range. More detailed remapping in this area during the course of this study shows the anticline to contain several parasitic mesofolds. These are open, asymmetric folds, inclined to the west (Figure 5.3.1). They have a wavelength of c. 40 m, and an amplitude of c.20 m. A rough, disjunctive fracture cleavage is developed in these folds, due to the lack of competency contrast between the quartzite beds.

Seismic data suggest the existence of intense reverse faulting associated with the eastern margin of the Bancannia Trough (Schroeder, 1987). These faults occur within

## Figure 5.3.1 Mesoscopic fold in Mootwingee Group sandstones

Looking south-southeast. 626163 mE 6546928 mN AMG zone 54.

Equal area net showing poles to bedding for the Nootumbulla Sandstone (pictured above)

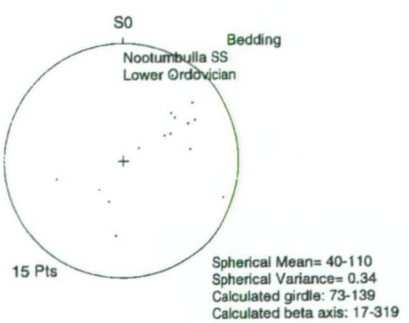

a sequence of reflectors correlated with the Mootwingee Group and are interpreted as low-angle thrusts. Schroeder (ibid.) suggested that these faults also disrupt Devonian sequences which unconformably overlie the Cambro-Ordovician reflectors. However, the data quality at early times is so poor that this further interpretation is difficult to sustain, and no interpretive section or time-depth map of the Devonian was provided by Schroeder (ibid.). Reactivation of post-Ordovician, pre-Devonian thrusts as dip-slip or strike-slip faults, analogous to the Koonenberry Fault movements, may be responsible for this complexity above depths of 3000 m.

Unconformably overlying the Mootwingee Group is the Late Devonian Snake Cave Sandstone of the Mulga Downs Group (Davidson, 1981). The Late Devonian Ravendale Sandstone that forms the Mt Wright massif unconformably overlies the Ponto Complex to the west of the Mt Wright Fault. It is faulted against the Gnalta Group at the Mt Wright Fault, indicating a final syn- to post-Carboniferous movement for this structure. A strike-slip component to this movement has produced drag folds in the Ravendale Sandstone.

### *5.3.2 Summary*

Although the Mt Wright-Cymbric Vale area has good exposure and age control, it is clearly a zone of structural complexity.

The Bald Hill Fault has a complex history (Davidson, 1981), which may conceal southwest-directed thrust transport of the greenschist Wilandra beds and the overlying Ordovician Rowena Formation over the ?Late Cambrian-Early Ordovician Ponto Complex. Thrusting may account for the apparent imposition of a macroscale asymmetric F1 chevron fold in the Wilandra beds, and the northwest trend of bedding and cleavage.

The ?Late Cambrian Ponto Complex, in turn, is thrust across both the Neoproterozoic MAV and the Early-Middle Cambrian Gnalta Group rocks at the Mt Wright Fault. F2 (the dominant folding) in the Ponto Complex may correlate with F1 in the Wilandra beds, having similar trends and an asymmetry to the southwest.

The Gnalta Group preserves relatively little evidence of folding related to the post-Ordovician, pre-Late Devonian event. Most of the beds referred to the Gnalta Group strike northwest, in the same trend as F1 in the Wilandra beds and F2 in the Ponto

Complex, suggesting some response to this event. The possible reasons for this are discussed below.

The Mootwingee Group also contains evidence of folding related to a northeast-southwest shortening event, with asymmetric open folds with southeasterly plunge. This constrains the oldest age limit of this event to post-Ordovician.

Finally, the Ravendale Formation contains none of the features observed in the older rocks of the area. It contains gentle open folds and drag folds related to Carboniferous or later movements on the Mt Wright Fault (Davidson, 1981). These folds may correlate with late kinking observed in the Wilandra beds and Ponto Complex near the Mt Wright and Bald Hill Faults. The lack of asymmetric northwest-southeast trending folds in the Ravendale Formation constrains the youngest limit of this deformation event to pre-Late Devonian. In view of observations in the Late Silurian-Early Devonian Mt Daubeny Formation, described elsewhere, it is likely that this event is in fact Silurian.

## 5.4 Questions arising from previous studies

### 5.4.1 What are the Wilandra beds?

Davidson (1981) correlated the Wilandra beds with the top of the Gnalta Group using lithological criteria. Mills (1992) ignored this correlation, grouping the area containing the Wilandra beds with the Kara beds. Crawford et al. (1997) showed that the MAV and the MWV and Cymbric Vale Formation volcanic units each have distinctive compositions, as well as age differences. A detailed study of the igneous geochemistry, and sedimentary rocks of the Wilandra beds is outlined below in an attempt to assign these beds to their correct stratigraphic position.

### *5.4.2 What is the significance of the Macs Tank and Baroorangee Creek Complexes?*

Johnson (1972) described an ultramafic complex near Macs Tank, outcropping immediately to the east of the Mt Wright Fault. Davidson (1981) described a second serpentinite melange at Baroorangee Creek, some 18 km to the south. The structural relationships, geochemistry, and affinities of these bodies to each other, the Gnalta Group and Ponto Complex are examined below.

*5.4.3 Coherency of the Gnalta Group*

All previous workers in this area have noted the lack of continuity of bedding that characterises the Gnalta Group (Warris, 1967; Kruse, 1979 & 1982; Leitch et al., 1978; Davidson, 1981). Most ascribed this to the presence of "cryptic" faulting and folding. This hypothesis is investigated below, using geophysical interpretation and new mapping.

*5.4.4 Setting of the Gnalta Group within the Koonenberry Belt*

A related question to the coherency of the Gnalta Group, is its tectonic and stratigraphic relationship to rocks of equivalent age within the rest of the Koonenberry Belt. In particular, there is no recognised stratigraphic or tectonic contact between the ?Lower-Middle Cambrian Teltawongee Group and the Gnalta Group (Mills, 1992). This has led to the hypothesis that the Gnalta Group may represent a separate allochthonous terrane (Leitch et al., 1978). Mills (1992) considered all the Lower to Middle Cambrian stratigraphy of the Koonenberry Belt was essentially autochthonous, and argued that the Teltawongee Group is a distal, basinal equivalent to the Gnalta Group. This correlation was made despite the lack of any interfingering relationships between the two packages. The affinities of the Gnalta Group are examined below in an attempt to resolve this conflict.

**5.5 Geophysical Mapping**

*5.5.1 Methods*

The approached used in mapping the Nuchea 7335 1:100 000 sheet is essentially similar to that described at Chapter 4.12. Interpretations were aided by field mapping traverses in the Baroorangee Creek, Cymbric Vale, Mt Wright Creek, Bynguano Range and Macs Tank areas. These traverses involved the description of lithological units, collection of structural data and lithological sampling. To this end, over 150 thin sections have been petrographically examined. To support the geophysical interpretation, over 50 samples were taken for bulk density measurements, and more than 600 magnetic susceptibility measurements were made on outcrops in the field (see Chapter 2 for summary)

*5.5.2 Stratigraphy*

Nuchea 7335 contains more formally defined stratigraphic units than any other sheet in the Koonenberry region. Because the stratigraphy is generally formalised, the following discussion will centre around formal units, rather than domains, in contrast to other 1:100 000 sheets mapped as part of this study.

Kara beds (NPrz3ka)

The most important exposure of Kara beds on Nuchea 7335 occurs around 641350 mE 6545540 mN. It outcrops as a yellow-buff shale to slate with a well-developed spaced slaty cleavage; it has an average magnetic susceptibility of 25 x $10^{-5}$ SI. In the magnetic image, this unit is very close to a high frequency folded lineament of 300 nT amplitude; it is unlikely that the shale is responsible for this anomaly.

A poorly exposed magnetic domain in the northern extremity of the map area is correlated with the Swamp Domain of Wonnaminta 7336, based on continuity of magnetic character.

Mt Arrowsmith Volcanics (NPrz3kv)

The formation occurs as a single, north trending broad magnetic high of 400 nT. On the ground, units include basaltic to andesitic flows and dykes intruding or interbedded with shale and/or unfossiliferous limestone.

Nundora Formation (Etn)

A sequence of graded, eastward-younging mudstone-sandstone couplets correlated with the Teltawongee Group outcrops at 641675 mE 6545575 mN. Up section eastward, medium- to coarse-grained feldspathic-lithic arenites interbedded with shale are tightly folded around a north-plunging syncline. This can be seen defined in the magnetics and is confirmed by cleavage and younging data.

Undifferentiated Gnalta Group (?Eg)

Occurs as a broad, high magnetic domain in the southeastern corner of the sheet. Mesozoic and Cainozoic units obscure this area.

Gnalta Group intrusive (?Egi)

An ovoid magnetic feature of c.1500 m diameter with high frequency overprint, intruding the Cymbric Vale Formation. The anomaly has a typical "bulls eye" pattern with an external zone of 125 nT and an internal zones of 75 and 100 nT. This feature probably corresponds to a small porphyry body reported by Davidson (1981).

Mt Wright Volcanics (Egv)

The formation outcrops as a broad magnetic high in the footwall of the Mt Wright Fault zone. Lithologies include basalt, basaltic andesite, and andesite lavas, dykes and volcaniclastics interbedded with archaeocyathan limestone lenses. Discrete high zones related to outcropping volcanics occur further to the west, and are probably fault bounded blocks of a broken formation. Magnetic susceptibilities for the MWV average 3100 x $10^{-5}$ SI.

Cymbric Vale Formation (Egcy)

Outcropping in the centre of the map sheet, the Cymbric Vale Formation has a generally flat magnetic response of c. 70 nT. It overlies some significant magnetic sources at depth, probably volcanics of the MWV. These produce longer wavelength anomalies. The average susceptibility of the Cymbric Vale Formation is essentially non-magnetic at 12 x $10^{-5}$ SI.

Two tectonised slices of tuffaceous origin are found in the hangingwall of the Mt Wright Fault. These have been correlated with the Cymbric Vale Formation.

Coonigan Formation (Egc)

Mapped exposures of the Coonigan Formation correspond with magnetic high zones e.g. 627210 mE 6548580mN, despite outcropping as relatively non-magnetic shale and limestone. Anomalies associated with the Coonigan Formation continue into the northwest corner of the sheet, where they appear to be folded around a northwest-plunging tight anticline broken by later north-trending brittle faults. These faults do not break the unconformably overlying Mootwingee Group, suggesting a post-Templetonian, pre-Payntonian deformation age. Early fold and fault deformation is consistent with interpretation of the Gnalta Group as a broken formation (see below)

Wilandra beds

The Wilandra beds contain basalts with shales, limestone and sandstones, fining upwards to a shale-dominated section. Outcrop of the Wilandra Formation is constrained by the Bald Hill Fault to the west, and inferred fault contacts with the Ponto Group to the north and east, and with the Teltawongee Group to the south.

Ponto Complex (Epo)

Well Paddock Subdomain (Epwp)

This subdomain is the hangingwall of the west-vergent Mt Wright Fault. It is a high strain zone, and was investigated by Davidson (1981) and Zhou (1993). Davidson (1981) reported gneisses, schists, phyllites and metabasites of amphibolite and upper greenschist grade. This was confirmed by sodic blue hornblendes (Zhou, 1993) indicating minimum pressures of formation of c.8 kB at temperatures of c.350°C. The rocks of this subdomain contrast strongly with the prehnite-pumpellyite facies basalts found in the footwall of the Mt Wright Fault (Crawford et al., 1997). It is likely that the Grasmere Creek Fault which transects this subdomain has in part repeated and translated some units of this subdomain.

The subdomain is characterised by a series of linear magnetic highs of c. 30 nT superimposed on a background level of c. 100 nT. Schists and phyllites average $50 \times 10^{-5}$ SI, whereas metabasites have susceptibilities averaging $350 \times 10^{-5}$ SI.

Amphitheatre Subdomain (Epam)

This subdomain occurs in the northeastern corner of the map sheet in an area of poor outcrop, and has received very little attention in the past. Reconnaissance mapping revealed crenulated phyllite and metasandstone with an average susceptibility of $25 \times 10^{-5}$ SI. Magnetically, the Amphitheatre Subdomain is subdued with responses between 0 and 25 nT.

Baroorangee Creek Mafic-Ultramafic Complex (MUMC) (Ebcc)

The Baroorangee Creek MUMC is a melange of mostly basalt, dolerite and metabasite blocks in a scaly serpentinite matrix. The susceptibility of blocks ranges between $3000 \times 10^{-5}$ and $30 \times 10^{-5}$ SI. These respond as a 300 nT asymmetric linear high.

Macs Tank MUMC (Emtc)

Like the Baroorangee Creek MUMC, the Macs Tank MUMC is a serpentinite melange in the hangingwall of the Mt Wright Fault system. It consists of blocks of predominantly tholeiitic volcanics mixed with minor metaharzburgites and some calc-alkaline volcanics from the footwall of the fault. Susceptibilities range from 3 to > $3000 \times 10^{-5}$ SI. These produce a composite high of 1250 nT. This is the highest response of any lithology in the Koonenberry region.

Mootwingee Group (E-Om) (includes Nootumbulla Sandstone E-Omn, Rowena Formation E-Omr, Bynguano Quartzite Member E-Omb)

These units comprise siliciclastic and carbonate sequences. The Bynguano Quartzite, originally proposed by Warris as a formation, has been downgraded to a member bed

of the Rowena Formation, due to lack of conclusive evidence for its distinctive mappability (Davidson, 1981).

All three units are essentially non-magnetic (average susc. 8 x $10^{-5}$ SI), and they respond as broad wavelength gradients influenced by underlying magnetic sources.

Mulga Downs Group (Dm) (includes Snake Cave Sandstone Dms, Ravendale Formation, Dmr)
These units consist of various packages of clean, porous fluvial sandstones of Frasnian to Famennian age (Bembrick, 1997). The average susceptibility of these rocks is 6 x $10^{-5}$ SI, producing a response akin to that of the Mootwingee Group. The Mulga Downs Group forms the first "solid geology" layer of the Bancannia Trough, and thus covers the western half of the sheet.

?Permian diatreme pipe ?Pi
A circular magnetic feature of c. 2000m diameter intruding the Ravendale Formation in the northeast corner of the map sheet. Kimberlitic diatreme pipes occur at Turkey Creek on Kayrunnera 7436; these features have been dated at 264 ± 18 Ma using fission track methods (Gleadow & Edwards, 1978).

### *5.5.2 Synthesis*

The Nuchea map sheet contains "solid geology" ranging in age from Late Neoproterozoic through to Permian. The susceptibility, density and radionuclide concentration contrasts between many units renders geophysics a useful tool in extending mapping particularly in the northern and eastern parts of the sheet.

The overall structural style revealed by the technique shows north-northwest—trending sinuous, reactivated thrusts and high-angle reverse fault systems. The two fundamental structures within the sheet are of this type: the Lawrence and Mt Wright Fault systems. The zone between these two major faults is characterised by complexly deformed geology with detached post-Middle Cambrian, pre-Ordovician synclinal hinges and intense north-northeast—trending fault arrays. West of the Lawrence Fault the geology is relatively simple open folded and faulted Late Devonian sedimentary rocks. East of the Mt Wright Fault zone is a high-strain folded and possibly overthrust domain of Late Neoproterozoic to Late Cambrian rocks.

## 5.6 Affinities and Correlation of the Wilandra beds

Davidson (1981) noted that he had only limited resources to investigate the geochemistry of volcanics in the Mt Wright area, and most of these were spent on determining the tholeiitic affinities of volcanics in the Ponto Complex, and the nature of the Baroorangee Creek Mafic-Ultramafic Complex. Furthermore, he had no resources for the analysis of immobile trace element data, a key to the investigation of altered volcanics such as occur in the Wilandra beds. The present study used a combination of petrographic and major and trace element analyses to determine the affinities of volcanic units within the Wilandra beds. In the following discussion, the term "Wilandra volcanics" is used as an informal stratigraphic term to refer to these rocks.

Davidson (1981) described the Wilandra volcanics as ab-chl-epi altered spilites. To ascertain the affinities of these rocks, 17 samples of lavas and dykes, and volcanogenic, clastic and carbonate sedimentary rocks were collected from creek traverses of the Wilandra beds. Figure 5.6.1 shows the sample distribution. Thin sections of all of these rocks were prepared and petrographically examined.

Dacite, andesite, diorite, basalt and dolerite were all present in the volcanic suite (Fig 5.6.2 a-d), with an even distribution of mafic rocks (6 samples) and intermediate samples (5 samples). In outcrop most lavas have chilled-margin textures, with some large vesicles developed. Some are intimately interbedded with carbonate breccias. Coarser grained rocks are generally thin sills, 0.2 -1 m in width.

Two dacite dykes are quartz- or quartz + plagioclase-phyric with strong ser-epi alteration of the glassy groundmass. Metabasaltic samples are plagioclase-phyric with relict clinopyroxene phenocrysts comprising up to 10 modal percent. Plag is albitised, and cpx altered to epi-act; the often glassy groundmass is pervasively altered to a mixture of carb-qz-ser-chl and hm (after chl). Of the coarser intrusive rocks, one sample of diorite (9701) is strongly plag+cpx-phyric with minor qz; textures suggestive of granophyre have been preserved in this sample, suggesting it is a late phase fractionation product of more mafic magmas. The remainder of the intrusives are plag+cpx+op-phyric ophitic dolerites, with the alteration assemblage epi-ab-ser. Sample 9706 has been strongly silicified. The composite metamorphic assemblage ab-chl-epi±act, indicates that the Wilandra volcanics were metamorphosed under middle greenschist facies conditions.

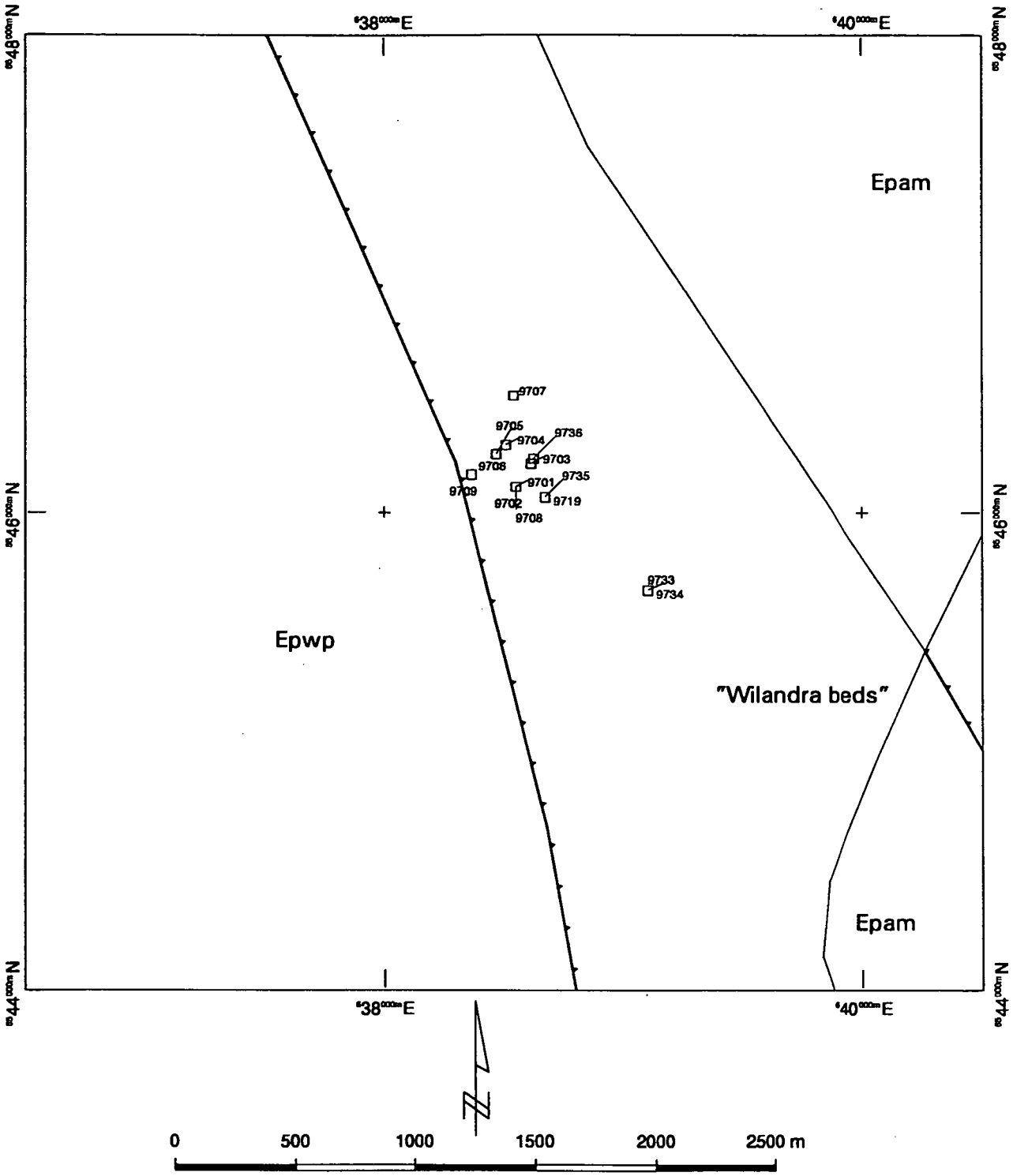


Figure 5.6.1

Sample Locations, "Wilandra beds"

Sample numbers given.
For ciphers, see Nuchea 7335 sheet, back pocket

From these samples, 2 dacites, 1 dolerite and 4 basalts were selected for standard whole rock XRF major- and trace-element analysis. Sample preparation and analysis was carried out in accordance with the procedures outlined in Chapter 3.

Data from the Wilandra volcanics is presented in Table 5.6.1, and Figures 5.6.2-5. Because these are altered rocks with some high LOI values (2 to 13 %), the data are recalculated volatile free, with loss on ignition values reported separately. Figure 5.6.2 contains normal Harker diagrams for both major oxides and trace elements. Plots of trace elements versus Zr (not shown) indicate that Nb, Y, P Sc and possibly V follow magmatic trends, and were immobile under the conditions of alteration, whereas Ba, Sr and Rb all show scatter indicative of remobilisation. Major oxide data (except $TiO_2$, $P_2O_5$ and possibly FeO*) should therefore be treated with caution. Also plotted for reference are fields for the Early Cambrian calc-alkaline Mooracoochie Volcanics (Gatehouse, 1986) and Middle Cambrian alkaline Murteree-Jena Volcanics (Sun, 1996) both from the Warburton Basin in South Australia. The reasons for comparison of these suites is discussed below.

The major element plots show that the metabasaltic rocks tend to group with the alkaline Murteree-Jena Volcanics in FeO*, $TiO_2$, $Al_2O_3$, MgO and $P_2O_5$, all of which have limited mobility, whereas the intrusive dacites and one dolerite tend to form a trend with the calc-alkaline Mooracoochie Volcanics.

The immobile trace elements Nb, Zr, Y and V also show the bimodal nature of the Wilandra volcanics. However, one metabasalt sample (9708) has lower Nb and Zr, more akin to the dacite-dolerite suite. The Nb/Y v Zr/Ti discrimination plot (after Winchester & Floyd, 1977) confirms that the Wilandra volcanics contain two distinct suites: a sub-alkaline suite composed of the dacites, dolerite and metabasalt (9708); and an alkaline suite of metabasalts.

MORB-normalised spidergrams of incompatible elements for the two suites are plotted with data from potential correlates (Figures 5.6.35-5.6.5). Figure 5.6.3 shows the alkaline suite with the samples of basalt from the Murteree-A1 and Jena wells in the Warburton Basin (Sun, 1996), indicating many similarities. These rocks are generally incompatible element enriched. High Nb is characteristic of within-plate basalts. Figure 5.6.4 shows a distinctively different pattern, based on the calc-alkaline suite and samples from the MWV. A clear relationship exists between these two suites, except for sample 9626 (a dacite) which, although petrographically similar, is anomalously enriched in Th and Nb. Figure 5.6.5 shows the alkaline suite plotted against the field of

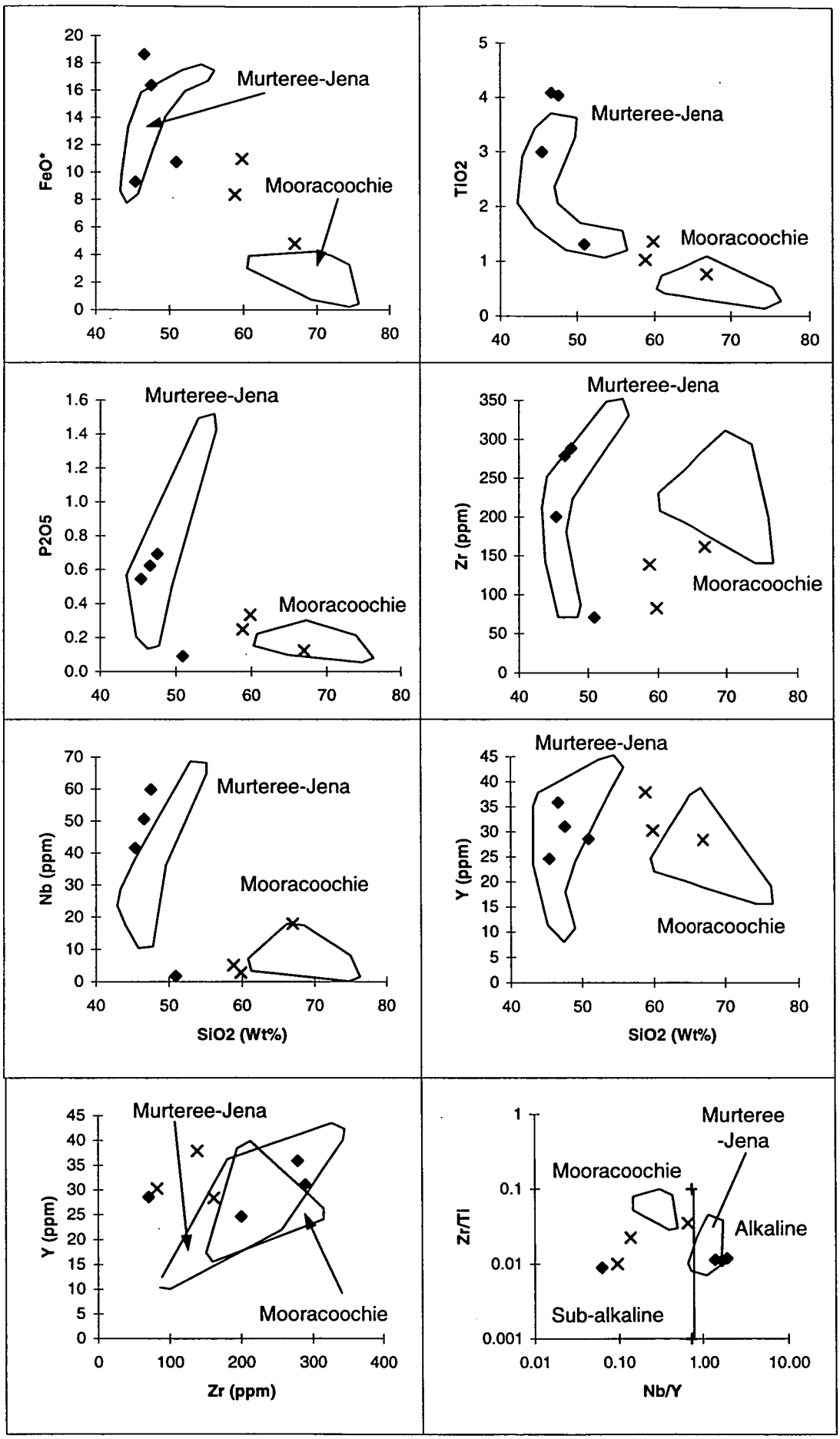


**Figure 5.6.2 Major and trace element diagrams, "Wilandra volcanics"**
diamonds = basalts; crosses = dacite and dolerite dykes

**Table 5.6.1 Whole-rock analyses recalculated volatile-free for the Wilandra volcanics**

| Sample | 9703 | 9707 | 9719 | 9708 | 9626 | 9627 | 9702 |
|---|---|---|---|---|---|---|---|
| Rock | basalt | basalt | basalt | basalt | dacite | dacite | dolerite |
| SiO2 | 46.65 | 47.59 | 45.41 | 50.92 | 66.95 | 58.86 | 59.86 |
| TiO2 | 4.09 | 4.04 | 3.00 | 1.32 | 0.77 | 1.03 | 1.37 |
| Al2O3 | 16.51 | 17.64 | 13.90 | 15.03 | 16.00 | 17.45 | 16.16 |
| Fe2O3 | 20.73 | 18.20 | 10.34 | 11.97 | 5.35 | 9.33 | 12.23 |
| FeO* | 18.65 | 16.37 | 9.31 | 10.77 | 4.82 | 8.39 | 11.01 |
| MnO | 0.08 | 0.11 | 0.23 | 0.36 | 0.11 | 0.14 | 0.09 |
| MgO | 5.22 | 5.03 | 2.81 | 6.72 | 3.22 | 3.07 | 4.29 |
| CaO | 1.07 | 1.16 | 17.45 | 10.19 | 1.03 | 3.28 | 0.97 |
| Na2O | 4.81 | 4.75 | 5.37 | 2.63 | 5.94 | 6.35 | 4.27 |
| K2O | 0.23 | 0.80 | 0.94 | 0.78 | 0.49 | 0.23 | 0.42 |
| P2O5 | 0.62 | 0.69 | 0.54 | 0.09 | 0.12 | 0.25 | 0.33 |
| LOI | 6.59 | 5.88 | 13.62 | 11.47 | 2.76 | 3.04 | 4.32 |
| | | | | | | | |
| Rb | 6 | 12 | 11 | 33 | 21 | 6 | 14 |
| Ba | 174 | 354 | 313 | 155 | 85 | 77 | 146 |
| Th | 2 | 4 | 2 | 1 | 23 | 2 | 2 |
| Nb | 51 | 60 | 42 | 2 | 18 | 5 | 3 |
| La | 39 | 38 | 29 | <2 | 43 | 10 | 12 |
| Ce | 73 | 65 | 65 | 10 | 82 | 21 | 25 |
| Nd | 40 | 37 | 31 | 7 | 42 | 15 | 15 |
| Pb | 9 | 4 | 9 | 10 | 11 | 162 | 2 |
| Sr | 207 | 454 | 466 | 168 | 123 | 205 | 180 |
| Zr | 279 | 289 | 200 | 71 | 162 | 139 | 83 |
| Ti | 24510 | 24214 | 17982 | 7888 | 4630 | 6184 | 8204 |
| Y | 36 | 31 | 25 | 29 | 28 | 38 | 30 |
| Ni | 11 | 4 | 2 | 53 | 44 | 9 | 13 |
| Cr | 20 | 11 | 18 | 355 | 140 | 67 | 55 |
| V | 287 | 302 | 267 | 331 | 338 | 220 | 171 |
| Sc | 20 | 15 | 14 | 45 | 17 | 20 | 24 |
| Cu | 26 | 24 | 14 | 97 | 16 | 69 | 151 |
| Zn | 99 | 719 | 63 | 99 | 65 | 93 | 125 |
| | | | | | | | |
| Nb/Y | 1.412256 | 1.927595 | 1.688769 | 0.062937 | 0.633803 | 0.137203 | 0.09571 |
| Zr/Ti | 0.011375 | 0.011931 | 0.011128 | 0.009001 | 0.034949 | 0.022444 | 0.010081 |

**Figure 5.6.3 Wilandra volcanics (alkaline suite) & Murteree-Jena Volcanics*, Warburton Basin** *(data from Sun, 1996)

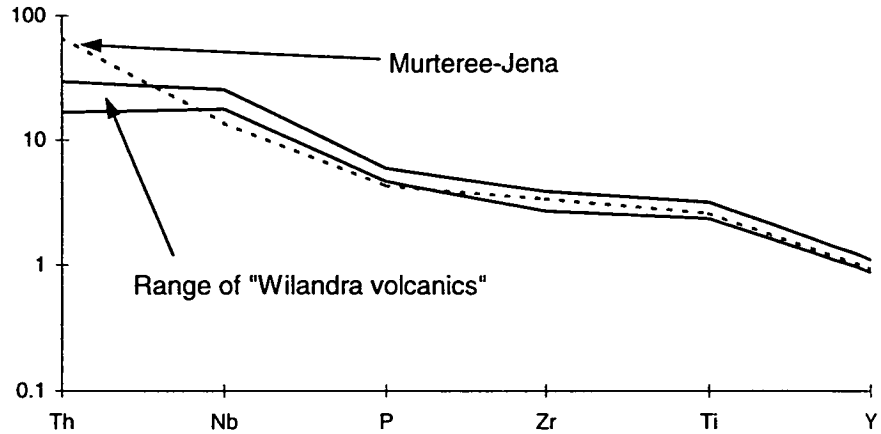


**Figure 5.6.4 Wilandra volcanics (calk-alkaline suite) & MWV***
(*data from Crawford et al., 1997)

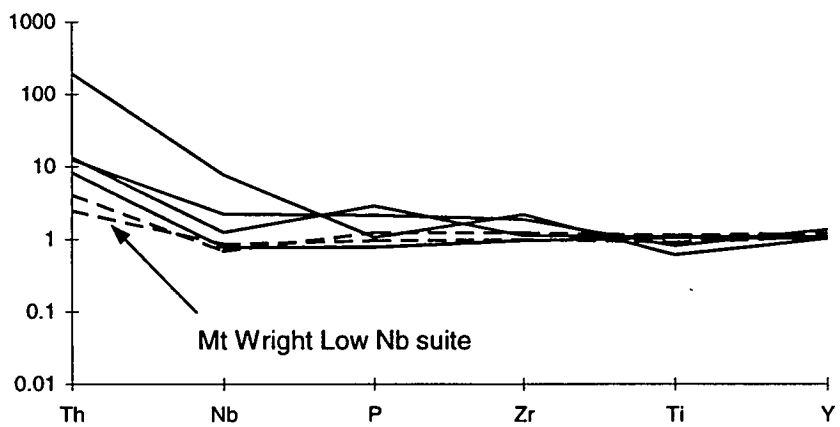


**Figure 5.6.5 Wilandra volcanics (alkaline suite) & MAV***
*(data from Crawford et al., 1997)

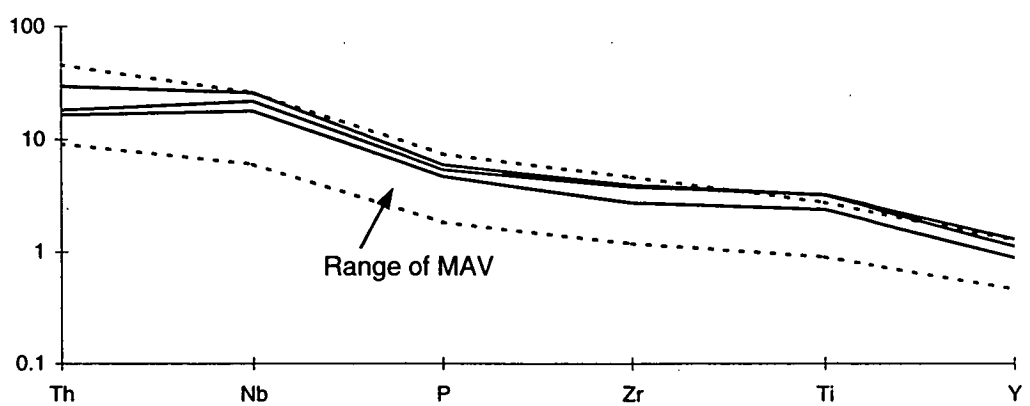


**Figures 5.6.3-5.6.5 N-MORB normalised spidergarms, "Wilandra volcanics"**
(normalising values from Sun & McDonough, 1989)

MAV data from Crawford et al., 1997. Again there is a close similarity between the Wilandra alkaline suite and the MAV.

The data described above imply that the Wilandra volcanics, and thus the Wilandra beds, are in fact a series of fault slices of Early Cambrian MWV and Late Neoproterozoic MAV. This has ramifications for the interpretation of the Mt Wright Fault: although clearly a major thrust structure, it is unlikely to be a major terrane boundary as suggested by Leitch et al. (1978), because two separate suites of different ages can be correlated to both west and east of it. The preferred interpretation of the Wilandra beds is a series of fault slices or nappes interleaved by thrusts into the Ponto Complex during west directed thrusting, or alternatively, as a set of later east-directed backthrusts. The timing of fault intercalation is constrained to be post-Late Cambrian (the age of the Ponto Complex, see below) and pre-Ordovician, due to Mootwingee Group sediments which unconformably overlie the Wilandra beds east of the Bald Hill Fault (Davidson, 1981).

The correlation of the MAV-Wilandra alkaline suite with the Murteree-Jena Volcanics casts some doubt on Boucher's (1994) correlation of the Murteree-Jena rocks with the Early Cambrian Truro Volcanics. Furthermore, if the new correlation indicated by these data is correct, it implies that the extensional tectonism related to the MAV and later MWV extended further to the north and west. This idea has already been postulated by various authors including Gatehouse (1986) and Sun (1996), although on the erroneous assumption that these volcanics represent a magmatic island arc suite.

For the sake of comparison to the local lithologies which might be the source of these fault slices, the enclosing Wilandra beds were also sampled. A volcaniclastic sandstone, 2 quartzose sandstones and 2 limestones were collected from very poor outcrops. Thin sections of each were prepared and examined. Limestones were both impure, recrystallised sparry varieties. Sample 9735 contained very altered basaltic intraclasts, suggesting a correlation with the MWV-Wilandra calc-alkaline suite. Of the clastic rocks, sample 9632 is a very immature, matrix-rich lithic-arkosic sandstone, containing poorly-sorted angular clasts of plagioclase, K-feldspar and quartz, with muscovite, hornblende and chromite. This rock also contained metamorphic biotite, indicating upper greenschist metamorphic grade. The chemical and physical immaturity of this rock implies a local source, and it is probably part of the Cymbric Vale Formation. Samples 9733 and 9734 come from cleaner quartzite horizons. Sample 9733, from a cross-laminated bed, is a recrystallised quartzite with distinctive muscovite cleavage. It also contains tourmaline, garnet, monazite and opaques. It is

distinctive from 9734, sampled from a massive sand bed, which is a biotite grade feldspathic quartz sandstone also containing zircon and monazite. The accessory metamorphic component within these rocks (garnet, monazite, tourmaline) has not been described from any parts of the Gnalta Group. The cross-laminated, clean quartzite is reminiscent of horizons within the Kara beds (Mills, 1992), with which these beds are tentatively correlated. These types of rocks within the Wilandra beds may have been the reason for Mills' (1992) incorporation of the Wilandra beds into the Kara beds.

## 5.7 Geophysics

### *5.7.1 Methods chosen*

Gravity and magnetics were selected to study the dip of the Mt Wright Fault at Macs Tank and Baroorangee Creek. At these locations the fault is marked by the amphibolitic metabasalts and metadolerites in serpentinite melange. These could be expected to have strong density and magnetic susceptibility contrasts with the rocks of the surrounding Gnalta Group and Ponto Complex. This initial assumption is borne out by the petrophysical investigations conducted at both sites (see below).

### *5.7.2 Gravity survey: acquisition and processing*

A total of 133 optically surveyed gravity stations were acquired in the area, consisting of two lines at 100 m station spacing. Ninety-two stations were acquired across the Mt Wright Fault on "Cymbric Vale" and a further 41 at Macs Tank (Figure 5.7.1).

These data were acquired using a Lacoste & Romberg Model G gravimeter, serial no. 651.

All data were processed using the algorithm described at 3.12.2. The base station for these gravity surveys was at "Wilandra". This is located at 31° 16' 59.3147"S 141° 39' 01.1220"E with an observed gravity value of 979394.59 mGal. This is a second order base to the Isogal 84 network station at Broken Hill airport.

### *5.7.3 Magnetic surveys*

Fourteen line kilometres were acquired in the course of this study, using a GSM-19 Overhauser Effect fast-sampling magnetometer, triggered by a hip-chain. Ten line

**Figure 5.7.1 Modelled traverses, Mt Wright-Cymbric Vale area**

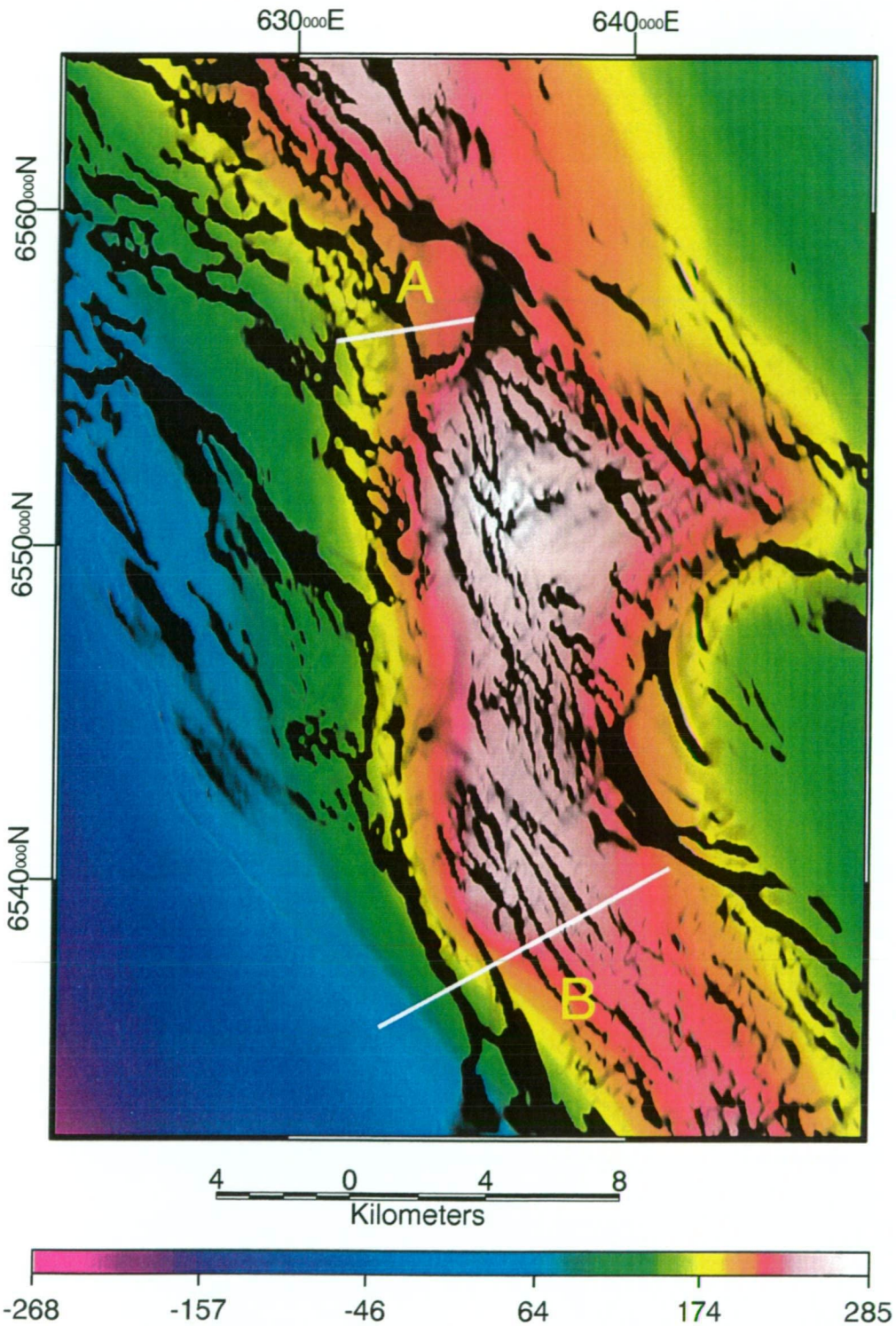


Bouguer anomaly pseudocolour with TMI intensity shaded at 45 degrees from the northeast. Grid is AMG zone 54. Z scale is in micrometres/sec/sec. A = Macs Tank traverse; B = Baroorangee Creek traverse.

kilometres of data were acquired at 0.5m spacing on "Cymbric Vale" and a further 4 line kilometres at Macs Tank. The sensor height of the magnetometer was 3m.

All magnetics have been diurnally corrected, using 60 second sampled records from a G-856 Geoinstruments proton precession magnetometer. The corrected data have been least-squares linear fitted to hand-held GPS control points (accurate to ± 20 m) observed along the lines of traverse.

## 5.8 The Gnalta Group: broken formation?

### *5.8.1 Structural style of the Mt Wright Fault Zone*

Magnetic data acquired across the Mt Wright Fault at both Macs Tank and Baroorangee Creek show high-amplitude, asymmetric anomalies (Figure 5.8.1). Data extracted from the regional magnetics coverage was modelled using the simple sensitivity analysis procedure outlined at 3.11.2 to predict the dip of magnetic sources throughout the Mt Wright-Cymbric Vale area . The results are shown in Figure 5.8.2. These suggest that the Mt Wright Fault is vertical near the surface, separating vertical Ponto Complex from steeply west-dipping MAV.

The Mt Wright Fault has developed a number of splays in the vicinity of Mt Wright. Most of these are easily mapped where they break up the continuity of the flat-lying Ravendale Formation. However one important splay is only identified in magnetic data (Figure 5.8.2), truncating magnetic anomalies in the Ponto Complex mapped to its east. This splay rejoins the Mt Wright Fault at Baroorangee Creek. Within the fault zone between the main fault and the splay lie a variety of stratigraphic and structural units. The principal lithology is high (amphibolite?) grade metasediments and metavolcanics of the Ponto Complex. These contain boudinage, rodding and stretching lineations parallel to the fault system (N-S). In addition, they contain a well-defined east-dipping schistosity, indicating west-directed transport (Figure 5.8.4).

Tectonically interleaved with the Ponto Complex in several locations is a crumbly, reddish or greenish cherty rock, which has a well-developed shear fabric, mylonitic in places (Figure 5.8.4B). The fabric appears to be parallel to a compositional banding, which it transposes.

Inspection of outcrops in creek exposures at 635398 mE, 6542522 mN and 635416 mE, 6542383 mN, shows that this rock contains an abundance of rootless folds, box folds, mesoscale shears, opposed microscale antiforms and synforms, and

**Figure 5.8.1 Dip sensitivity traverses, Mt Wright-Cymbric Vale**

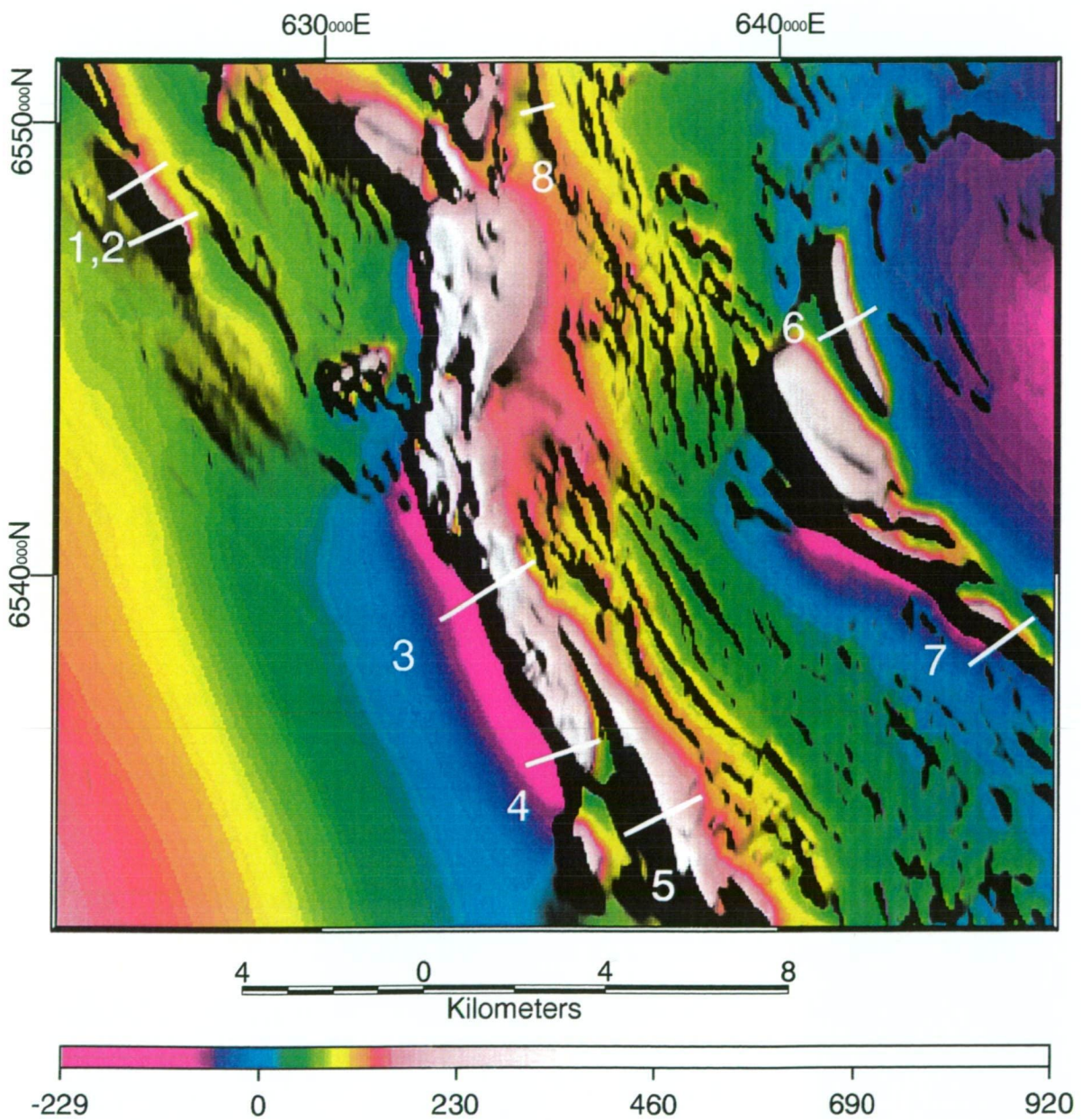


TMI pseudocolour and intensity layer shaded at 45 degrees from the northeast. Grid is AMG zone 54. Z scale in nT. Dip sensitivities shown in Fig. 5.8.2.
1,2: Lawrence Fault footwall. 3,4: Mt Wright Fault footwall. 5: Baroorangee Creek
6: Mt Wright FZ. .6: Kara beds. 7: Well Paddock Subdomain.
8: Bald Hill Fault hangingwall. Macs Tank traverses in Fig 5.8.2 are shown in Fig.5.7.1.

# Figure 5.8.2 Results of dip sensitivity modelling, Mt Wright -Cymbric Vale area

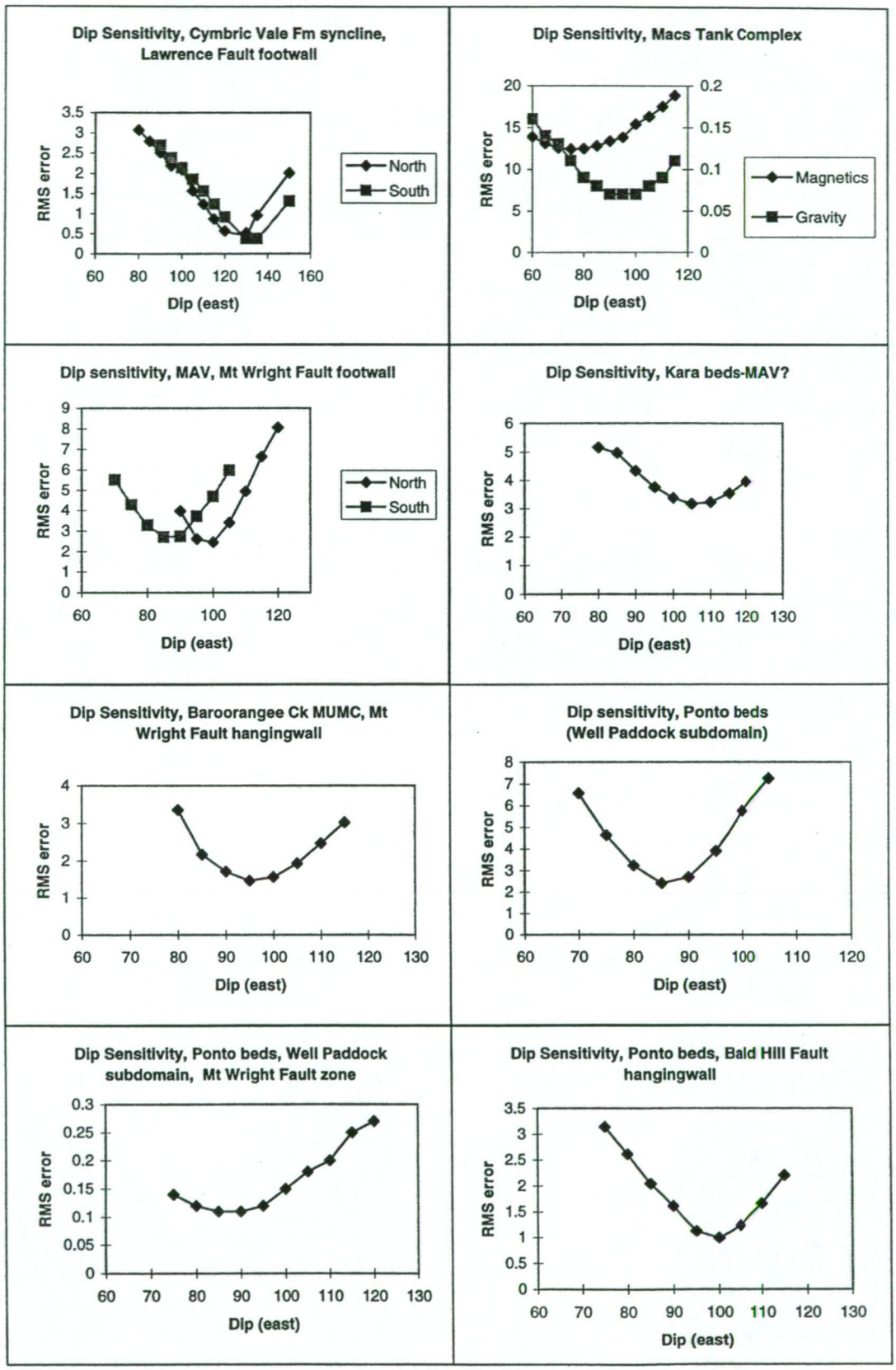

**Figure 5.8.3 Structures in the Mt Wright Fault hanging-wall: I**

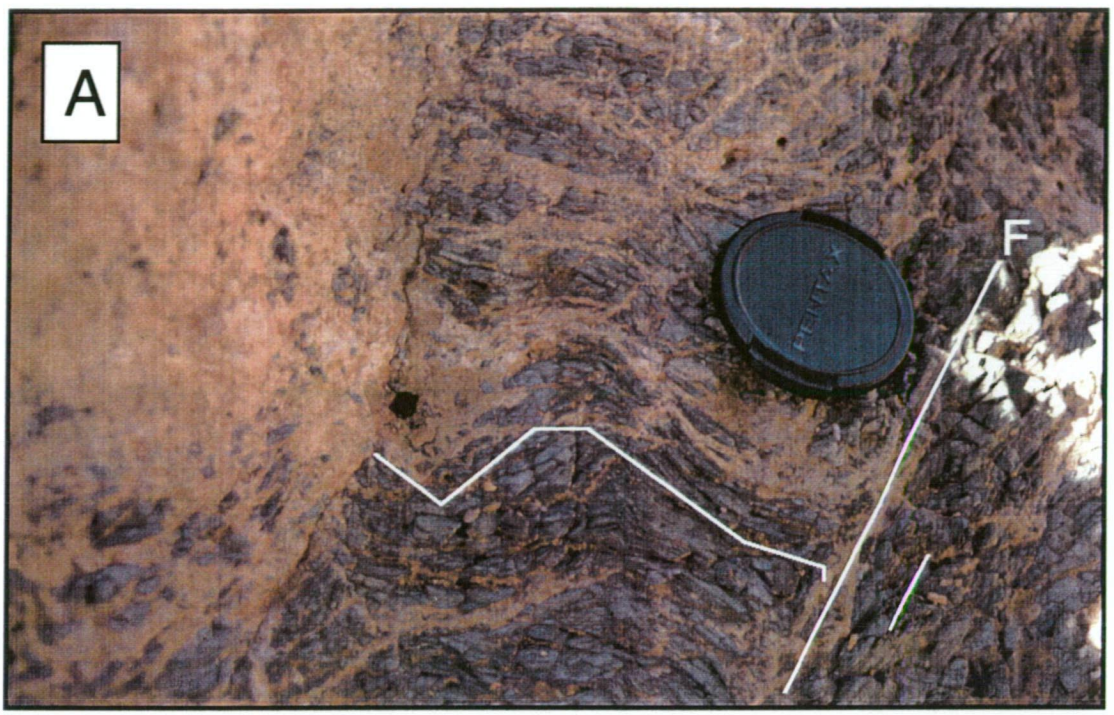


A (above) small-scale faulting and folding in cherty tuffs, Cymbric Vale Formation

B (below) kink and box folding in cherty tuff, Cymbric Vale Formation

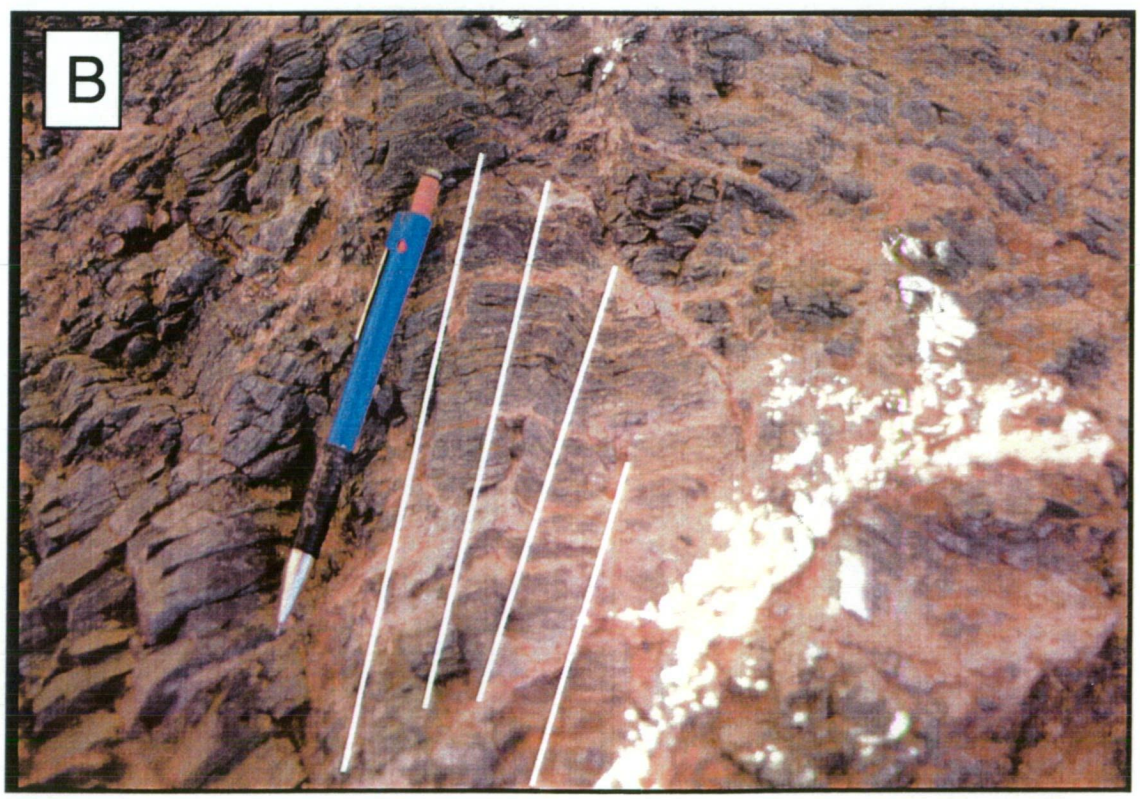

**Figure 5.8.4 Structures in the Mt Wright Fault hanging-wall: II**


A(above): west-directed F1 chevron folds, Ponto Complex

B(below): down-dip (east-directed) L-S fabric in tectonised cherty tuff

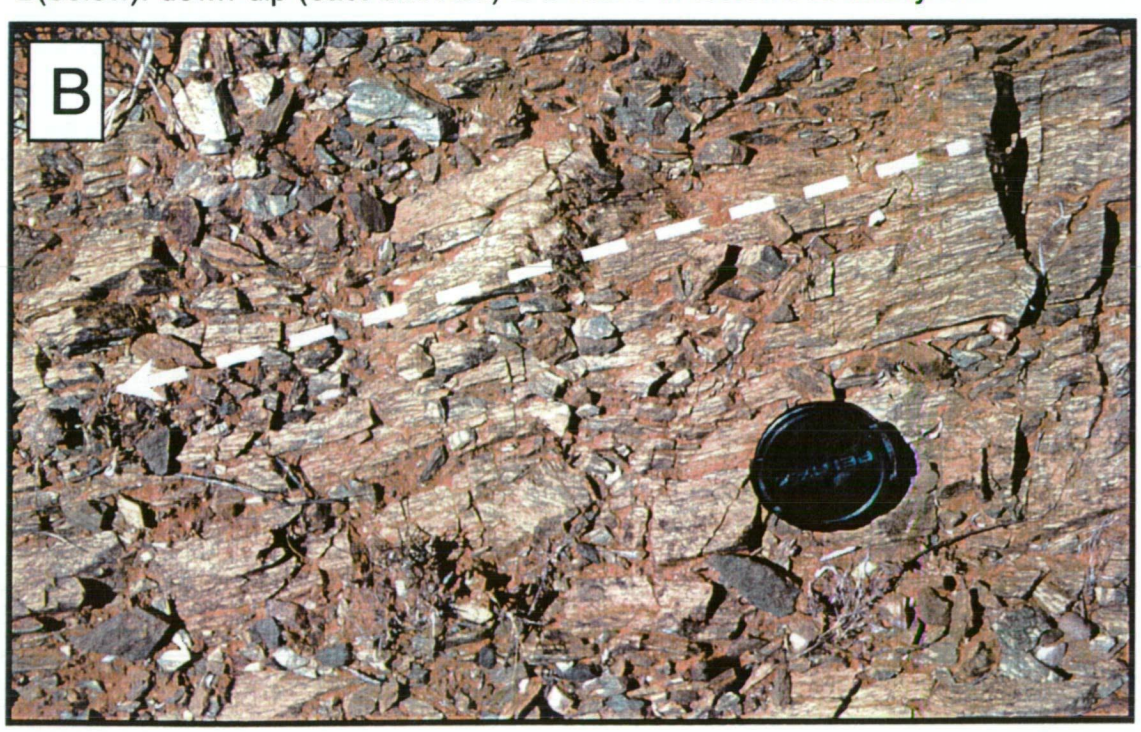

other non-cylindrical features. These fabrics are contained within broader mesoscale folds of a similar nature. Figure 5.8.5 shows the distinctive nature of this fabric relative to regional structural domains.

In thin section, these rocks consist of varying components of a recrystallised mosaic of silica and white mica, with a minor volcanic fragment component, usually broken clinopyroxene clasts. They do not contain original or altered feldspars. None of the tuffs described from the Ponto Complex contains a significant ferro-magnesian mineral component. However, some Cymbric Vale Formation airfall crystal-rich tuffs do contain altered euhedral ferro-magnesian mineral clasts, probably incorporated during explosive, shallow water felsic volcanism. I therefore correlate these tuffaceous fault slices east of the Mt Wright Fault with the volcanogenic sediments of the Gnalta Group, the MWV being the likely source of the clinopyroxene.

A second chert unit containing a similar tectonised fabric has been located at 636087 mE, 6537246 mN, adjacent to the Baroorangee Creek Serpentinite. Another, less tectonised slice of Cymbric Vale Formation. has recently been located at the northern tip of a fault splay, north of Mt Wright (G. Neef, unpublished data, 1998).

In an attempt to provide an age for this lithology, chert from 3 locations (635398 mE, 6542522 mN; 635416 mE, 6542383 mN; and 636087 mE, 6537246 mN) was etched with hydrofluoric acid and the residues sieved to 25 μm. This produced silicified trilobite fragments. These were not identifiable to even family taxon (C. F. Burrett, pers. comm. 1998). Nevertheless, the occurrence of trilobite fragments in this lithology strongly suggests a correlation with the Gnalta Group, in particular either the Cymbric Vale Formation or the Coonigan Formation, both of which contain trilobite faunas (Öpik, 1967; Jago et al, 1997). Trilobites are not known from any other stratigraphic unit in the area except the Mootwingee Group, which does not contain any tuff members.

The Baroorangee Creek Serpentinite, which abuts the tectonised tuff, is a serpentinite melange. At outcrop scale, it contains blocks of MAV alkaline type and Ponto tholeiitic type amphibolite grade metadolerites in a serpentinised matrix.

Thus the splay of the Mt Wright Fault can be considered a melange zone, where lithologies ranging in age from Neoproterozoic to Late Cambrian, are interleaved and metamorphosed to amphibolite grade. Related, simultaneous deformation can also explain irregularities in the stratigraphy of the Gnalta Group in the hanging wall of this fault (see below).

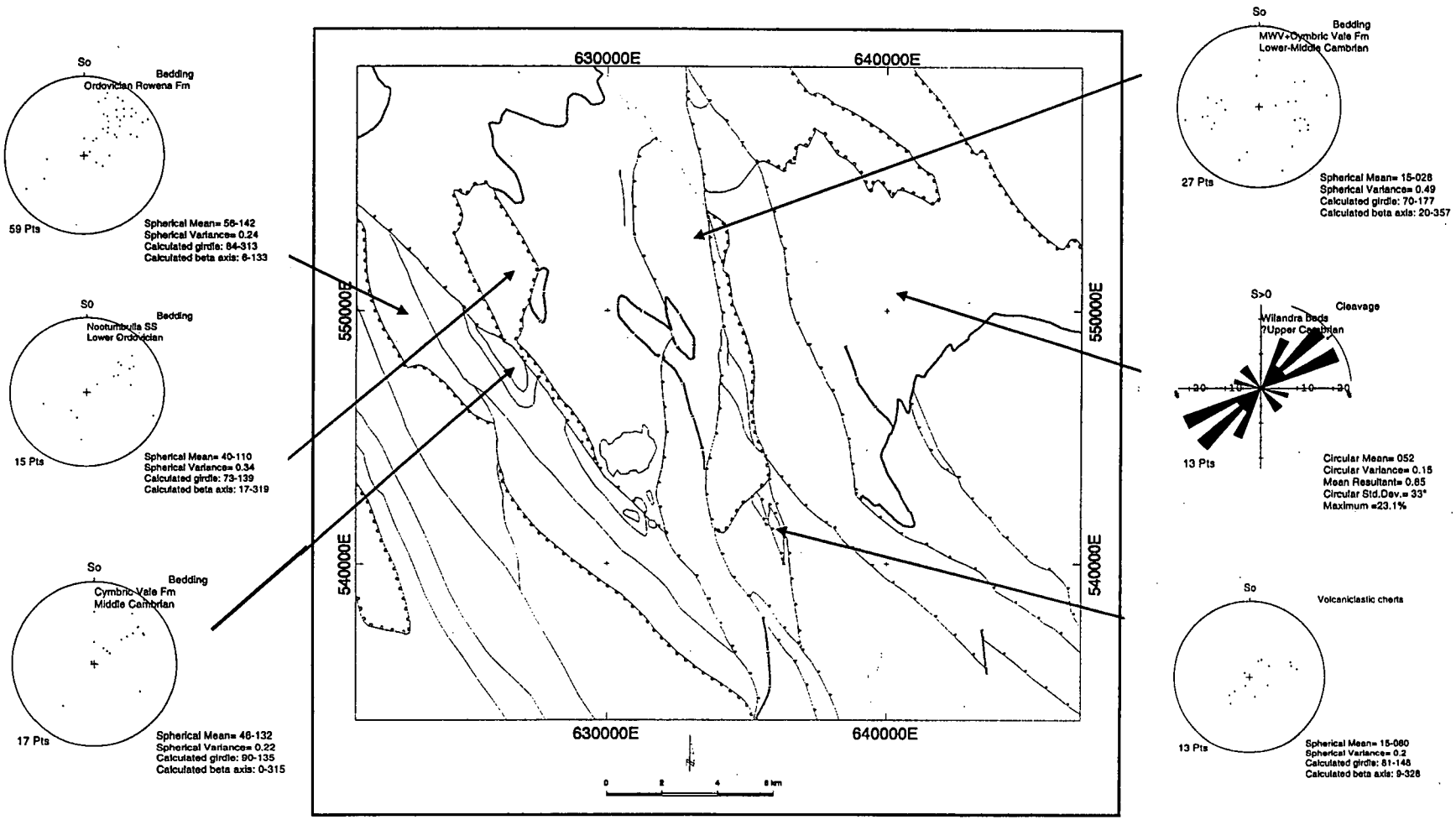


*Grid is AMG Zone 54; map is an inset from Nuchea 7335 1:100 000 interpretation in back pocket

**Figure 5.8.5 Structural domain map, Mt Wright-Cymbric Vale area**

*5.8.3 Distribution and nature of lithologies in the Gnalta Group*

The primary character of the Gnalta Group which draws attention to the possibility of a non-coherent stratigraphy is its distribution in outcrop (Figure 5.8.6). Lithologies assigned to the group outcrop over an area of 1000 $km^2$, yet most individual beds cannot be traced for more than a few tens of meters. This is despite the fact that the group contains welded tuffs and lavas, which are highly resistant to weathering, and make up significant topographic ridges in the region.

Instead, the group consists of small, scattered outcrops, usually <10 $m^2$, many of which are not petrogenetically related, e.g. limestones near basalts.

In the TMI image, the zone between the Mt Wright and Lawrence Faults consists of a series of flat zones, together with contorted and point anomalies of highly variable geometry, amplitude and spatial frequency. As well as suggesting non-continuity of magnetic sources, even beneath later cover, these trends are at variance with those of the surrounding regions to the north, south and east, which present strongly north-northwest—trending anomalies of high spatial frequency. The variability of magnetic signature within this internal region strongly suggests a complex tectonic history, but one which is different to the rocks to the west and east, producing a different structural pattern. In the internal zone, there is no magnetic evidence for buried synclines or anticlines, which produce simple, folded magnetic traces (e.g. Jessell et al., 1993).

In explaining the discontinuous outcrop, previous authors have noted the complexity of the area in local and regional mapping, and suggested cryptic faulting and folding as the cause (cf. Warris, 1967; Edwards, 1979; Kruse, 1982; Crawford et al., 1997). However, despite the previous insistence on cryptic deformation, limited structural analysis of the area (Figure 5.8.6) shows that outcropping beds of various lithotypes strike roughly parallel to the regional trend of the surrounding rocks, that is c. north-northwest.

Also apparent from this structural analysis is the lack of fold hinges in the area, relative to limb measurements. Two fold hinges have been mapped: a macroscopic syncline to the west, near the Lawrence Fault, has a magnetic core giving a predicted axial planar dip of 50° west; and an inferred anticline near the Mt. Wright Fault which appears to be upright.

**Figure 5.8.6 Mapped distribution of Gnalta Group lithologies, Mt Wright Fault**

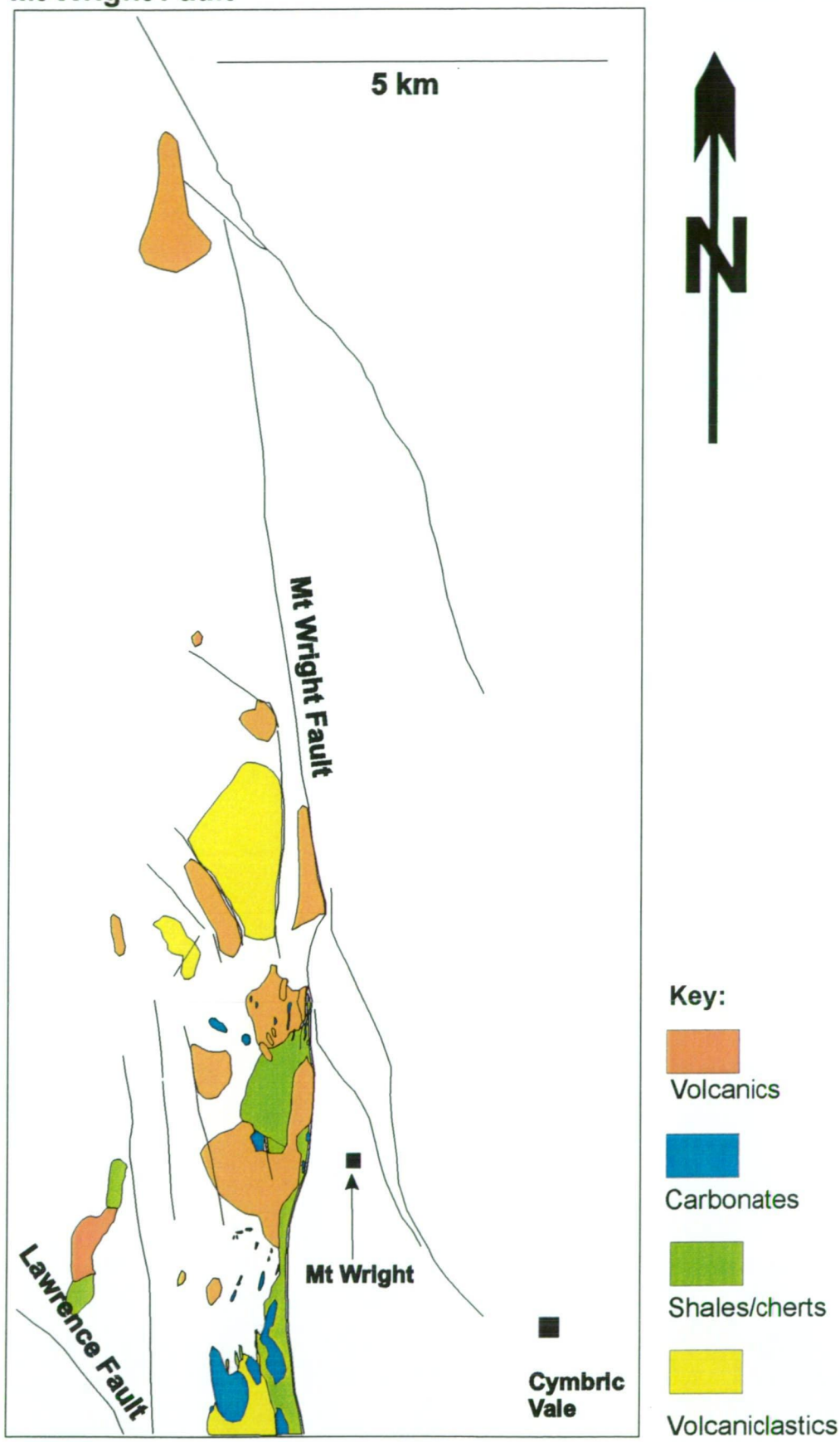


* modified from Stevens et al., Unpublished data

Cleavage data from the Gnalta Group are virtually non-existent (see Davidson, 1981), despite previous authors' insistence on severe folding. From the discussion of the structural geology above (5.3 ff), it is clear that there has been a tectonic event between the Early Ordovician and the Late Devonian, which has folded all the surrounding regional lithologies in a systematic fashion. Despite this event, which clearly post-dates deposition/extrusion of the Gnalta Group, these rocks contain no good evidence for the folding so well-developed in the younger rocks.

In conjunction with earlier authors' insistence on cryptic faulting within the Gnalta Group. (cf. Warris, 1967; Davidson, 1981; Kruse, 1982; Crawford et al., 1997), I interpret the structural-stratigraphic complexity as indicating that the Gnalta Group was tectonically broken in a post-Templetonian deformation. The lithologies of the Gnalta Group, consist predominantly of lavas, tuffs, limestones and volcanogenic sandstones. This favoured the development of broken formation rather than melange, due to the lack of a suitable, low competency matrix material such as shale. Broken fragments ranging in size from $< 1m^2$ to c.2 $km^2$ were then realigned during the regional north-northwest trending Silurian deformation.

The northern, poorly exposed domain abutting the Lawrence Fault shows a contrasting deformation style. This area contains scattered occurrences of the shale-rich, limestone-poor Coonigan Formation., which displays a high degree of faulting and folding in the magnetics (Figure 5.8.7). I interpret this low competency unit to have formed true melange, containing matrix and blocks, which were only partially realigned during the Silurian.

This model can explain the highly contorted nature of some lithologies relative to the virtually undeformed, fault juxtaposed beds of the same age.

## 5.9 Affinities of the Macs Tank and Baroorangee Creek Mafic-Ultramafic Complexes

The Macs Tank Mafic-Ultramafic Complex (MUMC) was originally mapped by Johnston (1972), and the Baroorangee Creek "Serpentinite" was mapped by Davidson (1981). No work on either body exists within the published literature.

### *5.9.1 Geophysical Interpretation of the Macs Tank MUMC*

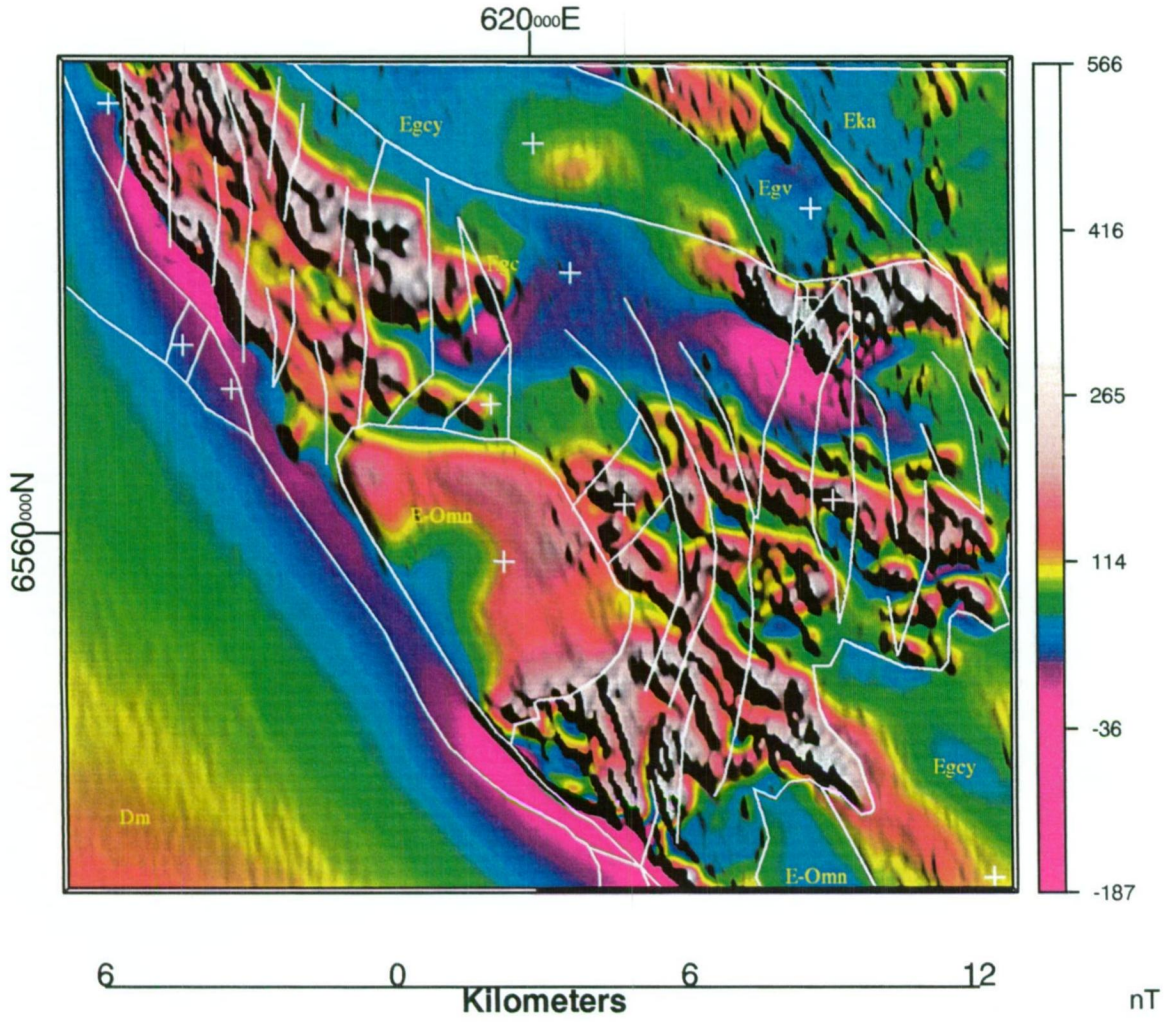


## Figure 5.8.7
## Interpretation of areas of Coonigan Formation

TMI pseudocolour with
1st VD intensity layer shaded
at 45 degrees from the northeast.

Geology layer interpreted; see
back pocket for Nuchea 7335 map.
Ciphers discussed in text.

Note high degree of faulting in
Coonigan (Egc) relative to other
units

**Figure 5.8.8 Broken formation within Coonigan Formation**

White arrows indicate faults within more competent sandy layer.

Overlying shale layer has flowed to accommodate deformation.

The Macs Tank Complex has a high magnetic signature, almost 2000 nT greater than the surrounding rocks, suggesting elevated magnetite values due to serpentinitsation of primary olivine. This is supported by magnetic susceptibility measurements made in the field (Table 5.9.1), and by petrographic observations (see below).

The other feature of the field around the body is the spiky, irregular high-frequency character; this is not observed in the aeromagnetic coverage of the area, as the flight height (60 m) has effectively low-pass filtered the data, leaving only the 2 km half wavelength.

**Table 5.9.1 Petrophysical summary, MUMC**

| *MUMC* | *Max* | *Min* | *Av* | *Median* | *1 sigma* |
|---|---|---|---|---|---|
| Macs Tank | 0.028 | 0.00003 | 0.009 | 0.01 | 0.007 |
| Baroorangee Creek | 0.034 | 0.0003 | 0.016 | 0.021 | 0.013 |

*Values in SI.

Ground geophysical data were forward modelled in two dimensions using the petrophysical properties listed in Table 5.9.1. The best-fit model for Macs Tank is presented in Figure 5.9.1. The solution shows three imbricate thrust sheets between the Ponto Complex and the Gnalta Group. Two of these, MWV and LMS represent slices of the Mt Wright Volcanics thrust up from the base of the Gnalta Group by breakthrough splays from the main fault. The Macs Tank Complex is an imbricate sheet in the hanging wall of the fault. Note that the solution cannot represent the degree of shearing (hangingwall) or tectonic mixing (footwall) observed in outcrop, as these features do not, of themselves produce magnetic or gravimetric contrasts. Dip sensitivity modelling (Figure 5.9.2) indicates that the Macs Tank Complex probably dips east at about 75° at the surface. The fault geometry indicated by the solution is an east-dipping listric thrust, consistent with the modelled section and field evidence from along strike. Modelling of the depth to detachment indicates the fault flattens at 8 km (Figures 5.9.3).

The best-fit forward model for Baroorangee Creek is shown in Figure 5.9.4. The Mt Wright Fault is the contact between steeply-dipping imbricated units to the east and more flat-lying section to the west. These flat-lying units reflect the late (post-Devonian) west-side down dip-slip movement of the fault as indicated by Crawford et al. (1997). Underneath the Ordovician Mootwingee Group, the base of the Gnalta Group dips to the east, suggesting this unit has been involved in the thrusting. In the immediate hangingwall of the fault is the approximately vertically dipping Baroorangee

## Figure 5.9.1 2D model of the Macs Tank Complex

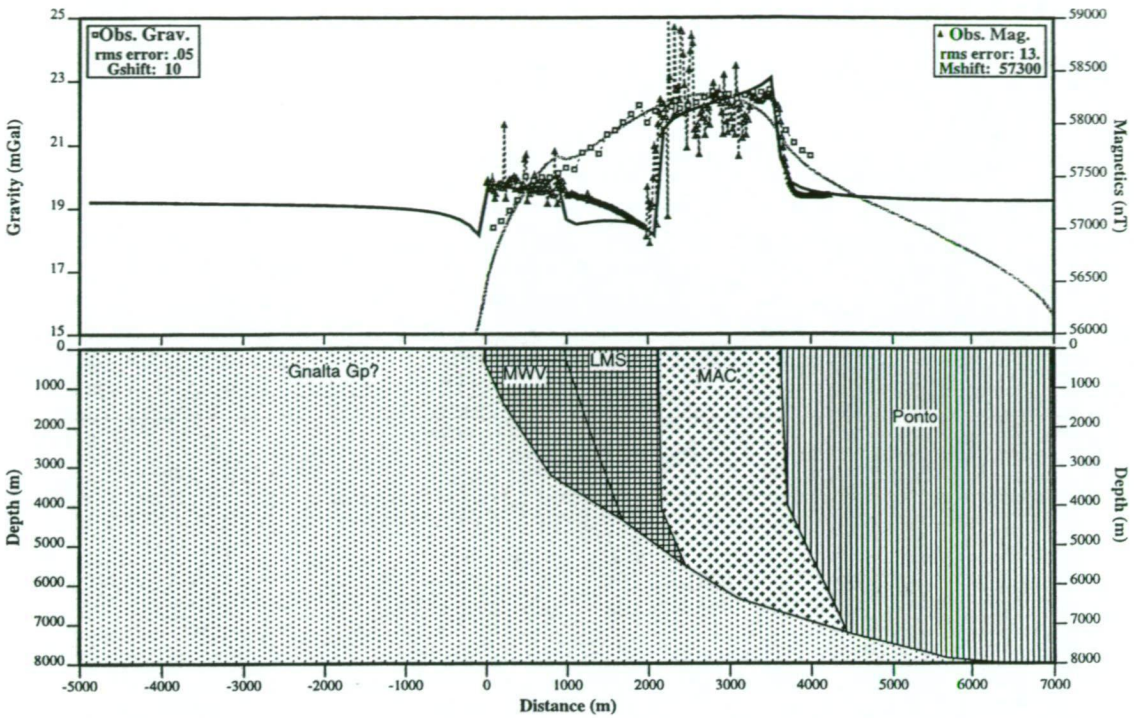


V. E. = 1.5. Key: MWV = Mt Wright Volcanics; LMS = limestone within Mt Wright Volcanics
MAC = serpentinite melange; Ponto = Ponto Complex schists

## Figure 5.9.2 Dip sensitivity of the Macs Tank Complex

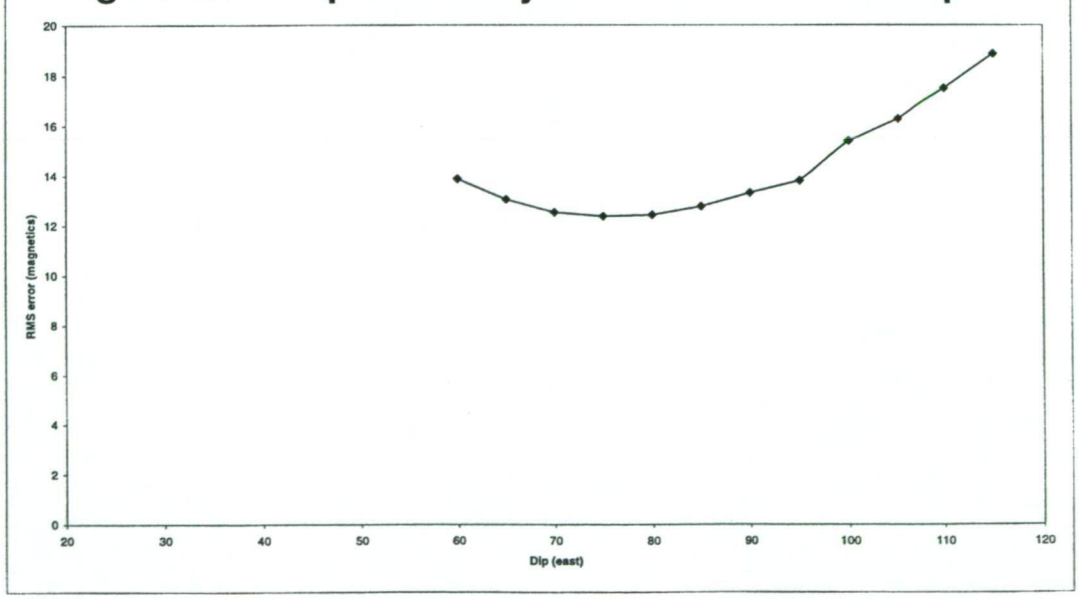

## Figure 5.9.3 Sensitivity of depth to detachment, Mt Wright Fault

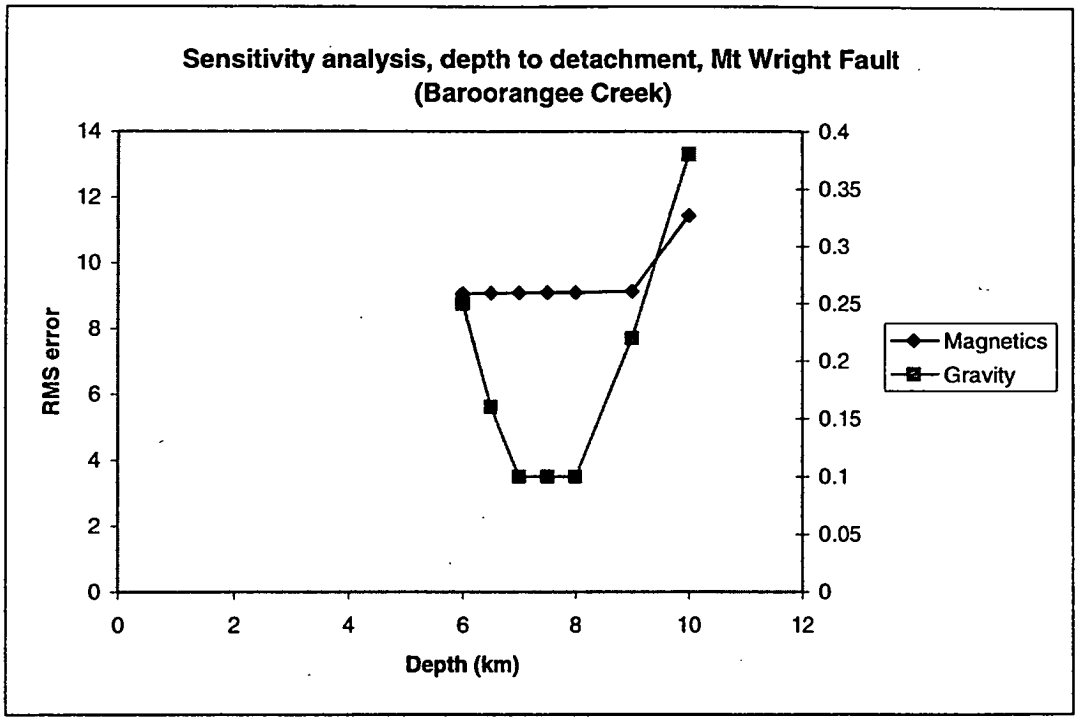


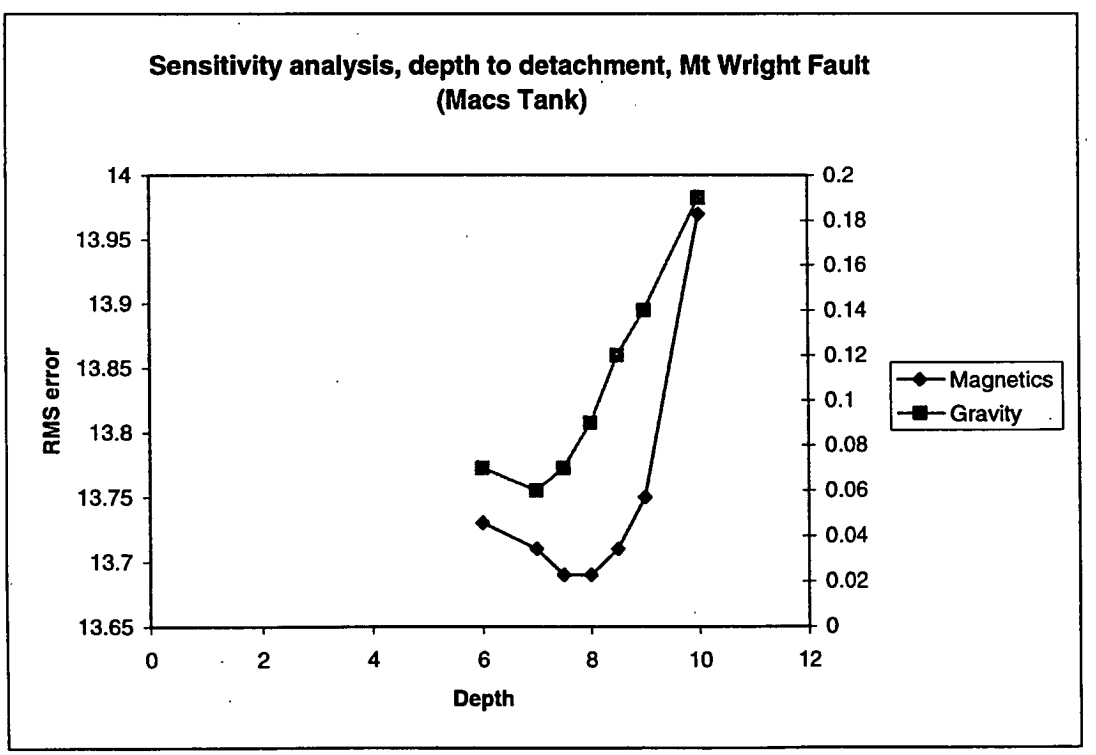

Creek MUMC. West of this lie four imbricate slices of Ponto Complex rocks of the Well Paddock subdomain. These have been attributed decreasing densities away from the fault zone (2.85 t/m$^3$ I; 2.82 t/m$^3$ II; 2.75 t/m$^3$ III; 2.72 t/m$^3$ IV), representing the decrease from amphibolite to middle greenschist grade. Two of the slices are separated by dense (2.85 t/m$^3$) magnetic (0.024 SI) slices interpreted as amphibolitic metabasalt.

*5.9.2 Geochemistry*

The igneous affinities of the Macs Tank and Baroorangee Creek Complex have never been thoroughly investigated. These two complexes are the only rocks of this sort known from the Koonenberry Belt, and it must be more than coincidence that they lie in equivalent structural positions on the Mt Wright Fault. Aside from each other, potential correlates for these bodies within the belt are non-existent, and must be looked for elsewhere in the Lachlan Fold Belt.

Sixteen samples from Macs Tank were prepared for petrographic analysis, including reflected light microscopy. Petrographically, samples from this suite range from upper greenschist grade through to blue hornblende-bearing amphibolites. Most olivine-bearing protoliths have been altered to messy serpentine-talc rock. The most common protolith in the samples gathered was aphyric basalt metamorphosed to greenschist grade (ab-act-epi). Dolerites, retaining ophitic textures and primary cpx-plag-mt mineralogy again with the metamorphic assemblage ab-epi-act, were the next most common. Three samples of serpentinised coarser rocks were found to contain pseudomorphs after the assemblages opx-ol and opx-plag, indicating original harzburgite (9638, 9640) and gabbronorite (9635). A single sample of plagioclase+magnetite-phyric andesite was also described (AJC 140a).

Davidson (1981) described metadolerites as tectonic blocks within a serpentinite matrix at Baroorangee Creek. These blocks occasionally retained some ophitic textures, and original phenocryst phases including cpx (diopside) and plagioclase. These were variably altered up to amphibolite grade, with the assemblage ab-hbl-clz-gt-epi-sp, or greenschist grade (act-epi-ab). Davidson also cites evidence for an overprinting Ca-Al metasomatism developing the assemblage epi-pre-talc-clz. The tectonic matrix at Baroorangee Creek contains the prograde assemblage serp-talc-chl-mt-antigorite-lizardite after tectonised opx+cpx-cumulate protoliths (websterite). This has been overprinted by a late veins containing pre-zeo-qz-clay.

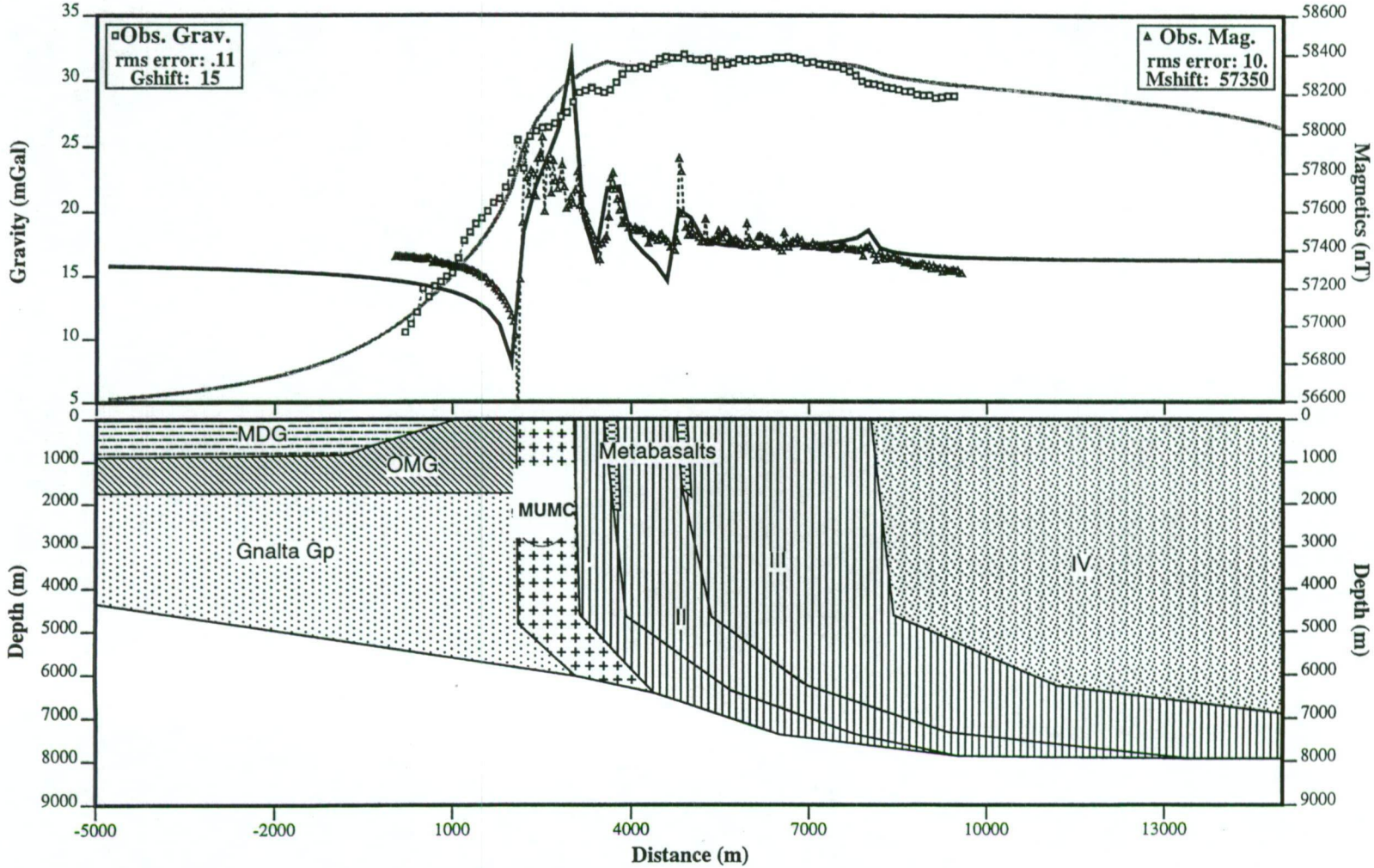


## Figure 5.9.4 2D model, Baroorangee Creek Complex

V.E. = 2.22. Key: MDG = Devonian Mulga Downs Group; OMG = Ordovician Mootwingee Group; MUMC = Baroorangee Creek serpentinite melange (Mafic-Ultramafic Complex); Metabasalts = slices of Ponto Complex metabasalts; Vertical stripe(I-III) = Ponto Complex upper greenschist facies metasediments; IV = Ponto Complex lower greenschist facies metasediments.

This study sampled metabasalt and metadolerite blocks metamorphosed to upper greenschist or amphibolite grade. These sometimes retained primary phenocryst phases including plag, as well as original ophitic and glomeroporphyritic textures. The metamorphic minerals in these blocks include act-chl-epi-clz ± blue-green hbl. This was overprinted by rare quartz-zeolite veins.

Ten samples from Macs Tank and seven from Baroorangee Creek were analysed for major and trace elements using standard whole-rock XRF techniques. Major and trace element data for these rocks are shown in Table 5.9.2. Because of hydrous alteration minerals, the data are recalculated volatile free, with loss on ignition values reported separately. LOI values are surprisingly low (1.5 to 4.1%) for such an altered batch of rocks.

Major oxide data are plotted against MgO (Figure 5.9.5, 5.9.6). Major oxide data show a high degree of scatter, and few discernible magmatic trends due to strong recrystallisation and metasomatism. There is a suggestion of increasing $TiO_2$ with decreasing MgO, which may be indicative of a tholeiitic fractionation trend; however, this must be interpreted carefully in the light of other data.

Immobile trace elements (Zr, Nb, Y) however do show indications of magmatic trends; Nb v MgO shows the data groups as three distinct clusters with increasing Nb as MgO decreases; this may reflect a fractionation trend. Note that Macs Tank appears bimodal, with both quite evolved (MW 137, MW 146) and relatively unfractionated samples. This trend is also displayed in Zr. However, Y appears relatively constant at all MgO levels.

Immobile element plots (Figure 5.9.7) show the coherency of the two MUMC in both Ti and Y versus Zr; the increase in both with Zr probably reflects increasing fractionation at higher Zr contents. A discrimination diagram of Zr/Ti v Nb/Y (after Winchester & Floyd, 1977) shows that the complexes form a coherent sub-alkaline trend.

Metadolerite from Macs Tank (MW135), and metadolerite (MW2) and metabasalt (MW2A) from Baroorangee Creek were analysed for incompatible elements including La, Ce and Nd. N-MORB normalised spidergrams for these rocks(Figure 5.9.8) show quite flat patterns, indicating a depleted mantle source. Elevation in Th, while requiring caution to interpret due to the altered nature of these rocks, may indicate a crustal component. Further support for this hypothesis can be gained by considering a larger data set which omits the LREE and Pb (Figure 5.9.9). Data for 7 samples from Macs

**Baroorangee Ck**

| Sample | MW2di | MW2e | MW2f | MW2l | MW2A | MW2J | MW2 |
|---|---|---|---|---|---|---|---|
| Rock | Amphibolite | Amphibolite | Amphibolite | Amphibolite | metabasalt | metabasalt | metabasalt |
| SiO2 | 44.34 | 50.03 | 49.65 | 49.42 | 49.70 | 48.87 | 48.22 |
| TiO2 | 1.65 | 1.35 | 1.66 | 1.67 | 1.39 | 1.45 | 1.40 |
| Al2O3 | 14.68 | 16.23 | 14.85 | 15.07 | 15.01 | 16.51 | 16.50 |
| Fe2O3 | 11.28 | 9.18 | 11.48 | 11.38 | 10.00 | 10.84 | 9.83 |
| FeO* | 10.15 | 8.26 | 10.33 | 10.24 | 9.00 | 9.75 | 8.85 |
| MnO | 0.24 | 0.19 | 0.19 | 0.19 | 0.18 | 0.18 | 0.20 |
| MgO | 8.36 | 7.28 | 7.43 | 7.27 | 8.03 | 6.51 | 7.11 |
| CaO | 17.71 | 11.32 | 10.18 | 10.72 | 11.38 | 11.31 | 14.00 |
| Na2O | 1.38 | 3.66 | 3.53 | 3.45 | 3.77 | 3.45 | 2.75 |
| K2O | 0.16 | 0.60 | 0.82 | 0.64 | 0.36 | 0.70 | 0.34 |
| P2O5 | 0.21 | 0.15 | 0.20 | 0.19 | 0.17 | 0.17 | 0.14 |
| LOI | 2.66 | 1.31 | 1.31 | 1.14 | 1.11 | 1.49 | 2.51 |
| | | | | | | | |
| Ni | 109 | 141 | 307 | 252 | 286 | 322 | 134 |
| Cr | 218 | 109 | 70 | 78 | 118 | 69 | 140 |
| V | 302 | 275 | 311 | 312 | 278 | 272 | 281 |
| Sc | 48 | 46 | 47 | 47 | 48 | 43 | 33 |
| Zr | 115 | 85 | 119 | 115 | 89 | 98 | 75 |
| Nb | 12 | 9 | 13 | 12 | 11 | 10 | 5 |
| Y | 34 | 30 | 38 | 37 | 29 | 32 | 29 |
| Sr | 201 | 463 | 466 | 332 | 313 | 554 | 570 |
| Rb | 1 | 16 | 20 | 15 | 9 | 16 | 10 |
| Ba | 35 | 587 | 967 | 881 | 312 | 863 | 280 |
| | | | | | | | |
| FeO*/MgO | 1.21 | 1.13 | 1.39 | 1.41 | 1.12 | 1.50 | 1.24 |
| Ti/Zr | 85.64 | 94.92 | 84.03 | 87.01 | 93.65 | 88.96 | 112.00 |
| Nb/Y | 0.37 | 0.30 | 0.34 | 0.33 | 0.38 | 0.31 | 0.17 |

**Table 5.9.2 Whole-rock analyses recalculated volatile-free for the Macs Tank and Baroorangee Creek Mafic-Ultramafic Complexes**

20 Analyses in Table 5.9.2

**Macs Tank**

| Sample | MW113 | MW117 | MW118 | MW120a | MW145 | MW135 | MW124 | MW126 | MW121 | MW123 | MW146 | MW126A | MW137 |
|---|---|---|---|---|---|---|---|---|---|---|---|---|---|
| Rock | Dolerite | Dolerite | Dolerite | Dolerite | Dolerite | Dolerite | Dolerite | Dolerite | metabasalt | metabasalt | Dolerite | metabasalt | Amphibolite |
| SiO2 | 48.80 | 45.62 | 48.77 | 49.04 | 46.98 | 49.68 | 48.33 | 47.96 | 48.47 | 48.13 | 49.35 | 57.05 | 49.09 |
| TiO2 | 1.23 | 1.41 | 1.29 | 1.40 | 1.40 | 1.45 | 1.52 | 1.15 | 1.36 | 1.38 | 1.88 | 2.35 | 1.84 |
| Al2O3 | 15.13 | 13.83 | 15.15 | 14.78 | 14.19 | 14.40 | 14.12 | 16.93 | 15.05 | 14.50 | 15.28 | 14.26 | 14.79 |
| Fe2O3 | 11.35 | 12.66 | 9.22 | 11.78 | 12.42 | 12.85 | 12.99 | 9.84 | 10.55 | 12.17 | 11.38 | 15.36 | 11.72 |
| FeO* | 10.22 | 11.39 | 8.30 | 10.60 | 11.17 | 11.57 | 11.69 | 8.85 | 9.49 | 10.96 | 10.24 | 13.82 | 10.54 |
| MnO | 0.18 | 0.21 | 0.09 | 0.19 | 0.21 | 0.21 | 0.20 | 0.16 | 0.13 | 0.22 | 0.19 | 0.04 | 0.17 |
| MgO | 8.14 | 9.08 | 9.40 | 7.57 | 8.20 | 7.87 | 9.24 | 8.67 | 9.64 | 8.35 | 6.28 | 0.19 | 7.02 |
| CaO | 11.62 | 15.33 | 11.46 | 12.23 | 14.20 | 8.60 | 9.53 | 11.02 | 11.04 | 12.18 | 10.65 | 1.73 | 10.88 |
| Na2O | 2.87 | 1.48 | 4.24 | 2.44 | 1.95 | 3.70 | 3.67 | 3.83 | 3.53 | 2.64 | 4.33 | 7.45 | 3.83 |
| K2O | 0.49 | 0.24 | 0.18 | 0.42 | 0.30 | 1.11 | 0.27 | 0.32 | 0.09 | 0.31 | 0.37 | 0.43 | 0.43 |
| P2O5 | 0.18 | 0.15 | 0.18 | 0.15 | 0.14 | 0.14 | 0.14 | 0.11 | 109.35 | 110.83 | 0.29 | 1.13 | 0.24 |
| LOI | 2.85 | 3.58 | 2.46 | 1.5 | 3.24 | 2.55 | 4.12 | 1.52 | | | 1.11 | 0.79 | 0.71 |
| | | | | | | | | | 1.02 | 2.83 | | | |
| Ni | 212.7 | 193.2 | 228.2 | 73 | 102.5 | 93.1 | 168 | 200 | 189 | 83 | 50.3 | 3.9 | 91 |
| Cr | 266.1 | 237.1 | 363.5 | 216 | 226.1 | 193 | 229.5 | 413.8 | 329 | 233 | 48.2 | 2.2 | 66 |
| V | 266.8 | 318.4 | 230.8 | 289 | 309.4 | 302.4 | 320.1 | 244.3 | 244 | 318 | 302.9 | 46.8 | 324 |
| Sc | 37.8 | 47.3 | 38.3 | 39 | 45 | 41.4 | 45.1 | 42.2 | 39 | 44 | 42.2 | 14.5 | 45 |
| Zr | 70.1 | 88.3 | 96.8 | 101 | 86.8 | 90.5 | 94.7 | 73.2 | 90 | 89 | 145.4 | 406.7 | 130 |
| Nb | 1.9 | 1.8 | 4.9 | 3.0 | 1.8 | 1.6 | 2.3 | 2 | 3.1 | 2.3 | 20.3 | 53.8 | 18.1 |
| Y | 29.1 | 37 | 34 | 36 | 35.8 | 33.7 | 35.4 | 29.7 | 34 | 35 | 37.8 | 64.6 | 41 |
| Sr | 250.1 | 238 | 392.4 | 288 | 488.1 | 578.5 | 344.6 | 221.5 | 346 | 654 | 273.8 | 127.1 | 255 |
| Rb | 16.1 | 9.8 | 2.4 | 37 | 14.1 | 31.4 | 15.1 | 7.8 | 1 | 25 | 5.7 | 7.6 | 13 |
| Ba | 1101.9 | 874.3 | 330.8 | 571 | 923.7 | 334.5 | 746.9 | 308.7 | 284 | 923 | 194.4 | 59.2 | 203 |
| | | | | | | | | | | | | | |
| FeO*/MgO | 1.26 | 1.25 | 0.88 | 1.40 | 1.36 | 1.47 | 1.27 | 1.02 | 0.99 | 1.31 | 1.63 | 72.14 | 1.50 |
| Ti/Zr | 105.07 | 95.71 | 80.14 | 83.10 | 96.55 | 95.95 | 96.45 | 94.47 | 90.26 | 92.71 | 77.69 | 34.63 | 84.50 |
| Nb/Y | 0.07 | 0.05 | 0.14 | 0.08 | 0.05 | 0.05 | 0.06 | 0.07 | 0.09 | 0.06 | 0.54 | 0.83 | 0.44 |

**Table 5.9.2 Whole-rock analyses recalculated volatile-free for the Macs Tank and Baroorangee Creek Mafic-Ultramafic Complexes** (cont.)

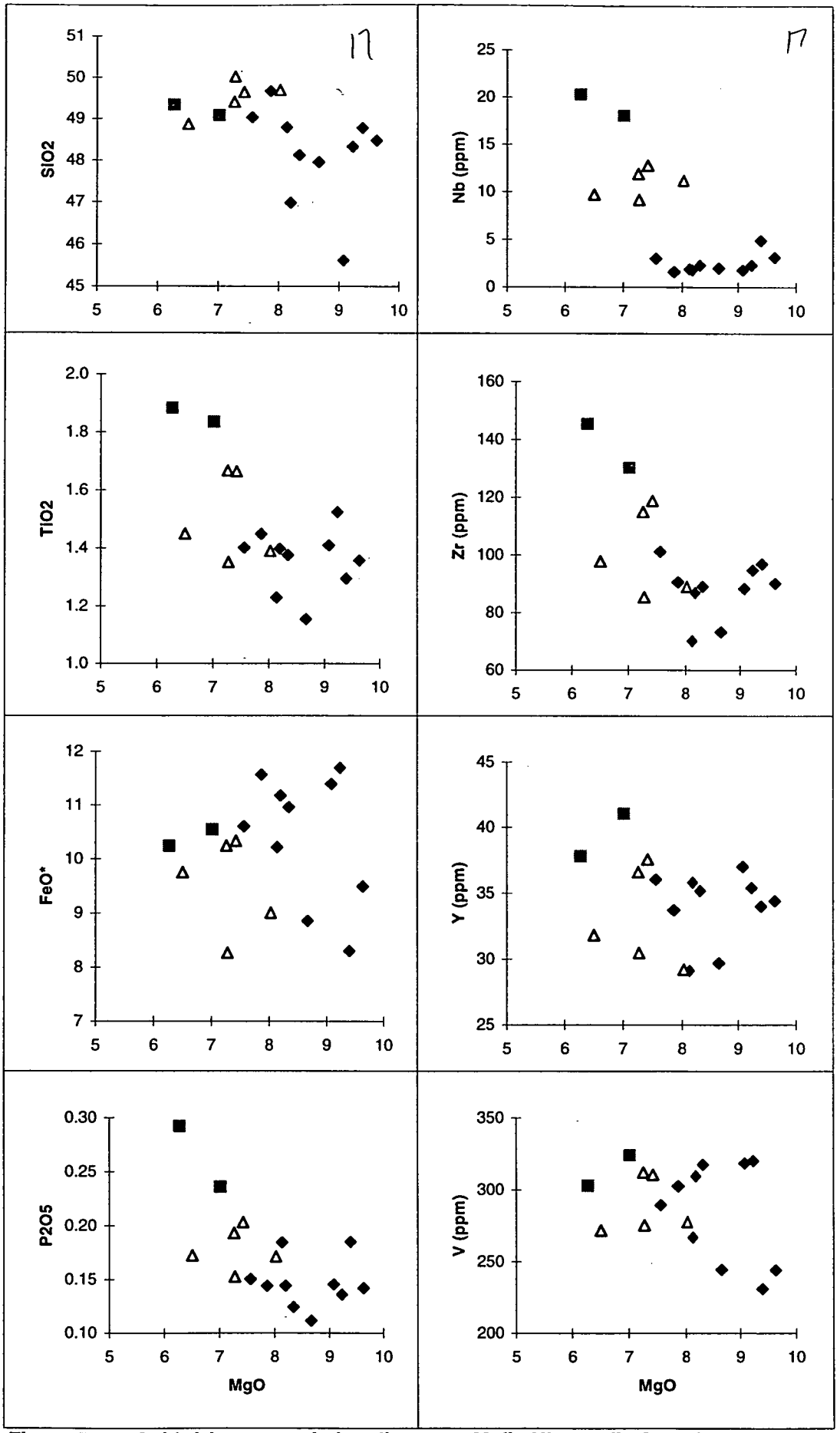


**Figure 5.9.5 Oxide/element variation diagrams, Mafic-Ultramafic Complexes**
squares = Macs Tank evolved; triangles = Baroorangee Creek; diamonds = Macs Tank

**Samples MW2 & MW2di have been omitted due to higher LOI

**Sample MW126a = trachyte, not metabasalt

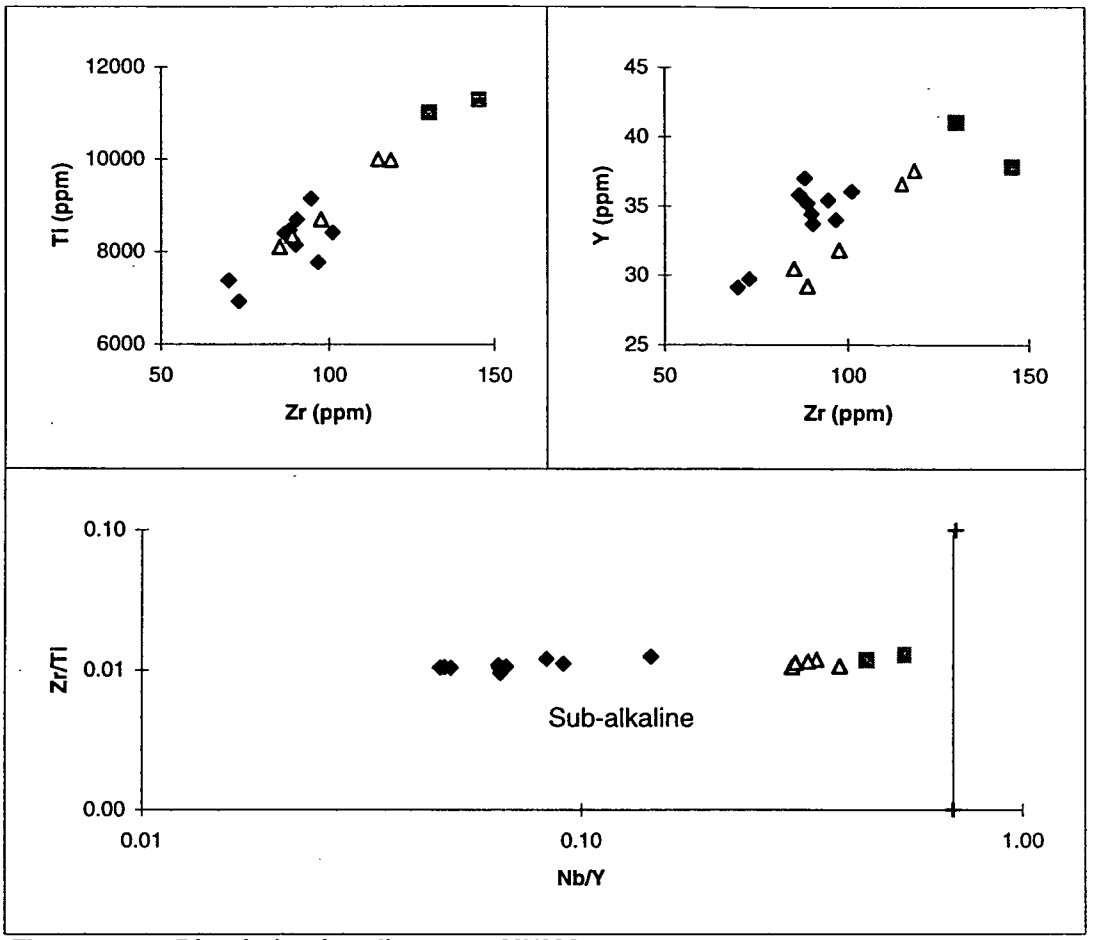


**Figure 5.9.6 Discrimination diagrams, MUMC**
Symbols as for Fig.5.9.5

**Figure 5.9.7 N-MORB normalised spidergram, Mafic-Ultramafic Complexes, Mt Wright Fault**
(normalising data from Sun & McDonough, 1989)

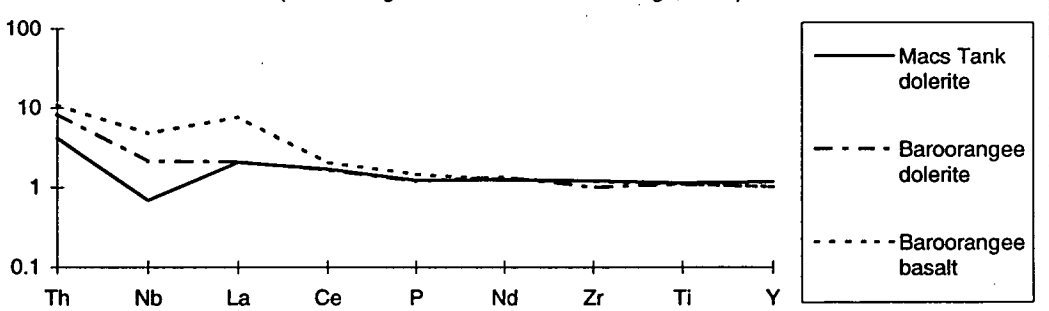


**Figure 5.9.8 N-MORB normalised incompatible element diagram, MUMC, Mt Wright Fault**

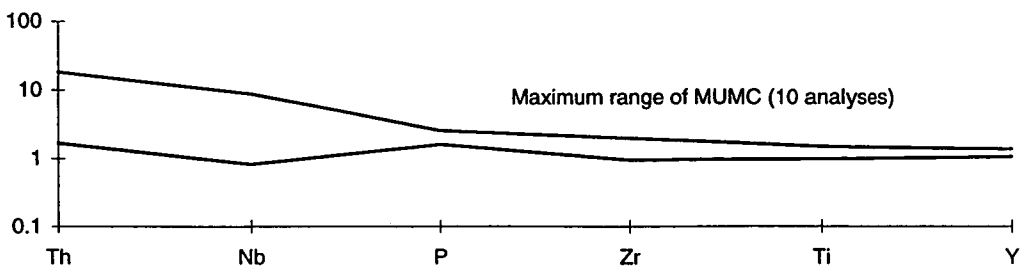

Tank and 3 samples for Baroorangee Creek show coherent flat patterns in most elements, again with elevated Th. The order of magnitude variation in Nb is still quite low (1 to 10 ppm), and reflects fractionation.

*5.9.3 Summary*

The Macs Tank and Baroorangee Creek Mafic-Ultramafic Complexes are serpentinite melanges with block-in-matrix character. Tectonic inclusions include metabasalt and metadolerite, as well as ultramafic meta-websterites and metaharzburgites. Analyses of greenschist and amphibolite grade mafic blocks from both complexes show a surprising coherency in terms of magmatic origin. These blocks appear to represent a tholeiitic suite derived from a MORB-like source.

Inclusions within the two MUMC closely match the chemistry of igneous rocks of the Ponto Complex (Zhou, 1993) which crop out to the north, south and east of both complexes.

*5.9.4 Chromite Geochemistry*

Samples of serpentinised ultramafic rocks collected from the Macs Tank Complex contain chromite phenocrysts. These occur in a serpentine-magnetite matrix within relict metaharzburgites.

Polished thin sections of samples containing chromites from both complexes were analysed for major oxide compositions using the University of Tasmania's Cameca SX-50 electron microprobe. Results for a suite of major oxides from individual spinels are shown in Table 5.9.3 and Figure 5.9.9.

Samples 124A and 126 from Macs Tank samples display two populations, with Cr# (= 100.Cr/[Cr+Al] atomic) between 39 and 56 (Figure 5.9.9 A). Spinels from a metaharzburgite from Macs Tank, and serpentinite from Baroorangee Creek were found to be too altered, with virtually all $Cr_2O_3$ replaced by $Fe_2O_3$, and will not be discussed further.

The range of both Cr# populations is indicative of equilibrium with a moderately refractory peridotite source, either in a MOR setting, where spinels typically have Cr# values of 10-60, or in a backarc setting where Cr# in spinel has a more limited range of 40-60 (Arai, 1994). Low $TiO_2$ (<1 wt%, Figure 5.9.9 B) may also be indicative of a

| Grain | 126 3-1 | 126 3-2 | 126 3-3 | 126 3-4 | 126 3-5 | 124A 1-1 | 124A 1-2 | 124A 1-3 | 124A 2a-1 | 124A 2a-2 | 124A 2a-3 | 124A 2b-1 | 124A 2b-2 |
|---|---|---|---|---|---|---|---|---|---|---|---|---|---|
| MgO | 1.78 | 2.06 | 1.67 | 1.67 | 1.75 | 1.48 | 1.41 | 1.35 | 1.23 | 1.25 | 1.11 | 1.20 | 1.37 |
| Al2O3 | 28.80 | 27.62 | 28.91 | 28.91 | 29.07 | 24.99 | 25.15 | 25.20 | 23.22 | 23.29 | 22.82 | 24.16 | 24.12 |
| SiO2 | 0.23 | 1.08 | 0.34 | 0.08 | 0.29 | 0.12 | 0.09 | 0.09 | 0.09 | 0.10 | 0.13 | 0.13 | 0.15 |
| TiO2 | 0.09 | 0.05 | 0.11 | 0.06 | 0.15 | 0.20 | 0.22 | 0.27 | 0.28 | 0.29 | 0.33 | 0.21 | 0.24 |
| Cr2O3 | 31.98 | 31.83 | 31.94 | 32.18 | 31.85 | 35.79 | 35.16 | 34.64 | 36.90 | 36.06 | 37.08 | 36.36 | 36.18 |
| MnO | 1.68 | 1.59 | 1.44 | 1.59 | 1.35 | 1.63 | 1.42 | 1.46 | 1.57 | 1.51 | 1.93 | 1.57 | 1.43 |
| FeO* | 35.57 | 34.59 | 35.65 | 34.80 | 35.77 | 36.02 | 36.27 | 36.35 | 37.22 | 37.12 | 36.81 | 36.39 | 36.65 |
| Fe2O3 | 3.21 | 2.02 | 2.67 | 2.60 | 2.79 | 3.80 | 3.91 | 4.00 | 4.81 | 4.93 | 4.63 | 3.87 | 4.18 |
| FeIIO | 32.68 | 32.78 | 33.24 | 32.47 | 33.26 | 32.60 | 32.76 | 32.75 | 32.89 | 32.69 | 32.65 | 32.91 | 32.89 |
| Mg# | 8.88 | 10.10 | 8.26 | 8.40 | 8.61 | 7.49 | 7.13 | 6.86 | 6.28 | 6.38 | 5.75 | 6.13 | 6.92 |
| Fe# | 91.12 | 89.90 | 91.74 | 91.60 | 91.39 | 92.51 | 92.87 | 93.14 | 93.72 | 93.62 | 94.25 | 93.87 | 93.08 |
| Cr# | 42.68 | 43.60 | 42.56 | 42.75 | 42.36 | 49.00 | 48.40 | 47.97 | 51.60 | 50.95 | 52.15 | 50.24 | 50.16 |

| Grain | 124A 2b-3 | 124A 2c-1 | 124A 2c-2 | 124A 2c-3 | 124A 3-1 | 124A 3-2 | 124A 3-3 | 124A 3-4 | 124A 3-5 | 124A 4-1 | 124A 4-2 |
|---|---|---|---|---|---|---|---|---|---|---|---|
| MgO | 1.22 | 1.09 | 1.05 | 1.04 | 1.67 | 1.64 | 2.15 | 1.63 | 1.46 | 0.82 | 0.87 |
| Al2O3 | 23.12 | 23.22 | 22.40 | 22.77 | 30.39 | 29.69 | 28.27 | 30.74 | 29.80 | 21.01 | 20.80 |
| SiO2 | 0.14 | 0.14 | 0.15 | 0.13 | 0.08 | 0.77 | 1.70 | 0.06 | 0.03 | 0.02 | 0.12 |
| TiO2 | 0.29 | 0.32 | 0.41 | 0.37 | 0.05 | 0.09 | 0.08 | 0.08 | 0.12 | 0.37 | 0.31 |
| Cr2O3 | 36.53 | 35.97 | 36.27 | 36.04 | 30.11 | 29.65 | 30.44 | 29.88 | 31.23 | 38.34 | 39.09 |
| MnO | 1.62 | 1.99 | 1.71 | 2.11 | 1.61 | 1.93 | 1.77 | 1.49 | 1.64 | 1.95 | 1.85 |
| FeO* | 36.68 | 37.59 | 37.95 | 37.80 | 35.67 | 35.81 | 34.43 | 35.96 | 36.16 | 37.09 | 37.13 |
| Fe2O3 | 4.51 | 5.39 | 5.57 | 5.73 | 3.23 | 2.79 | 1.17 | 3.19 | 3.25 | 5.10 | 4.87 |
| FeIIO | 32.62 | 32.74 | 32.94 | 32.65 | 32.76 | 33.30 | 33.38 | 33.08 | 33.24 | 32.50 | 32.74 |
| Mg# | 6.28 | 5.59 | 5.37 | 5.38 | 8.37 | 8.11 | 10.33 | 8.09 | 7.26 | 4.34 | 4.52 |
| Fe# | 93.72 | 94.41 | 94.63 | 94.62 | 91.63 | 91.89 | 89.67 | 91.91 | 92.74 | 95.66 | 95.48 |
| Cr# | 51.45 | 50.96 | 52.07 | 51.50 | 39.93 | 40.11 | 41.94 | 39.46 | 41.28 | 55.04 | 55.77 |

**Table 5.9.3 Major oxide data for spinels, Macs Tank Mafic-Ultramafic Complex**
FeII and FeIII are recalculated stoichiometrically
#'s are atomic ratios

**Figure 5.9.9 Discriminant diagrams for Cr-spinels, Macs Tank MUMC**

A

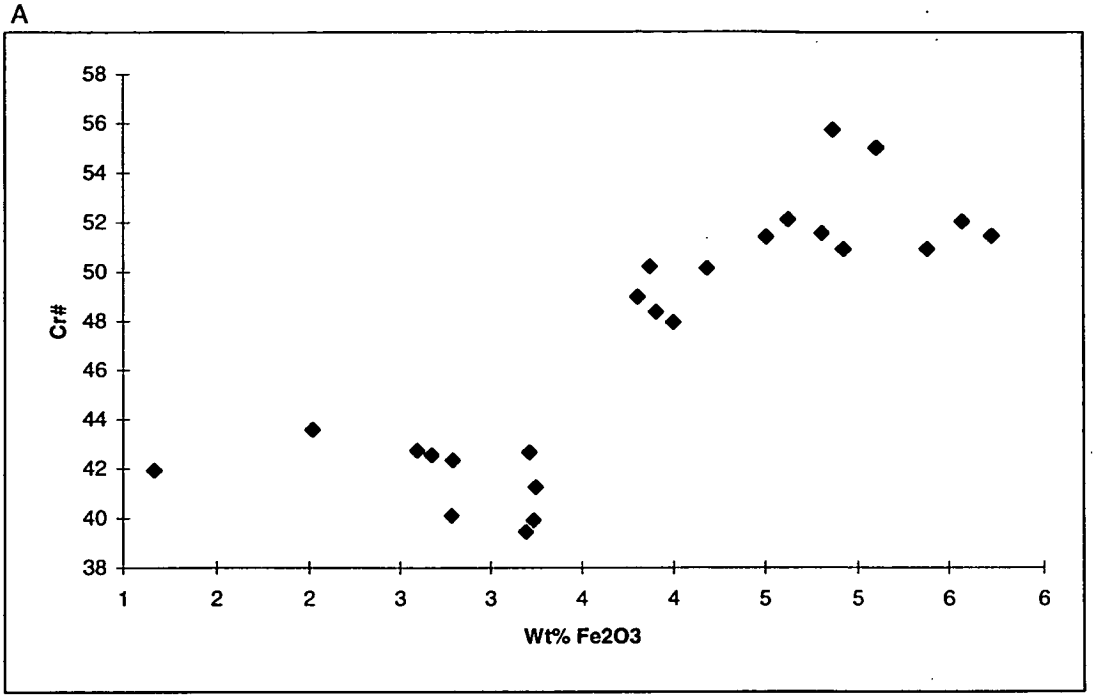


B

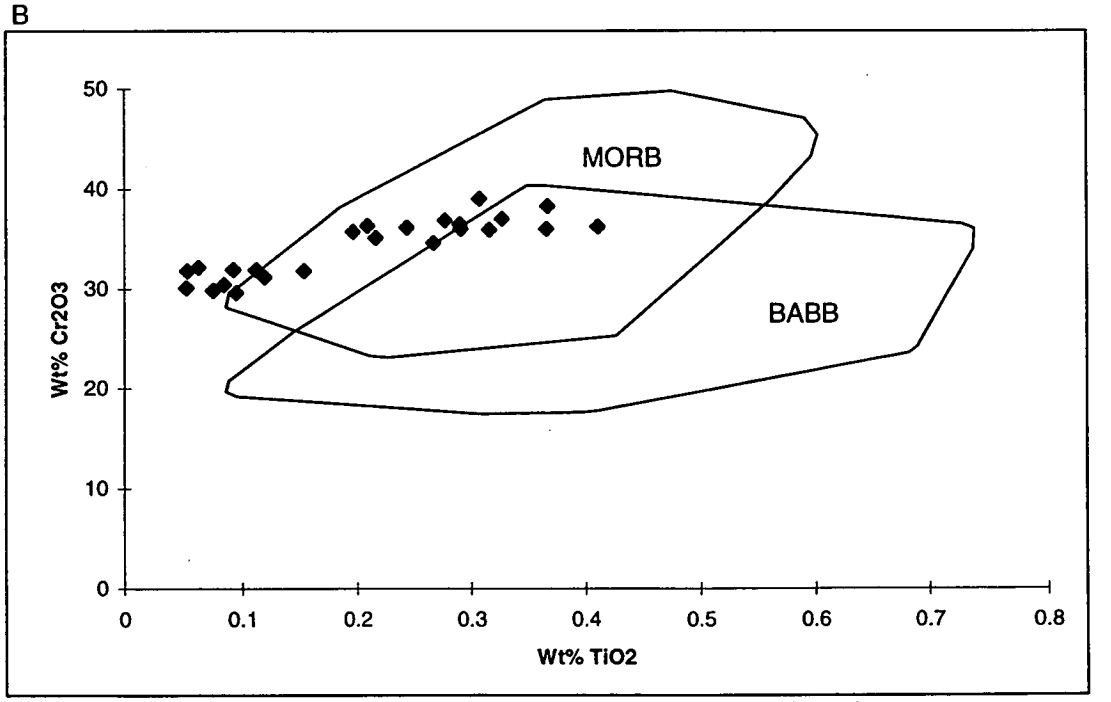


Fields are 95% of data from Crawford & Kamanetsky (unpublished data).

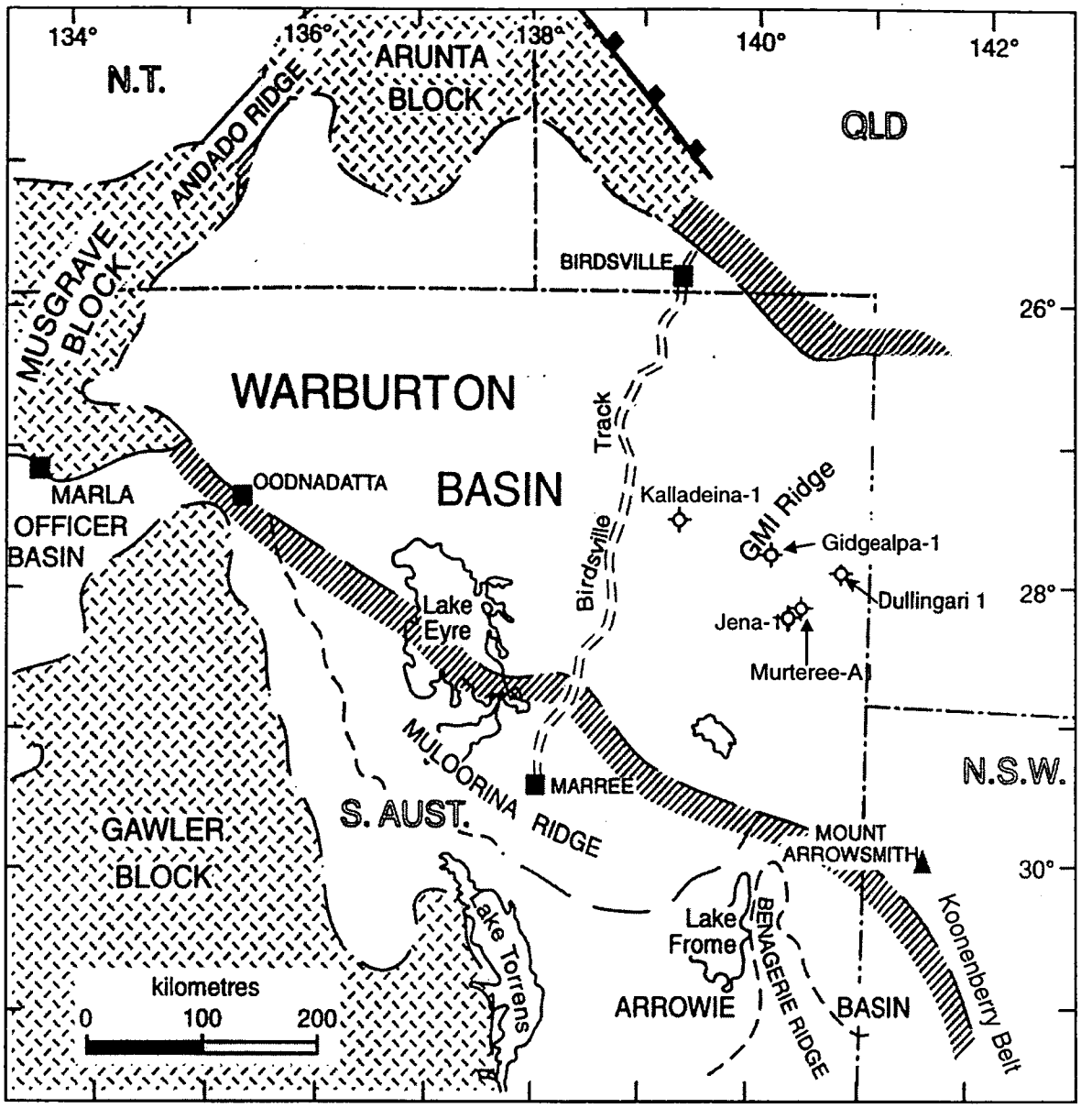


**Figure 5.10.1 Locality Map. Warburton Basin.**
(modified from Sun, 1996)

MOR setting (Allan et al., 1988). Figure 5.9.9 B shows that spinel compositions from Macs Tank overlap with the field of spinel compositions from MOR peridotites at a variety of locations

The Macs Tank samples are unlikely to be derived from a boninitic peridotite source as the Cr# values are too low; boninitic spinels typically attain Cr# values of > 80 (Roeder, 1994); similarly, a subcontinental peridotite source is ruled out because the values are much higher than the typically < 20 Cr# of spinels from this setting (Arai, 1994).

A backarc environment of intrusion of these rocks strengthens the correlation of parts of the Macs Tank Complex with the Ponto Complex (cf. Zhou & Mills, 1994) rather than the alkaline MAV or calc-alkaline MWV (Crawford et al., 1997).

*5.9.5 Tectonic Interpretation of the MUMC- Ponto Complex at Mt. Wright*

The Ponto Complex-MUMC on the Mt Wright Fault are best interpreted as a fragment of oceanic crust, possibly from a backarc or marginal basin setting. This fragment appears to have been overthrust from east to west as a leading imbricate fan. It is likely that this event was coincident with the development of broken formation in the Gnalta Group, which probably represents a continental shelf carbonate-clastic wedge (Mills, 1992).

The timing of emplacement of the Ponto Complex and MUMC at the Mt Wright Fault is constrained by relative dates and SHRIMP zircon U-Pb dating on several key units. The Ponto Complex has not been dated in the Cymbric Vale area. However, dates have been obtained using the SHRIMP U-Pb method at Grasmere prospect, 35 km to the east. These dates form a cluster around 500 Ma (506 ± 8 Ma; 501 ± 9 Ma; 497 ± 8 Ma: BHP Minerals Exploration, unpublished data). Using the AGSO timescale (Laurie & Young, 1996), these dates fall in the Late Cambrian (Undillan to Mindyallan) and give the earliest possible age for deformation.

Deposition of the Mootwingee Group, which unconformably overlies the imbricated "Wilandra beds" at Bald Hill (639000 mE 6543500 mN), commenced in the Late Cambrian (Payntonian) (Shergold, 1971), giving a minimum age for the termination of the deformation event.

These events constrain the timing of the formation of F1 structures in the Ponto Complex. This deformation event must post-date deposition of the Ponto Complex

(post-Mindyallan) and be pre-Payntonian. This limits the deformation to the Iverian and/or Idamean stages (497.5 Ma to 492.5 Ma, after Shergold, 1995).

## 5.10 The Warburton Basin: a less-deformed analogue of the Gnalta Group?

### *5.10.1 Introduction*

In 1964, some 3 years after the discovery of the Cymbric Vale faunas, Delhi-Santos drilled the Gidgealpa -1 well through the Permian sediments of the Cooper Basin into a Cambro-Ordovician infra-basin. This well in the far north-eastern corner of South Australia (Figure 5.10.1) intersected an essentially flat-lying sequence of interbedded sandstone, siltstone, carbonates and volcanics (Gatehouse, 1986).

Daily (1964) listed a rich fossil fauna from these rocks ranging in age from the early Middle Cambrian to Payntonian-Datsonian (=Latest Cambrian). Up to 150 subsequent wells penetrating the Warburton Basin allowed Gatehouse (1983, 1986) and subsequently Sun (1996) to define the stratigraphy (Figure 5.10.2).

Dullingari Group: Early to early Late Ordovician graptolitic shales + Innamincka Red beds
(unconformity)
Kalladeina Formation (1658m): Middle to Late Cambrian mixed sequence including acid volcanics cf. Coonigan Formation)
Mooracoochie Volcanics (1000+m): pre-Middle Cambrian acid calc-alkaline rift volcanics
(fault or unconformity)
Murteree-Jena Volcanics (this study): ?Late Neoproterozoic alkaline rift volcanics

### *5.10.2 Correlations*

Gatehouse (1986) correlated the lower Kalladeina Formation. with the upper parts of the Coonigan Formation at Mt Wright, on the basis of similar age (Ordian-Templetonian) and faunal assemblages.

The Kalladeina Formation overlies the pre-early Middle Cambrian Mooracoochie Volcanics. These are a sequence of tuffs, lapilli tuffs, agglomerates, trachytes, dacites, rhyodacites and rhyolites over 1000 m in thickness. Geochemical data presented in Gatehouse (1986) suggest a correlation with the MWV (*sensu* Crawford et al.1997),

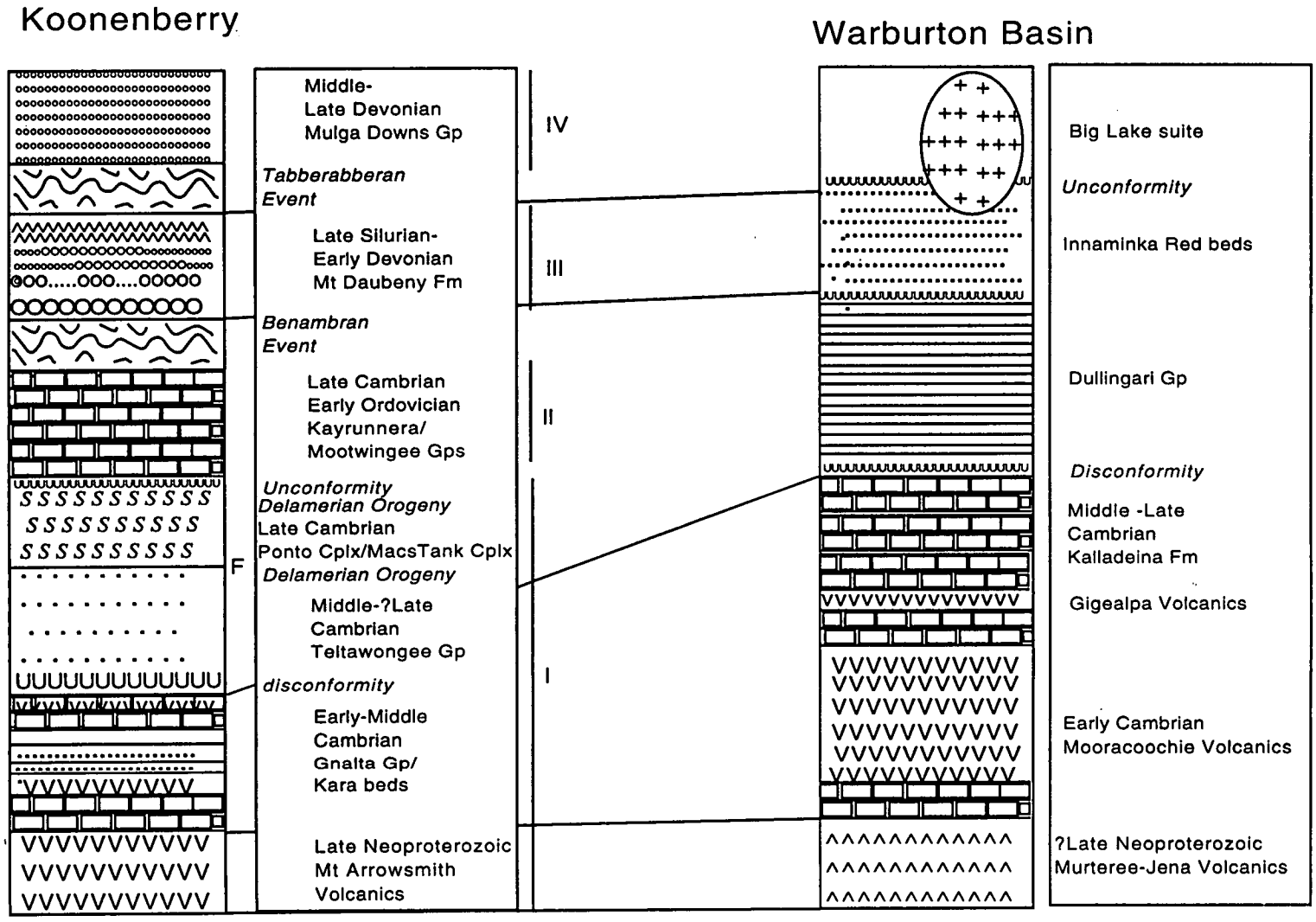


**Figure 5.10.2 Comparative Stratigraphy and correlations, Koonenberry FTB and Warburton Basin**
(Warburton data from Gatehouse, 1986; Sun, 1996; this study)

although these rocks are more likely to be related to calc-alkaline rifting rather than a magmatic island arc (Crawford et al., 1997).

The stratigraphic thicknesses for the Mooracoochie Volcanics compare favourably with the somewhat dubious thicknesses for the MWV-Cymbric Vale Formation. Leaving out Warris' (1967) upper and lower sections of the MWV which have been struck down, the thickness the MWV at Mt Wright is 2134 m. This figure can be considered indicative only, as dismemberment may have repeated or removed parts of the sequence. Nevertheless, this figure is of the same order as the 1000+ m quoted by Gatehouse (1986) for the Mooracoochie Volcanics. However, the stratigraphic thickness of the Kalladeina Formation (minimum 906 m, max. 1658 m) does not compare well with the abbreviated Coonigan Formation (113 m).

As shown in section 5.6, basaltic volcanics from the Murteree A1 and Jena wells are best geochemically correlated with the MAV, which have a Late Neoproterozoic age (Crawford et al., 1997). These volcanics have no biostratigraphic control (Sun, 1996), but were believed to be at least as old as Early Cambrian (Boucher, 1994).

In general, the thicknesses of the Warburton Basin sediments were emphasised as being close to true thicknesses by Gatehouse (1986), with near-horizontal dips broken by normal faults and possible "gentle" folds. Although the deformation of the Middle Cambrian Warburton section is not severe, Wopfner (1966) records a stratigraphic break between the Late Cambrian and Early Ordovician sequences, as at Mt Wright; this was interpreted by Wopfner (1966) and Roberts et al. (1990) as evidence of the Delamerian Orogeny.

The Ordovician Dullingari Formation is more deformed than the beds beneath, having steep dips and a cleavage: this relationship has not been satisfactorily explained in Gatehouse (1986) and indicates thrusting of the younger rocks over the older. Thrusts within the Kalladeina Formation are evident in seismic sections presented in Roberts et al. (1990) and from biostratigraphic repetitions (Daily *in* Gatehouse, 1986), and is clearly of post-Early Ordovician age. This disqualifies the thrusting from being Delamerian.

### *5.10.3 Structure*

Sun (1996) described four styles of thrust-related deformation in seismic records. These were zones of severe faulting and folding; zones of reverse, wrench and high

angle faults with pop-up blocks; ramp and imbricate thrust faulted domains; and areas with tight to gentle folds. Roberts et al. (1990) also demonstrated low angle overthrusting in seismic section.

Aspects of the thrust systems within the Warburton Basin have much in common with those inferred within the Mt Wright-Cymbric Vale area. These include episodic reactivation (cf. Mt Wright and Lawrence Faults); leading imbricate fan geometry; and internal and external nappe and horse development (after Sun, 1996). The main differences between the two areas are the north-east trend of the main Warburton structures, and the intensity of metamorphism, folding and faulting in the Mt Wright-Cymbric Vale area.

### *5.10.4 Timing of Deformation*

Timing of deformation within the Warburton Basin is coarsely controlled by biostratigraphic means. The involvement of the Early Ordovician "Innamincka Red beds" and the erosion of all thrusted packages under an Early Carboniferous unconformity constrains the major deformation to the Late Ordovician through to the Late Devonian (after Sun, 1996). It is likely that this correlates with the Silurian event recognised in the Mt Wright area and elsewhere in the Koonenberry Belt as proposed by Gatehouse (1986) and Wopfner (1972). Importantly, there appears to be no tectonic evidence of a Late Cambrian deformation other than a hiatus in sedimentation (Gatehouse, 1986); in addition delicate Early and Middle Cambrian body fossils are preserved in many parts of the sequence.

### *5.10.5 Implications*

The similarities and differences between the Warburton Basin and the Mt Wright area have important ramifications for the tectonic interpretation of both areas. The similarity in ?Late Neoproterozoic to Middle Cambrian igneous suites implies two areally extensive phases of rifting (Crawford et al., 1997). The present dimensions of this rift basin system covers a width of 200 km (Benagerie Ridge to Koonenberry Fault) across 4.5° of latitude (Figure 5.10.1); this does not take into account additional original width shortened during the Late Cambrian and Silurian, which implies an even broader rift system.

Sun (1996) interpreted the more extensive Middle Cambrian of the Warburton Basin as shelf-edge, slope and deep water basinal environments. This interpretation is

consistent with interpretation of the Pincally, Wydjah Formations, and the Wyarra Shale at Mt Arrowsmith, as well as the Coonigan Formation and suggests that the basin was open to the ocean. This implies that the Late Neoproterozoic to Late Middle Cambrian represents a sector of the multiply-rifted passive continental margin of Gondwana.

The association of significant volumes of early alkaline rift volcanics and later calc-alkaline rift volcanics with passive margin-style sedimentation above and below reflects multiple rifting. Initial rifting and breakup with development of transitional alkali seaward dipping reflector sequences (SDRS) (Mutter, 1985) with passive margin formation appears to have occurred between at 600 Ma and c.580 Ma. The margin so-formed remained passive until subsequent secondary rifting at 525 Ma to form either a backarc or marginal basin. The initial rifting with large volumes of mafic volcanics in SDRS is analogous to the Palaeogene North Atlantic Norwegian margin (ODP Leg 104: Viereck et al., 1988; Eldholm et al., 1989), whereas the formation of a marginal or backarc basin on a previous passive margin is analogous to the present Eastern Australian margin (Bryan et al., 1997) or Neogene Sardinian passive margin (Beccaluva et al., 1990). This sequence of margin development was proposed by Direen & Crawford (1998a). More evidence, particularly from outside the Mt Wright-Cymbric Vale area is required to validate this hypothesis.

### 5.11 Summary

This chapter set out to address the following questions:
*What are the affinities and correlations of the Wilandra beds?*
*What is the significance of the Macs Tank and Baroorangee Creek Mafic-Ultramafic Complexes?*
*Is the Gnalta Group a coherent stratigraphic unit?*
*And, is the Gnalta Group an integral part of the Koonenberry Belt, or allochthonous; and what is its tectonic setting?*

Again, a combination of geophysics, mapping, and geochemistry has been applied to the resolution of these problems. The following solutions have been suggested.

The Wilandra beds, an informal stratigraphic unit, are a series of imbricated slices of Late Neoproterozoic and Early Cambrian volcanic and sedimentary rocks belonging to the Mt Arrowsmith Volcanics, Kara beds and Gnalta Group. These rocks have been caught up in Late Cambrian-pre-Ordovician deformation, possibly as a nappe or

backthrust slice. It is therefore recommended that the use of the term "Wilandra beds" cease.

Mafic-Ultramafic Complexes on the Mt Wright Fault are serpentinite melanges that have greatest affinity with the Late Cambrian Ponto Complex. West-directed thrusting of this package up the Mt Wright Fault in the Iverian-Idamean (Latest Cambrian) led to the development of these melanges, incorporating igneous rocks from both the upper plate (Ponto Complex) and lower plate (Mt Wright Volcanics / Mt Arrowsmith Volcanics). In general tectonic terms, the overthrust plate has a strong E-MORB affinity and may represent a fragment of a backarc or marginal basin.

In response to this deformation event, the Gnalta Group appears to have developed into a zone of broken formation and sediment melange. This is particularly evident in the incompetent Coonigan Formation at the top of the sequence. The more competent Mt Wright Volcanics and Cymbric Vale Formation have formed a series of rigid blocks which were reorganised into a regional north-northwest grain during subsequent Silurian deformation.

The Gnalta Group has strong similarities in age, facies, tectonic history and Silurian structural style to the weakly-deformed, better-studied Warburton Basin of inland South Australia. It is likely that the two regions once formed part of a continuous basin system linked through the Mt Arrowsmith inlier. This argues strongly against the Gnalta Group being an exotic terrane as proposed by Leitch et al. (1978). Early-Middle Cambrian deep water turbiditic sediments such as the Teltawongee Group are not known from the Warburton Basin. This may suggest either of two solutions to the problem of the Teltawongee / Gnalta Group relationship: either Mills (1992) is correct and the Teltawongee Group represents abyssal plain and continental rise sedimentation in relation to the continental shelf sedimentation of the Gnalta Group; or the Teltawongee Group is allochthonous with respect to the Gnalta Group. In the first case, interfingering facies relationships could be prevented by having a rim or topographic plateau at the shelf-slope break (cf. Western Australian passive margin bathymetry, Veevers & Cotterill, 1978). Either interpretation is currently allowed on the data.

Like the Nundora-Wonnaminta-Marrapina-Nuntherungie region to the north, the Mt Wright-Cymbric Vale area preserves elements of a Late Neoproterozoic-Middle Cambrian passive margin, including shelf environments, and an allochthonous Late Cambrian volcanosedimentary sequence. The latter formed part of a collider in the

Iverian-Idamean stages of the Late Cambrian. This collision event led to strong disruption of both the passive margin and collider, although with strongly contrasting deformation style across the Mt Wright Fault Zone.

**Chapter 6: Grasmere Area and Southern Koonenberry Bend Zone**

# Chapter 6: Grasmere Area and Southern Koonenberry Bend Zone

## 6.1 Study area defined. Reasons for study.

The Grasmere-Southern Koonenberry zone is situated within the Grasmere 7435, Nuchea 7335 and Bunda 7434 1: 100 000 map sheets, in an area defined by the AMG Zone 54 coordinates 640000-673000 mE and 6493000-6550000 mN (Figure 6.1.1)

The area was selected for study because it contains two 90° strike changes in magnetic and gravity trends (Figure 6.1.2), observable at continental scale, reflecting some large-scale tectonic process that is yet to be satisfactorily explained. In addition, the area contains known base metal mineralisation that has been the subject of considerable exploration efforts. The metallogenic and structural controls on this mineralisation are not well understood.

## 6.2 Topography, hydrology, access.

The topography and road network are shown in Figure 6.2.1. The topography of the southwestern third of the Grasmere 7435 1:100 000 sheet consists of low rolling hills dissected by a dendritic drainage network. Further to the south onto the Bunda 7434 1:100 000 sheet, this topography passes into ?Recent aeolian sand dunes on a broad fluvial-aeolian plain. The principal points of relief in the area are the unnamed hills corresponding to the structural Menamurtee Dome, north of "Wilandra" airstrip. These reach 340 masl. West of the major Grasmere Creek, the eastern termination of the Ramparts Hills continues onto the Nuchea 7335 sheet, attaining a height of 380 masl. The only other major topographic feature in the area is Peveril Peak and its unnamed twin. These are north-south striking slices on the Koonenberry Fault, and are both 280 masl.

Access to the Grasmere 7435 sheet is gained by turning north from the sealed Barrier Highway past Little Topar (via "Glenora" and "Boorungie", or further east via "Grasmere"). A network of rough tracks maintained by the pastoral properties, gives four-wheel drive or motorcycle access to most parts of this area, caveats applying.

Figure 6.1.1 Locality Map. Grasmere Area.

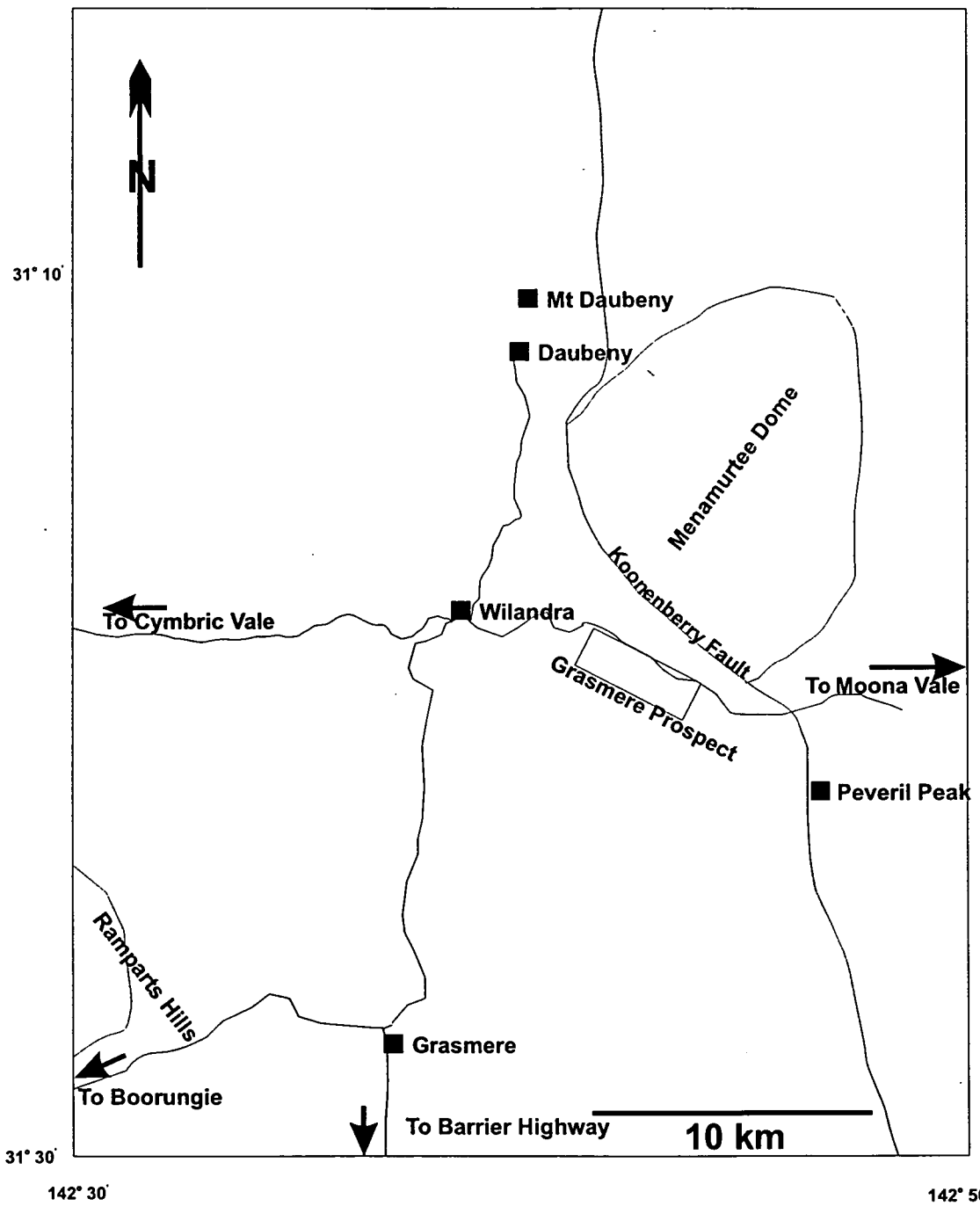

## Figure 6.1.2 Bouguer gravity and TMI image of the Grasmere area

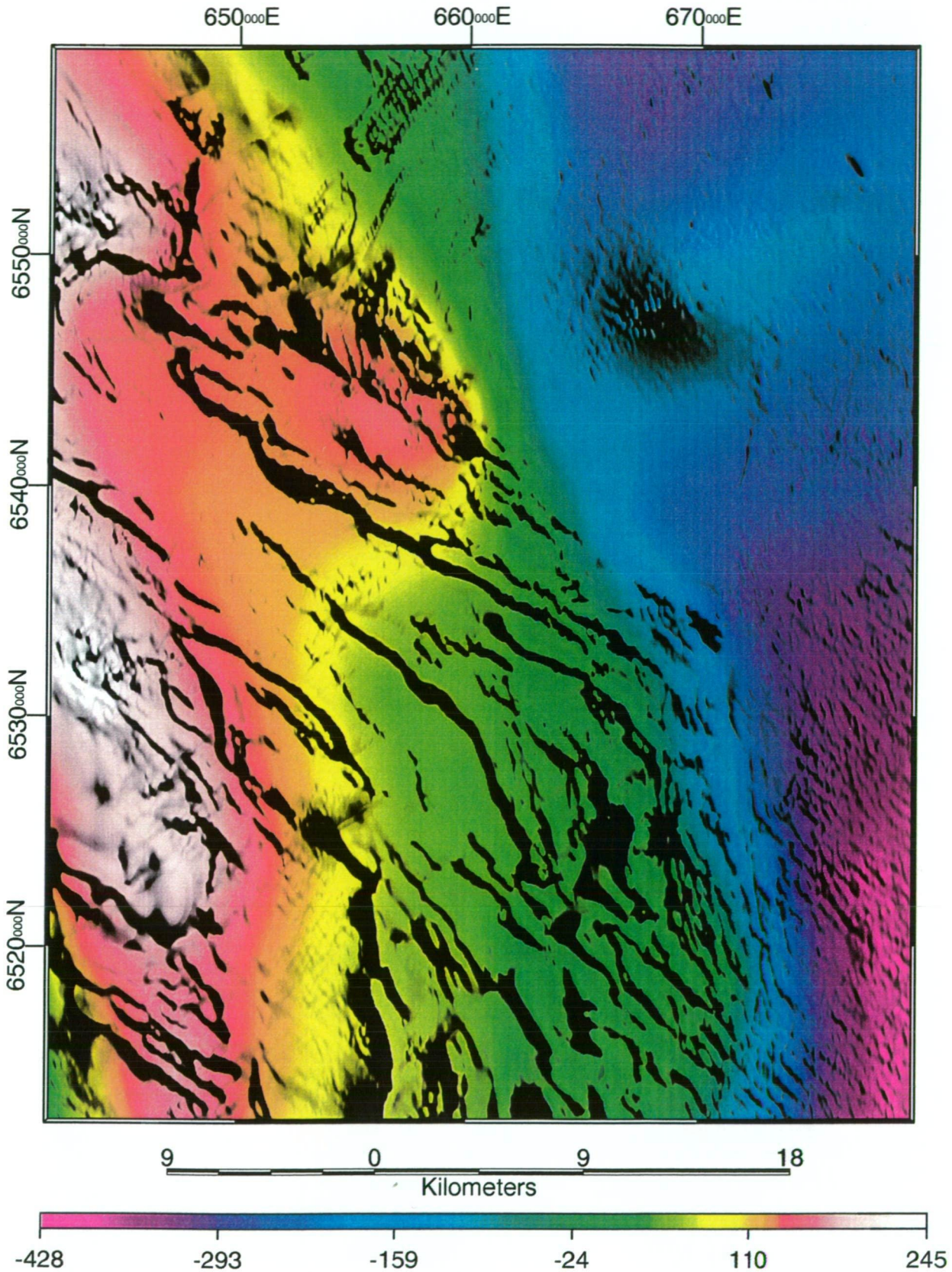


Bouguer anomaly pseudocolour and TMI intensity layer shaded at 45 degrees from the northeast. Z scale in micrometres/sec/sec. Grid is AMG zone 54.

## Figure 6.2.1 DEM and road network, Grasmere area

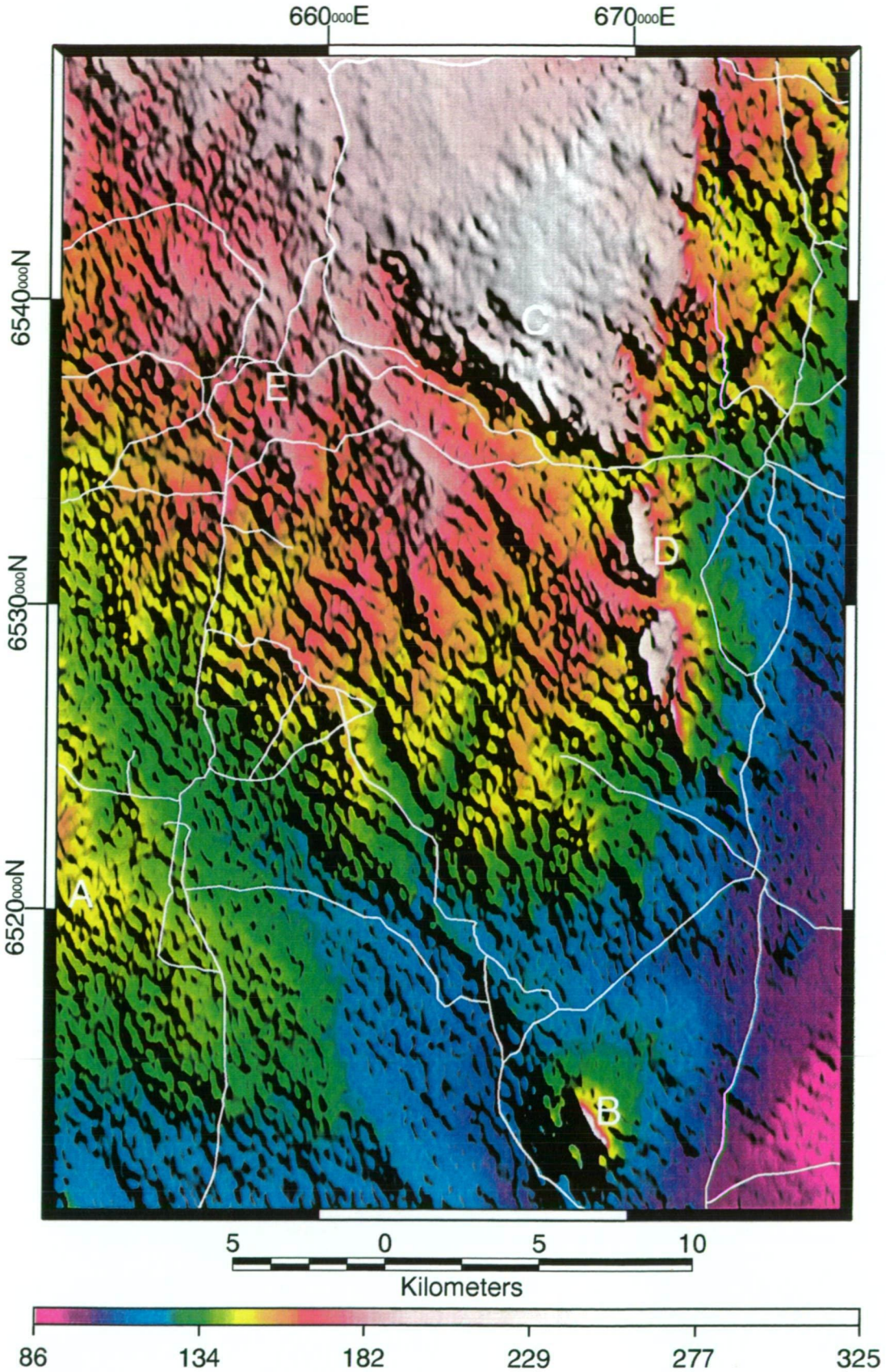


Digital elevation model pseudocolour and intensity layer shaded at 45 degrees from the northeast. Z scale in masl. A = Ramparts Hills; B = Comarto Peak; C = Menamurtee Dome; D = Peveril Peak; E = Wilandra

## 6.3 Local Structure & Metamorphism

### *6.3.1 Observations*

The structure of the Wilandra area has been locally elucidated by diamond drilling and geophysics during extensive mineral exploration at the Grasmere mine prospect (McPhar Geophysical, 1970; Davis & Chenhall, 1970; Esso, 1976; Amoco, 1982; CRAE 1989, 1990; BHP Exploration, 1998). Drillholes intersected low angle (<15° dip) reverse faults and shears, chevron folds, overprinting kink folds and rare late buckle folds (Davis & Chenhall, 1970). These relations imply at least three phases of deformation.

Senior & Senior (1995) produced a brief summary of the structural geology of the Grasmere 7435 sheet. They described near vertical to vertical north-northwest— and west-trending cleavages within the Ponto Complex. These were overprinted by a conjugate set of kink crenulation cleavages, but the attitude of these fabric elements was not described.

Faults cutting the Ponto Complex mapped by Senior & Senior (1995) appear to be of two types: early strike-parallel west-northwest striking faults ("Grasmere Fault", Koonenberry Fault), and later north-northwest— to north-northeast—trending faults which break the Complex into discrete fault blocks visible in remotely sensed data.

The metamorphic geology of the Ponto Complex in the Grasmere-Wilandra area was examined by Zhou (1993), who concentrated on mapping the distribution of metabasites. These investigations were restricted to a c.1km wide belt striking from the "Wilandra" airstrip along the "Moona Vale" Road on "Wilandra". This belt contains metabasic volcanic and intrusive rocks hosted by schist and phyllite.

Mafic rocks contained relict cpx, with two overprinted metamorphic assemblages. The first of these is act-epi-cz-mu±chl; the second, retrograde, assemblage comprises mu-epi-cz±chl±pump. He interpreted this evidence to suggest an initial middle greenschist facies metamorphic event (c. 2-3 kB, c.350°C), with a second higher pressure, lower temperature event (c. 3-6 kB, c.200 °C).

Zhou (1993) did not comment on the change of grade in the Ponto Complex from amphibolite grade at the Mt Wright Fault to greenschist / prehnite-pumpellyite at the Koonenberry Fault, over a distance of approximately 35 km.

Senior & Senior (1995) also described structures in the Late Silurian-Early Devonian Mt Daubeny Formation, in the northern central portion of Grasmere 7435. Both faults and fold-axes were described as following north- and west-striking trends. More complete data were recorded by Neef et al. (1989) who showed north-northeast and west-northwest trending fold axes cut by north-northeast and northeast striking dip-slip faults; the faults are often intruded by dykes in the type area. These data are summarised in Figure 6.3.1. The style of folding, faulting and metamorphic grade is described in more detail at 3.3; briefly, it consists of prehnite-pumpellyite grade rocks folded into gentle-open folds without axial planar cleavage, and broken up by brittle faults with crush zones.

Senior & Senior (1995) summarised structural data for the Late Devonian-Early Carboniferous Mulga Downs Group, cropping out to the east of the Koonenberry Fault. The most prominent feature is the Menamurtee Anticline, a gentle, upright, long-wavelength (6 km 1/2$\lambda$), southwest-plunging macroscopic anticline. The hinge and limbs of this structure are cut by brittle northeast-trending faults. Close to the Koonenberry Fault, bedding is dragged into tight folds, in much the same manner as at Koonenberry Mountain to the north (Mills, 1992).

### *6.3.2 Summary*

The latest structures in the Grasmere area appear to be post-Early Carboniferous northeast- trending brittle faults and related drag folds, and very rare macroscopic warps affecting the Mt Daubeny Formation and Mulga Downs Group. This event, regionally equated with the Kanimblan Orogeny by Mills (1992), was not accompanied by regional metamorphism.

The next-oldest regional metamorphic and deformation event seems to have occurred between the Early and Late Devonian (post-Mt. Daubeny Formation time and pre-Mulga Downs Group time). This event developed a prehnite-pumpellyite facies metamorphism in the Mt Daubeny Formation and a related retrogressive metamorphic overprint in the Ponto Complex. Folding at this time produced open west-northwest and north-northeast

## Figure 6.3.1 Rose diagrams. Fold axial and fault trends, Mt Daubeny Formation, Grasmere Area

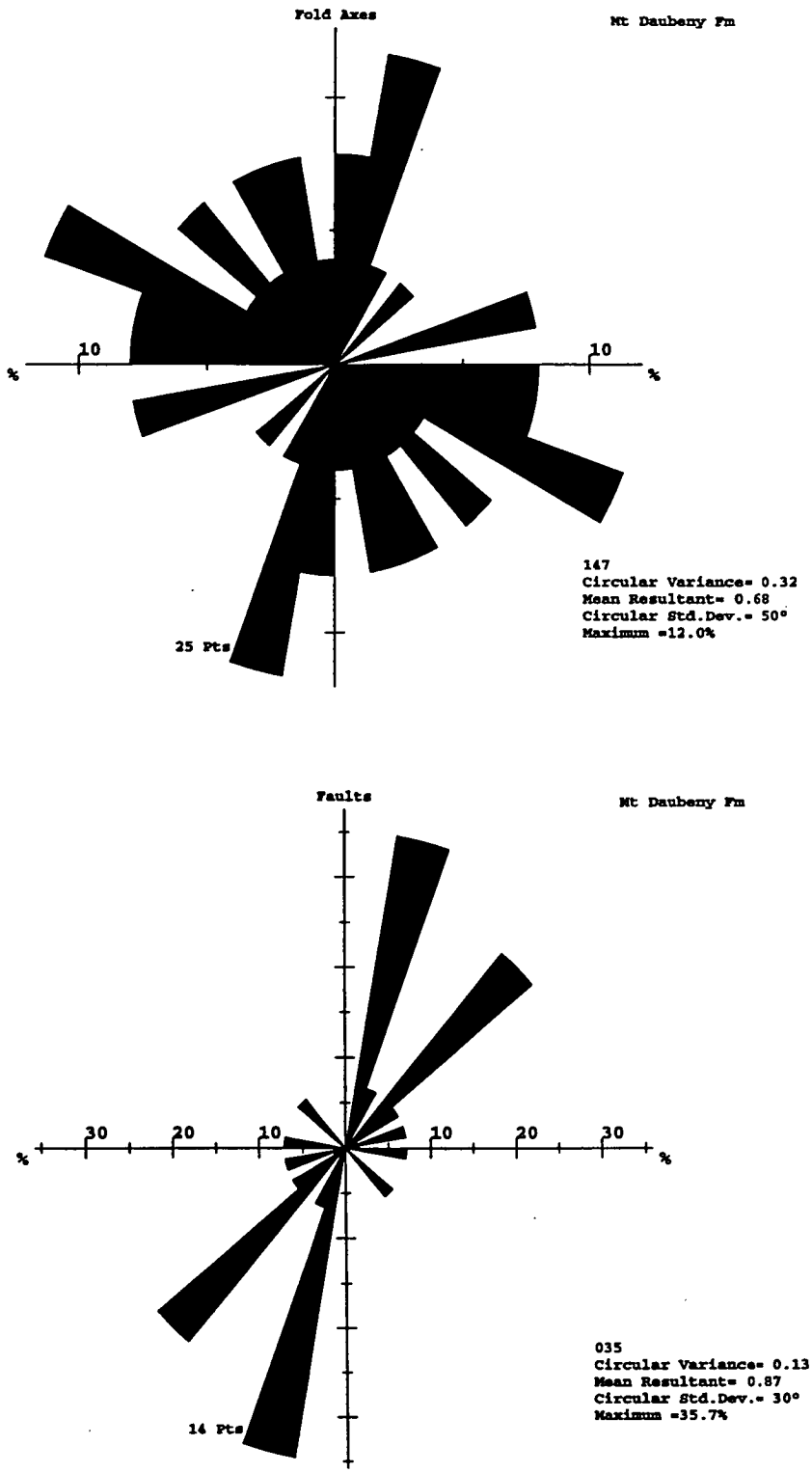

interfering folds; this implies at least two near-orthogonal phases of compression. Metamorphic mineral growth does not appear to be related to any axial plane cleavage development, which is weak to non-existent. These deformations have been tied to the Tabberabberan event in the Lachlan Orogen.

Fabrics described in the Ponto Complex have a completely different style and orientations to those outlined above, and relate to an earlier folding and thrusting event or events with high strain and greenschist facies metamorphism. The timing of deformation in this area is unconstrained by the published data.

### 6.4 Problems arising

The Grasmere area is probably the most prospective, and most explored area in the Koonenberry Belt, containing lodes of Banded Iron Formation (BIF)- hosted massive sulphide mineralisation at the Grasmere mine prospect (McPhar Geophysical, 1970; Davis & Chenhall, 1970; Esso, 1976). These lodes are hosted within the Ponto Complex (Senior & Senior, 1995). The oxidised zone contains higher grade mineralisation occurring as cuprite-malachite-azurite-tenorite with quartz-haematite-goethite gossan; the primary lodes comprise pyrite-pyrrhotite ± chalcopyrite-sphalerite (Lewis, 1976). Primary sulphides have a Cambrian Pb isotopic age (Zhou et al., 1992).

Opinion differs on the controls on the mineralisation. Senior & Senior (1995) reported a stratigraphic control within a dolomitic metasiltstone-chloritic schist horizon. Drillholes by CRAE (e.g. GR 7, logged by the author) show that massive sulphide intersections occur structurally above a horizon identified as "BIF" or quartz-magnetite rock. Leahey (1982, quoted in Senior & Senior, 1995) considered the quartz-magnetite horizon to be stratigraphically *higher* than the mineralised horizon, introducing the possibility of thrusting. Low-angle shears and thrusts were reported by Davis & Chenhall (1970), and are obvious in GR 7 (see below). This style of deformation may mean the ore horizon has been structurally repeated, requiring an analysis of the local and regional structure and stratigraphy before efficient exploration can proceed.

However the mapped distribution of units and structures on the Grasmere 7435 1:100 000 sheet has recently been found to be inaccurate, due to problems in the identification of

weathered lithologies (B.Stevens, pers. comm., 11/97). A program of geophysical interpretation and mapping designed to address this question is outlined below.

Of more regional tectonic significance is the nature of the deformation processes responsible for the bending of the Koonenberry fold belt through a c. 90° strike change in the south of the area. Two end-member mechanisms are possible for this deformation: oroclinal bending or dextral shearing (Figure 6.4.1). The age of this structuring is also not well-constrained. These problems were also addressed in the context of geophysical interpretation and mapping, described below.

### 6.5 Stratigraphy, Volcanic Facies and Structure of Early Palaeozoic rocks

In order to address the structural questions outlined above, some time was devoted to field mapping of stratigraphic and structural relationships in the "Wilandra" and "Grasmere" areas. Figure 6.5.1 shows an interpretative geological map for Palaeozoic units on Grasmere. This map is based primarily on interpretation of geophysical data including magnetics and magnetic vertical derivatives, both reduced to the pole; gravity; radiometrics; and Landsat Thematic Mapper visible and IR spectral imagery. The methods used are essentially similar to those described at 4.12.

Zhou (1993) geochemically analysed 26 samples for major and trace elements from the Cymbric Vale-Wilandra area. These all displayed sub-alkaline, tholeiitic characteristics, regardless of degree of metamorphism and protolith type (intrusive/extrusive). REE analysis of 5 samples showed the rocks have strong affinity to MORB, but include strong Nb depletion, suggesting early backarc-type MORB.

Senior & Senior (1995) mapped the Wilandra area as part of the Grasmere 7435 1:100 000 geological map. They defined nine map units within the Ponto Complex vis.
**Elpd** Diorite & olivine gabbro... forming plug-like intrusives
**Elpu** Finely crystalline, small, basic or ultrabasic dykes & plugs
**Ep** Undifferentiated lower greenschist grade metasediments
**Epa** Fine to medium crystalline intermediate to acid volcanics, comprising schistose andesite, andesitic tuff, flow banded rhyolite & intercalated sedimentary rocks
**Epb** Green tholeiitic basalt, trachybasalt & andesite

**Figure 6.4.1 Possible kinematics of bending, Koonenberry Fault, Grasmere**

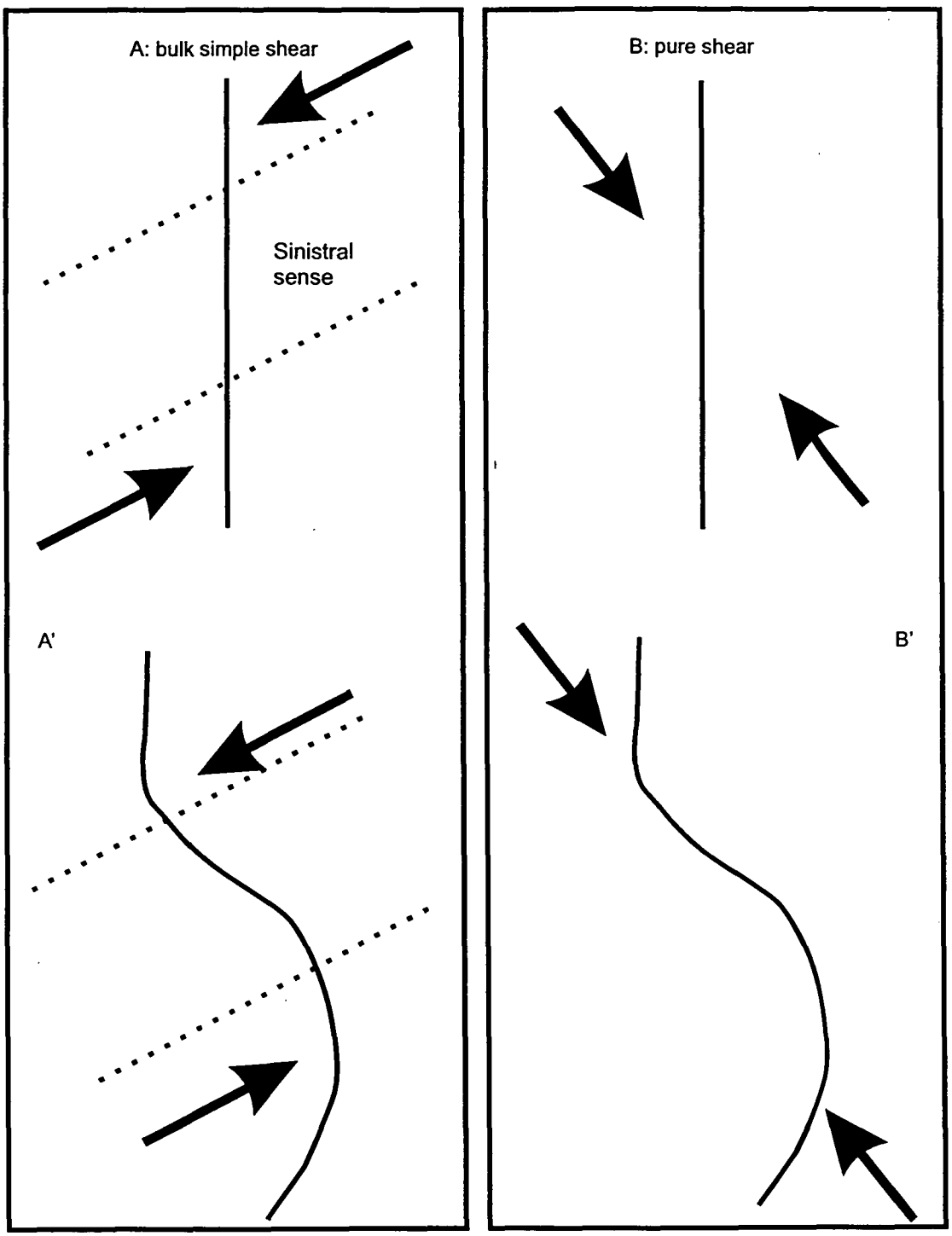

**Epm** Interbedded meta-lithic sandstone, siltstone, mudstone & dolomite, repetitively interlayered with tuffaceous arenite, andesitic tuff...schistose andesite and basalt flows
**Epsa** Silicified quartz sandstone with minor siltstone
**Eps** Strongly cleaved meta-lithic sandstone, siltstone, mudstone
**Epp** Strongly deformed phyllite in fine (meta-)lithic sandstone and siltstone.

Field checking of Senior & Senior's (1995) data has shown that various phyllites, basalts and quartz-magnetite rocks have been misinterpreted to form the units Elpd and Elpu. Also, many areas marked as Epb are in fact Epp in this scheme.

Thin section descriptions (L.Barron, pers. comm.1997) of samples from units Epa and Epm show that "andesitic" rocks are in fact either sandstones or basalt/gabbro. Clearly, there is a need for the stratigraphy of the Ponto Complex on the Grasmere 7435 1:100 000 sheet to be revised.

Ten subdomains have been defined within the Ponto Complex in the Wilandra area on the basis of geophysical interpretation checked by field traversing. These subdomains form the Grasmere and Division Tank Domains.

*6.5.2 Grasmere Domain (Epg)*

Blue Well Subdomain (Epbw)
A zone of diffuse anomalies, bounded by the Koonenberry Fault to the north, and a high (Epgp) to the south. Most of the subdomain has intensities of -100 nT, which are related to weakly magnetic phyllite, meta-fine sandstone, and metasiltstone (average $k = 25 \times 10^{-5}$ SI). A linear high (Gum Creek anomaly) is spatially related to outcrops of highly magnetic phyllite ($k = 3000 \times 10^{-5}$ SI). Other lithologies encountered on the ground include basalt flows and pillows, dolerite, gabbro, quartz dolerite, diorite, minor quartz-magnetite rock and magnetic phyllite, with basalt being the most common. Some of these rocks were investigated by Zhou (1993). They do not contribute to the Gum Creek anomaly, having an average magnetic susceptibility of only $45 \times 10^{-5}$ SI.

Metasediments of the Blue Well Subdomain have well-developed spaced phyllitic or slaty, continuous cleavages, (sub-)parallel to bedding; metaigneous rocks have rough, anastomosing cleavages.

Grasmere Prospect Subdomain (Epgp)

A series of intense 300 nT linear highs, related to quartz-magnetite rock (also called BIF in company exploration reports). This horizon is associated with sulphide lodes in the Grasmere Prospect. The average magnetic susceptibility of this rock is 3700 x $10^{-5}$ SI. Other lithologies in this subdomain include weakly magnetic phyllite (k 30 x $10^{-5}$ SI) and magnetic basalt (k 1100 x $10^{-5}$ SI).

Tuffs within this subdomain have been dated using SHRIMP derived U-Pb isotopes from magmatic zircons (BHP Exploration, unpublished data). Three dates cluster around 500 Ma (497 ± 8 Ma; 506 ± 8 Ma; & 501 ± 9 Ma), agreeing with a 500 Ma model Pb isotope age derived from sulphides in the Grasmere lodes (Zhou et al., 1992). This age is Undillan to Boomerangian (Late Cambrian). Sulphide isotope data indicate a mantle-derived Pb source for the syngenetic mineralisation, confirming the MORB-like affinity of the volcanics in the Grasmere Domain (after Zhou et al., 1992).

Metasediments of the Grasmere Prospect Subdomain have excellent structural textures preserved in diamond drillcore, such as in CRAE DDH GR7 which was examined by the author. This hole was collared at 663125 mE 6535570 mN, inclined at -63° to 12°, and reached a total depth of 247 m. Whereas outcrops in this subdomain show that the Ponto Complex has a prominent slaty cleavage dipping steeply (c.80°) to the southwest (Figure 6.5.2), three dimensional structures within the core show development of chevron-elliptical folds, microscale thrusts, box folding and kinking with pressure solution cleavages. Thrusts are preferentially developed in sandier or dolomitic units which are mechanically stronger than shaly units. These features, here called D2 fabrics, deform an earlier transposed fabric, S1, represented by mesoscale lenticles, boudins and hook-folds of pelite and quartz mica schist. Bedding and cleavage data from field traverses (Figure 6.5.2) display parallel bedding and cleavage dips, and indicate tight, asymmetric chevron folds with northwest plunge; northeast- dipping limbs are generally shallower than steeply southwest-dipping limbs.

The sum of this evidence suggests that the Ponto Complex is a series of imbricated southwest-vergent thrust sheets which have taken up two deformations. The earlier event, D1, produced northwest-trending isoclinal folds, thrusting and transposition of bedding. The second event, D2, produced further shortening by chevron folding and transposition

## Figure 6.5.2 Equal area nets, fabrics within the Ponto Complex Grasmere area

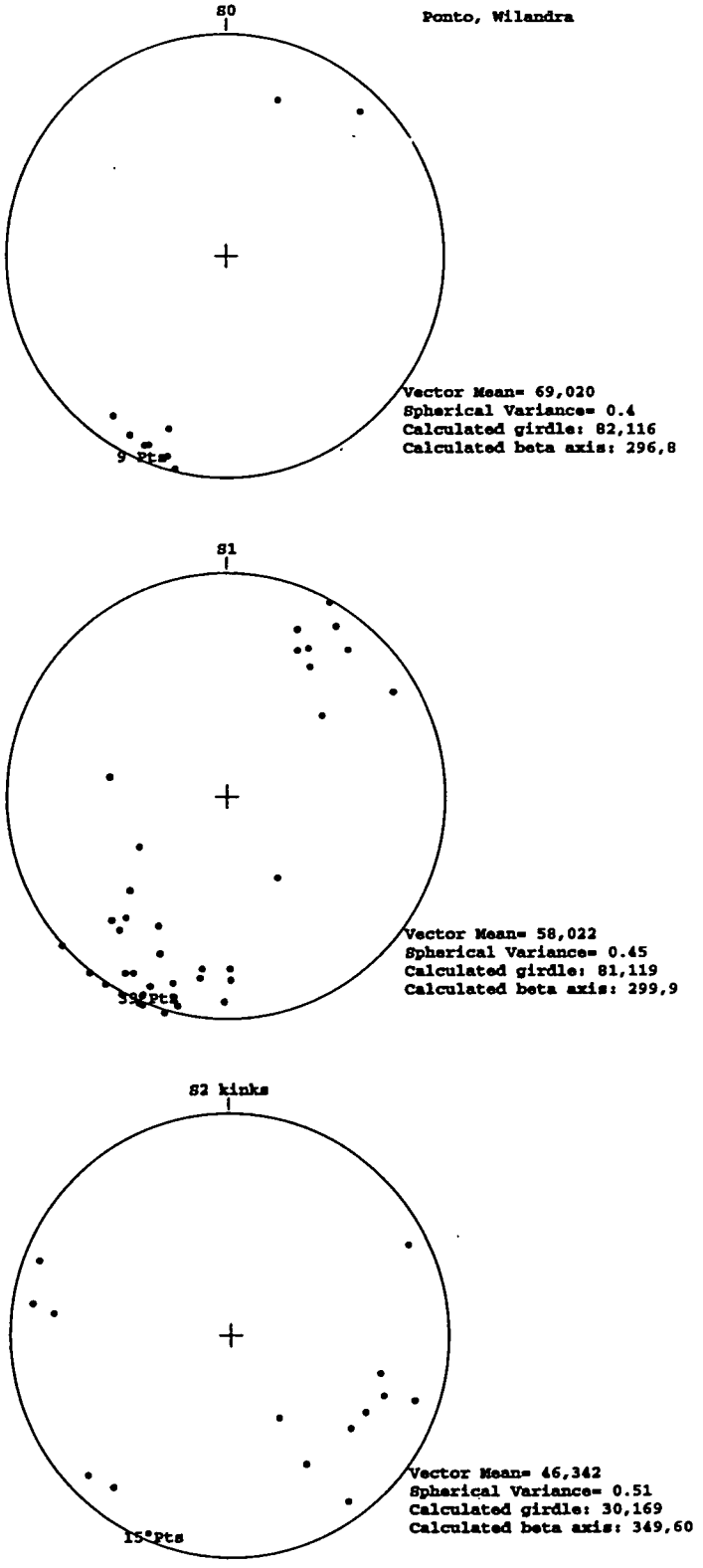

fabric slip, then later by thrusting. Field traversing and aeromagnetic evidence support this interpretation.

These observations confirm reports by Western Copper P.L. (1970) of kink (i.e. chevron) folding with layer parallel movement observed in drillholes DDH 2 & 3. These were associated with low-angle (< 15°) faults in both holes at depths of 94.5 m (DDH 2), 50.1 m & 52.7 m (DDH 3).

No links were drawn by Western Copper (1970) or subsequent licence holders between low angle faulting and the fold style observed in the Ponto Complex. However, recent work by Hill (1998) in turbidite sequences at Cape Liptrap, Victoria has shown that these two structural features can be linked mechanically and geometrically. The well-exposed, well-understood Cape Liptrap structures make good mesoscopic analogues for the poorly outcropping structures on Grasmere 7435 (e.g. Figure 6.5.6).

Transmitted light microscopy in this study revealed evidence for four distinct fabrics within these rocks. The earliest recognisable fabric is defined by discontinuous, smeared-out domains of quartz-biotite, with a gradation of grain size in some cases. This probably reflects original depositional grading from sand to silt, as seen in outcrop; this fabric thus represents bedding, S0. Discontinuous, recrystallised, interlocking, cleaner quartz domains are interpreted as early veins. These veins are the hooks seen in hand specimen, commonly contain decussate muscovite, and are probably related to the transposed F1 folds. This fabric is therefore S1.

The dominant fabric in these rocks is a moderately to strongly developed qz-mu-chl-bio spaced to continuous slaty cleavage, with spacing of domains being inversely proportional to the apparent strain. Domains containing earlier fabrics have been rotated into parallelism with this cleavage.

A weak- to well-developed dissolution crenulation cleavage (S3) cuts across all earlier fabrics and is associated with kink-style deformation. Observed cleavage transection of kink bands implies a strong rotational component to this phase of deformation.

The three microscopic deformation fabrics observed equate well with what is expected from map-view analysis and field traversing.

Meeninta Subdomain (Epme)

A series of linear magnetic lows, -80 nT below datum. On the ground, this zone is related to a weakly magnetic interbedded metasandstone-phyllite package ($k = 25 \times 10^{-5}$ SI) containing minor metabasalt and metabasaltic tuff ($k = 500 \times 10^{-5}$ SI).

Blanche Subdomain (Epbl)

Broad, west-northwest—east-southeast trending linear magnetic highs of 300 nT total amplitude. These are related to moderately magnetic phyllites ($k = 360 \times 10^{-5}$ SI) with tuffaceous horizons. The difference in magnetic lithologies between the Blanche and Grasmere Subdomains means that the magnetic pattern is probably not a fold or thrust repetition of the mineralised horizon.

Weinteriga Subdomain (Epwe)

A broad magnetic gradient from c.0 nT to -100 nT, northeast to southwest, associated with moderate to weakly magnetic phyllites-metamudstones ($k = 120 \times 10^{-5}$ SI).

Darts Subdomain (Epda)

A very broad magnetic low, c.2 km in width, between -100 and -200 nT, modulating eastwards along strike into a series of 600 nT total amplitude linear highs (Peveril anomaly). A variety of rock types outcrops in this subdomain: associated with the low zone are very weakly magnetic ($k = 30 \times 10^{-5}$ SI) metasandstones and slates, whereas the Peveril anomaly is associated with magnetic phyllite ($k = 800 \times 10^{-5}$ SI), thin (< 2 m wide) basalt flows or dykes ($k = 2500 \times 10^{-5}$ SI), diorite, non-magnetic phyllite ($k = 0$) and minor quartz-magnetite rock. The Peveril anomaly is c. 1500 m wide, suggesting an integration of linear magnetic sources such as dykes.

Paddys Creek Subdomain (Eppc)

A second broad (c. 2km) low , -200 nT in amplitude, related to a sandy metasedimentary package (coarse metasandstones to metasiltstone). These have weak magnetic susceptibility ($k < 20 \times 10^{-5}$ SI).

Bendee Subdomain (Epbn)

A fault-truncated, fold repeated series of magnetic highs with c. 350 nT total amplitude in an area of extremely poor outcrop. A weakly magnetic ($k = 25 \times 10^{-5}$ SI) phyllite is found in

this zone together with a series of alkaline intrusive rocks, including alkali diorite, monzodiorite, monzonite, and isolated outcrops of dolerite and basalt (B. Stevens & L. Barron, pers. comm). These rocks may be late intrusive related to similar rocks in the Darling River Lineament (see Chapter 7), but were not sampled during this study. The basalt has a susceptibility of 1000 x $10^{-5}$ SI. The anomaly appears to be folded, and is truncated against the Division Tank Subdomain boundary, which has been interpreted as a thrust.

Rainbow Subdomain (Epra)
Probably the oldest unit in the Grasmere domain, the Rainbow Subdomain occupies the core of a regional northwest-plunging anticline that truncates against the Division Tank Subdomain; it is surrounded by the Bendee Subdomain. It is associated with non-magnetic psammite and phyllite intruded by small plugs of moderately magnetic monzodiorite.

### *6.5.3 Faulting in the Grasmere Domain*

Evidence from the truncation of fold limbs and changes in cleavage dip suggests the Grasmere Domain is bounded to the southwest by a major reverse fault (Christmas Well Fault), and divided into two packages by a second reverse fault (Griffiths Fault). Both of these, and several other interpreted fault boundaries trend northwest, parallel to bedding trends (see Figure 6.5.3). Apparent eastward-younging and non-repetition of magnetic horizons such as the Grasmere Prospect Subdomain suggests that the enveloping surface of the Grasmere Domain is ramping up to the southwest, where the package is cut out by the Christmas Well Fault. This is consistent with structural and geophysical evidence from the Nuchea 7335 1:100 000 sheet that the Ponto Complex is a west- and southwest-vergent thrust package (Direen & Crawford, 1998b).

The Grasmere Domain between the Prospectors Creek Fault and the Christmas Well Fault is also broken up by a series of wrench faults trending at a high angle to bedding (see Figure 6.5.4). These faults almost invariably have apparent dextral displacements, with slips of more than 1 km in some cases. From changes in anomaly spatial wavelength, blocks in the east appear upthrown relative to those in the west, with the major displacement occurring as the mineralised zone is approached (near CRAE drillhole DDH GR1). As these wrench faults do not appear to interact with the bedding parallel-thrusts in

Figure 6.5.3

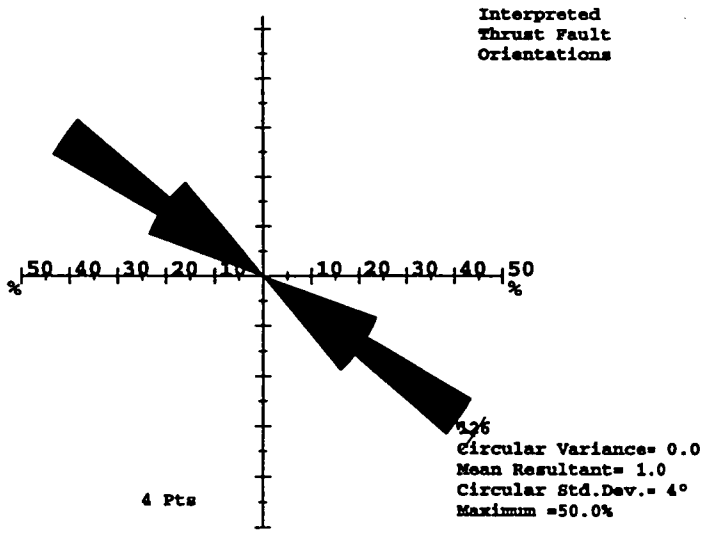


Figure 6.5.4

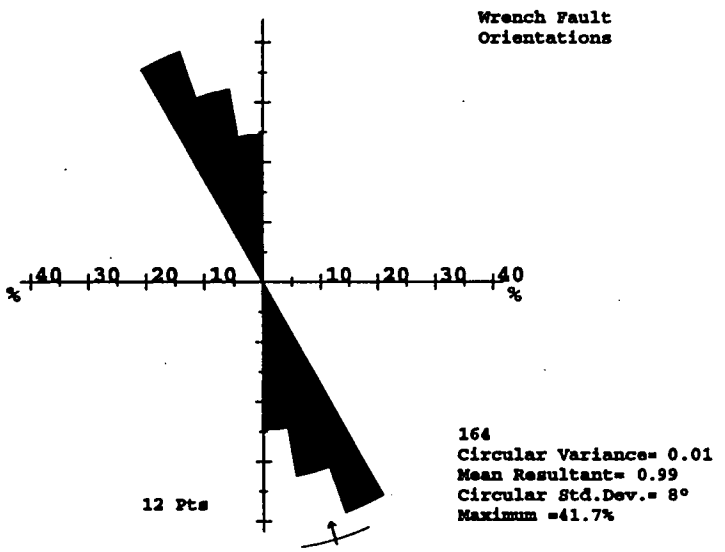


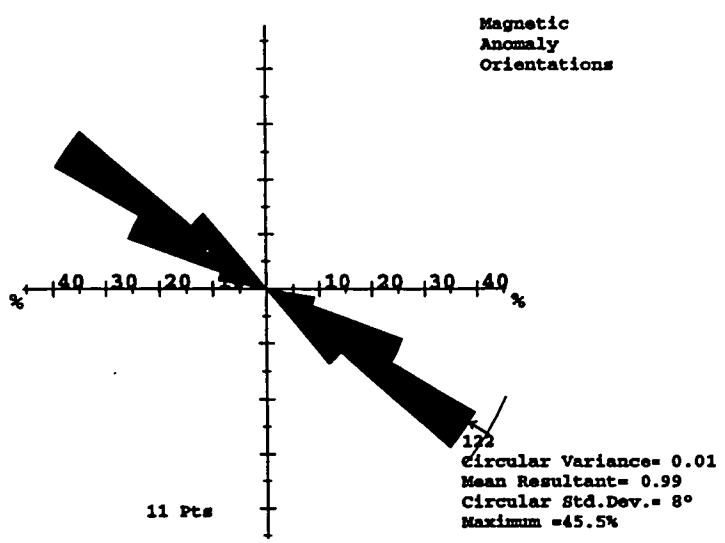

map view, the relative timing of these events can not be readily discriminated. These faults may be related to similarly trending faults that opened the small north-northwest—trending basin accommodating the Late Silurian Mt Daubeny Formation; in this case they would post-date the Late Cambrian (Iverian-Idamaean) thrust emplacement of the Ponto Complex.

### *6.5.4 Division Tank Domain (Epdt)*

This domain has a completely different character to those previously described, being an arcuate, composite magnetic high, 2.5 km wide by c.16 km arc length. The two highs comprising the domain have amplitudes c.400 nT. These are apparently related to magnetic phyllites (k = 125 to 600 x $10^{-5}$ SI) and are macroscopically folded into a series of southwest-vergent, northwest-plunging asymmetric folds. This fold trend is truncated against a northwest-trending linear feature interpreted as a thrust. The core of the anticline is represented by a broad magnetic low of -100 nT relative to the datum. On the ground, this feature is occupied by non-magnetic psammites, and approaching the thrust, extremely crenulated phyllite. The footwall of the thrust is occupied by a buff coloured laminated shale correlated with the Kara beds. The dip of the primary slaty cleavage within the hangingwall of the fault is 30° to 60° (T), whereas in the footwall, cleavage in the shale is vertical, striking 145°(T). These dips support an east-over-west sense of transport on a listric fault.

### *6.5.5 Other Domains*

E.B.L Domain (Ekeb)

This subdomain lies to the southwest of the Grasmere Domain, and is bounded by the Christmas Well Fault (to the northeast) and the Grasmere Creek Fault (to the southwest). Yellow-buff laminated shale correlated with the Kara beds is found within this domain. Two weak magnetic highs represented a single folded unit with a maximum amplitude of 30 nT, reflecting the weak susceptibility (av. 25 x $10^{-5}$ SI) of the Kara beds.

Mulga Tanks Domain (Ekmt)

This domain is a macroscale, refolded anticline of 4.5 km half wavelength; the feature is visible on magnetic images at scales up to 1: 5 000 000, defining the c. 90° trend change in magnetic and gravity lineaments. The amplitude of the single folded horizon is about

200 nT, but peaks at 25 nT, due to strong contrast with non-magnetic rocks to the east and west. There is no known outcrop of Kara beds in this area, but the domain is similar in form and character to the E.B.L Domain. The fold continues onto the Bunda 7434 1:100 000 sheet, where it has been interpreted as belonging to the Kara beds (Mills & Hicks, 1997).

Boorungie Domain (?Eg; undifferentiated Gnalta Group)
This domain is continuous under cover with that mapped in the southeastern corner of the Nuchea 7335 1:100 000 sheet. This unit does not crop out.

Johns Domain (Etn Nundora Formation)
In the south central region of the sheet, this domain occurs as a broad, negative magnetic gradient of –150 nT. The lowest values are associated with red feldspathic lithic sandstones of the Nundora Formation, the basal formation of the Teltawongee Group. These are found in the core of a macroscale syncline, visible in the aeromagnetics and defined by changes in younging direction in graded turbidite units. The average susceptibility of sandstones in the Nundora Formation is $< 20 \times 10^{-5}$ SI.

At the eastern margin of the mapped area, a second syncline defined by grading in turbidites is represented by a negative gradient of –60 nT. This syncline is also visible in the magnetics.

Paddock Well Subdomain (Epwp)
This is the continuation of higher grade Ponto Group rocks from the Nuchea 7335 sheet. The main feature of the subdomain on the Grasmere 7435 sheet is the presence of a macroscopic tightly folded, northwest-plunging anticline of 4 km half-wavelength. The Grasmere Creek Fault appears to duplicate parts of this package.

Amphitheatre Subdomain (Epam)
The continuation of low grade Ponto Group rocks from the Nuchea sheet.

S-Dd (Mt Daubeny Formation)
This unit is treated in detail by Senior & Senior (1995). The main magnetic feature of the domain corresponding to this formation is a series of north-northeast—trending linear features, which are probably an andesitic dyke swarm: andesitic dykes and lavas have

been mapped in the Mt Daubeny Formation on the Kayrunnera 7436 sheet (Neef et al, 1989). The bodies responsible must be only weakly magnetised, as the maximum response is 50 nT above a background of –100 nT.

*6.5.10 Summary of Structural and Stratigraphic Data*

The following are key points:

- The Kara beds and Teltawongee Group crop out on Grasmere 7435, in structural and probably stratigraphic conformity. This contact is the same as that observed at Teltawongee Dam, and has not previously been recognised (cf. Senior & Senior, 1995).

- The proposed Nundora Formation (see chapter 4.6) is present in this succession. Its stratigraphic thickness is c. 1000 m. Facies replicated from the type section include basal massive amalgamated sand beds, rare classic turbidites, and red, oxidised turbidites. Also present are thin laminar shale facies. A comparative stratigraphic column is given (see Figure 6.5.5).

- Re-occurrence of the Kara beds / Nundora Formation contact in a different structural position confirms the presence of large scale, regional thrust repetition of stratigraphy.

- Thrusts can be identified near locations of significant rotation of the dominant cleavage from the vertical (e.g. Ponto-Kara fault contact 660282 mE 6529210 mN)

- Southwest-vergent thrusting has occurred internally in the Nundora Formation, and has also been the mechanism for the emplacement of Late Cambrian Ponto Complex over older Kara beds/Teltawongee Group

- Dextral strike-slip faulting in the hangingwall sheet occurred after thrusting. This fault array trends north-northwest—south-southeast. Faults tip into zones of north-northwest—directed crenulations, and north-northwest and north-northeast—trending kink bands that are the hinges to fanning box folds (Figure 6.5.6). The extension caused by this episode of faulting may be responsible for providing the accommodation space for the Mt. Daubeny Formation, which is unaffected by north-northwest—trending faults (Figure 6.5.4).

# Figure 6.5.5 Comparative stratigraphic sections, Nundora Formation, Grasmere & Nundora

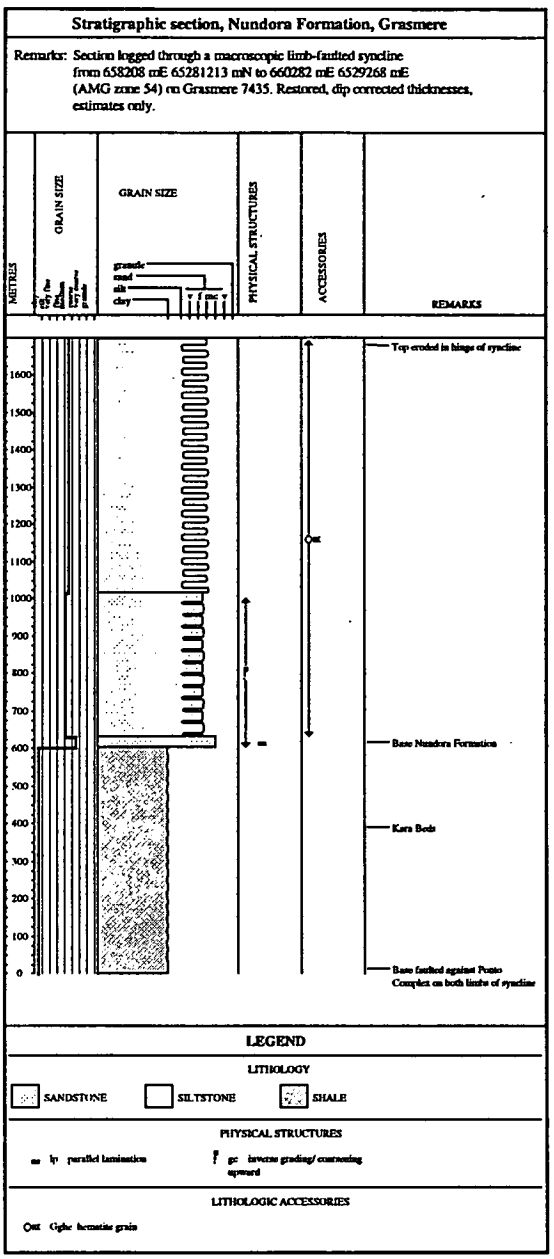


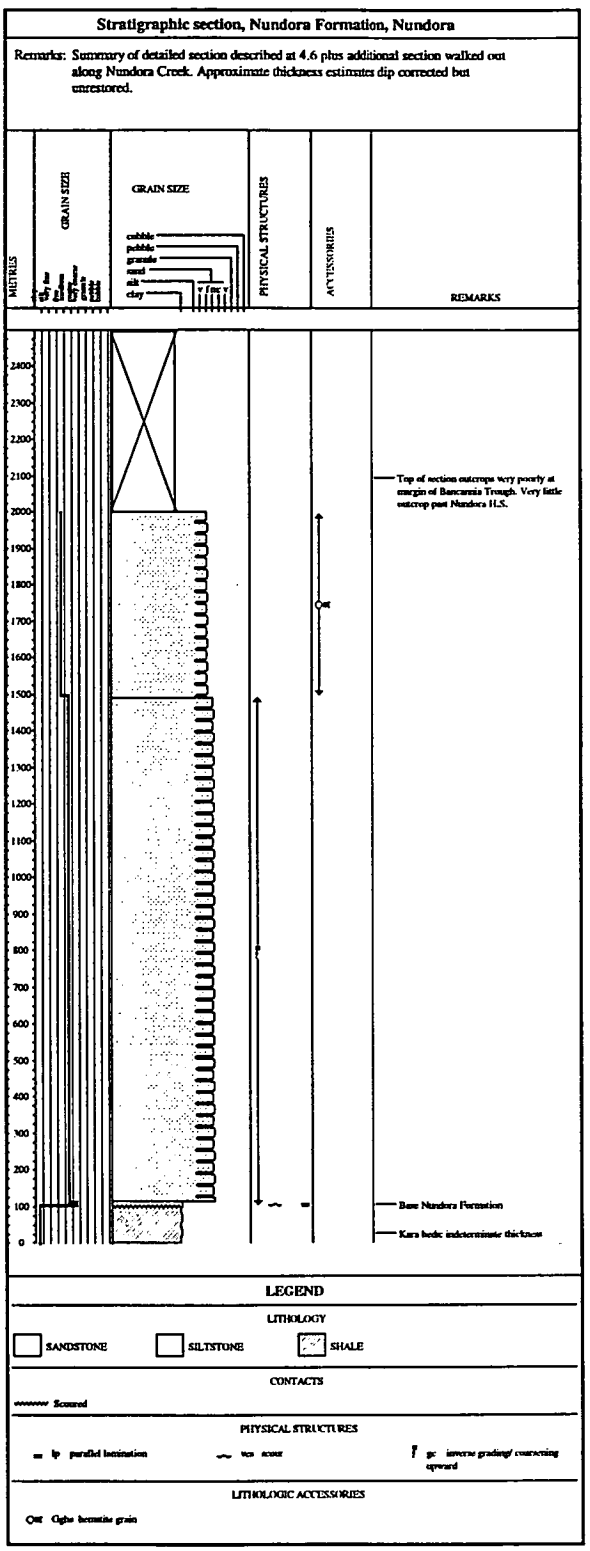

**Figure 6.5.6 Style of late deformation in the Ponto Complex, Grasmere**

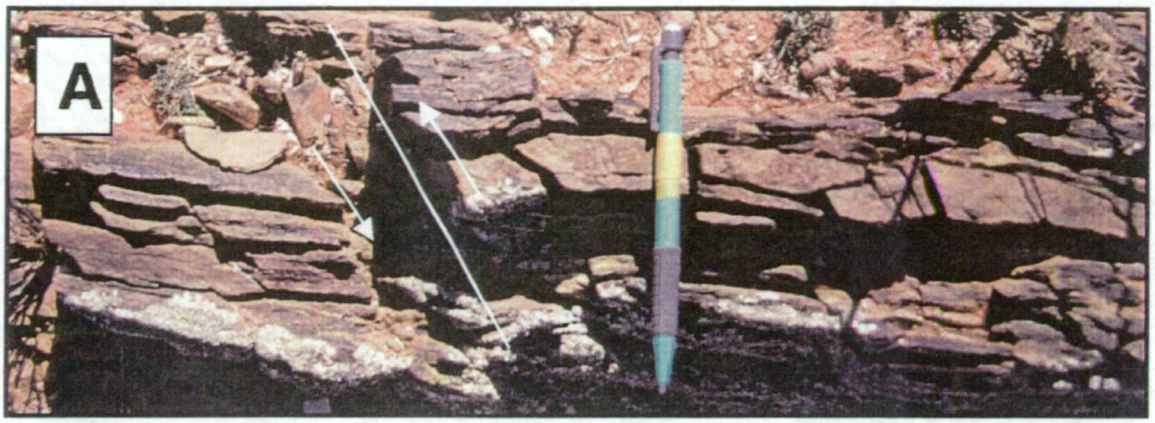


A: Sinistral fault in metasiltstone. Fault trends 170°True, dipping 86° E. Pen points in facing direction of beds

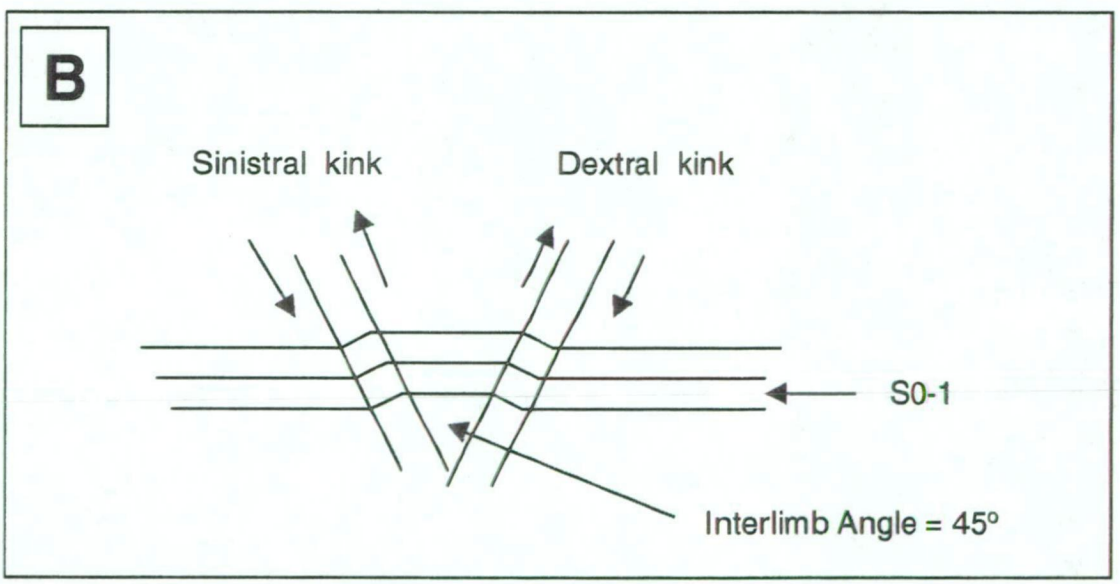


B: sketch of a mesoscopic fanning box-fold deforming a composite bedding-cleavage fabric (S0-1) in metasiltstones at 659309 mE 6534105 mN (AMG Zone 54). Sinistral kink trends 190°(true); dextral kink trends 235°(true). Bedding cleavage fabric dips 85° to 115° (true).

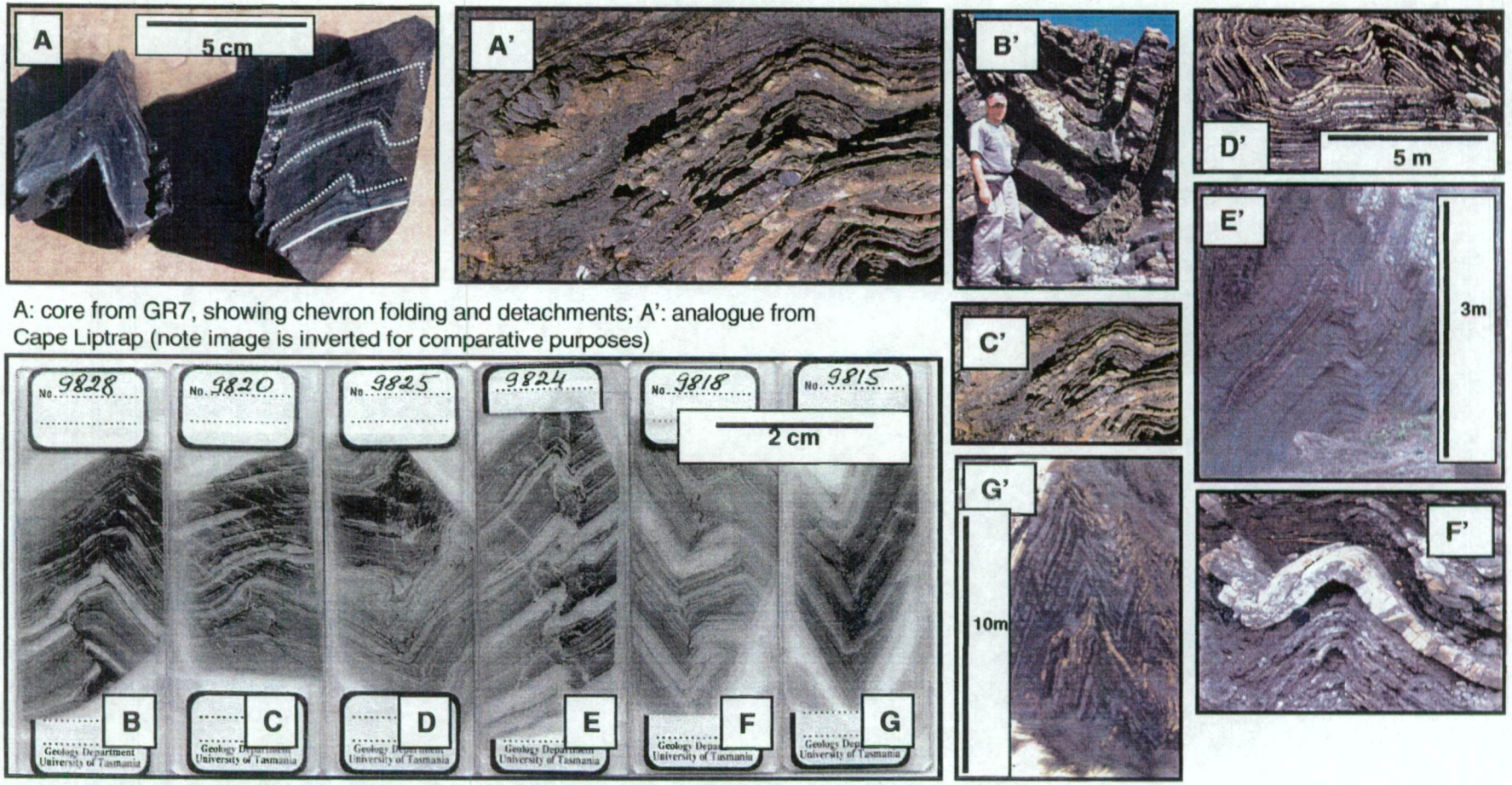


A: core from GR7, showing chevron folding and detachments; A': analogue from Cape Liptrap (note image is inverted for comparative purposes)

B-G:Thin sections of structures in core, and some mesoscopic analogues from Cape Liptrap, Victoria, in folded and thrusted turbidites (B'-G'). Lens cap (A', C', F') is 5 cm in diameter.

**Figure 6.5.7 Mesoscopic structures, GR 7drillhole, and analogues, Cape Liptrap (Victoria)**

## Figure 6.6.1 Dip sensitivity traverses, Grasmere area

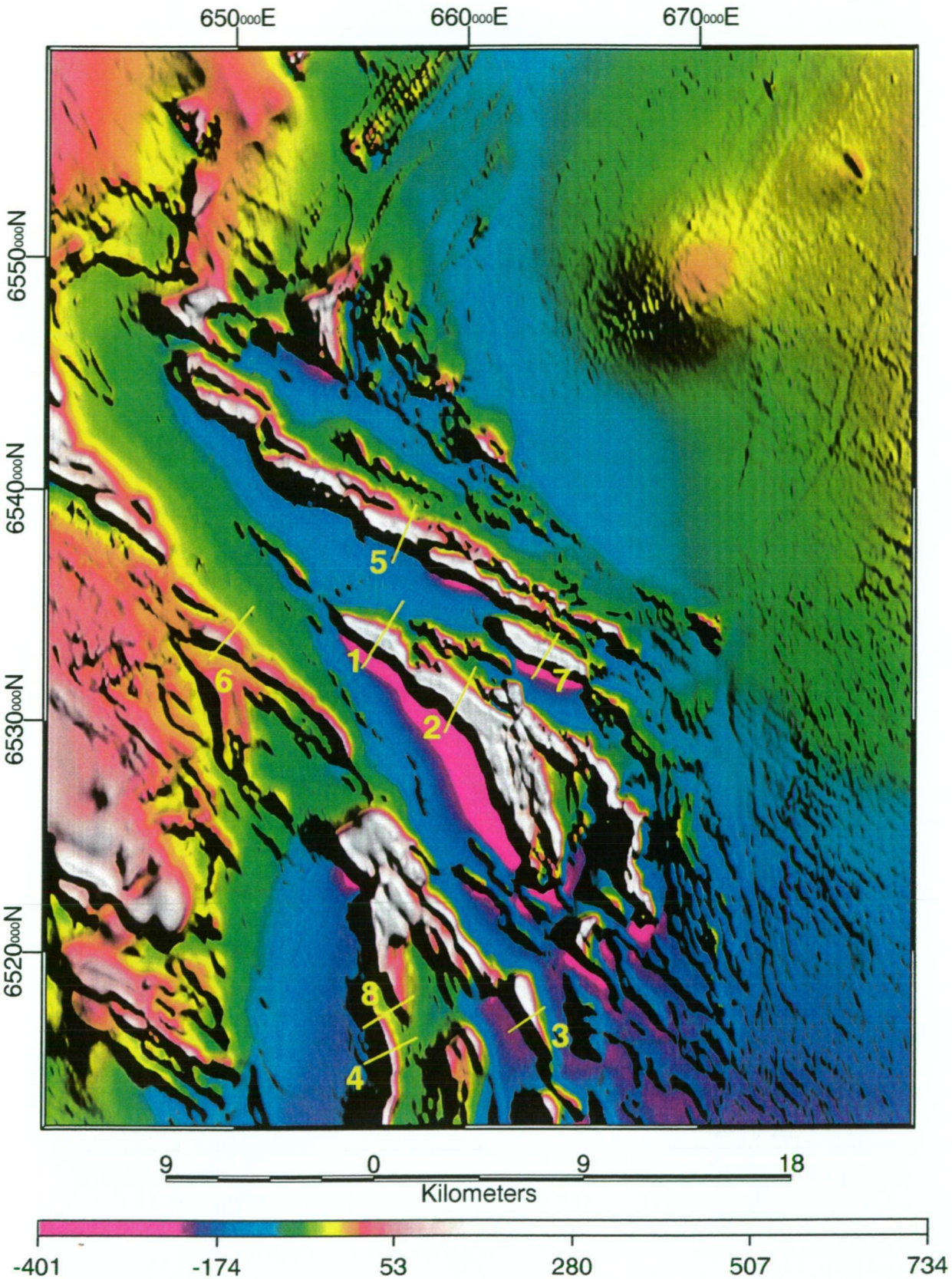


TMI pseudocolour and intensity layer shaded at 45 degrees from the northeast.
Z scale in nT. Grid is AMG zone 54. 1 ,2 = Division Tank subdomain; 3, 4 = Mulga Tanks subdomain east & west; 5 = Grasmere Prospect subdomain; 6 = Well Paddock subdomain; 7 =Peveril anomaly; 8 = Mulga Tanks west (2).

## 6.6 Geophysical modelling of structures and structural analysis

In order to further constrain structural information, a series of simple magnetic forward models was constructed for various anomalies within the Grasmere, Johns and Mulga Tanks Domains (Figure 6.6.1).The procedure used is the same as that outlined in Chapter 4 and Direen (1998). The following interpretations have resulted from this exercise, with results shown in Figure 6.6.2.

- Dip of the Grasmere Prospect Subdomain: this feature dips almost vertically or very steeply to the southwest.

- Dip of the Peveril Anomaly, Darts Subdomain: this feature dips steeply northeast to vertically.

- Dip of the Division Tank Subdomain: two profiles indicate that this feature dips between 80° to near-vertically to the northeast.

- Mulga Tanks Subdomain: three profiles were extracted from this apparently folded feature, two from the western limb and one from the eastern limb. The eastern limb dips c.70° east, whereas the western limb dips between vertical to 80° to the south-southwest. These data indicate that the Mulga Tanks Domain is an inclined-to-the-west asymmetric antiform. Data from Hicks & Mills (1997) suggest this feature is an anticline.

These results are consistent with steeply northeast-dipping imbricate slices within the Ponto Complex that become listric at depth as suggested by map-view analysis. The inclined anticlinal structure in the underthrust block and the structures within the Ponto Complex imply west- to southwest-directed transport and compression post-500 Ma (Figure 6.6.3).

The thrust stack was then disrupted by a north-northwest—south-southeast-directed extension which caused dextral dip-slip and strike-slip fault motions on northwest to north-northwest—directed fault arrays. (Figure 6.6.3)

# Figure 6.6.2 Results of dip sensitivity analysis, Grasmere area

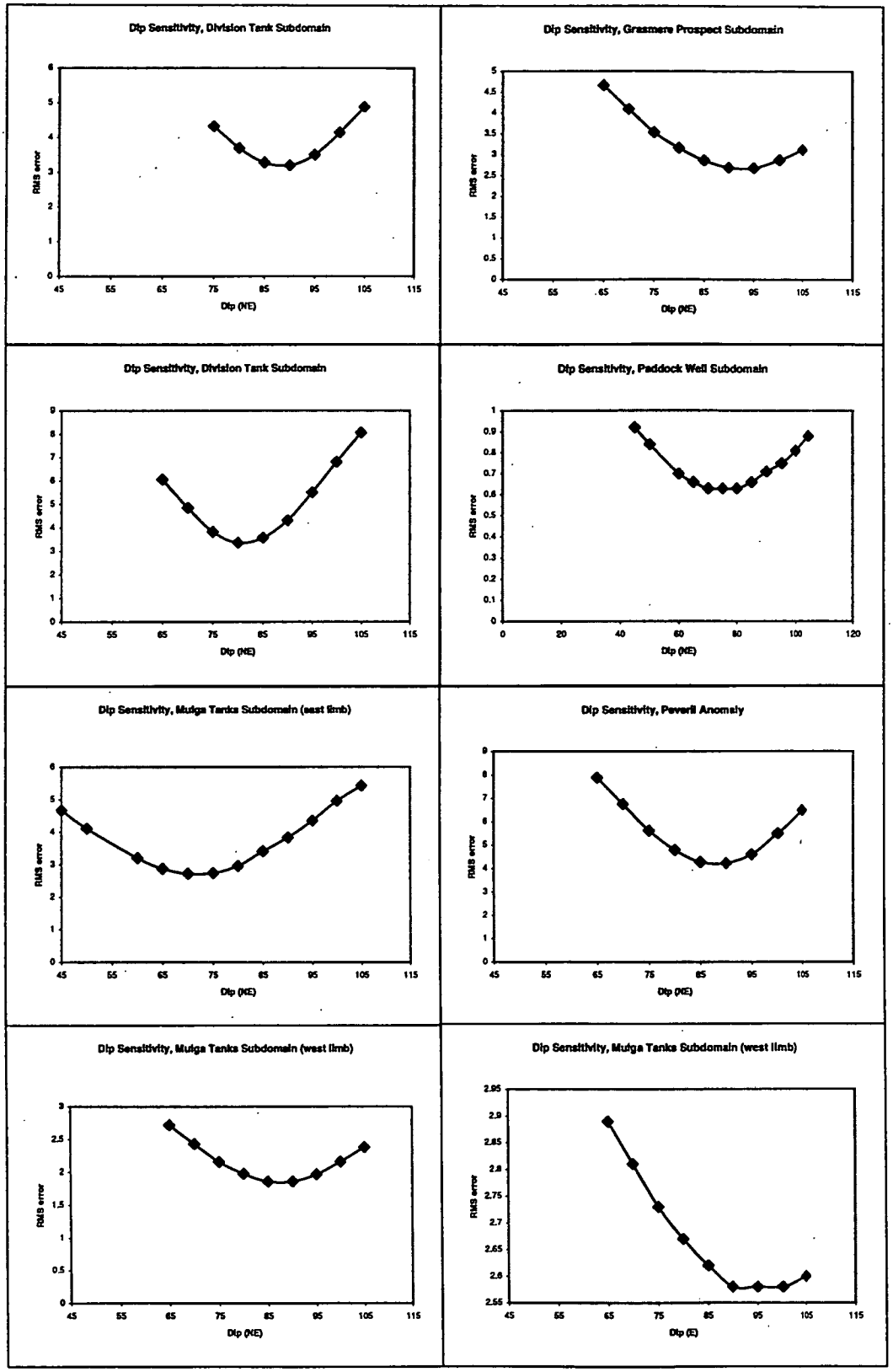

## Figure 6.6.3 Interpreted kinematic history, Grasmere Area

Late Cambrian

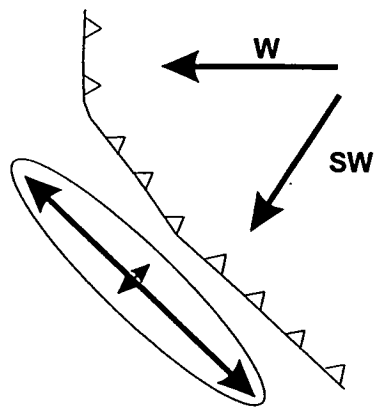


Formation of a series of west- and southwest vergent thrusts and folds

Post-Cambrian, pre-late Silurian

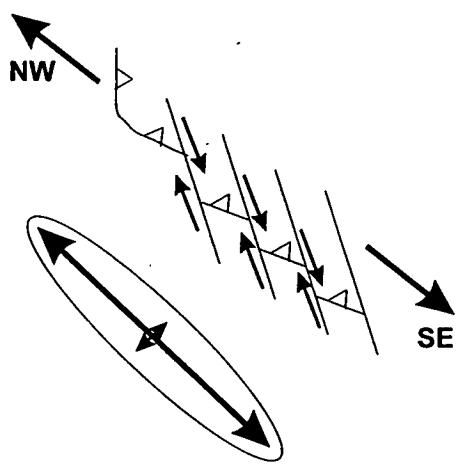


Northwest-southeast directed extension, disrupting internal parts of the thrust stack; the leading edge towards the west is unaffected

Post Late Devonian

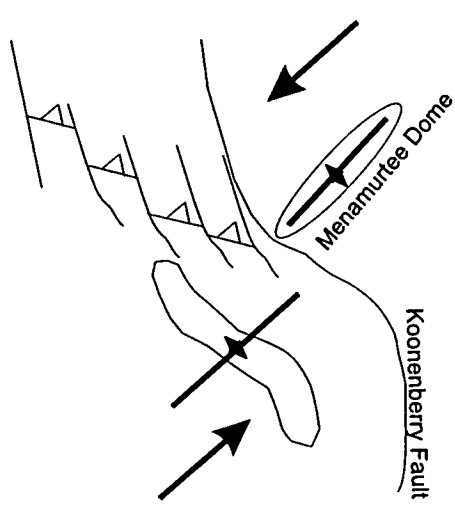


Sinistral southwest-northeast directed shearing; earlier faults and folds deformed; Menamurtee Dome forms as a restraining bend fold on the Koonenberry Fault

The formation of the "oroclinal" bend in the Late Cambrian underthrust plate and bending of the Mulga Tanks Domain from a north-northwest to a north-northeast strike was probably brought about by north-northeast oriented sinistral shear; this type of deformation explains the sigmoidal trace of the Koonenberry Fault on the Grasmere sheet, and also the north-northeast trend of the Menamurtee Anticline which has formed in a restraining bend. North-northeast— trending brittle faults found within the Mt Daubeny Formation and Mulga Downs Group are also consistent with this type of deformation, and constrain its age to Carboniferous or later. (Figure 6.6.3).

## 6.7 Igneous petrology of mafic rocks from the Blue Well Subdomain

Rocks sampled from the Blue Well Subdomain include metagabbro, metadolerite, metabasalt and altered metavolcaniclastic rocks (lava breccia and lapilli tuff). Metabasalts and dolerites are all cpx + plag-phyric. All samples have been more or less altered with calcic plag being replaced by ab-ser, and cpx replaced by epi-chl ± act, indicating greenschist facies metamorphic conditions. Other alteration minerals include qz-carb, and ser-mu in the volcaniclastics and glassy mesostasis of the basalts. These assemblages accord with the findings of Zhou (1993), who recorded a metamorphic assemblage of act-epi-cz-mu±chl in relict cpx bearing metabasalts. In contrast with Zhou (1993), no evidence for pumpellyite was found in any of the samples described above.

Seven samples (four metadolerites, two metabasalts and one metaandesite) were analysed for major and trace elements using standard whole rock XRF techniques. Major and trace element data for these rocks are shown in Table 6.7.1. Data are recalculated volatile free, with loss on ignition values reported separately. LOI values ranged from relatively low (1.8%) to high (9.23%).

Major oxide data are plotted against MgO (Figure 6.7.1). A selection of trace elements expected to have been immobile under the alteration conditions is plotted against both MgO and FeO*/MgO as an index of fractionation (Figure 6.7.2).

These data represent the only geochemical dataset for the Ponto Complex *sensu stricto* acquired by this study. For this reason, 9 analyses from the correlated Macs Tank MUMC (see chapter 5) have been used to augment the data. A field for the Ponto Complex from

**Table 6.7.1 Whole-rock analyses recalculated volatile-free for the Ponto Complex**

| Sample | 9709 | 9713 | 9811 | 9835 | 9840 | 9845 | 9862 |
|---|---|---|---|---|---|---|---|
| Rock | dolerite | basalt | basalt | dolerite | dolerite | dolerite | basalt |
| SiO2 | 50.98 | 50.99 | 53.81 | 48.38 | 47.85 | 50.45 | 51.14 |
| TiO2 | 1.56 | 1.59 | 1.61 | 1.54 | 1.30 | 1.44 | 1.60 |
| Al2O3 | 15.24 | 14.62 | 17.03 | 19.39 | 21.06 | 15.09 | 15.30 |
| Fe2O3 | 12.22 | 12.48 | 12.83 | 9.79 | 8.57 | 11.54 | 12.04 |
| FeO* | 10.99 | 11.23 | 11.54 | 8.81 | 7.72 | 10.39 | 10.83 |
| MnO | 0.24 | 0.19 | 0.13 | 0.16 | 0.13 | 0.18 | 0.24 |
| MgO | 7.00 | 5.03 | 2.38 | 4.95 | 4.85 | 7.47 | 2.02 |
| CaO | 8.99 | 11.19 | 5.40 | 11.15 | 12.29 | 10.47 | 9.51 |
| Na2O | 2.38 | 3.47 | 6.44 | 3.20 | 2.77 | 3.09 | 7.36 |
| K2O | 1.26 | 0.25 | 0.19 | 1.26 | 1.05 | 0.14 | 0.35 |
| P2O5 | 0.13 | 0.17 | 0.17 | 0.18 | 0.12 | 0.12 | 0.45 |
| LOI | 3.86 | 1.98 | 1.8 | 3.16 | 2.61 | 2.58 | 7.38 |
| | | | | | | | |
| Rb | 66 | 3 | 6 | 10 | 13 | 3 | 13 |
| Ba | 250 | 44 | 209 | 689 | 317 | 64 | 58 |
| Th | <1.5 | <1.5 | <1.5 | <1.5 | 2 | <1.5 | <1.5 |
| Nb | 3 | 3 | 1 | 8 | 6 | 3 | 1 |
| Sr | 176 | 73 | 142 | 344 | 331 | 291 | 539 |
| Zr | 101 | 98 | 98 | 119 | 93 | 98 | 113 |
| Ti | 9336 | 9524 | 9650 | 9246 | 7776 | 8611 | 9597 |
| Y | 33 | 38 | 44 | 26 | 23 | 33 | 53 |
| Ni | 65 | 109 | 83 | 39 | 44 | 57 | 68 |
| Cr | 227 | 386 | 273 | 95 | 107 | 272 | 287 |
| Pb | 6 | 2 | <1.5 | <1.5 | <1.5 | <1.5 | 15 |
| V | 102 | 249 | 272 | 244 | 205 | 300 | 270 |
| Sc | 49 | 48 | 38 | 37 | 36 | 48 | 48 |
| La | 6 | 4 | 6 | 7 | 6 | 7 | 7 |
| Ce | 12 | 12 | 12 | 19 | 14 | 13 | 12 |
| Nd | 9 | 9 | 12 | 16 | 10 | 10 | 12 |
| Zn | 122 | 102 | 70 | 73 | 69 | 88 | 80 |
| Cu | 92 | 62 | 67 | 66 | 61 | 98 | 18 |
| | | | | | | | |
| Nb/Y | 0.10 | 0.07 | 0.02 | 0.31 | 0.25 | 0.10 | 0.03 |
| Zr/Ti | 0.01 | 0.01 | 0.01 | 0.01 | 0.01 | 0.01 | 0.01 |
| FeO*/MgO | 1.57 | 2.23 | 4.85 | 1.78 | 1.59 | 1.39 | 5.38 |

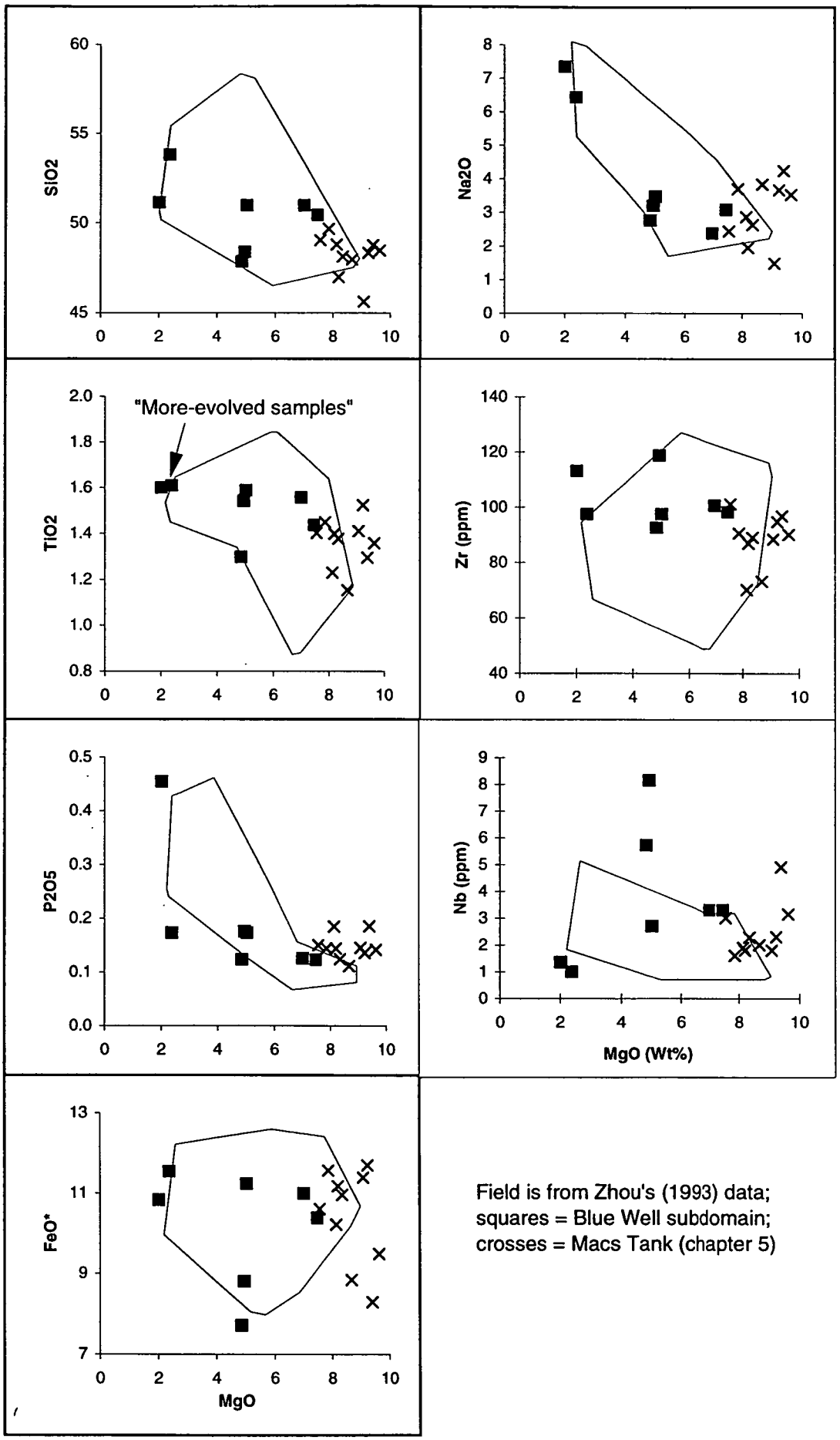


**Figure 6.7.1 Oxide/element diagrams, Ponto Complex, Grasmere**

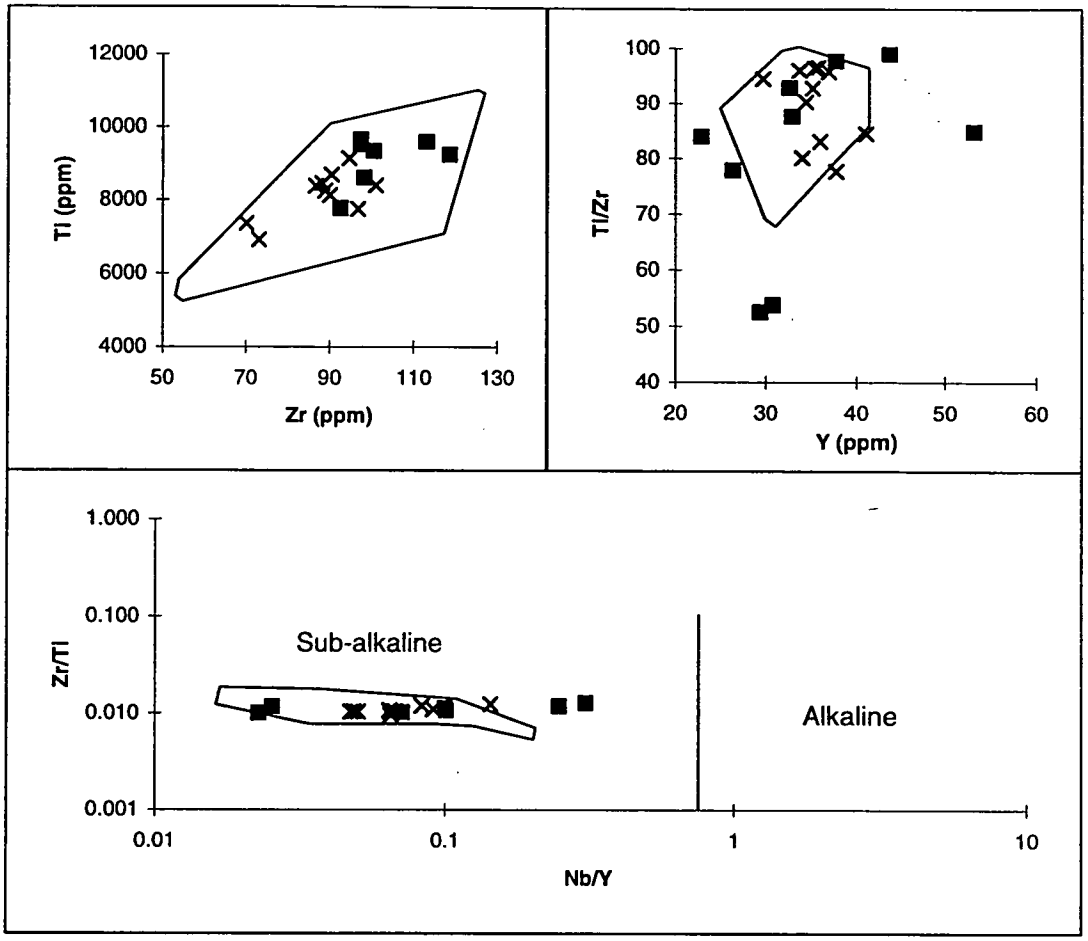


**Figure 6.7.2 Trace element discriminant diagrams, Ponto Complex Grasmere**
Field is from Zhou's (1993) data. Symbols as for Figure 6.7.1.

**Figure 6.7.3 N-MORB normalised spidergram, Ponto Complex, Grasmere**

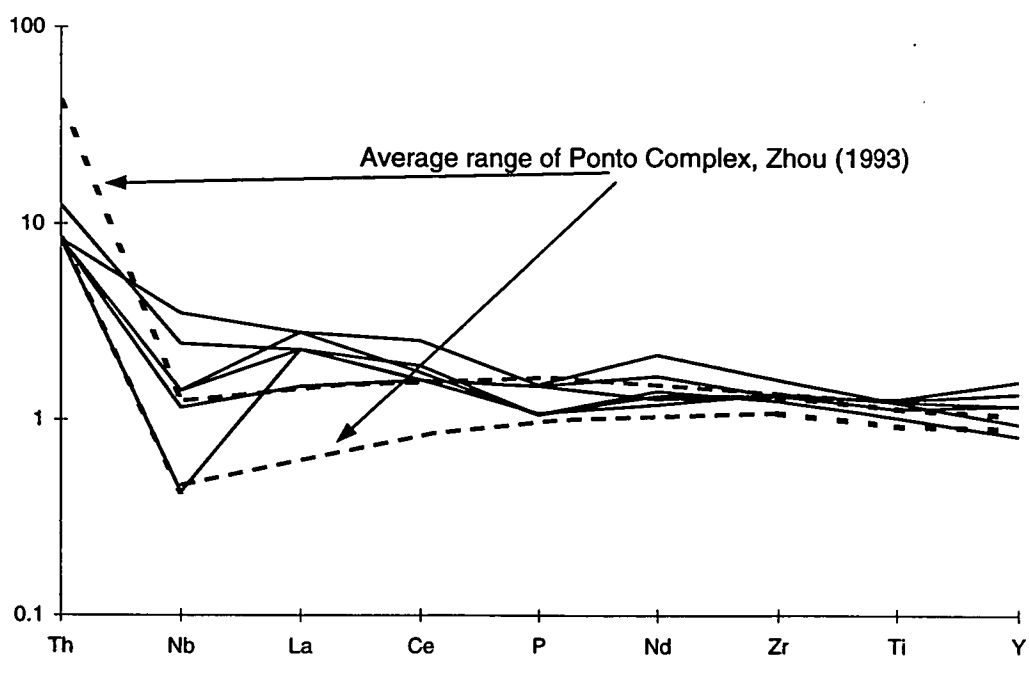

Zhou (1993) is also plotted for reference; these points represent Ponto rocks sampled from areas throughout the fold belt.

Metabasalts in the Ponto Complex in the Grasmere area include compositions very similar to those MORB-type tholeiites recorded by Zhou (1993) from the Ponto Complex, and from blocks in the Macs Tank Complex. However, two Grasmere metabasalts are notably more evolved (2-3% MgO) than most Ponto metabasalts, yet show similar Fe, Ti, Zr and Nb contents to the less-evolved compositions. This is unexpected for manifestly subalkaline tholeiitic magmas, which normally show a strong increase in FeO*, $TiO_2$ and Zr with increasing fractionation. Since these apparently evolved metabasalts have Ti/Zr values in the same range as the less-evolved Ponto metabasalts, it is likely that the these low MgO rocks are simply 'typical' Ponto metabasalts which have undergone MgO depleting metasomatism, an assumption reinforced by the exceptionally high $Na_2O$ (6-8%) in these samples compared to 2-3.5% in other Ponto metabasalts.

In summary, the suite of Ponto rocks from the Blue Well subdomain in the Grasmere-Wilandra area shows the distinctive character of igneous rocks from this complex throughout the belt: that is tholeiitic with an enriched MORB source.

### 6.8 Summary

This chapter presents new mapping, stratigraphic information, geochemistry, and integrated geophysical and structural analysis for the Grasmere 7435 1: 100 000 map sheet. These data have the potential to constrain exploration models for BIF-hosted massive sulphide mineralisation in this prospective area. They also provide clues to the timing of major tectonic features within the Koonenberry Belt, and support for the fold and thrust belt model advanced in earlier chapters and by Direen (1998).

Geophysical mapping shows the distribution of the Ponto Complex is strongly controlled by two major faults, in analogous situation to the Gnalta Group at Mt Wright. The Grasmere Creek Fault appears to represent the leading edge of an imbricate fan and, unsurprisingly, splays from the Mt Wright Fault on the Nuchea 7335 map sheet. The footwall of the Grasmere Creek Fault contains poorly exposed and deformed equivalents of the Gnalta Group, analogous to the footwall of the Mt Wright Fault.

Between the Grasmere Creek Fault and Prospectors Creek Fault, the Ponto Complex comprises at least two distinct slices, containing internal imbrications. Horses within the Ponto appear from the magnetics to be largely transposed northeast dipping limbs of asymmetric isoclinal folds inclined to the southwest. The northern of the two domains contains igneous rocks equivalent to the Macs Tank Mafic-Ultramafic Complex which crops out in the same thrust sheet on Nuchea 7335. The two domains within the Ponto Complex, the Grasmere and Division Tank Domains, are separated by an out-of-sequence nappe of Kara beds and Teltawongee Group This repetition of stratigraphy from the Nundora area confirms the validity of a fold-and-thrust model for the Koonenberry Belt.

The tectonic history of the Grasmere area is consistent with that of the areas to the north and west examined in previous chapters. A post-Boomerangian folding and thrusting event emplaced a marginal or backarc basin fragment (the Ponto Complex) over continental shelf sediments (Gnalta Group, Kara beds equivalents). Post-Early Ordovician, pre-Late Silurian deformation involved further southwest-directed thrusting, producing out-of-sequence nappes and a new penetrative fabric in Palaeozoic rocks. This was followed by a phase of late west-northwest-southeast—directed extension, opening accommodation space for the Mt Daubeny basin, and producing dextral fault arrays in the thrust stack. In post-Early Carboniferous times, the whole area was subject to a northeast-directed dextral shear couple which produced ductile and brittle responses in basement and cover, respectively.

**Chapter 7 Palaeozoic rocks of the Darling River Lineament and Scopes Range**

# Chapter 7 Palaeozoic rocks of the Darling River Lineament and Scopes Range

## 7.1 Study area defined. Reasons for study.

The Scopes Range- Darling River Lineament is situated on the Bunda 7434, Topar 7334 and Menindee 7333 1: 100 000 map sheets, in an area approximately defined by the AMG Zone 54 coordinates 595000 mE 6430000 mN - 595000 mE 6513000 mN - 689000 mE 6510000 mN (Figure 7.1.1)

The east-north east trending Darling River Lineament (DRL) (Scheibner, 1973; Katz, 1976; Stevens, 1986) is a continental scale tectonic lineament extending into Queensland and South Australia (Scheibner, 1973). It has been cited as comprising a part of the so-called "Tasman Line" (e.g. Powell, 1996).

Magnetic anomalies in the DRL strike west-southwest—east-northeast, and have been drilled for a variety of commodities, including copper-gold (CRAE, 1996), diamonds (CRAE, 1985), Broken Hill Type (BHT) massive sulphide (Pasminco, 1996) and Volcanic Hosted Massive Sulphide (VHMS) (BHP, 1997). No economic discoveries have been made to date. Many drillholes (Wahratta; Eaglehawk 1,2 & 3; Dolo 19 & 20; Inkerman 1,2,4,5,6,7 & 8: see Figure 7.3.1) have intersected interpreted Palaeozoic volcanic and intrusive rocks, ranging in composition from rhyolite through to kimberlite. Also of interest are some poorly exposed mafic pipe-like intrusions at Comarto, at the intersection of the lineament and the northwest-trending Koonenberry Belt. The tectonic environments of all these igneous rocks, and thus to postulated models for the tectonic significance of the Darling River Lineament are the subject of this chapter.

## 7.2 Access to samples

No field work was conducted in this area, obviating the need for descriptions of access and topography in the area.

Diamond core samples for the Wahratta and Dolo prospects were obtained from the CRAE / Rio Tinto core yard in Broken Hill. At the time of writing, the Wahratta core was being administered by Eaglehawk Consulting for the new licence holders, Platsearch N.L. Diamond core samples for the Eaglehawk prospect were obtained from the Pasminco Exploration core yard, also in Broken Hill. Rock chip samples from an RC drilling program on the Inkerman prospect were obtained from the BHP Exploration

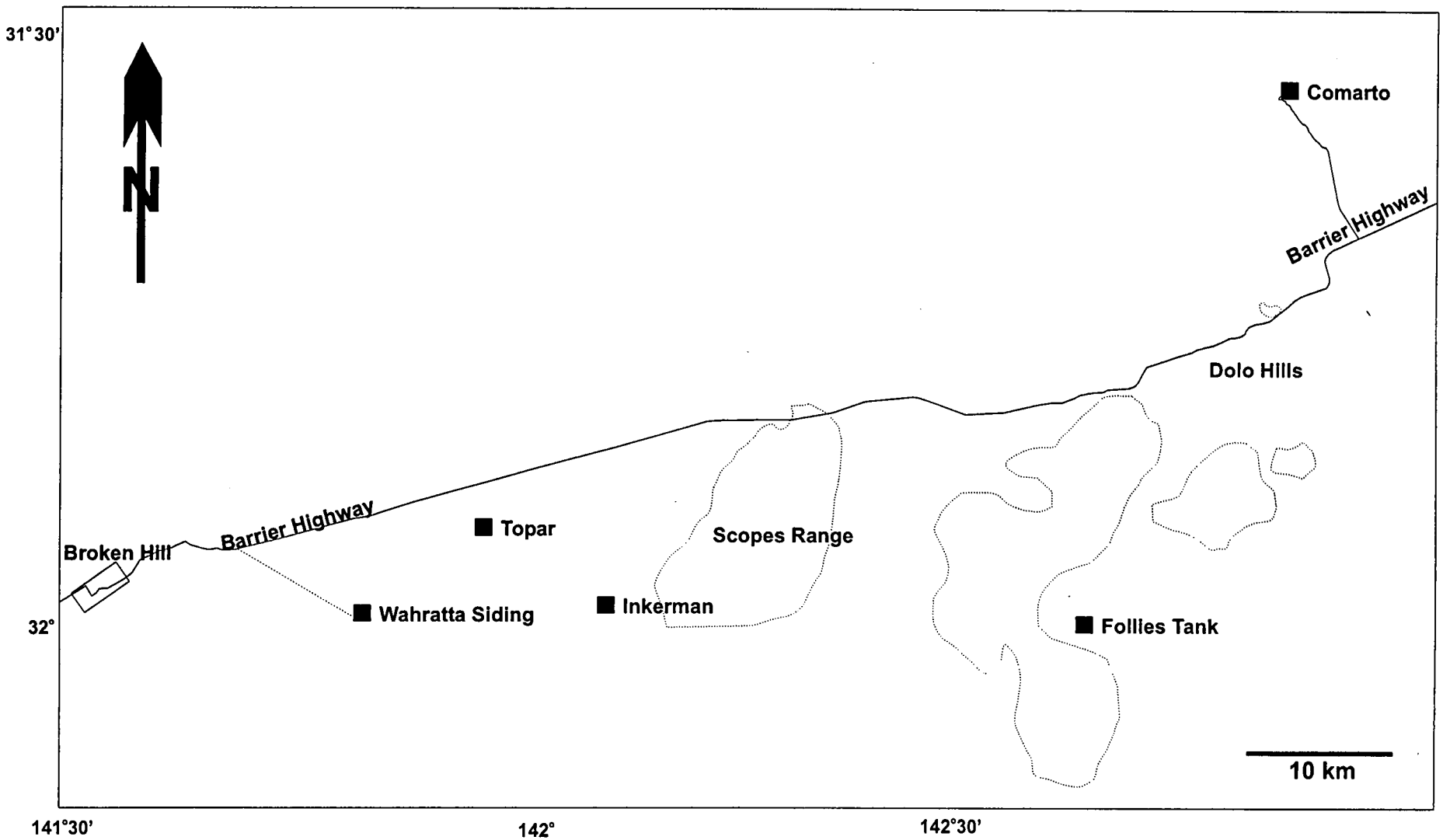


**Figure 7.1.1 Locality Map. Scopes Range - Darling River Lineament Area.**

house in Broken Hill; however, the unprotected outdoor storage of these samples at that location has since led to significant degradation. All diamond core samples, thin sections, powders and XRF pills used in this study are lodged with the Curator of the School of Earth Sciences, University of Tasmania.

### 7.3 Drilling Locations. Additional Information: drilling, mapping, geochemistry.

The distribution of the drillholes selected for study is shown in Figure 7.3.1. In addition, 12 other drillholes by CRAE are shown. These drillholes intersected a variety of sedimentary rocks that put the igneous intersections into context.

The oldest rocks mapped within the DRL studied are the Kara beds on the Bunda 7434 sheet. These crop out poorly at Scrubbys Tank, north of the Scopes Range and on the hangingwall side of the Koonenberry Fault. Although none of the igneous units to be examined in this chapter was found intruding the Kara beds, this occurrence is mentioned because of it is believed to represent the position of the (now) parautochthonous ?Late Neoproterozoic rift system (see Chapter 4).

Holes DL7, 9, 10, 14, 19 & 20 all intersected red or green-grey metasiltstone-sandstone and minor shale correlated with the Teltawongee Group (Mills, pers. comm. 1998; and core logging, this study). These are intruded by quartz-feldspar porphyries in holes DL 19 & 20, indicating a post-?Middle Cambrian age of intrusion.

Magnetic metasiltstone was described in DL 13; this may correlate with the Ponto Complex. Rocks assigned to the Ponto Complex were mapped by Hicks & Mills (1997) on Bunda at Dolo Hill, indicating that these rocks also make up part of the DRL.

Clean, cross-bedded quartzites of the Cambro-Ordovician Scopes Range Beds were intersected in drillholes DL 8, 12, 17 & 18. Hicks & Mills (1997) mentioned "rare felsic volcanic units" in the Scopes Range Beds, but no drillhole has intersected these.

Zhou (1993) analysed 10 samples of metabasalt and metadolerite collected from pipe-like bodies at Comarto. These pipes, mapped by Hicks & Mills (1997) in the hangingwall (western side) of the Koonenberry Fault, are only metamorphosed to prehnite-pumpellyite facies (Zhou, 1993) and show no penetrative cleavage (Hicks & Mills, 1997). Zhou (1993) inferred these rocks to have an Early Cambrian age based on their metamorphic grade and a dubious correlation with the "Mt Wright Volcanics" (actually Mt Arrowsmith Volcanics, Crawford et al., 1997; see chapter 5). However,

TMI pseudocolour and intensity layer, shaded at 45 degrees from the northeast. Key:
J = Jupiter-1;
PR = Pondie Range-1;
D345 = Dolo 3-5;
D7-9;17-20 = Dolo 7-9 & 17-20;
FT = Follies Tank 1-5;
BG = Black Gate-1;
P = Pamamaroo-1;
M = Inkerman 7&8, Little Topar A1-8, B1-2 & C1, Dolo 10-16 & 20-21, Byrnedale-1;
W = Wahratta;
I1-6 = Inkerman 1-6;
K = Kars-1;
E1-3 = Eaglehawk 1-3

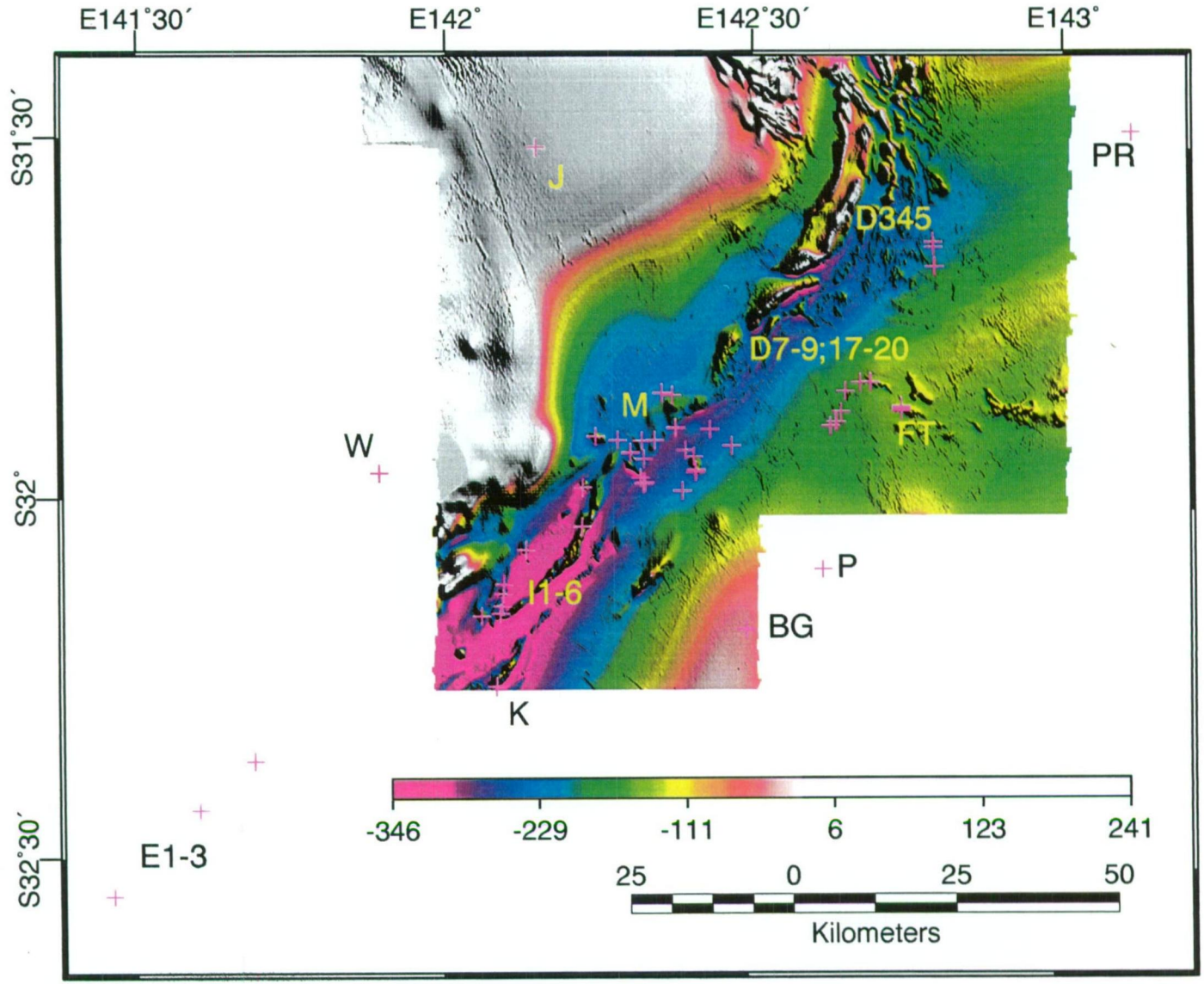


**Figure 7.3.1 Drillhole locations, Scopes Range and Darling River Lineament**

Hicks & Mills (1997) mapped and interpreted Ponto Complex lithologies all along the hangingwall of the Koonenberry Fault on Bunda 7434, consistent with areas to the north (see chapter 6). This means that the pipes at Comarto must be post-500 Ma, based on the SHRIMP zircon dates from the Ponto Complex at Grasmere (see Chapter 6.5). Prehnite-pumpellyite grade andesite lavas crop out west of the Koonenberry Fault on the Grasmere 7435 sheet (Senior & Senior, 1995); these are interbedded with the Late Silurian-Early Devonian Mt Daubeny Formation, and are interpreted to have been metamorphosed during the Middle Devonian Tabberabberan event in the Lachlan Orogen. Their similar metamorphic grade to the pipes could mean that the Comarto rocks have an intrusive age between Early Ordovician and Early Devonian.

Nb/Y versus Ti/Zr (Zhou, 1993) indicated that the Comarto pipes are sub-alkaline, and are predominantly tholeiitic. N-MORB normalised spidergrams of these samples showed E-MORB or OIB type patterns with strong Th and moderate P enrichment; K depletion, attributed to remobilisation, was also a feature of these rocks. On the basis of these characteristics, Zhou (ibid.) inferred a within-plate setting.

### 7.4 Questions arising from previous studies

The Darling River Lineament is a zone of faults (e.g. Redan Fault, Koonenberry Fault), shear zones (e.g. Anabama Fault) and geophysical linear features. Most authors have considered the DRL to be a zone of dextral shear (Scheibner, 1973; Katz, 1976; Stevens, 1986). However, the DRL was also believed by Powell (1998, 1996) and Veevers & Powell (1984) to represent a sinistral transform margin during breakup of Rodinia in the Mid Neoproterozoic (pre-755 Ma: Wingate, 1998)

Recent deep crustal-upper mantle seismic reflection investigations and gravity profile modelling (Owen et al., 1997) show that the DRL dips to the southeast at between 50° to 60°, and is a zone of crustal thinning of c.5 km on the downthrown (southeastern) side. This geometry is inconsistent with the vertical dip expected from a strike-slip fault.

The main apparent tectonism associated with the DRL is of Devonian age, when it acted as a series of down-to-the-southeast normal faults, accommodating several kilometres thickness of Mulga Downs Group sediments in the Menindee Trough (Owen et al., 1997). Younger, pre-Cretaceous faulting has deformed the Devonian sediments in accommodating Murray Basin sedimentation (Owen et al., 1997).

The affinities of ?Palaeozoic igneous rock suites at Comarto, and intersected in the Dolo, Inkerman, Wahratta and Eaglehawk prospects, and their relationships to different magnetic features within the DRL must shed new light on the nature of this continental scale lineament.

## 7.5 Petrography of igneous rocks from the Darling River Lineament-Scopes Range

Inkerman: These drillholes were targeted for VHMS style mineralisation associated with magnetic anomalies at the southwestern end of the Scopes Range (BHP, 1997) (Figures 7.1.1; 7.3.1). Twenty thin sections were made from rock chip samples acquired by sieving RC drill cuttings. Igneous samples ranged in composition from basalt to dacite and diorite. Two samples of phyllite were also investigated.

Diorite was intersected in holes IR 001, 004, 005 & 007. These rocks are all coarse, equigranular plag-cpx-hbl-op-bio diorites. Alteration of cpx to hbl-act and plag to ab-ser indicates metamorphism in the middle to upper greenschist facies. These intrusive rocks are all believed to be co-magmatic.

Cpx+hbl-phyric andesites with a groundmass of microlitic plag, bio and opaques were intersected in holes IR 002 & 008. These are believed to represent thin dykes that are co-magmatic with the diorites. These dykes also have an act-hbl + chl-ser metamorphic assemblage, indicating upper greenschist conditions.

Further variations of this suite were encountered in holes IR 007 & 008. These are cpx+plag+qz+hbl-phyric andesites and plag+qz+hbl-phyric dacite with chl-ser altered glassy groundmass. Resorbed quartz crystals and glassy groundmass in these rocks suggest that they are lavas.

Hole IR 005 intersected mafic basaltic andesites. These contain a phenocryst assemblage of plag-cpx-op in a chl-altered glassy groundmass. These rocks are probably also lavas.

Finally, hole IR 006 drilled quite different lithologies. Cpx+plag-phyric metabasalt with blue hbl metamorphic alteration of cpx occurs between two intervals of qz-mu-chl phyllite. This near-amphibolite-grade rock may represent a dyke in the phyllitic country rock to the basaltic andesite-andesite-dacite-diorite suite. The cleavage in the phyllite is a weak spaced slaty cleavage.

Dolo prospect: qz-ksp porphyritic rhyolite dykes were intersected in both DL 19 and DL 20. These also contain minor plagioclase and primary muscovite, with sericite alteration of both feldspar types. No cleavage was apparent in this suite. Drill logs (Mills, 1985, unpublished data) indicate that these porphyries intrude undifferentiated Teltawongee Group turbidites. A sample from DL 20, 70 m is a rhyolitic lava containing primary quartz, K-feldspar, plagioclase, hornblende and biotite, with sericite alteration of feldspars and the glassy groundmass.

Eaglehawk prospect: The Eaglehawk prospect lies to the southwest of Broken Hill, and was targeted for BHT mineralisation over magnetic and EM conductivity anomalies (Pasminco, 1996) (Figure 7.3.1). Two samples from EHK1 are cumulate monzogabbros, containing cpx phenocrysts + plag, ksp, bio, mt and blocky ap. These rocks were described in Pasminco (1996) as aug-bio microgabbro. EHK 2 contained a hornblende-bearing cumulate monzogabbro (plag + ksp + cpx-phyric + accessory hbl, bio, zrc and ap), which was also described in Pasminco (1996) as aug-bio-hbl microgabbro; and biotite monzodiorite (plag + ksp + bio phenocrysts + minor qz). EHK 3 intersected two main rock types: bio-hbl andesite lavas (bio-hbl-aug ± plag phenocrysts + plag-ksp ± ap, in an altered groundmass of plag, qz and glass); and dolerite dykes (plag-aug ± bio, mt, il). The dolerite dykes also contain the metamorphic assemblage epi-chl-act or epi-act-hbl, indicating upper greenschist facies metamorphic conditions.

Wahratta: This hole was drilled on a large magnetic anomaly on the southeastern edge of the Broken Hill block, outside the D2000 magnetic data coverage. The target was breccia-fill Cu-Au-U mineralisation. Twenty thin sections were examined from between 827 and 1081 metres depth, 1082 m being the total depth of the hole. There appear to be two distinct igneous suites intersected at Wahratta. The earlier is a suite of monzogabbros to monzodiorites similar to that described from Eaglehawk. These are coarse, sometimes cumulate textured, intrusives with ksp-plag-hbl-cpx-qz-op-ap-zrc all abundant. Plagioclase and K-feldspar in these rocks is often sericitised, and clinopyroxene has been metamorphosed to actinolite, indicating greenschist facies metamorphism. One sample (9926) has a carb-epi-pre assemblage, indicating calcic metasomatism.

Possibly associated with this suite are hornblende andesites intersected at depths of 1058-1060 m, and trachybasalt dykes or flows between 827 and 838 m. The hornblende andesite dykes have ksp-aug-plag-hbl + minor op-qz mineralogy, whereas

the trachybasalts are plag + ksp + cpx + ap- phyric with a strongly epidote altered groundmass of relict trachytic-textured plagioclase.

Evolved greenschist facies dolerite dykes intrude this suite between 919 and 1081 m. At shallower depths these dykes are strongly ab-chl-ser-epi altered, with little or no relict mafic phenocrysts, and a relict ksp-plag-op mineralogy. The deepest samples (1066 & 1081 m) retain primary biotite and clinopyroxene crystals interlocked with feldspar and opaques. Clinopyroxene has also been metamorphosed to actinolite in these dykes, indicating a pre-metamorphic age for the second intrusion event.

## 7.6 Geochemistry of igneous rocks from the Darling River Lineament-Scopes Range

Thirty-seven samples from the Darling River Lineament were analysed for major and trace elements using standard XRF techniques and sample preparation procedures as outlined in earlier chapters. The samples were chosen to give the broadest possible range of compositions in both volcanic and intrusive rocks, while avoiding alteration. The final set consisted of two rhyolites from the Dolo prospect; ten andesites, one dacite, six diorites and one dolerite from Inkerman; three andesites, three monzogabbros and three dolerites from Eaglehawk; and two trachybasalts, three monzogabbros, one monzodiorite and two dolerites from Wahratta. Results are given in Table 7.6.1.

The data are presented graphically for a selection of major oxides and trace elements (Figures 7.6.1 & 7.6.2). A tectonic discrimination diagram is also shown (Figure 7.6.2). Indicative major and trace elements from the intrusive suites at Wahratta are also plotted separately against FeO*/MgO as an index of fractionation (Figure 7.6.4).

Plotted also for reference are two analyses of dacite from volcanics intersected in Bancannia South-1. (B.Stevens, unpublished data). These included welded crystal-vitric rhyodacitic-dacitic and andesitic tuffs, and plagioclase-phyric dacite lavas interpreted to have shoshonitic affinities (Barron, 1990). SHRIMP zircon dating of a sample of dacite gave an imprecise age of 497 ± 11 Ma, which is Middle Cambrian (Ordian) to Early Ordovician (Warendan) (Stevens & Fanning, unpublished data). This date may help to constrain the ages of the other, undated intrusives.

Also included is an analysis from a mafic diorite drilled in the VIMP-11 drillhole within the Miga Subzone of western Victoria. This rock has been SHRIMP zircon dated at

| | Inkerman | | | | | | | | | |
|---|---|---|---|---|---|---|---|---|---|---|
| Sample | 007(132-134) | 007(150-152) | 008(42-44) | 008(48-50) | 008(50-52) | 008(58-60) | 005(174-176) | 005(178-180) | 002(136-137) | 002(137-138) |
| Rock | hbl andesite | hbl andesite | dacite | andesite | andesite | andesite | bas-andesite | bas-andesite | andesite | andesite |
| SiO2 | 71.13 | 70.83 | 68.85 | 69.78 | 68.12 | 68.42 | 58.81 | 55.78 | 56.15 | 56.45 |
| TiO2 | 0.36 | 0.35 | 0.48 | 0.40 | 0.46 | 0.46 | 0.70 | 0.82 | 0.90 | 0.91 |
| Al2O3 | 14.90 | 14.81 | 15.46 | 15.27 | 15.39 | 15.35 | 14.82 | 14.96 | 16.63 | 16.55 |
| Fe2O3 | 3.45 | 3.22 | 4.24 | 3.27 | 3.29 | 3.67 | 7.82 | 8.31 | 7.95 | 7.93 |
| FeO* | 3.10 | 2.89 | 3.81 | 2.94 | 2.96 | 3.30 | 7.03 | 7.48 | 7.15 | 7.14 |
| MnO | 0.02 | 0.03 | 0.05 | 0.04 | 0.05 | 0.06 | 0.15 | 0.15 | 0.15 | 0.13 |
| MgO | 0.82 | 1.16 | 3.38 | 1.95 | 1.78 | 1.88 | 5.70 | 7.38 | 4.70 | 4.73 |
| CaO | 1.52 | 1.75 | 0.78 | 1.96 | 2.27 | 1.87 | 6.60 | 7.92 | 7.71 | 7.38 |
| Na2O | 4.19 | 4.43 | 3.29 | 4.11 | 4.80 | 5.96 | 3.84 | 3.37 | 3.82 | 3.87 |
| K2O | 3.47 | 3.29 | 3.32 | 3.10 | 3.69 | 2.19 | 1.44 | 1.18 | 1.76 | 1.80 |
| P2O5 | 0.14 | 0.14 | 0.16 | 0.13 | 0.14 | 0.14 | 0.14 | 0.14 | 0.24 | 0.24 |
| LOI | 1.94 | 1.36 | 5.24 | 2.23 | 2.82 | 1.58 | 0.87 | 0.26 | 0.43 | 0.46 |
| | | | | | | | | | | |
| Nb | 17 | 18 | 13 | 14 | 15 | 15 | 6 | 8 | 7 | 8 |
| Zr | 202 | 205 | 178 | 201 | 182 | 205 | 112 | 113 | 129 | 134 |
| Sr | 320 | 341 | 103 | 254 | 180 | 248 | 585 | 544 | 1103 | 1071 |
| Ba | 883 | 909 | 983 | 976 | 1060 | 459 | 954 | 425 | 670 | 687 |
| Sc | 5 | 6 | 7 | 5 | 7 | 6 | 23 | 24 | 22 | 23 |
| V | 36 | 39 | 54 | 39 | 47 | 38 | 167 | 202 | 201 | 197 |
| Y | 21 | 20 | 16 | 15 | 16 | 15 | 20 | 20 | 23 | 23 |
| Rb | 114 | 104 | 90 | 70 | 90 | 58 | 41 | 32 | 39 | 39 |
| Pb | 7 | 7 | 6 | 6 | 6 | 7 | 8 | 5 | 12 | 11 |
| Zn | 42 | 38 | 42 | 31 | 33 | 49 | 97 | 81 | 82 | 83 |
| Cu | 9 | 11 | 13 | 13 | 9 | 10 | 42 | 50 | 85 | 25 |
| Ni | 6 | 7 | 18 | 10 | 17 | 15 | 102 | 118 | 31 | 30 |
| Ti | 2158 | 2082 | 2851 | 2396 | 2783 | 2744 | 4199 | 4933 | 5394 | 5440 |
| Zr/Ti | 0.09 | 0.10 | 0.06 | 0.08 | 0.07 | 0.07 | 0.03 | 0.02 | 0.02 | 0.02 |
| Zr/Nb | 11.81 | 11.39 | 14.02 | 14.06 | 12.47 | 13.58 | 18.06 | 15.07 | 18.70 | 17.40 |
| Nb/Y | 0.83 | 0.90 | 0.80 | 0.93 | 0.93 | 1.00 | 0.32 | 0.37 | 0.31 | 0.33 |
| FeO*/MgO | 3.77 | 2.49 | 1.13 | 1.51 | 1.66 | 1.76 | 1.23 | 1.01 | 1.52 | 1.51 |

**Table 7.6.1 Whole-rock analyses recalculated volatile-free for igneous suites, Darling River Lineament**

| | Inkerman (cont.) | | | | | | | | Bancannia South | | |
|---|---|---|---|---|---|---|---|---|---|---|---|
| Sample | 002(144-146) | 001(142-144) | 001(156-158) | 004(158-160) | 004(178-180) | 005(188-190) | 005(198-200) | 006(172-174) | Sample | BS10 | BS11 |
| Rock | andesite | diorite | diorite | diorite | diorite | diorite | diorite | dolerite | Rock | Dacite | Dacite |
| SiO2 | 56.52 | 53.07 | 53.68 | 59.02 | 62.98 | 55.41 | 54.82 | 49.94 | SiO2 | 64.98 | 65.17 |
| TiO2 | 0.91 | 0.89 | 0.90 | 0.86 | 0.59 | 0.85 | 0.57 | 1.41 | TiO2 | 0.76 | 0.79 |
| Al2O3 | 16.62 | 16.08 | 16.16 | 18.11 | 16.82 | 15.41 | 16.40 | 14.26 | Al2O3 | 16.15 | 16.01 |
| Fe2O3 | 7.82 | 9.27 | 8.87 | 6.92 | 5.22 | 8.74 | 7.84 | 13.41 | Fe2O3 | 2.83 | 2.86 |
| FeO* | 7.04 | 8.34 | 7.99 | 6.23 | 4.70 | 7.86 | 7.06 | 12.07 | FeO* | 2.30 | 2.28 |
| MnO | 0.12 | 0.15 | 0.14 | 0.13 | 0.09 | 0.15 | 0.14 | 0.29 | MnO | 0.09 | 0.09 |
| MgO | 4.79 | 7.05 | 7.05 | 3.37 | 3.04 | 6.98 | 8.00 | 7.70 | MgO | 1.66 | 1.72 |
| CaO | 7.29 | 9.13 | 8.91 | 5.09 | 4.72 | 7.76 | 8.43 | 10.06 | CaO | 1.67 | 1.69 |
| Na2O | 3.97 | 3.22 | 3.28 | 4.43 | 4.24 | 3.53 | 2.89 | 2.24 | Na2O | 5.11 | 4.90 |
| K2O | 1.71 | 0.94 | 0.95 | 1.83 | 2.16 | 1.06 | 0.89 | 0.66 | K2O | 4.20 | 4.24 |
| P2O5 | 0.24 | 0.21 | 0.15 | 0.30 | 0.21 | 0.18 | 0.05 | 0.11 | P2O5 | 0.24 | 0.24 |
| LOI | 0.87 | 0.77 | 0.83 | 1.88 | 1.93 | 2.05 | 1.89 | 1.92 | LOI | 1.53 | 1.54 |
| | | | | | | | | | | | |
| Nb | 7 | 4 | 5 | 12 | 10 | 4 | 3 | 1 | Nb | 14 | 21 |
| Zr | 136 | 60 | 77 | 163 | 166 | 83 | 71 | 82 | Zr | 260 | 250 |
| Sr | 1079 | 708 | 752 | 692 | 712 | 664 | 715 | 143 | Sr | 300 | 310 |
| Ba | 675 | 462 | 436 | 846 | 931 | 381 | 326 | 55 | Ba | 730 | 730 |
| Sc | 22 | 27 | 28 | 16 | 13 | 25 | 28 | 48 | La | 41.7 | 41.7 |
| V | 196 | 220 | 205 | 156 | 102 | 175 | 215 | 333 | Ce | 80.6 | 81.4 |
| Y | 23 | 20 | 19 | 21 | 15 | 15 | 16 | 35 | Nd | 38 | 38.1 |
| Rb | 35 | 24 | 27 | 67 | 74 | 32 | 31 | 31 | Sc | 11 | 12 |
| Pb | 11 | 8 | 9 | 13 | 11 | 20 | 26 | 6 | V | 66 | 60 |
| Zn | 80 | 83 | 84 | 76 | 54 | 108 | 136 | 102 | Y | 35 | 31 |
| Cu | 41 | 47 | 59 | 35 | 53 | 78 | 44 | 53 | Rb | 160 | 160 |
| Ni | 28 | 73 | 76 | 15 | 30 | 127 | 103 | 50 | Th | 17 | 12 |
| Ti | 5475 | 5334 | 5399 | 5139 | 3555 | 5078 | 3442 | 8449 | Pb | 250 | 105 |
| Zr/Ti | 0.02 | 0.01 | 0.01 | 0.03 | 0.05 | 0.02 | 0.02 | 0.01 | Ti | 4554 | 4738 |
| Zr/Nb | 19.15 | 15.00 | 16.38 | 13.47 | 16.77 | 18.86 | 20.88 | 68.33 | | | |
| Nb/Y | 0.31 | 0.20 | 0.25 | 0.58 | 0.64 | 0.30 | 0.21 | 0.03 | Nb/Y | 0.40 | 0.68 |
| FeO*/MgO | 1.47 | 1.18 | 1.13 | 1.85 | 1.55 | 1.13 | 0.88 | 1.57 | Zr/Ti | 0.06 | 0.05 |

**Table 7.6.1** (cont.)

| | Dolo | | Eaglehawk | | | | | | | | |
|---|---|---|---|---|---|---|---|---|---|---|---|
| Sample | DL19/126.8 | DL20/70 | EHK3/207.1 | EHK3/125.8 | EHK3/137.1 | EHK1/109. | EHK2/180. | EHK2/194 | EHK3/153. | EHK3/177. | EHK3/305.3 |
| Rock | rhyolite | rhyolite | andesite lava | andesite lava | andesite lava | mzgabbro | mzgabbro | mzdiorite | dolerite | dolerite | dolerite |
| SiO2 | 77.50 | 76.45 | 67.22 | 64.31 | 62.04 | 57.08 | 57.97 | 64.57 | 50.72 | 50.58 | 50.21 |
| TiO2 | 0.07 | 0.06 | 0.37 | 0.65 | 0.64 | 0.80 | 0.94 | 0.58 | 2.54 | 1.91 | 1.43 |
| Al2O3 | 13.08 | 13.37 | 17.00 | 17.68 | 16.88 | 15.70 | 16.19 | 17.30 | 16.41 | 15.43 | 18.20 |
| Fe2O3 | 1.16 | 1.52 | 3.06 | 4.23 | 5.59 | 6.86 | 7.05 | 4.55 | 11.69 | 10.56 | 9.12 |
| FeO* | 1.05 | 1.37 | 2.76 | 3.81 | 5.03 | 6.17 | 6.34 | 4.09 | 10.52 | 9.50 | 8.21 |
| MnO | 0.00 | 0.02 | 0.03 | 0.05 | 0.05 | 0.11 | 0.10 | 0.03 | 0.16 | 0.17 | 0.14 |
| MgO | 0.34 | 0.33 | 1.45 | 2.30 | 2.96 | 5.83 | 5.07 | 2.35 | 4.05 | 7.36 | 6.54 |
| CaO | 0.19 | 0.37 | 3.56 | 2.36 | 5.28 | 7.20 | 6.94 | 3.52 | 8.42 | 9.24 | 9.66 |
| Na2O | 2.96 | 3.37 | 5.40 | 6.42 | 5.67 | 3.91 | 3.64 | 4.91 | 4.57 | 3.56 | 3.19 |
| K2O | 4.66 | 4.48 | 1.73 | 1.67 | 0.61 | 2.14 | 1.88 | 1.97 | 1.02 | 0.92 | 1.10 |
| P2O5 | 0.03 | 0.03 | 0.17 | 0.33 | 0.28 | 0.36 | 0.21 | 0.22 | 0.42 | 0.28 | 0.41 |
| LOI | 1.11 | 1.19 | 0.95 | 3.35 | 2.49 | 1.09 | 1.65 | 1.24 | 1.74 | 0.87 | 0.95 |
| Nb | 10 | 12 | 11 | 13 | 23 | 8 | 8 | 18 | 13 | 15 | 24 |
| Zr | 90 | 75 | 190 | 188 | 208 | 141 | 118 | 193 | 182 | 144 | 160 |
| Sr | 52 | 77 | 808 | 682 | 403 | 885 | 881 | 1035 | 762 | 382 | 531 |
| Ba | 293 | 282 | 795 | 584 | 215 | 851 | 481 | 594 | 347 | 239 | 313 |
| Cr | 2 | 3 | 22 | 68 | 40 | 253 | 98 | 29 | 58 | 238 | 129 |
| La | 25 | 20 | 52 | 42 | 66 | 52 | 37 | 62 | 24 | 21 | 31 |
| Ce | 54 | 39 | 93 | 80 | 101 | 103 | 71 | 108 | 48 | 43 | 60 |
| Nd | 26 | 20 | 32 | 35 | 38 | 49 | 31 | 40 | 20 | 24 | 27 |
| Sc | 4 | 5 | 5 | 12 | 36 | 18 | 21 | 9 | 10 | 39 | 27 |
| V | 3 | 2 | 43 | 103 | 346 | 155 | 172 | 91 | 103 | 300 | 198 |
| Y | 25 | 27 | 14 | 17 | 42 | 23 | 21 | 20 | 16 | 30 | 22 |
| Rb | 198 | 204 | 46 | 41 | 26 | 55 | 54 | 80 | 18 | 24 | 24 |
| Th | 23 | 16 | 14 | 13 | 5 | 10 | 9 | 21 | 12 | 3 | 5 |
| Pb | 14 | 5 | 5 | 14 | 8 | 8 | 4 | 13 | 7 | <1.5 | 2 |
| Ti | 425 | 365 | 2198 | 3907 | 3819 | 4800 | 5611 | 3471 | 15222 | 11476 | 8578 |
| | | | | | | | | | | | |
| Nb/Y | 0.42 | 0.46 | 0.74 | 0.77 | 0.54 | 0.33 | 0.40 | 0.92 | 0.79 | 0.50 | 1.07 |
| Zr/Ti | 0.21 | 0.21 | 0.09 | 0.05 | 0.05 | 0.03 | 0.02 | 0.06 | 0.01 | 0.01 | 0.02 |

**Table 7.6.1** (cont.)

| | Wahratta | | | | | | | |
|---|---|---|---|---|---|---|---|---|
| Sample | WAH-827.4 | WAH-838.5 | WAH-873 | WAH-986.5 | WAH-995 | WAH-1053 | WAH-1055 | WAH-1081 |
| Rock | tr-basalt | tr-basalt | mzdiorite | mzgabbro | mzgabbro | mzgabbro | dolerite | dolerite |
| SiO2 | 54.70 | 51.00 | 56.96 | 56.32 | 56.37 | 55.68 | 49.74 | 51.08 |
| TiO2 | 1.01 | 1.13 | 1.02 | 1.04 | 1.07 | 1.03 | 3.22 | 2.98 |
| Al2O3 | 17.23 | 16.15 | 17.12 | 17.07 | 16.84 | 17.13 | 13.77 | 13.67 |
| Fe2O3 | 7.78 | 9.78 | 7.22 | 7.17 | 7.28 | 7.62 | 14.74 | 14.09 |
| FeO* | 7.00 | 8.80 | 6.50 | 6.46 | 6.55 | 6.86 | 13.26 | 12.67 |
| MnO | 0.08 | 0.13 | 0.10 | 0.13 | 0.14 | 0.13 | 0.22 | 0.26 |
| MgO | 5.07 | 6.41 | 3.29 | 3.64 | 3.66 | 3.66 | 4.41 | 4.13 |
| CaO | 7.96 | 9.54 | 5.71 | 6.06 | 5.80 | 5.91 | 8.38 | 7.46 |
| Na2O | 4.03 | 5.37 | 4.09 | 4.44 | 4.41 | 4.20 | 3.87 | 3.89 |
| K2O | 1.71 | 0.07 | 4.04 | 3.65 | 3.98 | 4.15 | 0.73 | 1.31 |
| P2O5 | 0.42 | 0.42 | 0.45 | 0.47 | 0.46 | 0.48 | 0.92 | 1.13 |
| LOI | 3.90 | 5.23 | 1.11 | 1.73 | 1.94 | 1.73 | 1.97 | 1.80 |
| | | | | | | | | |
| Nb | 26 | 13 | 33 | 40 | 36 | 34 | 19 | 16 |
| Zr | 209 | 128 | 224 | 287 | 367 | 198 | 321 | 252 |
| Sr | 807 | 675 | 755 | 892 | 786 | 713 | 381 | 469 |
| Ba | 477 | 11 | 917 | 1125 | 844 | 1211 | 246 | 278 |
| La | 42 | 30 | 66 | 67 | 71 | 66 | 30 | 29 |
| Ce | 90 | 56 | 126 | 137 | 142 | 129 | 76 | 68 |
| Nd | 40 | 29 | 51 | 57 | 57 | 54 | 46 | 44 |
| Sc | 23 | 31 | 16 | 19 | 19 | 17 | 33 | 29 |
| V | 218 | 290 | 158 | 188 | 190 | 183 | 337 | 228 |
| Y | 21 | 18 | 26 | 27 | 27 | 25 | 71 | 67 |
| Rb | 40 | <1 | 136 | 109 | 142 | 124 | 27 | 49 |
| Th | 19 | 9 | 26 | 33 | 32 | 24 | 4 | 7 |
| Pb | 3 | 3 | 12 | 11 | 15 | 14 | 3 | 4 |
| Ti | 6080 | 6779 | 6105 | 6232 | 6390 | 6163 | 19331 | 17867 |
| | | | | | | | | |
| Nb/Y | 1.20 | 0.74 | 1.29 | 1.47 | 1.34 | 1.35 | 0.26 | 0.24 |
| Zr/Ti | 0.03 | 0.02 | 0.04 | 0.05 | 0.06 | 0.03 | 0.02 | 0.01 |
| FeO*/MgO | 1.38 | 1.37 | 1.97 | 1.77 | 1.79 | 1.87 | 3.01 | 3.07 |

**Table 7.6.1** (cont.)

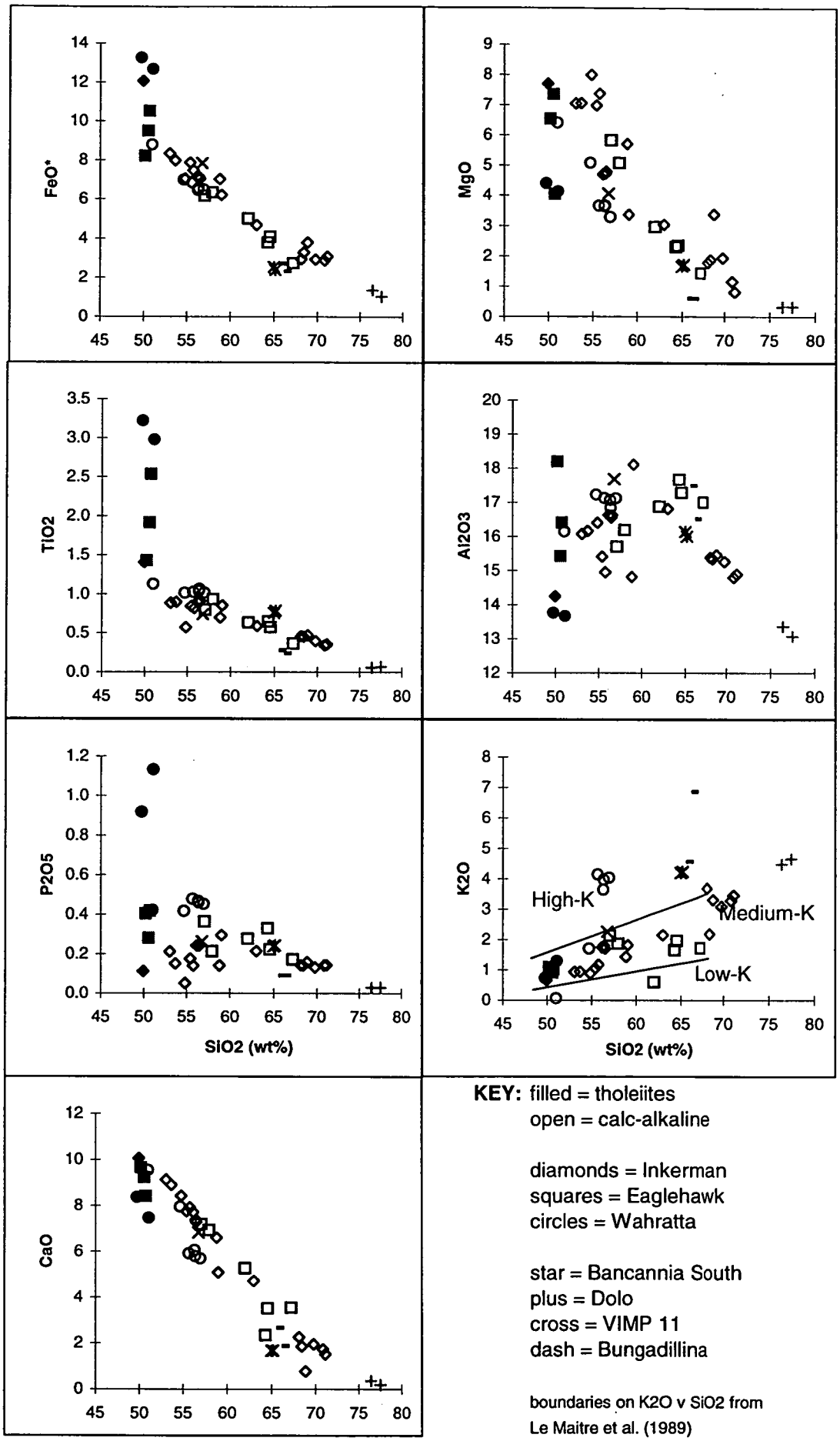


**Figure 7.6.1 Major element variation diagrams, calc-alkaline + tholeiitic suites Darling River Lineament**

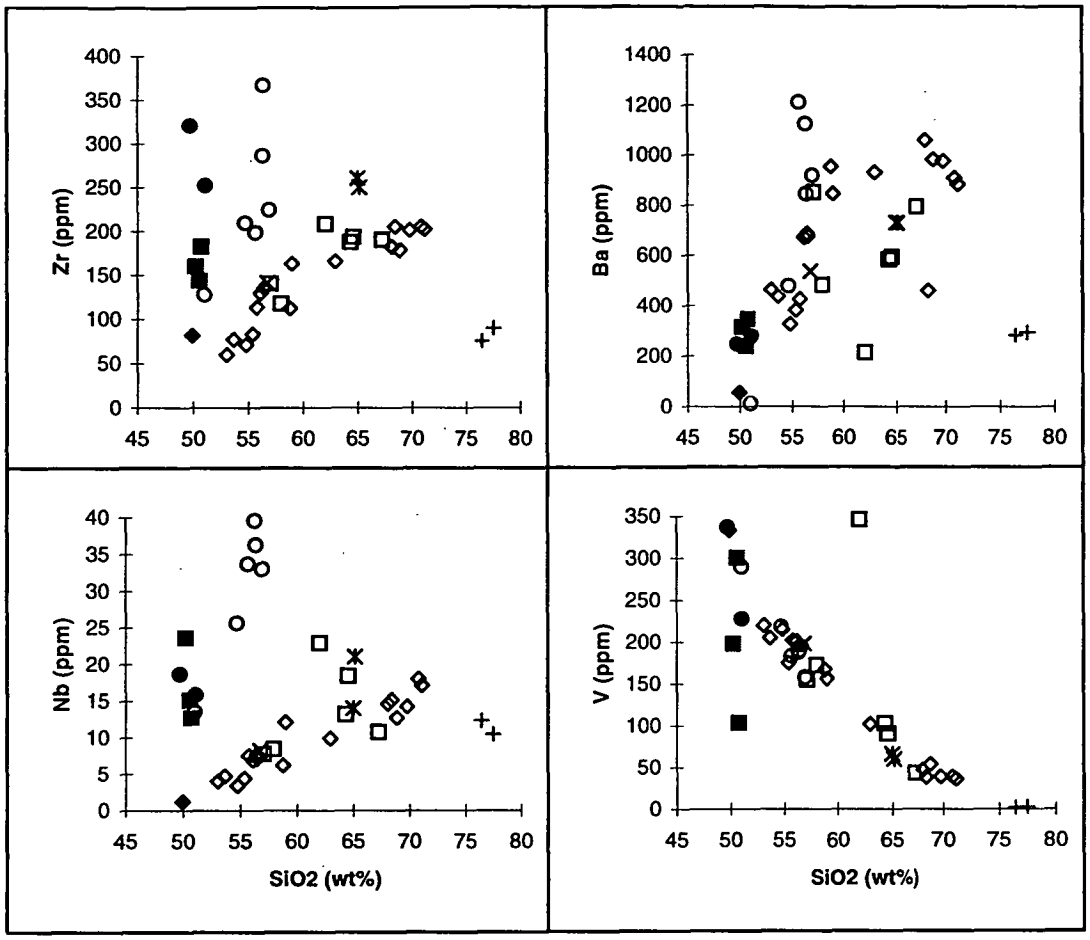


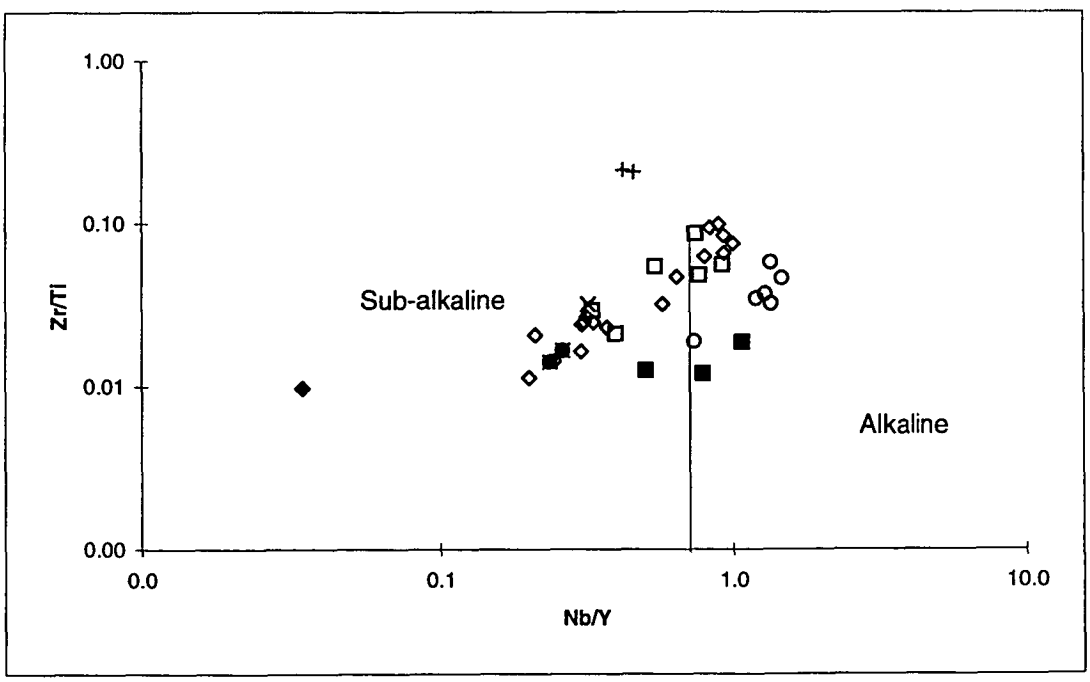


**Figure 7.6.2 Trace element variation and ratio diagrams, DRL suites**
Key: as for Fig. 7.6.1.

504 ± 8 Ma (Middle Cambrian) (Maher et al., 1997), which overlaps the age for the Bancannia South-1 dacite. This diorite was not assigned to a definite magmatic suite in the analysis of Crawford (in Maher et al., 1997); because of the similarity in petrographic character to rocks from Inkerman it has been included for comparison here.

A further two data points are from analyses of Bungadillina Monzonite of the Peake & Denison Ranges (Ambrose et al., 1981). These rocks, cropping out in far northern South Australia, have high-K affinities like rocks in the Wahratta drillhole. K-Ar dating on a variety of minerals in the Bungadillina suite gave ages centred on 500 Ma, and thus the Bungadillina Monzonite is interpreted as a far-flung, late stage intrusive of the Delamerian Orogeny (Ambrose et al., ibid.).

Major oxide data show surprising coherency given the diversity of data and alteration states of the rocks analysed; clear magmatic trends are visible in most elements, including the normally mobile $Na_2O$ and $K_2O$. FeO* and $TiO_2$ give the most useful information; the decreasing trend of both elements with increasing $SiO_2$ is indicative of calc-alkaline fractionation. This is the case for Inkerman diorites, hornblende andesites and dacite; Wahratta trachybasalts, monzogabbros and monzodiorite; Eaglehawk andesites and monzogabbros; the far-end member Dolo rhyolites; and samples from the Bancannia Trough, Victoria and South Australia.

In contrast, Inkerman dolerites, Eaglehawk dolerites and Wahratta dolerites all show evolution with increasing FeO* and $TiO_2$ at relatively constant $SiO_2$, indicative of tholeiitic fractionation with suppressed crystallisation of titano-magnetite.

Although requiring careful interpretation due to the age and metamorphosed state of the samples, $K_2O$ appears to show relatively coherent trends which may be useful in assigning tectonic affinities to the suites. Most samples on the $K_2O$ v $SiO_2$ plot fall in the medium- to high-K fields of Le Maitre et al. (1989). Two exceptions are likely to be due to K stripping during alteration. The high-K suite includes diorites from Wahratta and Inkerman, and the Victorian and South Australian samples. The remainder of the (calc-alkaline) rocks are all of medium-K affinity.

Trace element Harker diagrams for Zr, Nb, and V show three, usually distinct, groups. Tholeiitic dolerites from Eaglehawk, Wahratta and Inkerman form a group with low Zr and Nb, and show evidence of fractionation at constant $SiO_2$ in V. Calc-alkaline rocks show gradual increases in Zr and Nb, and decrease in V. High-K monzonitic rocks

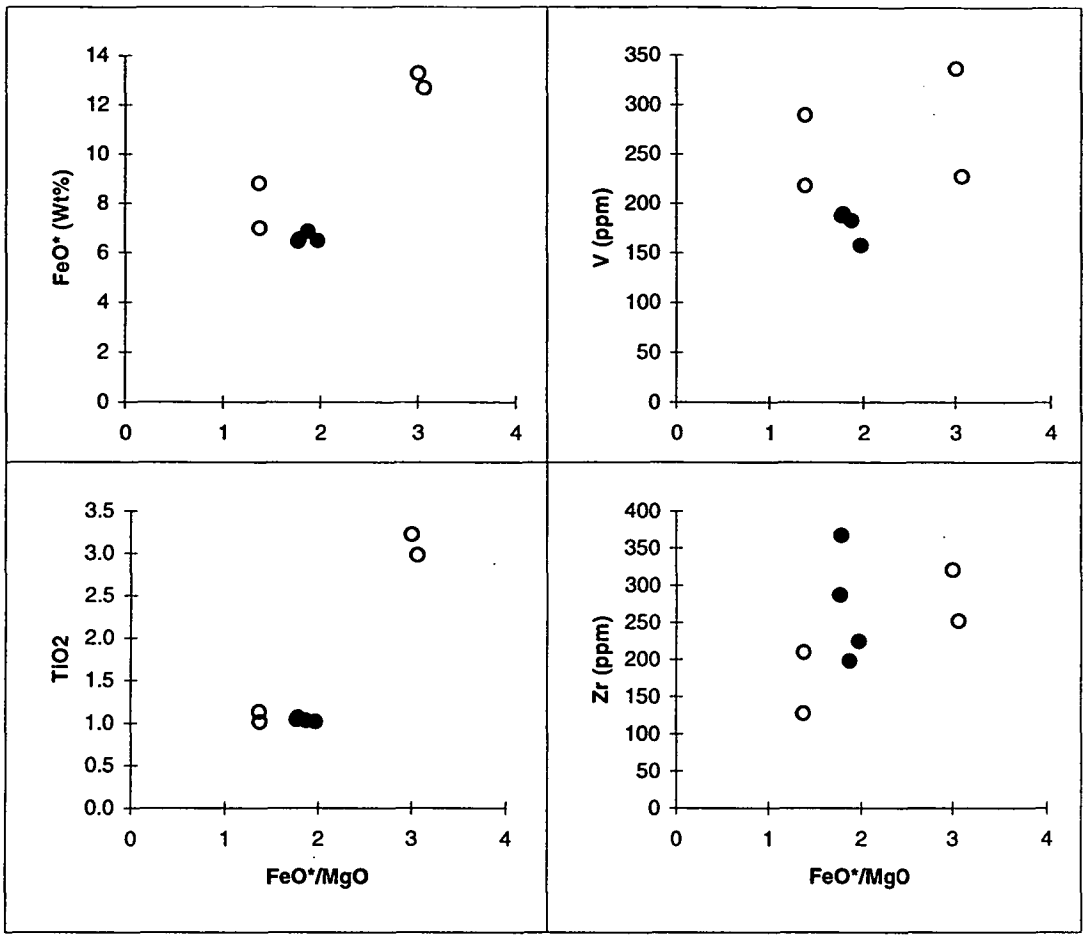


**Figure 7.6.3 Fractionation trend diagrams, Wahratta samples**

KEY: open circles = calc-alkaline lavas; solid circles = calc-alkaline intrusives; shaded circles = tholeiite dykes

Intrusives are cumulate monzodiorites and monzogabbros, accounting for elevated Zr at MgO ~2%

from Wahratta and Eaglehawk form a third group of high Zr and Nb, but fall within the calc-alkaline trend for V. On these diagrams, the very felsic Dolo rocks plot as outliers. Zr/Ti versus Nb/Y (after Winchester & Floyd, 1977) shows most samples fall within the field for sub-alkaline rocks; however a significant number of samples, including Wahratta lavas, Eaglehawk intrusives and lavas, and Inkerman lavas, all plot in the alkaline field.

Plots of the Wahratta samples against FeO*/MgO show two clear groupings: tholeiites have high FeO* and $TiO_2$ as well as higher FeO*/MgO at equivalent $SiO_2$. The tectonic discrimination plot of Zr/Ti versus Nb/Y shows that the dolerites fall in the sub-alkaline field as expected; cumulate monzonitic rocks, related lavas and dykes all fall in the alkaline field as shown above.

Incompatible element spidergrams normalised to N-MORB have been produced for both the tholeiitic and calc-alkaline suites (Figure 7.6.4 - 7.6.5). Analyses for the tholeiitic dolerites (Figure 7.6.4) generally vary smoothly from the LILE to HFSE, indicate an enriched MORB source with minor crustal influence suggested by Nb depletion. The implied sources are similar to those postulated for the Gneilwonga Volcanics (see Chapter 4.9.1), although the DRL suite is more enriched.

The calc-alkaline suite is very similar although with more pronounced Nb depletion. Sample "BS1 dac", a dacite from Bancannia South-1, has an extraordinarily enriched Pb signature (See Table 7.6.1); this may reflect sample contamination during preparation, as these samples were prepared and analysed by a commercial laboratory with a mixed suite of non-related, and possibly sulphide bearing, rocks. Alternatively, contamination from heavy drilling muds may be an explanation. Again, an E-MORB source with crustal influences is suggested; similarities between the early calc-alkaline suite and the later tholeiitic suite imply similar sources, with perhaps decreasing input from the crust with time.

## 7.7 Tectonic history of the DRL: deductions from magmatic suites

Two magmatic suites have been encountered in the DRL: an early calc-alkaline suite and, intruding it, a later tholeiitic suite. Both sets of rocks have been metamorphosed to greenschist facies, and calc-alkaline suite rocks intrude the ?Early-Middle Cambrian Teltawongee Group, also metamorphosed to greenschist facies. The metamorphic conformity of country rock and igneous intrusives, and cross-cutting relationships demand a post-Early Cambrian age for both intrusion events.

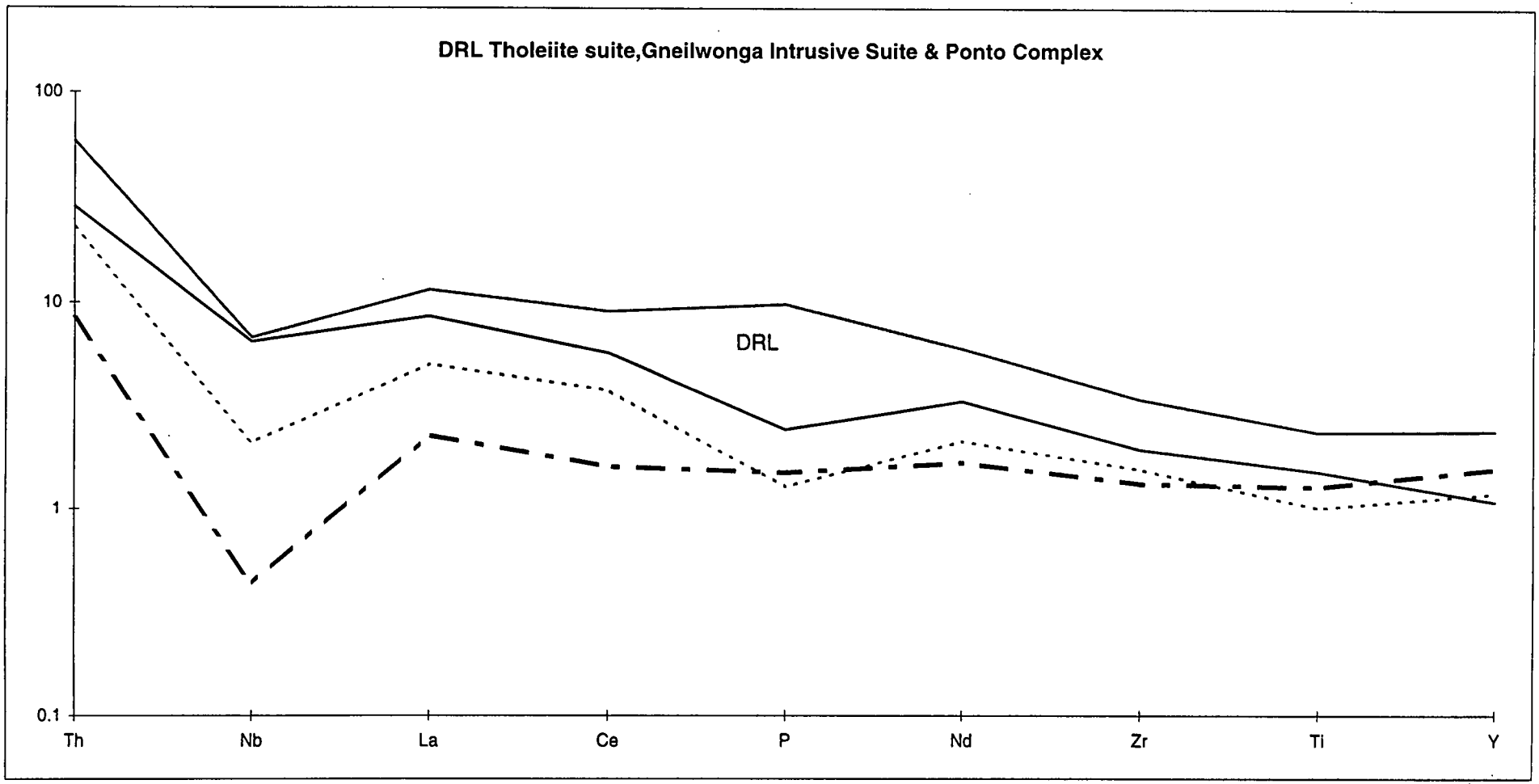


**Figure 7.6.4 N-MORB normalised spidergram, DRL tholeiite suite**
Normalising values from Sun & McDonough (1989)
Key: light stipple = Gneilwonga; heavy stipple = Ponto. DRL range from Wahratta and Eaglehawk samples only (5 analyses)

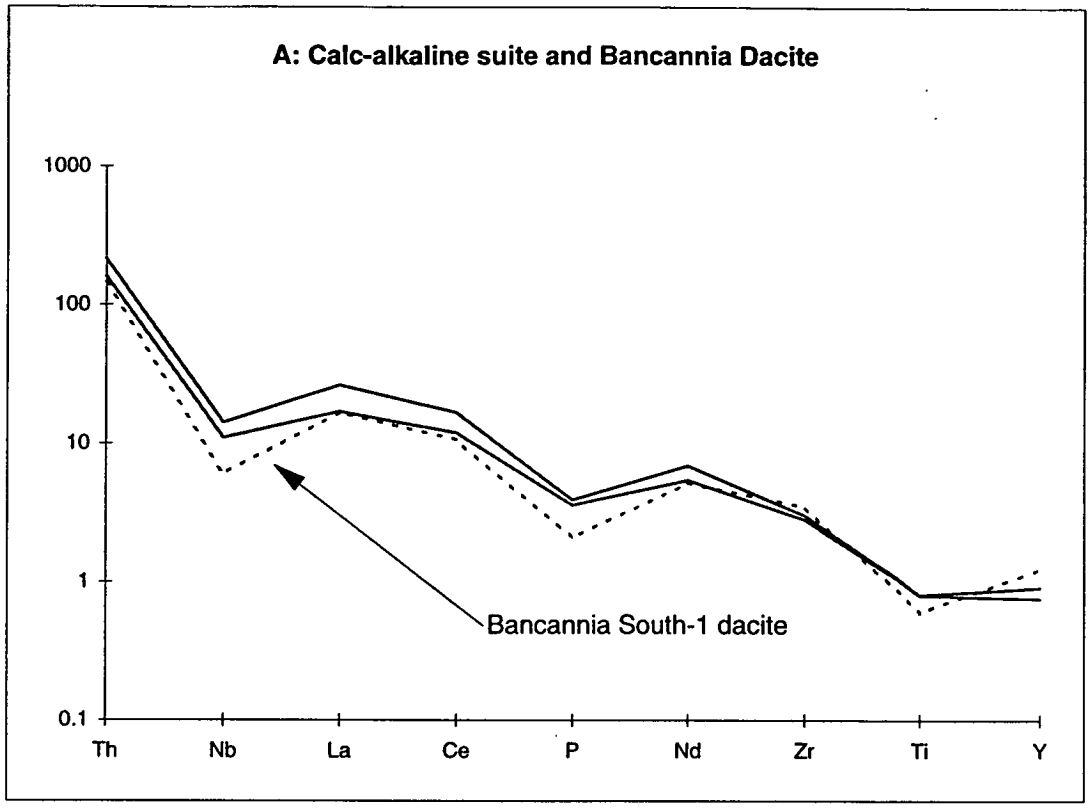


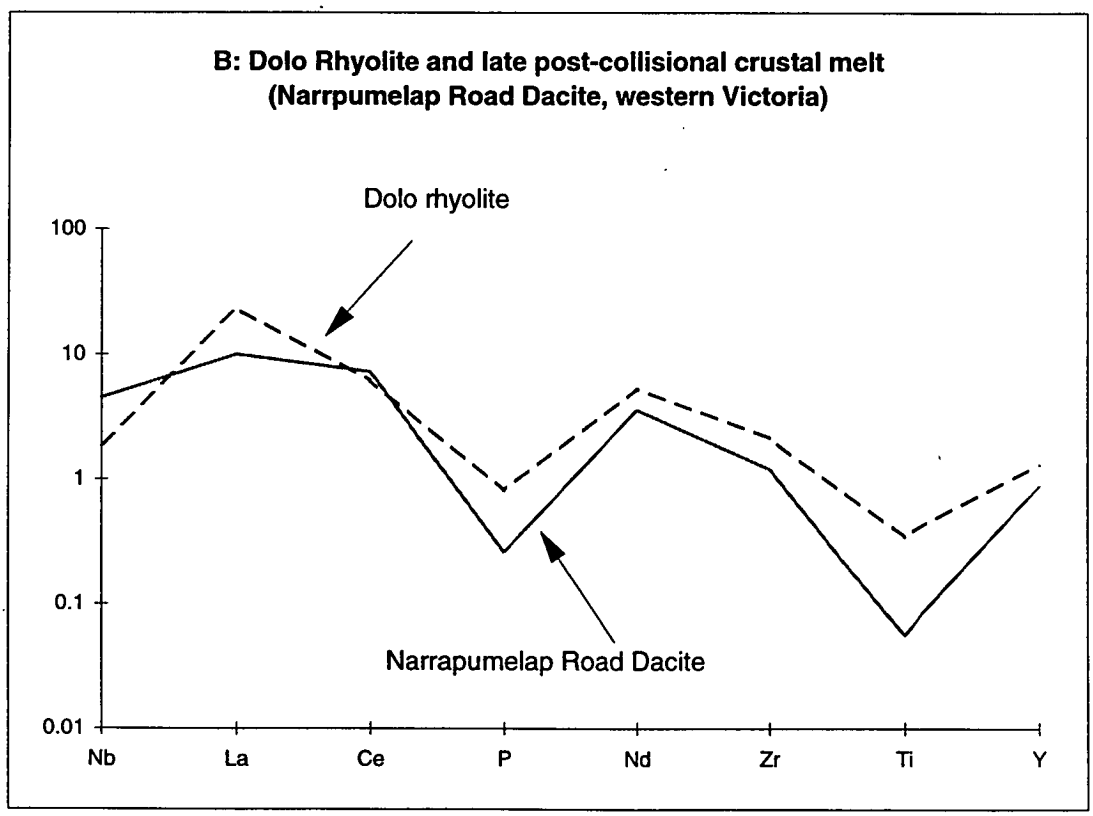


**Figure 7.6.5 N-MORB normalised spidergrams, DRL calc-alkaline suite**
Normalising data from Sun & McDonough (1989)

Constraint for the latest age for intrusion comes from two indirect lines of evidence. The DRL calc-alkaline suite is geochemically correlated with high-K dacites from the Bancannia Trough SHRIMP dated at 497 ± 11 Ma. This is a Middle Cambrian (Ordian) to Early Ordovician (Warendan) age. The calc-alkaline suite is also tentatively correlated with mafic diorite from the Miga Subzone of Victoria and the Bungadillina Monzonite of South Australia. These similar high-K rocks gave a SHRIMP zircon date at 504 ± 8 Ma (Middle Cambrian)(Ordian to Idamean), and a K-Ar date of c. 500 Ma respectively.

The second constraint on intrusive age is that neither of the DRL suites has been found to intrude the folded Early Ordovician (Warendan to Arenig) Scopes Range Beds (dates: Shergold et al., 1985).

The sum of these lines of evidence strongly suggest that both pulses of DRL magmatism occurred between 508 Ma (Ordian) and 496 Ma (Idamean). Both shared the same E-MORB source with minor crustal component, supporting a limited time range of magmatic activity. The range of ages inferred for this magmatism overlap those proposed for the emplacement of the Ponto beds onto the Gnalta Group (Iverian-Idamaean: 497.5 Ma to 492.5 Ma) (see Chapter 5.9)

The possibility of correlations of the DRL calc-alkaline suite with high-K rocks further afield suggest a major lithospheric event involving the mantle and the crust during this 5 to 10 Ma interval.

Alternatively, these rocks may be fractionated products of an extensive mafic crustal underplate melted during post-collisional lithospheric extension and decompression. This hypothesis was suggested by Foden et al. (1990) for the source of the Bungadillina Monzonite and related rocks in the Adelaide Fold Belt. There are some close similarities between these rocks and the post-collisional Mt Read Volcanics of western Tasmania (Crawford et al., 1992), and Mt Stavely Volcanics of western Victoria (Crawford et al., 1996a).

A third possibility is that the combined medium- and high-K chemistry, E-MORB and possible subduction-related source signatures of the NSW rocks may indicate that these suites represent part of an allochthonous island arc welded to the Gondwana craton late in the Delamerian Orogeny. In this variant, the major element and age correlation between the DRL rocks and the Bungadillina Monzonite would be fortuitous.

In support of this idea, $K_2O$-$SiO_2$ and Y-Zr compositions of the DRL suites show similarities to Early-Middle Ordovician island arc volcanics from central NSW (e.g. Glen et al., 1998: Figure 4). A corollary of this theory would be that part or all of the Teltawongee Group country rock is allochthonous with respect to the craton.

### 7.8 Conclusions

This chapter has attempted to examine the tectonic significance of the Darling River Lineament (DRL) through the examination of the geochemical affinities and timing of various igneous suites occurring within it. Although the main fault movements associated with the DRL are Devonian and Carboniferous (Owen et al., 1997), it has been the locus of several pulses of magmatic activity. The main igneous event occurred at around 500 Ma during the Delamerian Orogeny, producing a mixed mafic to felsic calc-alkaline suite and a later tholeiitic mafic suite. Potential correlates of these rocks are found in western Victoria and possibly northern South Australia, implying a large, widespread crust-mantle event. The cause of this event is unclear on the data available, but the calc-alkaline rocks do show some affinities to island arc suites, and also to post-collisional magmatic suites in western Tasmania and western Victoria.

A third intrusive event is inferred to have occurred after the Delamerian orogeny, possibly during the Late Silurian or Early Devonian. This produced mafic tholeiite pipes with pronounced within-plate signatures, confirming that cratonisation of the older Delamerian terrane had already occurred.

The tectonic elements represented in the DRL therefore include cratonic crust (Redan block to the north), Late Neoproterozoic-Early Cambrian shelf and basinal sequences (Kara beds; Teltawongee Group), syn-collisional volcanics of the Delamerian Orogen (Ponto Complex, DRL magmatic suites), post-collisional overlap sequences (Scopes Range Beds), and post-cratonisation volcanics (Comarto pipes). On the weight of this evidence, the importance of the DRL as a tectonic boundary dates back only to the Cambrian, and is largely related to events of the Delamerian Orogeny.

None of the suites examined is likely to be old enough to represent evidence for a continent-ocean transform margin at c.750 Ma as implied by Powell (1998).

**Chapter 8: Tectonostratigraphy and Prospectivity of the Koonenberry-Bancannia Region**

*8.0 Introduction*

*8.1 Summary of new findings*

*8.2 Ramifications of new observations*

*8.3 Resource Potential of the Koonenberry Fold Belt*

# Chapter 8: Tectonostratigraphy and Prospectivity of the Koonenberry-Bancannia Region

## 8.0 Introduction

This purpose of this chapter is to summarise and synthesise new datasets from the Koonenberry-Bancannia region which were elucidated separately in preceding chapters. The overall tectonic history of the belt is also presented, and the styles of tectonic setting discussed. The model developed is then used in a predictive way to examine the prospectivity of the belt for hydrocarbons and a range of ore deposits. It is not the intention of this study to develop a coherent metallogenic or hydrocarbon prospectivity model for this region; rather, this chapter provides a coherent framework and reference points for future, more detailed studies of those types.

## 8.1 Summary of New Findings

The Nundora-Wonnaminta-Marrapina-Nuntherungie area contains elements of a Late Neoproterozoic-Middle Cambrian continental passive margin, and an allochthonous Late Cambrian volcanosedimentary sequence from a backarc or marginal basin. These elements were amalgamated in a pre-Mindyallan event correlated with the Delamerian Orogeny. Post-collisional magmatism, in the form of tholeiitic dykes intruded the original passive margin sequences. Subsequent reorganisation of these elements occurred in a Silurian deformation, probably equivalent to the Benambran event in the Lachlan Fold Belt. Southwest-directed folding and thrusting with attendant regional metamorphism were the dominant modes of early deformation events, whereas northwest-trending brittle faulting (dip-slip with strike-slip components) and drag folding without widespread metamorphism characterises Devonian and Carboniferous deformations. Both deformation styles continue onto the craton edge (Euriowie Block). Geophysical modelling and structural considerations suggest that the area now under the Bancannia Trough was not immune from the early folding and thrusting events; however, its current identity as an intra-cratonic basin may have resulted from being floored by a more rigid, coherent thrust block of mafic volcanics.

The Mt Wright-Cymbric Vale area also preserves elements of a Late Neoproterozoic-Middle Cambrian passive margin, including shelf environments, and an allochthonous Late Cambrian volcanosedimentary sequence. The latter may have formed part of a colliding sequence in the Iverian-Idamean stages of the Late Cambrian. This collision

event led to strong disruption of both the passive margin and collider, although with strongly contrasting deformation style across the Mt Wright Fault Zone.

The tectonic history of the Grasmere area is consistent with that of the areas to the north and west, with a post-Boomerangian folding and thrusting event that emplaced a marginal or backarc basin fragment over continental shelf sediments. Post-Early Ordovician, pre-Late Silurian deformation involved further southwest-directed thrusting, producing out-of-sequence nappes and a new penetrative fabric in Palaeozoic rocks. This was followed by a phase of late northwest-southeast directed extension, opening accommodation space for the Mt Daubeny basin, and producing dextral fault arrays in the thrust stack. In post-Early Carboniferous times, this area was subject to a northeast- directed sinistral shear couple which produced ductile and brittle responses in basement and cover, respectively.

The tectonic elements represented in the Darling River Lineament include cratonic crust, Late Neoproterozoic-Early Cambrian shelf and basinal sequences, syn-or post-collisional volcanics of the Delamerian Orogen, syn- to post-collisional overlap sequences, and post-cratonisation intrusives. The main igneous event occurred at around 500 Ma, with potential correlates found in western Victoria and possibly northern South Australia, consistent with a widespread crust-mantle event. On the weight of this evidence, the importance of the DRL as a tectonic boundary dates back only to the Cambrian, and is largely related to events of the Delamerian Orogeny; however, the main fault movements in this area are Devonian and Carboniferous (Owen et al., 1997). None of the elements examined provides evidence for a continent-ocean transform margin in this location at c.750 Ma as implied by Powell (1998); however, such evidence cannot be ruled out at depth.

The lines of evidence above suggest a Late Neoproterozoic to Carboniferous tectonic history as shown in Table 8.1.1.

## 8.2 Ramifications of the new model

The proposed tectonic development is a significant change in understanding of the Koonenberry-Bancannia region in comparison to earlier models. The more important ramifications are reviewed below.

**Table 8.1.1 Tectonic history of the Koonenberry-Bancannia Region**

| Chronostratigraphic Units (intervals in Ma) | | Lithostratigraphic Units | Tectonic Setting | Plate regime |
|---|---|---|---|---|
| Carboniferous 344-298 | post-Tournaisian | "Kanimblan Event" | Intracratonic, extensional | ENE directed dextral megashear with brittle faulting, folding. |
| 354-344 | Tournaisian | Ravendale Fm | sag-basin | Intracratonic |
| Devonian | Late | Snake Cave SS | rift-sag basin | Intracratonic |
| 384-369 | Middle | Snake Cave SS<br>Tabberabberan Event | rift-sag basin<br>Tilting, minor folds | Intracratonic transpression |
| 410-384 | Early | Mt Daubeny Fm | post-Orogenic collapse | Intracratonic, extensional |
| Silurian 410-384 | post-Ludlow | Mt Daubeny Fm | post-Orogenic collapse | Intracratonic, extensional |
| 414-410 | Ludlow | Mt Daubeny Fm | post-Orogenic collapse | Intracratonic, extensional |
| 434-414 | pre-Ludlow | Benambran Event | Intracratonic | SW directed thrusting, folding |
| Ordovician | post-Arenig | hiatus | Erosional | Cratonic |
| c.486-c.467 | Arenig | Ponto Complex<br>Scopes Range beds | Ongoing collision | Collisional |
| 490-c.486 | Tremadoc | Ponto Complex;<br>Mootwingee Gp | Ongoing collision | Collisional |
| Cambrian 492.5-490 | Payntonian-Datsonian | Ponto Complex<br>Kandie Tank LMS,<br>Mootwingee Gp | Ongoing collision | Collisional |
| c.497-492.5 | Iverian-Idamean | Ponto Complex<br>Cupala Ck Fm<br>DRL igneous suites | Collision along Mt Wright FZ | Collisional |
| 498.5-c.497 | Mindyallan | Ponto Complex<br>Kayrunnera Gp<br>DRL igneous suites | Collision along Wonnaminta Flt<br>Post-collisional magmatism | Collisional |

| | | | | |
|---|---|---|---|---|
| 500-498.5 | Boomerangian | Ponto Complex | Collision onset | Convergent |
| 503-500 | Undillan | Ponto Complex | **Marginal Basin** | Convergent |
| 506-503 | Late Templetonian-Floran | Coonigan Fm ?Teltawongee Gp | Continental Shelf | ?Convergent |
| | | Ponto Complex | **Basin Floor** | |
| 509-506 | Ordian-Early Templetonian | Cymbric Vale Fm | Rift | ?Convergent |
| | | Teltawongee Gp | Shelf | |
| | | Ponto Complex | **Marginal Basin** | |
| c.527-509 | Toyonian | Cymbric Vale Fm | Rift | Extensional |
| | | Teltawongee Gp | Shelf | |
| | | Ponto Complex | **Marginal Basin** | |
| c.528-c.527 | Atdabanian -Botomian | MWV | Rift | Second rifting: NE-SW extension |
| | | Teltawongee Gp | Shelf | |
| | | Ponto Complex | **Marginal Basin** | |
| 533-528 | Tommotian | Teltawongee Gp | Shelf wedge | Passive margin |
| Late Neoproterozoic 600-580 | | Kara beds, MAV | Rift margin | First rifting: NE-SW extension |

Table 8.1.1 Tectonic history of the Koonenberry-Bancannia Region (cont.)

*8.2.1 Broad Tectonostratigraphy*

The most recent models for the development of the whole Koonenberry Belt were proposed by Zhou and co-workers (Zhou & Mills,1994; Zhou & Whitford, 1994; Zhou, 1993; and Mills, 1992). An alternative, if brief, interpretation was offered by Stevens et al. (1996). The view espoused by the first four papers was that the Ponto Complex represented a rift block of the Curnamona Craton (Zhou & Mills, 1994), underlying the stratigraphic equivalents of the Adelaide Fold Belt (Mills, 1992). This sequence, thought to be a continental margin (Zhou, 1993; Mills, 1992), was believed to have undergone a second phase of rifting at 525 Ma (Zhou & Whitford, 1994; Zhou, 1993) before orogenesis during the Middle to Late Cambrian Delamerian Orogeny (Mills, 1992). The effects of later deformation events were perceived to be minor (cf. Mills, 1992) compared to what were believed to be Delamerian and Mesoproterozoic orogenic fabrics.

The new model presented here (see Figure 8.2.1), developing ideas put forward in Stevens et al. (1996), offers an entirely different tectonostratigraphy. Continental passive margin formation by rifting between 600 and 580 Ma is the oldest recognised event. This was followed in the Early Cambrian (around 525 Ma) by an extensive second phase of crustal attenuation, related to the formation of a marginal basin along a large sector of the east-facing 600 Ma passive margin. This rifting continued into the present Warburton Basin area of South Australia. The Early Cambrian event is similar to that proposed in early models, except that radical revision of the stratigraphy requires that entirely different units are involved. It is believed that the Ponto Complex is a relic of this basin, consistent with its geochemical affinities.

Sometime in the Middle Cambrian, this margin changed to a compressional plate-kinematic regime. It is proposed that this event is associated with the onset of east-directed subduction at the western margin of the backarc basin, which now lies between the Koonenberry Fault and Cobar.

Subduction of the thin basin floor sequences continued until the end of the Middle Cambrian (Boomerangian). At this stage, rifted wedges of older Adelaidean age crust and piles of rift volcanics, both still preserved beneath the Koonenberry belt, began to be subducted. The buoyancy of these thicker cratonic slabs (currently 2.70 $t/m^3$) compared to thin, dense oceanic crust (2.90 $t/m^3$) is believed to have locked up the subduction zone. Transference of compression from the locked subduction zone to the

## Figure 8.2.1 Tectonostratigraphic development of the Koonenberry FTB

*Schematic and stylised, not to scale.

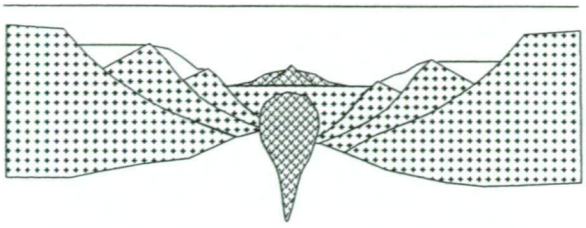

Late Neoproterozoic
(600-580 Ma)

Volcanic Passive Margin
& transitional alkaline volcanism
over a wide area
MAV + Kara beds

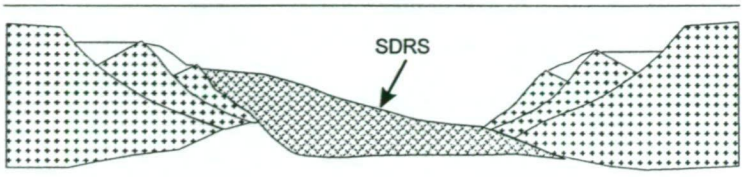


Late Neoproterozoic
(580-550 Ma)

Rifting and drifting phases
MAV + Kara beds

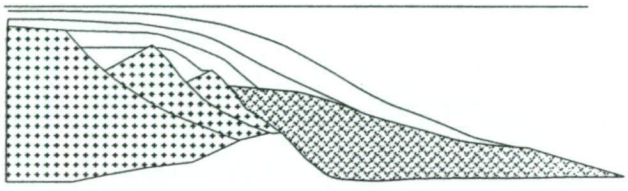

Early-Middle Cambrian
(?545-528 Ma)

Passive Margin Wedge
Teltawongee Group

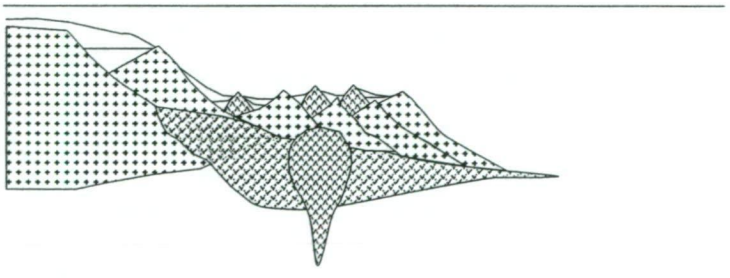

late Early Cambrian
(525 Ma)

Aborted continental rifting
& calc-alkaline volcanism
Gnalta Group

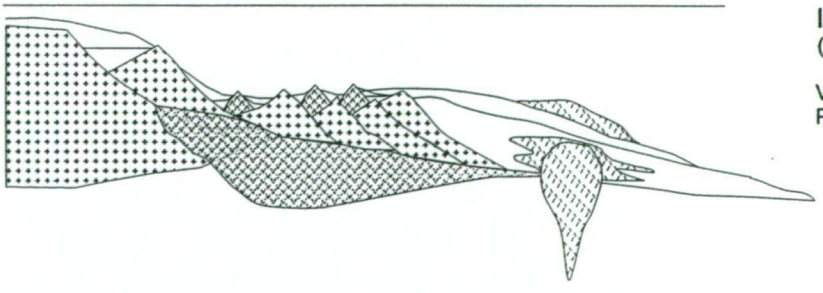

late Middle to Late Cambrian
(515-510 Ma)

Volcanic marginal basin formation
Ponto Complex

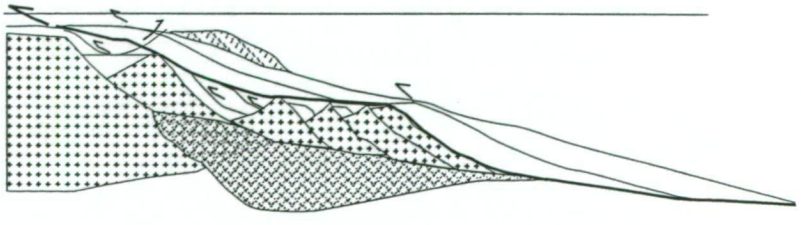

Late Cambrian
(c.505-498)

Marginal basin inversion
& thrust deformation

(cont. over page)

**Figure 8.2.1** (cont.)

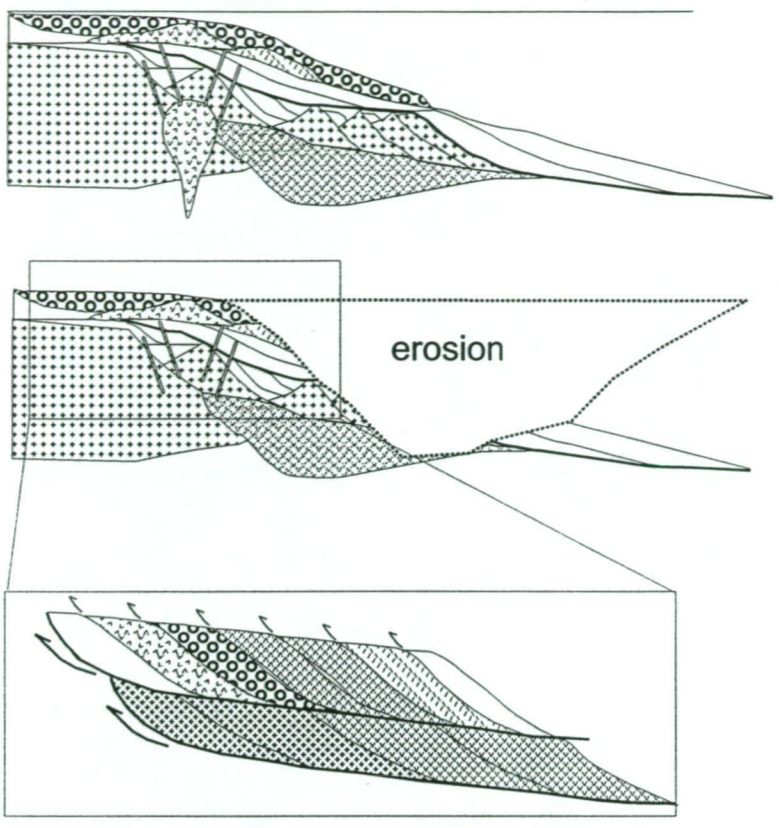


Late Cambrian
(c.498-480)

Post-collisional volcanism
& "molasse" basin formation
DRL suite; Mootwingee Gp
& correlates

Middle Ordovician-Silurian

Progressive cratonisation; eroded
material removed into Lachlan
Fold Belt quartz-rich flysch

Silurian

West vergent-thrusting on multiple
detatchments particularly between
post-580 and pre-580 sections

Late Silurian-Early Devonian

Erosion of thrust-stack and formation of
post-orogenic intermontane basins
Mt Daubeny Formation

Mid Devonian

Intracratonic basin formation
Mulga Downs Gp

Mid Devonian;
Mid Carboniferous

High crustal level deformation
Normal faulting and low-amplitude
long-wavelength folding;
Reactivation of early thrusts as normal
and strike-slip faults
Ongoing sedimenation in Devonian
(Ravendale Fm)

western margin of the basin then led to the thrust emplacement of marginal basin sequences onto the 600 Ma to 525 Ma "basement. This is likely to have occurred by reactivation of 525 Ma normal faults as reverse faults.

The diachroneity of the Late Cambrian- Early Ordovician siliciclastic-carbonate sequences developed on top of the inversion zone suggests that these deposits are not truly post-deformational, but rather late syn-deformation deposits. This idea is reinforced by an extended c.60 Ma hiatus in sedimentation following the Arenig, indicating the onset of cratonisation of the margin and accreted fragments, with the active plate margin "jumping" to a position well outboard to the east. I suggest that the relatively poorly known turbiditic Girilambone Group in the Cobar district represents the Ordovician locus of subduction. Biostratigraphic determinations for the Girilambone Group (Stewart & Glen, 1995; Iwata et al., 1995) give ages in the Llanvirnian to Caradoc epochs of the Ordovician (Darriwillian to Gisbornian) -ages which immediately post-date the last open marine deposition in the Koonenberry region.

In the Koonenberry, Silurian deformation in response to events outboard (see below) was followed by a phase of extension, possibly due to orogenic collapse of a portion of the developing Lachlan Fold Belt outboard. The continental red-bed facies of the Mt Daubeny Formation were the result, followed by a protracted sag phase of continental fluvial sedimentation with minor epicontinental marine influences.

Large scale orogenic events further to the east in the Lachlan and New England Fold Belts were responsible for internal adjustments in the Koonenberry Belt during the Middle Devonian to Carboniferous.

### *8.2.2 Structural Style*

The identification of widespread thrusting in the Koonenberry overturns all prior interpretations of this region. As outlined in Chapter 2, most previous structural models for the Koonenberry belt have tended to incorporate thick-skinned, vertical models of deformation processes, with little or no explanation of either the kinematics or dynamics of deformation (cf. Mills, 1992; Zhou, 1993). The exception to this was the terrane concept of Leitch et al. (1987). However, Mills (1992) showed that the timing of strike-slip faulting in the belt invalidated many of the assumptions of the terrane model, and this study has shown that there is no objective evidence for far-travelled exotic terranes accreted in the Koonenberry Belt.

The fold-and-thrust belt model developed in this study shows that the Koonenberry Fold Belt has similar structural characteristics to the Early Palaeozoic Tyennan Fold Belt of Tasmania and the Lachlan Fold Belt of mainland Australia. Common features include an imbricate thrust stack geometry involving linkage of large-scale thrusts, repeated stratigraphic slices, out-of-sequence-nappes, and multiple crustal detachments. These styles of deformation are linked to the plate tectonic regime occupied by the Koonenberry Belt during the Early Palaeozoic (see 8.2.3 below).

The Late Palaeozoic deformations in the Koonenberry belt are markedly different to earlier phases, with a dominance of high crustal-level structures, including dip-slip and strike-slip faults, warp- and drag-folding. Reactivation of earlier fractures is also common. The primary cause of deformation, which resulted in the oroclinal bending of the Koonenberry Belt and in particular, the Koonenberry Fault, appears to have been a sinistral megashear aligned with the northeast-southwest trending Darling River Lineament (Figure 8.2.2). Both Devonian and Carboniferous deformation styles have similarities to the neotectonics of China and central Asia (Molnar & Tapponnier, 1975; Molnar & Tapponnier, 1977; Molnar & Tapponnier, 1981; Tapponnier et al., 1982), which are the result of transmitted stresses through a rigid, cratonic landmass. This deformation style is also linked to the plate tectonic regime at this time (see below).

### *8.2.3 Plate tectonic context of fold-belt development*

In the Middle and Late Cambrian, rocks now found in the Koonenberry FTB formed part of the leading plate edge of Gondwana. Collision-related structures are thus typical of Mesozoic and Neogene continent-ocean accretionary plate boundaries in various locations, including Hokkaido (Arita et al., 1998), the Chugach Mountains of Alaska (Page et al., 1986, Kusky et al., 1997) and Taiwan (Yen et al., 1998). In all of the studies listed above, seismic, gravity and magnetics have played a major part in constraining the thrust geometry of the belts. In this respect, the Koonenberry Belt is a typical continental margin accretionary fold-and-thrust belt.

Deformation in the Koonenberry FTB occurred diachronously from the Boomerangian until the Tremadoc (Early Ordovician) and possibly up to the Arenig, a period of 20 Ma. The style of deformation was very much like the Palaeogene arc-continent collision preserved in New Caledonia (Collot et al., 1987; Aitchison et al., 1995), with very little orogenic relief being built-up: unconformably overlying post-collisional sequences are all marginal marine facies.

**Figure 8.2.2 Two-dimensional model for transmission of strain from a new orogenic front (NEFB) to neo-cratonic interior along the DarlingRiver Lineament and other lineaments during the Carboniferous**

Key : DRL = Darling River Lineament; CIL = Cobar-Inglewood Lineament;
Size of arrows is proportional to strain. Data are TMI, shaded from the west.

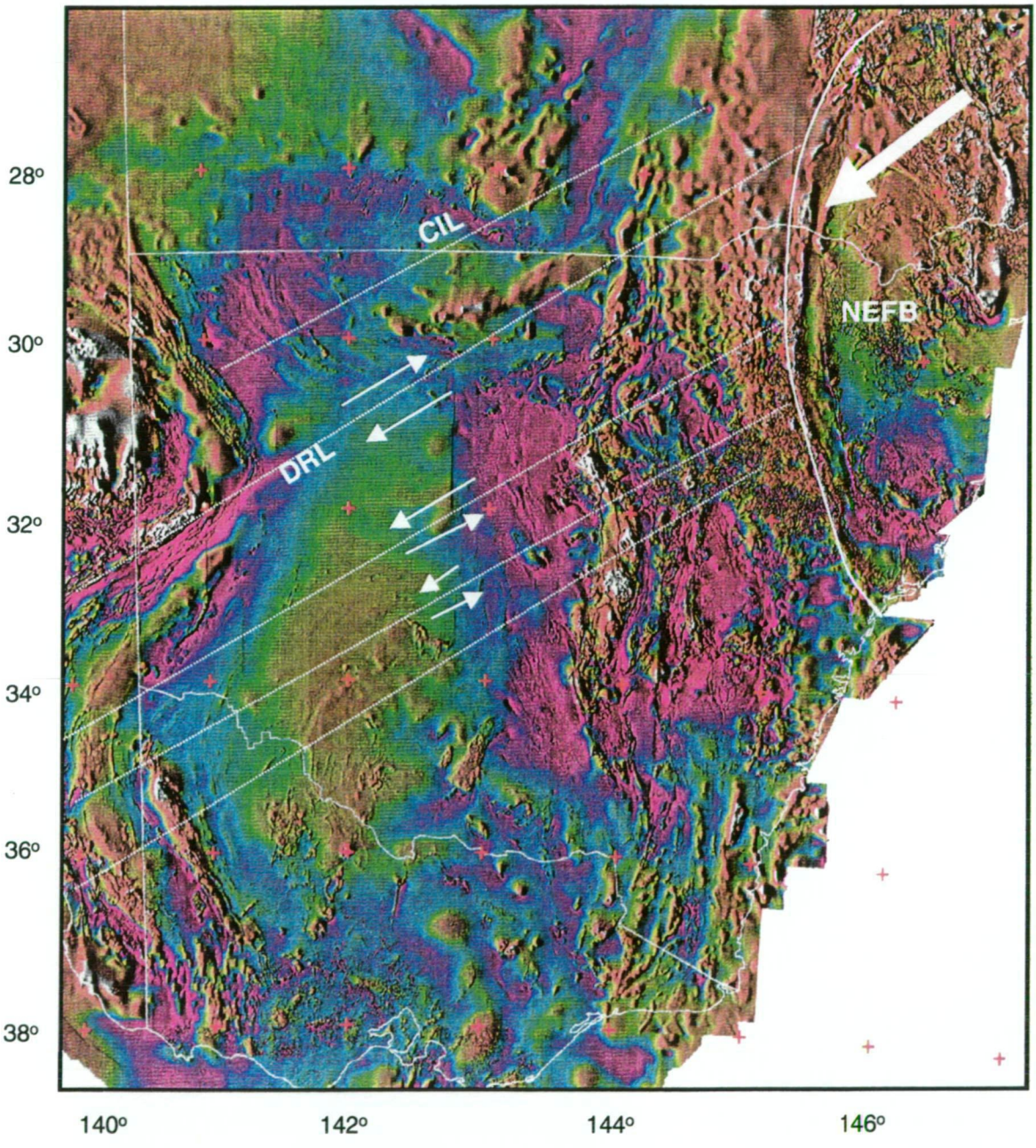

Fossil evidence from Ordovician sequences and limited dating on the emplaced sequences indicates that emplacement was achieved at different rates in different locations. Three explanations are possible for this. The first is that the geometry of both the margin and collider were irregular, leading to varying times between initial and final collision states if the rate of collision was constant along the collision zone. An alternative explanation is that the initial geometries may have been regular, but that ongoing spreading in the colliding block resulted in differential rates of collision in different sectors of the collision zone. The third explanation, a hybrid of these end-members, is probably more realistic when modern collision zones of this type are considered (e.g. Oman: Michard et al., 1991).

From the Late Cambrian to the Late Silurian, the Koonenberry FTB occupied a position inboard of the active plate margin, itself possibly located in the Cobar region. The first deformation in the Ordovician Girilambone Group occurred during the Benambran orogenic event, and developed thrusts and strong northwest-striking deformation fabrics from southwest-directed compression (Ingpen, 1996; Iwata et al, 1995). These features match similar Silurian fabrics developed in the Koonenberry FTB and the Warburton Basin, and indeed elsewhere throughout most of the Lachlan Fold Belt. This Late Ordovician-Silurian event has recently been recognised as the most significant to affect the eastern Australian mainland (Gray & Foster, 1997b). The previously unrecognised signature of this event in the Koonenberry FTB and further inboard demonstrates its extensive nature, and confirm the identity of the Koonenberry FTB as part of the Lachlan Orogen (Gray & Foster, 1997b; equivalent to Tasman Fold Belt System of Scheibner, 1996a).

The Devonian and Carboniferous saw the collision of a series of indenters far to the east of the Koonenberry Belt to form the Lachlan and New England Fold Belts (LFB; NEFB) (Scheibner, 1996b). The Early Devonian intracratonic Cobar Basin, outboard of the Koonenberry FTB, was inverted by thrusting in the Pragian (400-395 Ma) (Glen et al., 1992; Glen et al., 1994). This outboard event may have led to the demise of the Mt Daubeny sedimentation, and the Emsian unconformity separating it from the Mulga Downs Group. A further Devonian collision in the LFB is believed to be responsible for the Eifelian angular unconformity (Alder, 1998; Bembrick, 1997) in the Mulga Downs Group. Carboniferous collisions in the NEFB (Scheibner, 1996b) along a west-northwest-southeast striking collision axis at the northeastern end of the DRL may have been responsible for the megashear related deformation in the Koonenberry Belt at this time (Figure 8.2.1), via crustally transmitted plane strain.

The development of the Koonenberry FTB outlined in this study places it in the context of a long Palaeozoic history of continental accretion at the eastern margin of Gondwana, in much the same manner as proposed by Crook (1980a,b). This southwest Pacific-style of orogenesis (Crook, 1980a; Gray & Foster, 1997a) involves continuous accretion of oceanic tectonic elements, or in some cases, terranes, against the craton. An important feature of this model is the prediction of near-continuous deformation in the neocratonic margin, as all accreted blocks adjust to shear imparted by new additions and the demands of isostasy. However, despite the intuitive prediction that near-continuous and diachronous modes of deformation would be observed in the field, these features have only recently been proven in the Lachlan Fold Belt (Gray & Foster, 1997b; Gray et al., 1997; Bucher et al., 1996).

The recognition of near-continuous, diachronous deformation has cast doubt on the usefulness of regional stratigraphic unconformities as markers of discrete, cataclysmic "orogenies". More important for defining orogenic activity is the recognition of generations of fold and cleavage formation (Gray et al., 1997;Gray & Foster, 1997b) These findings have led Gray and co-workers to propose a long-lived Lachlan Orogeny, beginning at 440 Ma and ending in cratonisation by 340 Ma.

It is the finding of this study that, perhaps inevitably, the effects of the long-lasting Lachlan Orogeny have overprinted and modified the older accretionary margin and craton edge found in the Koonenberry FTB. As already noted by Mills (1992), geological consideration of the realities of fold-belt interference and overprinting means that some eastern Australian tectonic concepts, such as linear fold belt "boundaries" and the "Tasman Line", will have to be abandoned.

In particular, it is patently unrealistic to expect that linear geophysical anomalies along the approximate position of the Late Neoproterozoic craton edge still accurately represent the position of that margin. This study has shown that these anomalies represent a variety of lithological-structural associations of different ages, but are almost entirely associated with Palaeozoic deformation. The concept of a geophysically-defined "Tasman Line" as an extensional boundary (Gunn,1996) is thus a meaningless concept; a compressional "Tasman Line" is equally meaningless, as this study shows that Neoproterozoic "cratonic" crust is caught up in the Cambrian thrusting, both in the fold-belt proper, and on the craton as far west as the Corona Fault, and perhaps beyond (Haren et al, 1997; Gibson et al., 1996; Webster, 1996; Stevens & Rothery, 1997).

## 8.3 Resource potential of the Koonenberry FTB

To date, minerals exploration in the Koonenberry Belt has proceeded slowly and in piecemeal fashion. To a large extent, this prospecting approach was justified by the general lack of knowledge of the rock sequences present, their ages and structural relationships. Despite this, exploration has uncovered currently uneconomic deposits of high grade silver, gold and copper, mixed base metals (Barnes, 1975), diamonds (K.J. Mills, pers. comm) and shows of oil and gas (Bembrick, 1975). Whereas a detailed review of the occurrence and styles of this mineralisation is not the purpose of this study, it appears from the available exploration reports that these resources are strongly associated with three rock groups: Au, Ag, and Cu bearing veins and massive sulphides in the Late Cambrian Ponto Complex; hydrocarbons in the Devonian Mulga Downs Group; and diamonds as inclusions in Permian kimberlitic diatreme pipes.

Inasmuch as new geological interpretations of the geophysical data from this study clearly delineate these three host lithologies, target areas for future exploration are increased. However, a more integrated approach to resource exploration, based on the concept of ore deposit models (Roberts & Sheahan, 1988) is possible.

### *8.3.1 Potential metallic resources*

It has already been noted above that the belt preserves elements of a spectrum of tectonic regimes. At first appraisal, this makes it prospective for a wide variety of deposits. Rift associated deposits include sediment-hosted base metals; passive margin settings commonly host Mississippi Valley Type (MVT) and "Irish style" carbonate-hosted mineralisation; backarc basins are the site of extensive modern polymetallic volcanic hosted massive sulphide (VHMS) mineralisation, and ancient turbidite-hosted Au; volcanic arcs host both Cu-Au porphyry style and higher level epithermal Au-Ag deposits, and occasionally skarns of various types; collisional environments are also known to be prospective for Cyprus-style VHMS, in addition to "Alpine style" Platinum Group Element deposits; and finally, intracratonic basins may host sediment-hosted U ("rollfront" and "unconformity") and Cu ("red-bed") deposits.

The likelihood of any of these deposit types forming will have been determined by the interplay between four factors: a source for metals of the relevant type; a mechanism of transport to the site of mineralisation; an effective trapping and accumulation mechanism for the metals; and finally, tectonic preservation of the deposit (including from the effects of weathering). Full evaluation of these controls is not attempted here.

Despite its close proximity to the world-class Broken Hill district, the revised ages of most of the tectonostratigraphic packages renders the belt unprospective for Broken Hill Type Ag-Pb-Zn mineralisation.

Sediment-hosted base metal deposits (SHBM) such as those found in northern Australia, are found stratigraphically above large piles of mafic volcanics, and hosted in black-shale–carbonate sequences (Gustafson & Williams, 1981). Both of these are found in the MAV-Kara beds assemblage, which must therefore be considered prospective for this style of mineralisation. The approximate time-equivalence of these rocks to the Selwyn Basin deposits of Canada enhances the prospectivity for this temporally controlled style of mineralisation (Gustafson & Williams, 1981).

MVT deposits are by definition found in carbonate packages, which in turn are best developed in continental shelf sequences. MVT deposits also have a strong association with the development of secondary porosity in their host sequences. Both elements are found in the Cambrian Gnalta Group (and possibly equivalents in the Warburton Basin), a shelf sequence with porosity resulting from formation-breaking processes. MVT deposits also display a strong temporal control, with most examples occurring during the Cambrian -again enhancing the prospectivity of the Koonenberry target stratigraphy. "Irish-style" Ag-Pb-Zn deposits are a variant between the SHBM and MVT deposits, having both syngenetic and epigenetic characteristics (Muhling, 1990); because the Koonenberry belt is prospective for both end-members, "Irish" style deposits may also be found.

VHMS deposits are typically associated with submarine volcano-sedimentary sequences in regions of high heat-flow and hydrothermal activity (Lydon, 1988). Evidence of these features is preserved in the tholeiitic Ponto Complex volcanics and in the calc-alkaline DRL post-collisional volcanic sequences. Both packages are of Late Cambrian age, and temporally correlate with other VHMS-hosting packages in southeastern Australia (see chapters 10 & 11).

The mineralised porphyry system drilled in the Wahratta drillhole effectively attests to the prospectivity of the DRL region for Cu-Au mineralisation associated with monzonitic porphyry bodies, typical of arc environments (McMillan et al., 1997). In addition, if other such bodies have intruded carbonate packages in the Kara beds, or reactive lava packages in the Ponto Complex, various types of skarn mineralisation may have been developed. Later, non-arc related porphyritic intrusives in the Nuntherungie-Wertago-

Copper Mine Range area (Neef, 1991) are also spatially associated with Cu and Ag vein mineralisation which may be epithermal or mesothermal.

The collisional Ponto Complex is prospective for several deposit types. Where serpentinised peridotite-dunite assemblages are found along faults, spatially limited prospectivity exists for "Alpine style" podiform Cr-Ni-PGE deposits (Ballhaus, 1990). Higher in the volcanic stratigraphy, potential exists for clustered Cyprus-style (Constantinou & Govett, 1973) Cu massive sulphide deposits which are associated with major ophiolite sequences (e.g. Al Azry et al., 1993). It is possible that Cu mineralisation already noted in the Ponto Complex (Ponto Copper Mine: Carne, 1908; Grasmere Prospect: Lewis, 1976) may be an indicator of this type of mineralisation. The folded Ponto Complex turbidites are also prospective for structurally-controlled turbidite-hosted Au deposits, equivalent to major producers in western Victoria (e.g. Taylor et al., 1996).

The Mulga Downs Group and Mt Daubeny Formation are both sequences of porous red-bed sandstones with occasional marine facies that unconformably overlie older sequences rich in metallic sources (MAV, MWV, Ponto Complex, DRL intrusives). Carbonaceous marine packages in the Mulga Downs Group are thus prospective for sediment hosted Cu, whereas the cleaner sandstones, especially at the unconformity surface may be prospective for U. "Rollfront" deposits may have also developed where the Mulga Downs Group has acted as a hydrocarbon reservoir, thus providing a reducing agent for oxidised fluids carrying Cu, U and Au.

### *8.3.2 Summary*

Based on tectonostratigraphy and conceptual models of ore genesis, the Koonenberry FTB must be considered prospective for a wide variety of mineral deposits. Further, the indications of a fertile metallogeny are already present, with historical mining activity recorded as producing a variety of different commodities. Future detailed study of the metallogenesis of the Koonenberry FTB is recommended as part of ongoing exploration, and should be done on a fold-belt wide basis to include all the areas mentioned above.

### *8.3.3 Potential hydrocarbon resources*

The Koonenberry Fold Belt, and in particular, the Bancannia Trough, have been targets for petroleum exploration from the 1960's to the present. As outlined in Chapter

2, various studies have already been undertaken in attempts to define potential sources, migration paths and traps (e.g. Wilson, 1967; Evans, 1977; Brown et al., 1982; NSWGS, 1993). A series of dry holes with tantalising shows has generally dampened exploration activity. However, recent reports of gas flowing from water bores in the northern Bancannia Trough (B. Mullard, pers. comm. 1996) and oil seeps have stimulated the exploration process again, as at the time of writing.

In terms of conceptual models, petroleum exploration is very similar to ore deposit exploration, with a valid *play* the result of interplays between a mature source, hydrocarbon migration, adequate reservoir sites and reservoir integrity and preservation. Very recent work has indicated two possible mature sources -one Cambrian and one Devonian- but not the actual source rock (Alder, 1998). In general, the source potential of the marine parts of the Devonian has been rated as poor (Brown et al., 1982). Studies of oil shows and seeps, including some from outcrop at Cymbric Vale suggest relatively recent (Cainozoic) generation and migration of hydrocarbons; the possible causes for this remain unexplained (Alder, 1998).

Finally, it is to the trapping environment that more attention needs to be paid in future. Previous explorers worked on the assumption of vertical tectonics, and were rewarded with dry holes. New exploration models must take into account that the Koonenberry region is part of a polydeformed thrust belt, with deformation in the Cambrian, Silurian, Devonian and Carboniferous. Particular attention ought to be paid to the effects of the high-level Carboniferous deformation affecting the Mulga Downs Group, which is the only suitable reservoir rock in the region (Bembrick, 1997). Of key importance is that many potential reservoir structures (e.g. internal unconformities, Middle Devonian folds) will have been breached by the major Carboniferous fault deformation. If suitable seal rocks have not been emplaced against the reservoir sequence, then there is probably very little chance of finding an intact Devonian play (cf. Evans, 1977). Suitable fault seals may include Devonian shales, Gnalta Group shales or volcanics, Ponto Complex rocks or even Kara beds shales. Alternatively, due to overthrusting, migration may have taken place from younger to older porous sequences. This multiple-deformation scenario with older units acting as fault seals may explain why apparently Devonian oil is being found in Cambrian limestone at Cymbric Vale (cf. Alder, 1998). An equivalent scenario has also been proposed as a high-risk play in the producing Warburton Basin (Roberts et al., 1990). Despite this similarity, the Cambrian Gnalta Group limestones are unlikely to be an effective reservoir, due to their broken and discontinuous nature as a result of Late Cambrian tectonism.

In summary, while source potential exists and hydrocarbon generation has unarguably taken place, the highest risk element of any play in the Koonenberry FTB will be the trap. Exploration focus should be maintained on Mulga Downs Group reservoirs, with emphasis placed on structural plays with effective fault seal lithologies.

### *8.3.4 Diamonds*

A Permian pyrope-bearing kimberlite has been identified at Turkey Creek on Kayrunnera 7436 (Gleadow & Edwards, 1978; Mills & Hicks, unpublished mapping). The occurrence of several similar pipe-like intrusions has been noted on the Wonnaminta 7336 and Nuchea 7335 1:100 000 sheets. These may warrant further attention using ground magnetics, drilling and geochemistry.

## 8.4 Summary

Part 1 of this study has shown that the Koonenberry Belt of western NSW is a polydeformed fold and thrust belt of Palaeozoic age. Its development can be seen to have occurred as a consequence of its tectonic setting at an active plate margin for some of this time, and more generally, as the outcome of protracted and progressive accretion events on the eastern side of Gondwana. As a result of these processes, the region is highly prospective for a variety of resources, both metallic and non-metallic.

In the following Part, I seek to place the Koonenberry Fold Belt (KFB) in its broader continental context. This entails expanding the scale of investigation, moving from the limited New South Wales-focussed perspective of the previous chapters, to encompass possible correlative rocks of the Adelaide Fold Belt (AFB) of South Australia and Victoria, Tyennan Fold Belt of Tasmania, and even further afield to the Trans-Antarctic Mountains. In doing so, I hope to demonstrate that the Koonenberry Fold Belt is one element of a much larger continental margin-accretionary fold belt system, and that these relationships help constrain unresolved problems from the KFB: problems that cannot be solved with reference to NSW alone.